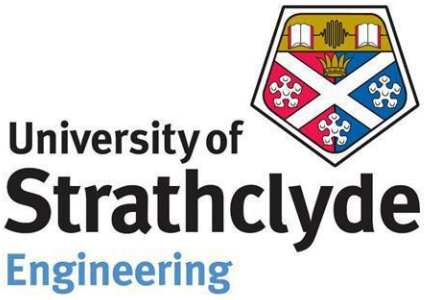

A Study of the Metallurgical and Mechanical Property Variability in a Dual Phase Low Alloy Material

David Gill

Department of Mechanical & Aerospace Engineering

University of Strathclyde, Glasgow

July 2017

Submitted to the Department of Mechanical & Aerospace Engineering

in partial fulfilment of the requirements of

Doctor of Philosophy

Abstract

AISI 4161H is a low alloy material that is currently used to manufacture coil springs for the TechnipFMC portfolio of actuated gate valves. The coil springs are designed to operate in a subsea service environment for a minimum of 25 years, which can equate to conditions of a working water depth of 10,000 feet (3048metres) and pressure of 10,000 psi. As the Coil Spring is the main method of valve closure, failure of the respective material can lead to catastrophic consequences. The design has no redundancy, therefore coil spring breakages and loss of load can lead to failure in the closure of the valve gate, which is the main failsafe system, controlling the flow of oil and gas from the seabed.

Throughout the initial development of the respective coil spring material, TechnipFMC has discovered that the necessary metallurgical properties requirements have not been consistently met. The initial work, which was conducted between 2012 and 2014, established that the material contained microstructural variability, which produced mechanical properties that did not meet the design intent of the coil spring. These findings were found with material procured from different mills and by two separate OEM's who hot formed the raw bar into final coil spring products. Failure to meet the design requirements, affects the functionality of the coil spring to have enough stored energy to act as failsafe mechanism to close the respective valve.

To address this problem, a comprehensive design of experiment programme has been developed as a series of characterisation and validation testing, to determine the fundamental properties of the AISI 4161H material type, using different heat treatment operations and conditions.

This is considered paramount, as current industry requirements do not mandate any testing or material characterization, other than a basic metallurgical assessment.

These requirements and level of governance are considered inadequate by the author, as the industry controlling standards do not define the correct pass / fail criterion that ensures such a critical product will not fail in-service.

The research programme contained within this thesis, addresses the reasons for the variability exhibited by the AISI 4161H material, and determines how the variation can be influenced by exposure to different hot working and heat treatment conditions.

The subsequent findings from the programme will enable engineers to determine the limitations of the material, and the effect variability has on the functionality of the coil spring for subsea applications.

The characterisation will also allow the industry governing bodies to align their respective test requirements and acceptance standards to that of a heterogeneous material, which contains variability throughout its cross-sectional thickness.

Declaration of Authenticity and Author's / Companies' Rights

This thesis is the result of the author's original research. It has been composed by the author and has not been previously submitted for examination, which has led to the award of a degree.

This thesis shall not be made available until a period of 7 years has lapsed from the date of publication. Until this time, the work shall be held within the department of Mechanical & Aerospace Engineering.

Author Signature:

Date:

Supervisor Signature:

Date:

Acknowledgements

I would like to express my sincere thanks and appreciation to Professor David Nash and Dr Andrew McLaren for their continual support and guidance in undertaking the academic and experimental research to produce this thesis. Their technical knowledge and experience within mechanics and material science disciplines has been invaluable.

Thanks, are due to other key members of the University staff, especially Dr Fiona Sillars for her continued support throughout the detailed analysis phase of this work.

My special thanks are extended to my friends and colleagues at TechnipFMC; Ravi Kapur, David Woodall, Dr Michael Roy, Andrew Cunningham and Sean Dobie. Their expert advice and selfless help throughout was exceptional.

Finally, I would like to thank my wife Lynne and children Marissa and Marcus, for their patience, support and encouragement, which has made the process of writing this thesis possible.

Table of Contents

List of Figures

List of Tables

Nomenclature

Ac1	Temperature at which austenite begins to form during heating
Ac3	Temperature during heating that the transformation of ferrite into austenite ends
AISI	American Iron and Steel Institute
ASME	American Society of Mechanical Engineers
ASTM	American Society for Testing and Materials
BCT	Body Centred Tetragonal
Bf	Bainite finish temperature
Bs	Bainite start temperature
BS EN	British Standard European Norm
C	Carbon
°C	Degrees Celsius
CCT	Continuous Cooling Transformation
CoC	Certificate of Conformity
Cr	Chromium
DI	Ideal Diameter
DoE	Design of Experiments
EDAX	Energy Dispersive Analysis X-Ray
El	Elongation
°F	Degrees Fahrenheit
F1	Coil Spring Preload
F2	Pinch Point Load
F3	End Load - maximum load
FCC	Face Centred Cubic
Fe_3C	Iron Carbide
FEA	Finite Element Analysis
FSC	Fail Safe Close
Fs	Solid Load - load achieved when the coils are fully compressed
Ft	Feet
HPHT	High Pressure High Temperature
HBN	Hardness Brinell Number
HBW	Hardness Brinell Tungsten Ball
HRC	Hardness Rockwell C
G	Shear modulus
ID	Inside Diameter
in "	inches
IST	Institute of Spring Technology

ITD	Isothermal Transformation Diagram (see also TTT)
K	thousand
ksi	Kilopound per square inch
KN	Kilo Newtons
L0	Free height / length
L1	Maximum working height / length
L2	Crack open / Pinch point height / length
L3	Minimum working height / length
Ls	Solid height / length
MPa	Megapascal
Mf	Martensite finish temperature
Mn	Manganese
Mo	Molybdenum
Ms	Martensite start temperature
NPI	New Product Introduction
OD	Outside Diameter
OEM	Original Equipment Manufacture
P	Phosphorous
psi	Pounds per square inch
Q & T	Quench and Temper
r	Radius
RoA	Reduction of Area
S	Sulphur
SEM	Scanning Electron Microscope
Si	Silicon
T	Thickness
TTT	Time Temperature Transformation (see also ITD)
wt	weight
UTS	Ultimate Tensile Strength
YS	Yield Strength

1 INTRODUCTION

1.1 Product Background

Mechanical springs are utilised globally for multiple purposes and industries, from consumable inexpensive operation to critical applications, where failure is not an option.

In basic terminology, mechanical springs can be defined as elastic bodies, which deform to a certain amount under a specific load, and return to their original shape when the applied load is removed [4]. There are many different spring types utilised, which range in size, design and material composition. However, these requirements are dependent on the application, operating environment and resultant load characteristics for the mechanical system selected.

Within the oil and gas sector, mechanical springs are used within subsea Christmas trees as the main mechanism for the fail-safe operation of actuated valves.

1.1.1 Subsea Christmas Trees

One of TechnipFMC main products is the Christmas tree, which plays a key role in the subsea oil production infrastructure. The primary functions of the tree, are the control and extraction of production fluid and gas from the oil field.

Following the initial drilling of a well the subsea tree is installed on the wellhead, which is cemented in the sea floor. The production tubing is run from within the subsea tree and is the route by which the hydrocarbons are extracted from the reservoir. It is typically designed for a minimum lifetime of twenty-five years subsea and controls the well for the duration of its operating life. Towards the end of a well's life, injection trees are often added to the system. These inject water or gas into the well to increase hydrocarbon recovery from the reservoir.

Throughout the subsea tree there are various flow paths. To open and close these flow paths a series of valves are utilised. These valves are controlled by subsea actuators attached to the valve stem. Figure 1-1 illustrates a subsea tree with the

actuator locations labelled, with Figure 1-2 identifying the stem and actuator interface.

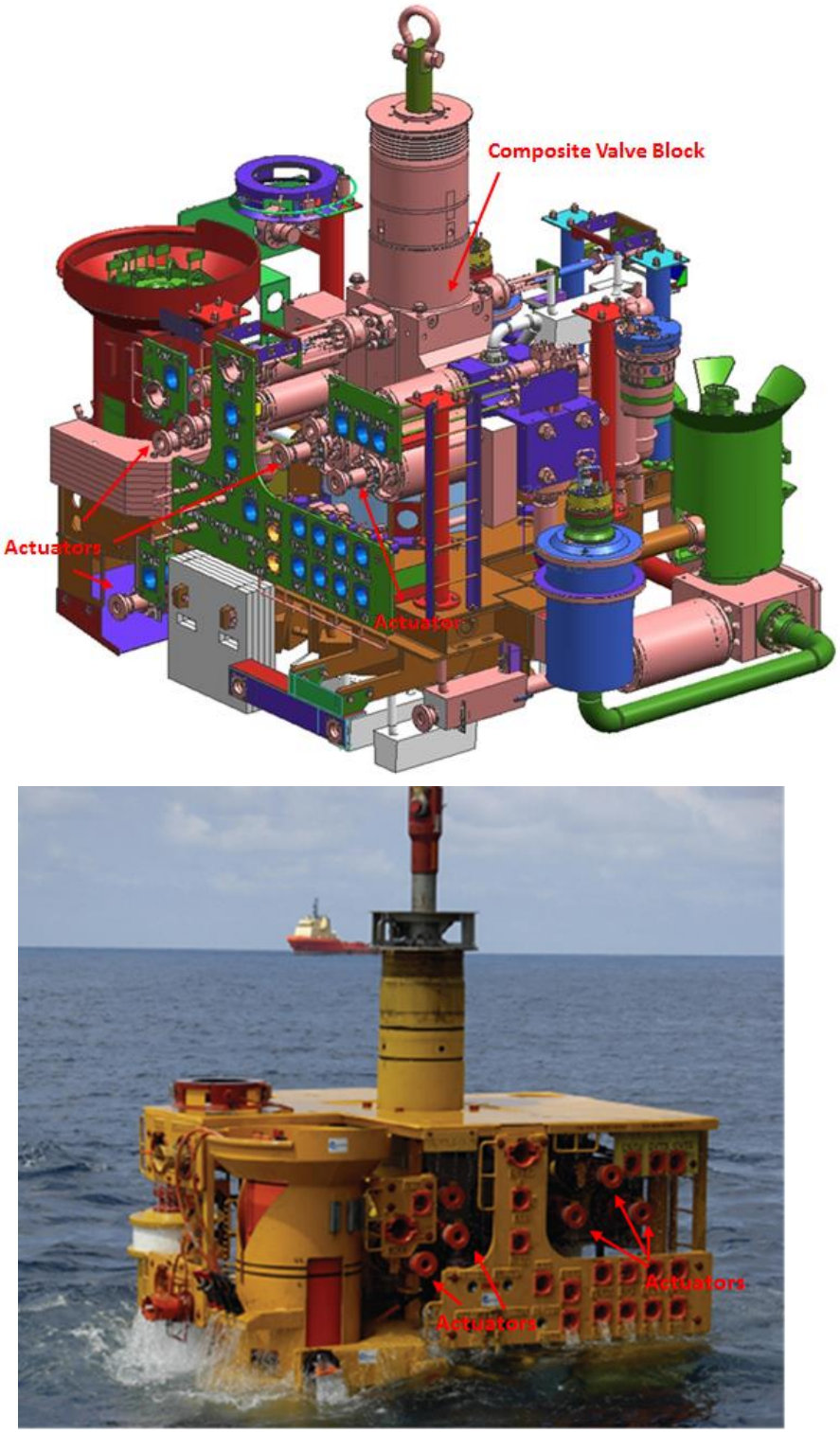

Figure 1-1: Subsea Christmas Tree (Top - Schematic View / Bottom - Full Tree)

1.1.2 Subsea Actuator Overview

Actuators can be operated by electrical, hydraulic or pneumatic signals. They are crucial for the oil and gas industry as the operator is distanced from the subsea installed equipment and it must be possible to remotely control the valves. Figure 1-2 displays two subsea valves and actuators with the main components identified.

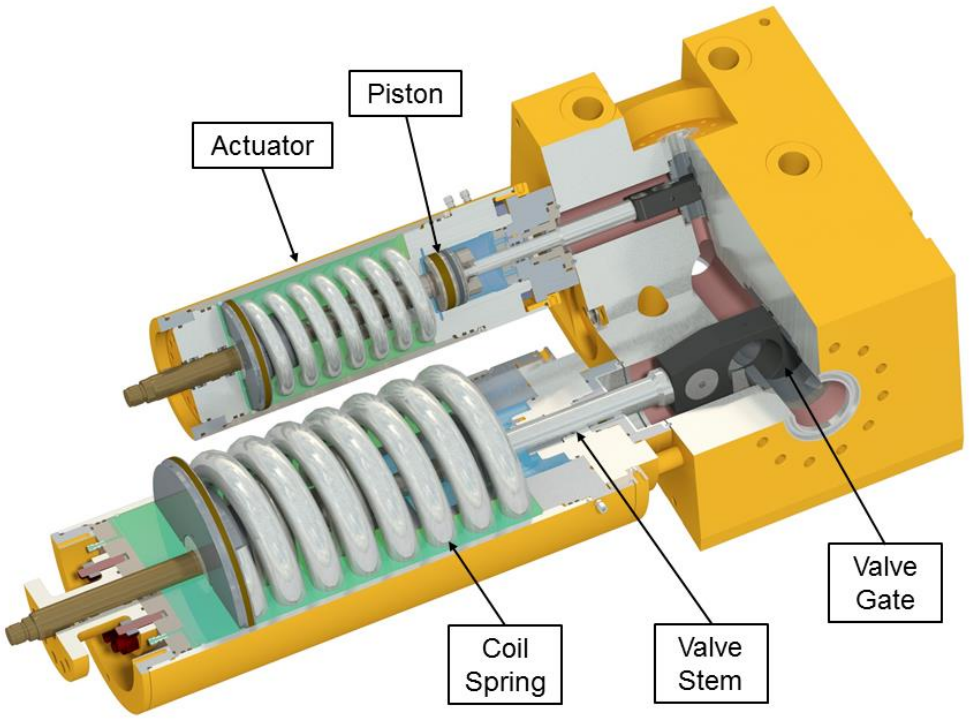

Figure 1-2: Subsea Valves and Actuators

Actuators are available in a variety of shapes and sizes. The smaller actuator in Figure 1-2 is for a 2 1/16" (52.4mm) valve and the larger one a 5 1/8" (130.2mm) valve. Within a subsea tree different valve sizes are required for each function. For the main production bore, where the hydrocarbons flow, it tends to be 5 1/8" (130.2mm) valves and actuators that are used. Smaller valves and actuators, such as the 2 1/16" (52.4mm) are found on the annulus bore which is used for chemical injection.

1.1.3 Coil Spring Purpose

In most cases, subsea valves are required to operate as a 'fail safe close' system. During normal operation, hydraulic pressure is applied to the actuator, compressing the spring and allowing the gate to remain in the open position. When hydraulic pressure to the actuator is relieved, the coil spring is primarily responsible for stroking the actuator, thereby closing the gate and stopping the flow of fluid. Inherently, this method requires the coil spring(s) within the actuator to remain in the compressed state for long intervals. It is essential that the coil spring retains its stored energy since the fluid flowing through the gate bore is itself pressurised, and will resist changes to the flow path. Refer to Figure 1-3 for a sectional view of a 5 1/8" (130.2mm) actuator demonstrating the key working parts.

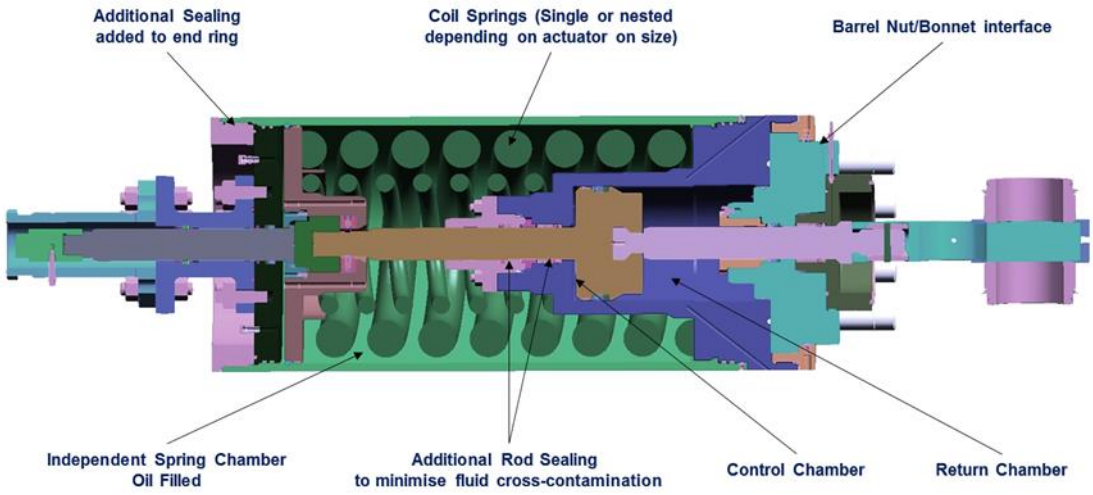

Figure 1-3: Typical Actuator and Gate Arrangement

In a typical actuated valve, the highest force required from the actuator is when the valve is just about to open (crack open) and conversely just before it closes (pinch point). Depending on the type of valve, control pressure is applied to the hydraulic piston within the actuator control chamber, which is used to open or close the valve. The coil spring assists in the function of the actuator return stroke. This assistance is provided both during normal operation and during abnormal conditions, where the actuator could be subjected to loss of control chamber pressure. In this situation, the

retained force within the compressed coil spring will react and overcome the production well and valve frictional forces and close the valve (fail safe close).

1.2 Statement of Problem

Currently TechnipFMC utilise AISI 4161H [5] material for the coil springs used to function its new generation of fail-safe close and open actuators. These coil springs are designed to operate in a subsea service environment for 25 years, which can equate to conditions of a working water depth of 10,000 feet (3048m) and pressure of 10,000 psi.

As the coil spring is the main and sole method of valve closure, failure of the respective material is not an option, as the design has no redundancy. If the material fails to retain its spring energy and load, or is subjected to a fatigue like fracture, the valve with fail to operate as the design intended. The consequences of this condition, will result in the removal of the Christmas tree from the subsea installation, which has a major impact on the customer's ability to extract oil from the sea bed. This situation incurs huge revenue losses for the operator, and effects the reputation of the subsea system manufacturer. Therefore, the spring material is critical in terms of its ability to provide consistent valve functionality with repeatable operation and no risk of failure.

Due to the volume of parts needed for subsea tress, TechnipFMC rely on 2 OEM's to manufacture the coil springs for the respective valves. The OEM's utilise the same material grade, however this can be supplied from 3 raw material mills.

Throughout the initial development of the respective coil spring, TechnipFMC has discovered that the desired metallurgical properties requirements have not been consistently met. This is specifically in relation to the AISI 4161H material that has been supplied via different raw material mills and coil spring Original Equipment Manufacture’s (OEM's) who operate different methods of manufacture to achieve the required design intent of the fully heat-treated material.

The initial development programme established that the required tensile properties could not be consistently met, with poor ductility and low yield and UTS values exhibited by the material. This was further investigated, with metallurgical analysis

discovering that the material did not contain a homogenous microstructure, but one that revealed a mixture of elongated bands and a matrix. The initial work also established the effect of changing bar sizes and material type; with increased diameters producing more banding and a greater hardness delta between the two phases within the microstructure (band and matrix).

To address this problem, TechnipFMC has initiated a pre-study to determine the fundamental properties of the AISI 4161H material type, in the Hot Wound / Coiled form. This is considered paramount, as current industry standards do not mandate any testing or material characterization, other than minimum metallurgical assessment (chemical composition / hardness), which is conducted on samples of raw bar processed at the same heat treatment conditions of the hot formed coil.

These requirements and level of governance are considered inadequate by the author, as they do not fully consider the extent of metallurgical and mechanical properties needed to ensure a critical product will operate at the required design conditions and service environment.

To date detailed investigation and testing, has shown that that a continuous cast material procured to the requirements of AISI 4161H, can exhibit variability in terms of resultant mechanical and metallurgical properties. This is specifically in relation to the tensile properties and microstructure, which has shown to change when different bar diameters are manufactured and exposed to different hot forming conditions, such as forging (forge reduction ratio). There are several potential factors that can induce variability, however this information is not readily available, or recognised by the industry or controlling bodies. The coil spring industry and controlling specifications do not consider variability in terms of microstructure, as they are more focused on physical testing such as surface hardness, as the controlling output to ensure material repeatability. Therefore, limited knowledge exists within the industry, on how variable the material can be, and the effects this can have on the properties of the final fully heat-treated coil spring.

1.3 Aim and Scope of Research

The aim of this research programme is to determine and characterize the key properties of a hot wound AISI 4161H material, and determine the effects of various heat treatment conditions to control and achieve the desired design of the coil spring used for critical subsea applications. This work will also be used to enable engineers to determine the limitations of the coil spring material, and help develop future industry standards that properly align with the actual manufactured product.

To meet the desired objective, the scope of the research includes:

1. Original work and conclusions already reported by the author and TechnipFMC
2. Design rationale of a coil spring
3. Operational conditions, considerations and external factors
4. Product limitations and failure mechanisms
5. Raw material - how is it made / considerations
6. Method of Manufacture of the coil spring
7. Effects of Heat Treatment
8. Design of Experiments - conduct experimental investigation into the mechanical and metallurgical properties for various bar sizes at the fundamental and extremities of the material heat treatment processing window
9. Discuss the experimental results in conjunction with the literature research
10. Detail the conclusions and recommendations of the complete work programme.

1.4 Outline of Thesis

The Thesis consists of 8 chapters.

Chapter 1 indicates the general objectives, background overview, and problem statement, which is driving the need for the research detailed within this thesis.

Chapter 2 describes the design and operating considerations of a coil spring and subsea valve.

Chapter 3 presents the initial work completed by the author and TechnipFMC; detailing the areas of concern regarding the variability in metallurgical properties, which was evident during the New Product Introduction (NPI) stage of development.

Chapter 4 describes the literature review of the related research.

Chapter 5 presents the experimental methodology / DoE, and details the metallurgical investigation and assessment of the heat treatment trials.

Chapter 6 reviews the results of both the literature and experimental research programme, detailing the reasons why material variability is exhibited.

Chapter 7 describes the effects material variability has on the coil spring functionality.

Chapter 8 summarizes the thesis, and provides conclusions and recommendations along with suggestions for future research.

2 COIL SPRING DESIGN CONSIDERATIONS

2.1 Introductory remarks

This chapter describes the key design considerations of a coil spring, in conjunction with the operating conditions related to subsea applications. It also states the important variables that need to be observed when developing this product type from design to full manufacture.

2.2 Terminology

The following terminology is used throughout to describe the design philosophy.

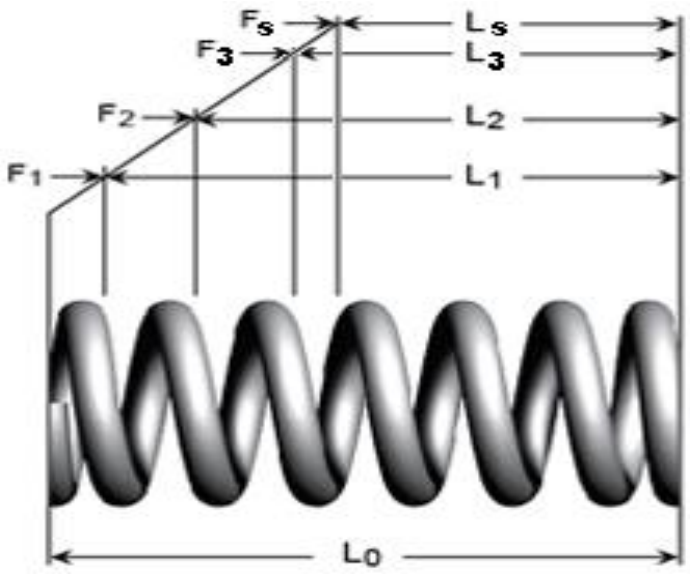

Figure 2-1: Coil Spring Deflections and Loads [1]

Table 2-1: Abbreviations

Abbreviation	Description
L0	Free Height/Length: The length of the spring when no load is applied
L1	Maximum Working Height/Length: The length of the spring at its longest position while in service inside the actuator
L2	Crack open / Pinch point Height/Length: The length of the spring when compressed to the point where the valve is at the crack open/pinch point
L3	Minimum Working Height/Length: The minimum efficient working length of the spring is designed to be where the valve is open (actuator fully stroked)
Ls	Solid Height/Length: The theoretical length of the spring at maximum compression where the coils of the spring are in contact.
F1	Preload: The minimum load produced by the spring in operation, it occurs at the maximum working height of the spring

F2	Pinch Point Load: The load produced at the pinch point height
F3	End Load: The maximum load produced by the spring in operation, which occurs at the minimum working height
Fs	Solid Load: The theoretical maximum load produced by the spring when fully compressed so that all coils are in contact

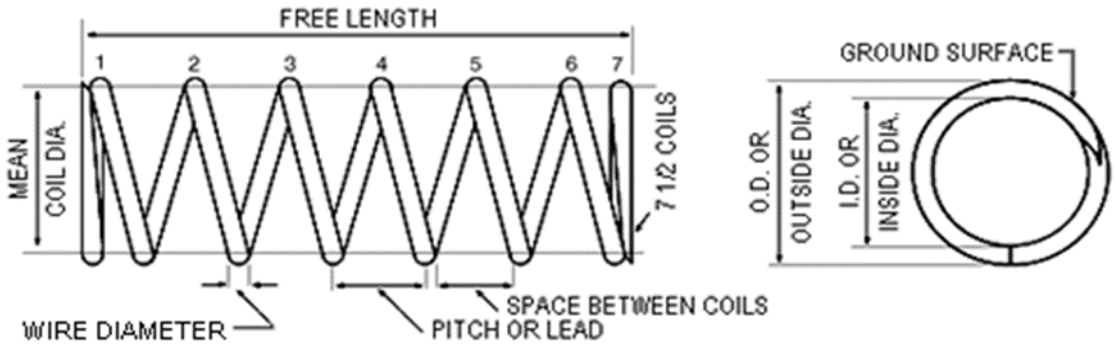

Figure 2-2: Coil Spring Definitions [1]

Table 2-2: Definition of Terms

Definition	Description
Wire Diameter	Diameter of the drawn bar from which the spring is manufactured
Free Length	Measured length of the spring in its "free" state, i.e. when there is no compressive load acting on it
Pitch	Mean distance between the centres of adjoining coils.
Ground Surface	The bearing area of the ends of the spring. Typically, a "3/4 grind" is specified for hot coiled springs - this refers to roughly 3/4 of the circumference being ground flat.
Theoretical Total Available Deflection	The distance between the free height of the spring and the theoretical solid height (= L0 - Ls).
Sa - Residual Range	Sum of all the minimum allowable gaps between adjoining active coils for the smallest permitted spring length.
Number of Active Coils	The number of coils which deflect during loading of the spring and contribute to the spring rate.
Number of Inactive Coils (Dead Coils)	The number of coils which do not deflect during the loading of the spring and therefore do not contribute to the spring rate. Inactive coils are usually the coils at either end of the spring, however dead coils can be introduced in the middle of the body of the spring to aid in the prevention of tangling. Typically for closed and ground ends of a hot coiled spring, the number of inactive coils is 2.
Total Number of Coils	The sum of the active and inactive coils. This is measured over the full length of the wire (or bar) from tip to tip including fractions of a coil.

2.3 Design and Coil Spring Arrangements

The main design objective of the coil spring(s), is to overcome the minimum hydraulic head of bore pressure to close the valve. This is achieved through the retained spring force / load, and depends on factors such as water depth and the pressure of the subsea installation. Each of these attributes along with the available space within the actuator (Figure 1-2) will dictate the geometry (Figure 2-2) and number of coils required for the specific application. Because the application is displacement dependent, required loads are always defined at specific spring heights with respect to a fixed datum, rather than deflection from free height (Figure 2-1). Therefore, the required spring performance determines the coil spring arrangement, size and material type.

In a single arrangement (Figure 1-2), one coil spring is utilised to meet the load and geometry requirements. However, within a nested arrangement (Figure 1-3) two or more springs are arranged coaxially, i.e. different sizes of springs are placed inside another concentrically on a common axis to create a parallel spring arrangement. This allows the spring designer to optimize the available volume for springs and hence give a greater load for a given deflection than for a single spring in the same envelope. Nested coil arrangements may be necessary in certain circumstances, such as:

- Where a greater load is required from a given envelope, which cannot be provided by a single spring.
- Where the design stress of a spring is too high - the design stress can be reduced by adding another spring in parallel to share the load.
- To reduce the risk of buckling of a long single spring by reducing the overall length, through use of an additional coil

2.4 Operating / Performance Requirements

For a Fail Safe Close (FSC) Valve, the actuator spring (or springs) must overcome the sum of all the forces within the valve and actuator, and cause the valve to close as intended. With respect to Figure 2-1:

- The preload force (F1) exerted by the spring(s) at preload height (L1) must be sufficient to overcome these loads.
- The load at Pinch point height (L2) must be sufficient to overcome the pinch point load (F2).
- The maximum load (F3) at the end of the stroke (minimum working height L3) must not exceed the hydraulic control capabilities.

The actuator coil springs are required to operate for 25 years subsea, and must be capable of a minimum 10,000 cycles without suffering premature failure or spring load relaxation. Actuators are also required to operate in any orientation. For this reason, coil springs require physical guidance and support at both ends. The effect of gravity must also be considered to eliminate any contact with the actuator housing.

In addition, the key operating conditions of the oil field must also be met, with no respective loss of actuator valve functionality:

- Water depth of 300 - 10,000 feet (91 - 3048m)
- Operating pressure of 5000 - 20,000 psi pressure
- Operating temperature of 4°F - 400°F (-15°C to 204°C)

2.5 Dimensional Tolerances and Stability

The spring must be sized, considering radial expansion under compression as well as tolerances, such that it does not come into contact with any other internal components. The free length (Figure 2-1) shall not change significantly after the pre-setting operation.

Actuator Coil springs must remain dimensionally stable during operation. Deviation from the original envelope after many cycles could cause interference or change to the valve signature (load response achieved by the coil spring).

2.6 Allowable Stress Limits

The design utilises a maximum allowable percentage of the UTS for a given material, to set the maximum stress limit for a coil spring. For a low alloy steel, which is pre-set during manufacture, the IST recommend that Springs shall be designed to have an upper uncorrected stress limit no greater than 56% of the UTS of the material at

the theoretical solid height [2]. Higher stress limits are not recommended because calculations used for spring designs do not take into consideration the full components of stress acting on the coil spring (Chapter 7).

The UTS of the material has a major influence on the resultant design of the coil spring, which will influence the overall performance in terms of resultant load and stress limits. For the design requirements and operating conditions, the UTS has been set at 210 Ksi for TechnipFMC applications [1].

2.7 Other Design Considerations

All manufactured coil springs must undergo a pre-setting operation, which is key to the functionality of the component in service. Pre-setting is used to increase the elastic range of the material by setting the coil beyond the maximum working height (L3 position in Figure 2-1). The IST recommends that the pre-setting height should set at a minimum of 90% of the available deflection [2]. This ensures that the coil spring can operate within the pre-set height without the risk of subsequent load loss.

2.8 Concluding Remarks

The design requirements and operating environment need to be fully understood when developing a coil spring as a subsea failsafe mechanism. The harsh operating conditions and component criticality demand that failure in-service is not an option. The coil spring must achieve the required tensile properties, in order to enable the material to retain its spring load throughout the functionality of the valve. The integrity of the material is therefore of the utmost importance, considering the coil spring is held at the highest stressed condition (valve fully open L3 position) for most of its subsea life (Figure 2-1).

Therefore, these fundamental points are used and considered throughout this thesis, and by engineers who are required to design and manufacture coil springs for this respective application.

3 INITIAL AUTHOR AND TECHNIPFMC WORK

3.1 Introductory remarks

This chapter describes the initial work completed by the author and TechnipFMC; in terms of the technical challenges faced with the material development of a new valve actuator design. The work detailed within, lists the issues related to changing from traditional industry subsea failsafe return mechanism (Disc Springs), to a single load displacement technology (Coil Springs). Throughout the chapter reference is made to the both company and industry requirements, including the governance of mechanical / metallurgical properties. The information presented also demonstrates why the work completed within this thesis was required, and hence the creation of the problem statement described in Chapter 1.

3.2 Background

Traditionally within the oil and gas industry, and companies such as TechnipFMC; Disc Springs have been utilised as the principal method for the return stroke and failsafe operation for subsea valves, reference Figure 3-1.

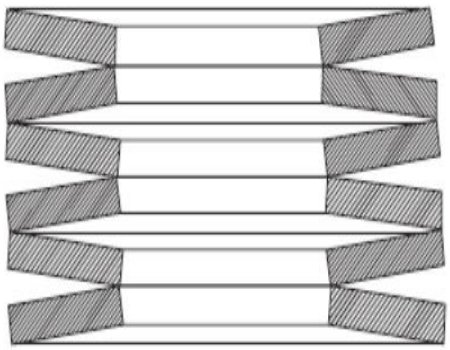

Figure 3-1: Example of the Disc-Springs layout arranged in parallel [4]

In 2014 TechnipFMC changed its design strategy, and decided to look at alternatives that would operate within a High Temperature High Pressure environment (HPHT). This drive was to meet customer requirements of deeper and more difficult oil extraction conditions. Hence the company decided to select the coil spring as its new failsafe valve return stroke mechanism.

The design characteristics of both mechanisms are different, with disc springs delivering the required load using multiple discs in either series, parallel or a combination of both. This orientation relies of each individual disc delivering a set amount of travel (deflection) and resultant load. Whereas the coil spring is required to deliver the complete load and deflection to close the respective valve. Both systems however, have their advantages / disadvantages. These include:

- Disc springs
    - Operate at extremely high stress levels – up to 120% of material yield stress, due to deflection loads applied to meet the required displacement
    - Have redundancy within the system. If several disc springs suffer radial cracking in service, the valve will still function
- Coil springs
    - Dependant on design, will operate at relatively lower stresses – up to 56% of the materials UTS
    - Have no redundancy. If the spring suffers failure (a material through-thickness fracture) the coil shall become redundant with complete loss in functionality.

The initial work scope therefore, was to specify a material for coil springs that would operate under HPHT applications.

3.3 Initial Material Investigation

The purpose of the initial material research was to develop coil springs for the companies' new portfolio of HPHT application valves. This included two valves, one with a single coil and the other with a dual nested arrangement.

- 2 inch 10K application - single coil
- 5 inch 10K application - dual coil

The main differences in terms of design is the respective raw material and the bar diameters utilised; reference Table 3-1.

Table 3-1: Valve Portfolio Initial Development

Valve Type	No of coils	Coil bar diameter	Coil material
2 inch bore 10ksi Pressure	1	1.687 inch (42.8mm)	AISI 51B60H
5 inch bore 10ksi Pressure	2	Inner - 1.375 inch (34.9mm)	AISI 51B60H
		Outer - 2.875 inch (73.0mm)	AISI 4161H

To validate the required design intent (mechanical / metallurgical properties), the industry governing body (ASTM) [54 - 58] was consulted. However, after a detailed review, it was clear that the governance standards were not adequate for critical components such as coil springs. This was evident through the consultation of the key fundamental specifications [54 - 58], which state that minimum metallurgical testing is required on a sample bar.

In summary, basic testing such as Hardness, Grain size determination, Chemical composition & Surface decarburization is the only test / qualification criteria required to ensure a product with no redundancy will survive 25 years subsea without failure. Due to the lack of governance and knowledge in the mechanical / metallurgical properties of an actual coil spring; this initiated the necessity to develop (by the author) a new set of qualification / testing criteria for fully manufactured coil springs. The testing criteria developed, is compared to current industry standards within Table 3-2, Figure 3-2, and Figure 3-3.

Figure 3-2: Example of sample bar required by ASTM standards

Table 3-2: Developed Conditions v ASTM Requirements

Developed requirements	Coil Spring	
Test type	***Location***	***Number of tests***
Visual assessment	All surfaces	1 per coil spring
Tensile	First full coil from each end plus mid-coil position	3 per coil spring
Hardness	HRC on each end of tensile test specimen	6 per coil spring
Surface Hardness	Machined ends & First full coil from each end plus mid-coil position	5 per coil spring
Through-thickness Hardness	Taken from a full a diameter slice at the first full coil from each end plus mid-coil position	3 per coil spring
Material Grain size determination	First full coil from each end plus mid-coil position	3 per coil spring
General Microstructural evaluation	First full coil from each end plus mid-coil position	3 per coil spring
Microstuctural Banding evaluation	2nd full coil poistion - longitudinal section at 5mm below surface, mid-radius & core	3 per coil spring
Surface Decarburization assessment	First full coil from each end plus mid-coil position	3 per coil spring
Material Macro Inclusion assessment	2nd full coil position	1 per coil spring
Quenched bar assessment - Grain size & Hardness	Additional bar quenched at the same conditions as coil spring	1 per Heat of Material
Chemical Compositon	Supplied by raw material Mill	1 per Heat of Material

ASTM requirements	Bar only	
Test type	***Location***	***Number of tests***
Visual assessment	Na	Na
Tensile	Na	Na
Hardness	Na	Na
Surface Hardness	On bar surface	1 per Heat of Material
Through-thickness Hardness	Na	Na
Material Grain size determination	Micro-section	1 per Heat of Material
General Microstructural evaluation	Na	Na
Microstuctural Banding evaluation	Na	Na
Surface Decarburization assessment	Micro-section	1 per Heat of Material
Material Macro Inclusion assessment	Na	Na
Quenched bar assessment - Grain size & Hardness	Additional bar quenched at the same conditions as coil spring	1 per Heat of Material
Chemical Compositon	Supplied by raw material Mill	1 per Heat of Material

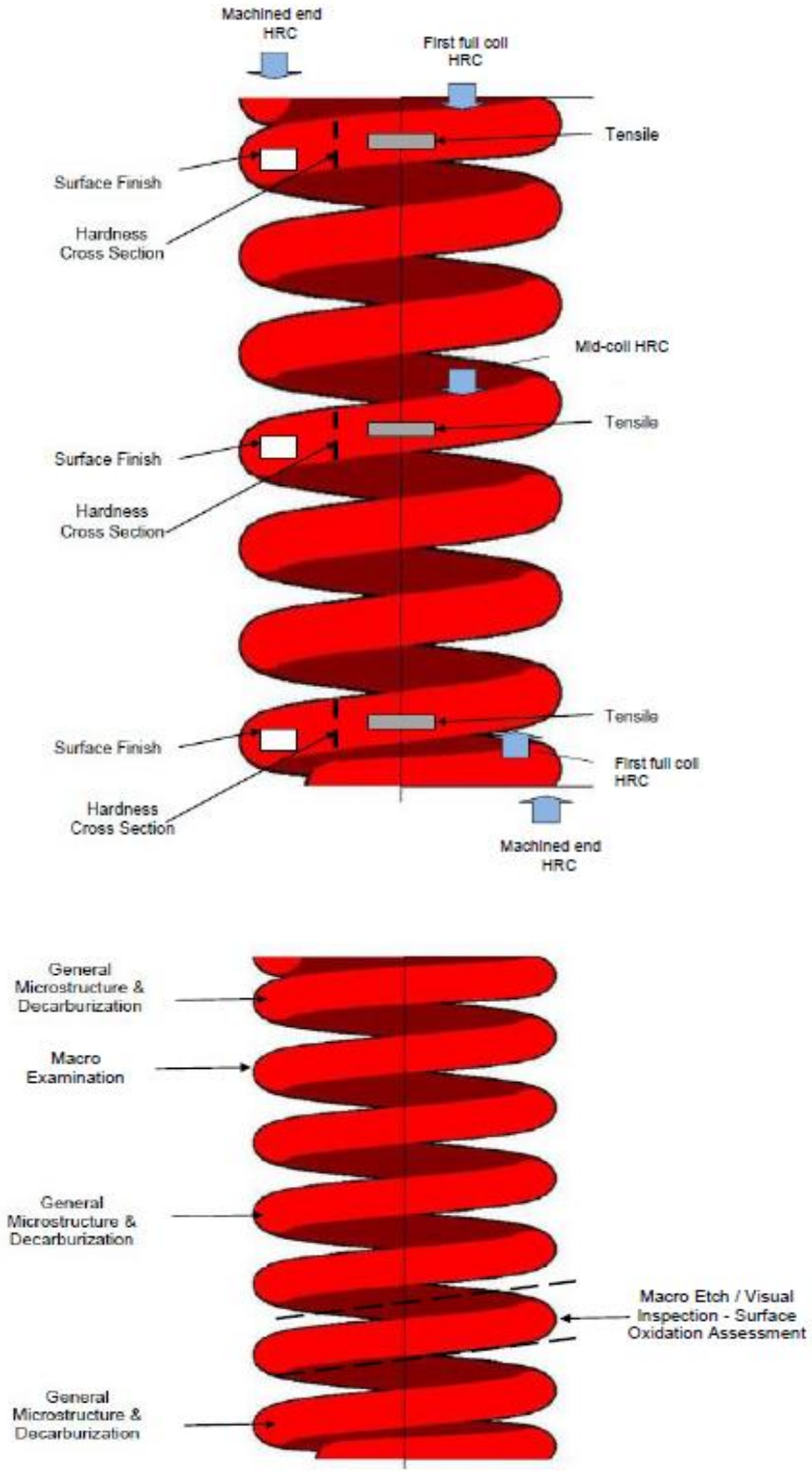

Figure 3-3: Metallurgical Sampling Plan Developed for Coil Spring Qualification

The developed requirements also take into consideration the life-cycle operations of the respective valve. During standard operation, a subsea valve will function over 600 cycles between the L1 & L3 position (minimum & maximum load conditions) within a 25-year time frame. Therefore, to fully understand the effect of operational cycling, and to ensure full material integrity, the development requirements / testing criteria detailed within Table 3-2 was repeated after 10,000 cycles.

These fundamental test requirements were set to fully understand the mechanical / metallurgical properties of the TechnipFMC coil spring.

3.3.1 Initial Material Investigation Results

The initial work scope assessed the coil springs detailed within Table 3-1, which consisted of the manufacture of 30 coils springs (10 x 3 bar sizes); and the full metallurgical assessment of 15 of the total produced.

The AISI 51B60H material coils, namely the 1.375 and 1.687-inch (34.9 and 42.8mm) diameter bar, exhibited uniform / repeatable results, which met the design intent and minimum mechanical properties required.

The AISI 4161H material however, which is made from 2.875-inch (73.0mm) diameter bar, produced inconsistent results in terms of meeting the material tensile properties (220Ksi UTS / 200Ksi YS / 7% El / 25% RoA); reference Figure 3-4.

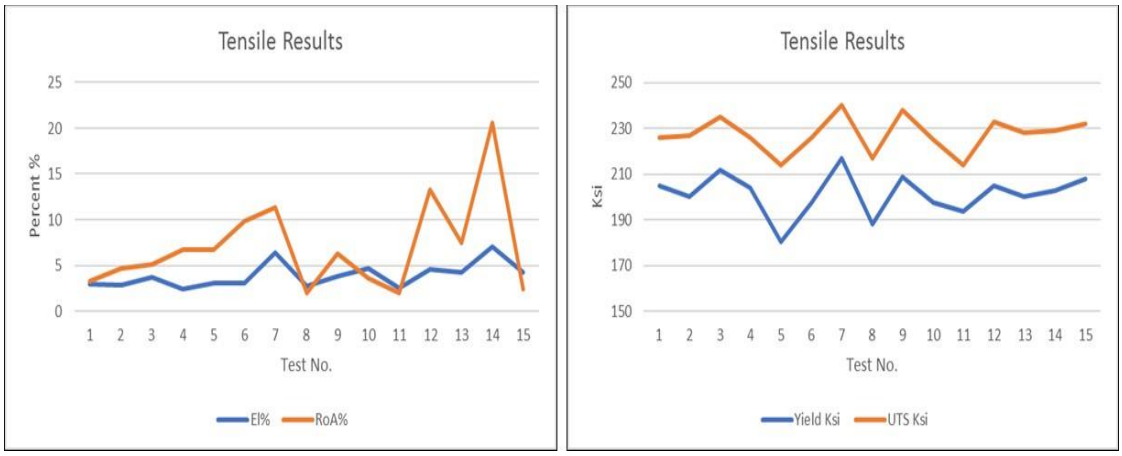

Figure 3-4: AISI 4161H Coil Spring Tensile Results

To understand why the 2.875-inch (73.0mm) diameter coils exhibited such erratic results, microstructural comparisons were made to the AISI 51B60H material parts. The analysis established that the material was not homogenous, and that the three bar diameters exhibited different levels of banding within the metallurgical matrix. The banding appeared as elongated zones with a microstructure that was different from the main material matrix. These zones also ran parallel with the rolling direction of the bar (longitudinal). In addition, the work also recognized that as the bar size increased in diameter, the forging reduction ratio (established by the raw material mill) reduced; in conjunction with an increase in the amount of apparent banding.

This breakthrough for TechnipFMC was further substantiated, when the 2.875-inch (73.0mm) parts were reproduced using material from a different Mill (Mill 1), which utilised higher reduction ratios. The original material (Mill 2) was found to have a forging ratio of 5.3:1, compared to the alternative (Mill 1), which was 21.1:1.
Ironically this change in raw material manufacture (Mill 1), produced more consistent metallurgical properties, which met the design requirements for full valve operation, reference Figure 3-5. In addition, key fundamental differences were observed, with the exhibited banding within the two sets of microstructures, which was greater with the material forged at a ratio of 5.3:1. These differences were further clarified when hardness points were taken in both the matrix and banded material at the 10% thickness location (0.2875-inch / 7.3mm). The resultant values had shown that higher reduction ratio material, exhibited a significantly lower average hardness delta (difference between banded zone & matrix) than that of the material produced using a ratio of 5.3: 1.

- 5.3:1 forge ratio AISI 461H material - Hardness delta 15.8 HRC
- 21:1 forge ratio AISI 461H material - Hardness delta 2.0 HRC

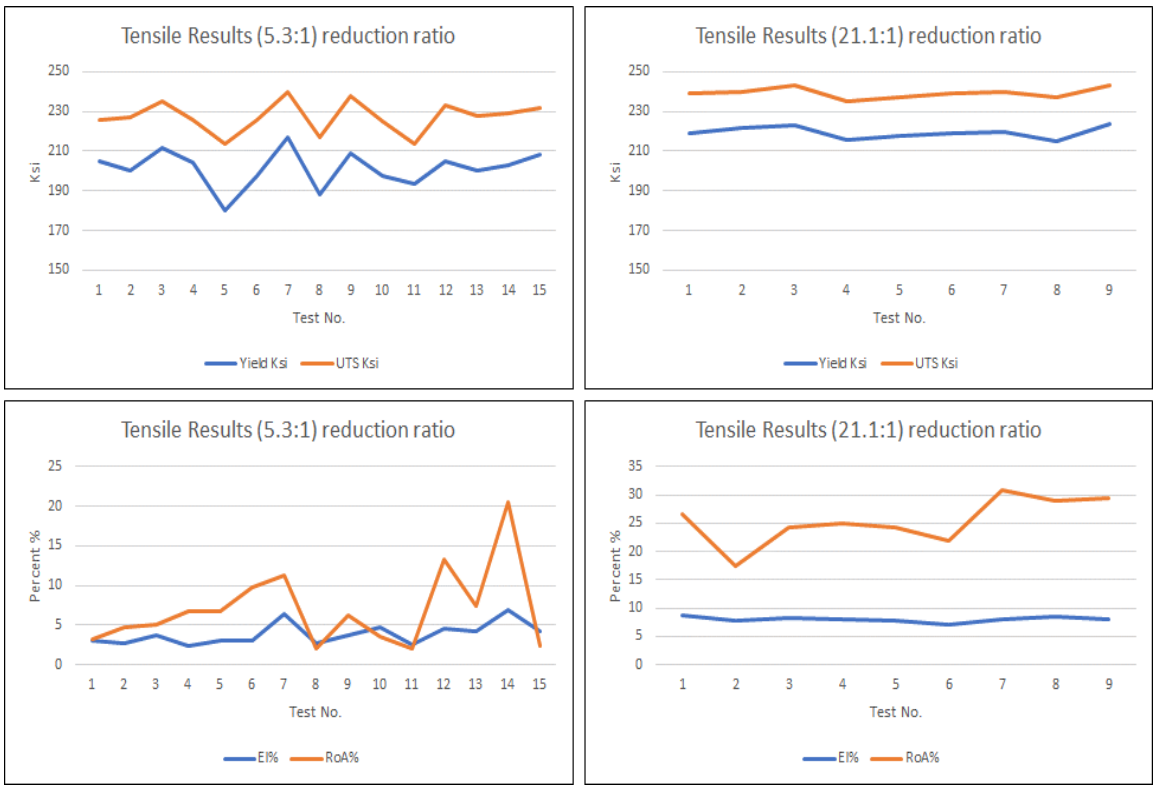

Figure 3-5: Tensile Property Comparison of the AISI 4161H Material (Forge Ratio 5.3:1-Left versus Forge Ratio 21:1-Right)

To capture this latest information, the company wrote its own governing specification. This mandated a minimum forging reduction ratio of 10:1, for all materials regardless of bar diameter; and a maximum allowable hardness delta of 5 HRC between microstructural bands and matrix. The premise of these new specification requirements was to ensure there would be an elevated level of process control; both with the in-coming raw material from the Mill (1 or 2) and at the OEM who conduct the subsequent hot coiling and heat treatment operations.

3.3.2 Phase 2 - Material Investigation Results

Although it appeared that the issue of the unusual tensile property behaviour had been identified, in conjunction with a respective governance to control metallurgical variability; the banding continued to be present.

This was two-fold:

- When the coil spring OEM started using different heats of material (with the high forging reduction ratio) for high volume production.

- When another coil spring OEM was asked to manufacture, the same part using the AISI 4161H material from 2 different Mills (1 & 3)

Figure 3-6 demonstrates the differences the two coil spring manufacturers experienced when processing the material supplied by Mill 1, with a similar forging reduction ratio. It was expected that with the work conducted during the initial development phase, this situation and set of results should not occur. However, the mechanical properties achieved using OEM 1, were far superior that that of OEM 2.
This was especially apparent with the resultant through-thickness hardness, yield stress and ultimate tensile strength values. OEM 1 produced a linear uniform hardness trend across the coil spring sectional thickness, whereas OEM 2 exhibited a consistent decline in values from the surface to the core (47-39 HRC). There were also marked differences in the ultimate tensile strength and yield stress, with average respective values of 200 and 170 Ksi achieved compared to 240 and 220 Ksi produced by OEM 1.
The variability was also exhibited when each OEM processed the AISI 4161H material from different Mills (2 and 3), utilising the same methods of hot forming and heat treatment (OEM 1 - Mill 1 and 2 & OEM 2- Mill 1 and 3).

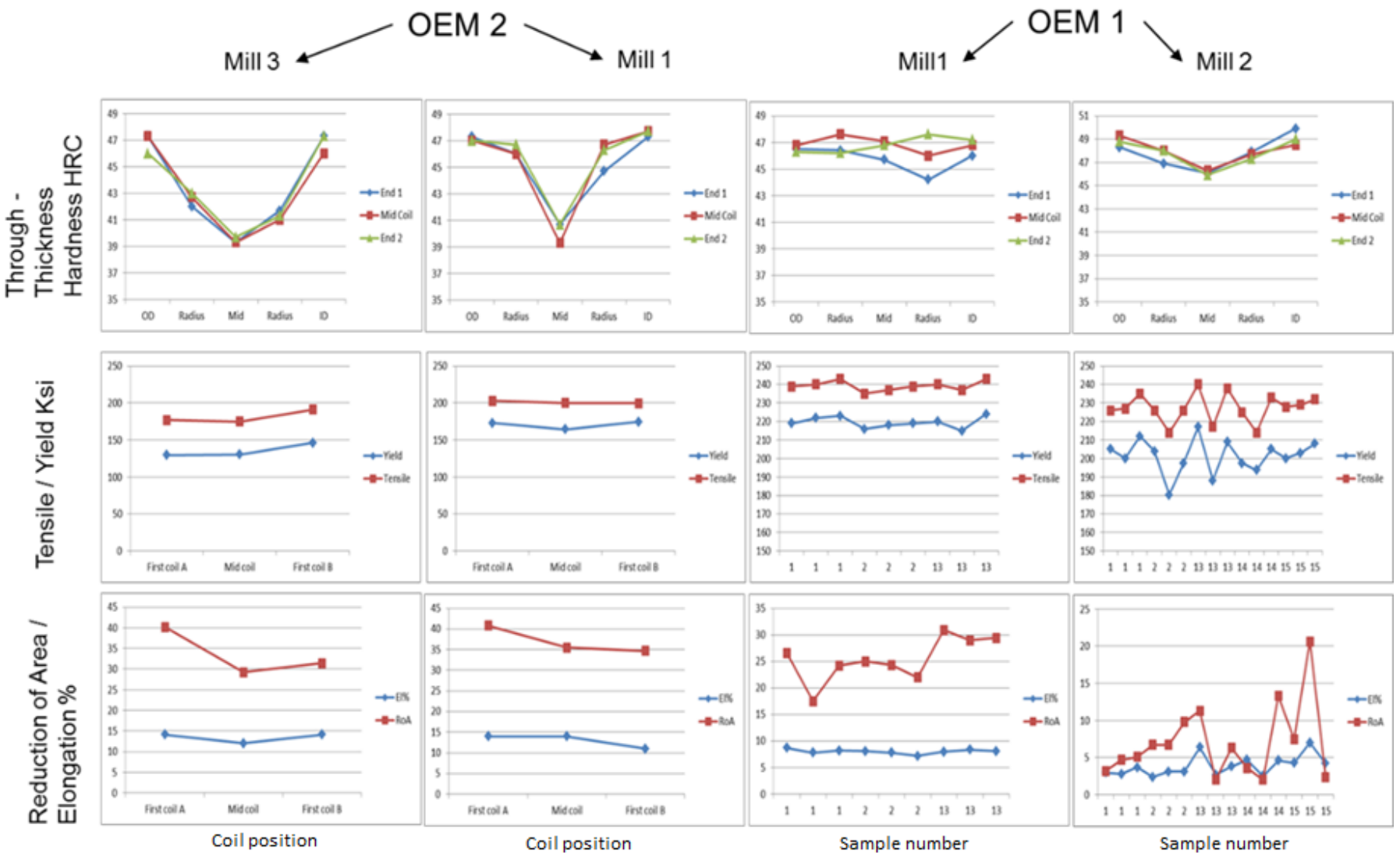

Figure 3-6: Metallurgical Property Comparison of Material Supplied from Different Mills, which has been processed by two separate OEM's

3.3.3 Phase 3 - Material Investigation Results

The purpose of the final phase of work, was to determine the effect of using three Heats of material from a new Mill source; separate from those identified within phases one and two. Mill 4 was selected, as they had offered TechnipFMC a material, which had a significantly low hardness delta (banded phase - minus the matrix phase) throughout the complete 2.875-inch (73.0mm) cross-section (sub-surface, mid-radius and core - centre). This was of great interest, as the microstructural phase hardness delta was only ever measured near the surface of the material, and a new source was stating that the governance requirement of <5 HRC could be met. In addition, Mill 4 had subsequently substantiated this finding by conducting analysis on seven (7) different Heats of material using the same heat treatment conditions - see Figure 3-7.

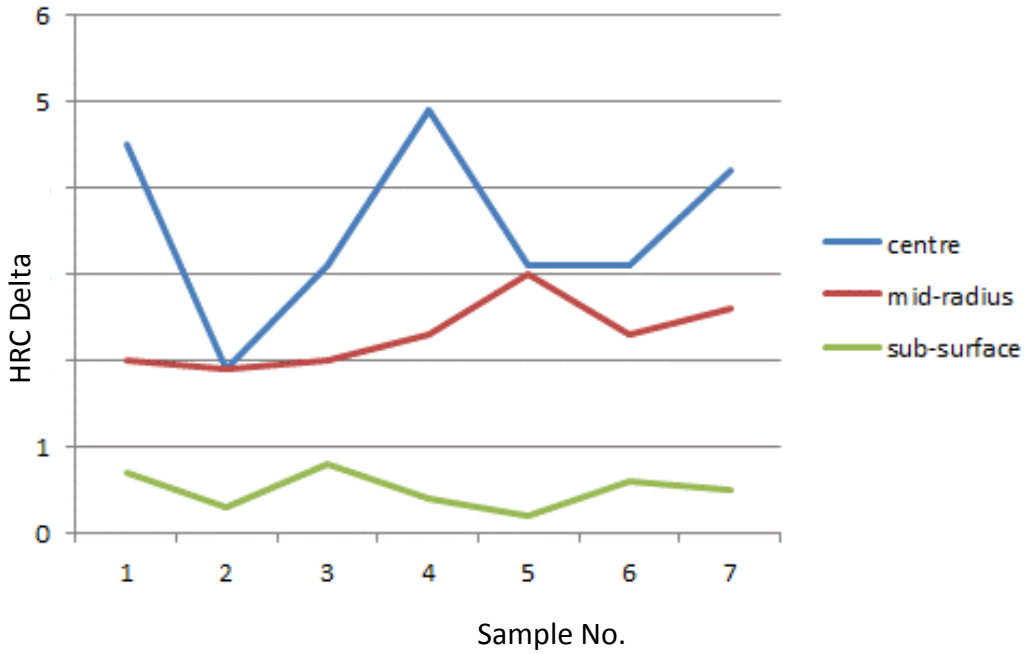

Figure 3-7: Metallurgical HRC Delta Comparison

However, the results were not linear as expected, with the actual coil springs that were manufactured using three of the material heats from new Mill source.

Testing had confirmed that the tensile properties failed to consistently meet the 220 Ksi UTS and 200 Ksi YS minimum requirement. Instead average values of 210 Ksi UTS and 190 Ksi YS were achieved, which were taken from a data set of over 40 tensile test results.

To understand whether these respective requirements were realistic for the AISI 4161 H material, a technical review of both BS EN 10089 [61] & ASM Engineers Handbook [50], was completed. This review confirmed that materials with similar chemical composition and heat treatment conditions, should achieve a resultant UTS of 210 - 254Ksi. In addition, the technical review established that there were no yield stress requirements, which was in line with ASTM (A29 and A689) governing specifications for the AISI 4161H material.

Based on this criterion, and the results achieved for the extensive tensile test study, is was decided to lower the tensile requirements from 220 to 210 Ksi. Further, it was agreed internally by TechnipFMC, that the resultant yield stress of the material was not a design requirement, and as such should be removed as a specification requirement.

In addition to the tensile test results, testing was conducted on microstructural specimens, to determine the HRC delta between the bands and material matrix. This analysis was completed on the same three material heats supplied from Mill 4, with both full and partial coils (known as wraps) assessed at the OD & ID locations - Reference Figure 3-8.

The results demonstrated, that unlike the initial assessment conducted by the Mill - Reference Figure 3-7, a maximum hardness delta of 12 HRC was achieved for the coiled material. Compared to the initial set of results, this is an increase of 11 HRC for the same test location.

When comparison was made to the initial testing conducted by Mill 4, it was established that the trials were conducted on a 1-inch slice of material, which was austenitised and tempered at 1700°F & 800°F (927°C & 427°C) respectively. Thus, indicating that different heating and cooling conditions could indeed vary the effect of the hardness delta experienced within the respective phases within the microstructure.

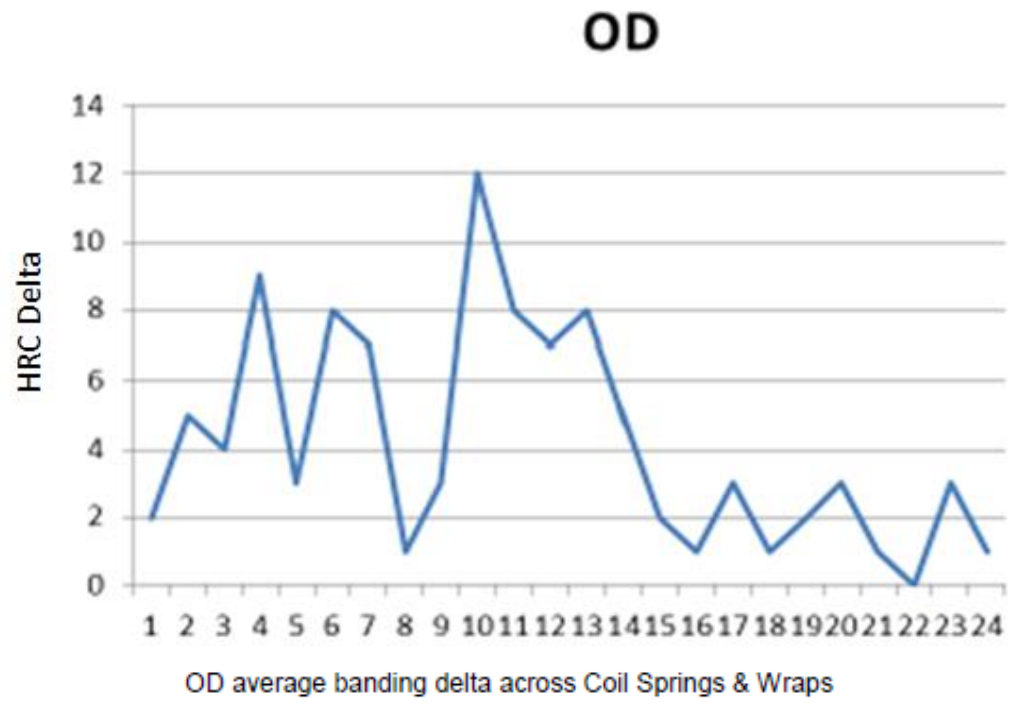

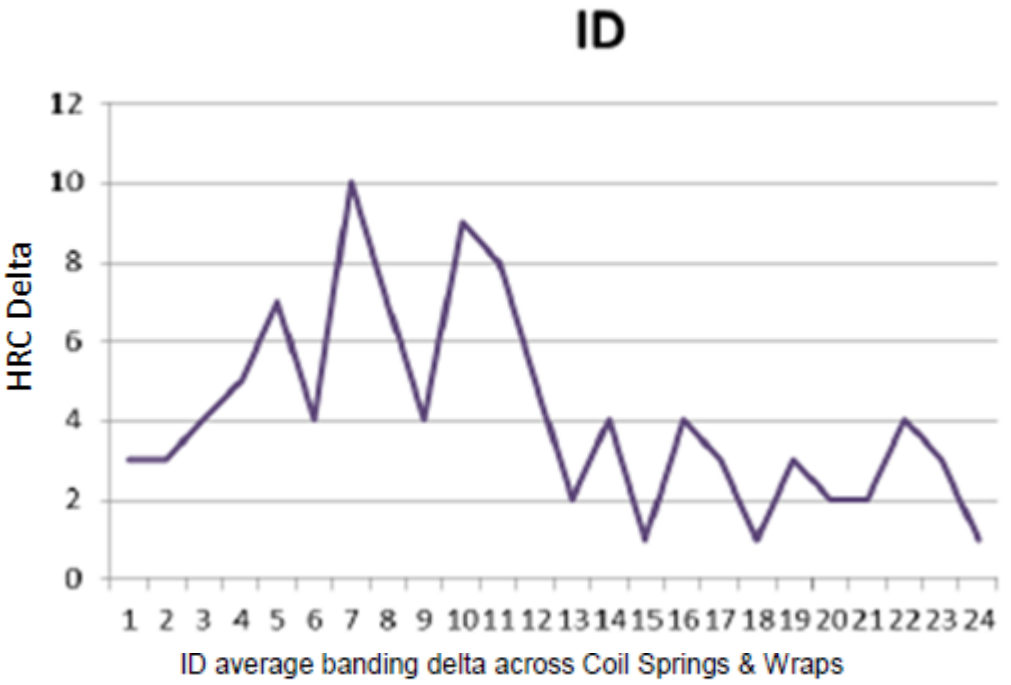

Figure 3-8: OD & ID Average HRC Phase Delta

3.4 Summary Remarks

The initial author and TechnipFMC work study, has established the rationale for a design change, for the valve return stroke mechanism. It has also confirmed that the industry governance in terms of material acceptance / testing for subsea applications was inadequate, especially for coil spring components, which operate under HPHT conditions with no redundancy. Subsequently this has driven the need to develop a new set of test criteria, which fully determines and substantiates both the mechanical / metallurgical properties of the coil spring in the fully heat-treated condition.

The investigation has also established that the smaller diameter coil springs made from the AISI 51B60H material, exhibited consistent metallurgical properties in terms of tensile and microstructural properties. However, the initial work found that the 2.875-inch (73.0mm) AISI 4161H tested parts exhibited unexpected mechanical properties, which was directly related to raw material forging reduction ratio and the amount of banding present within the resultant microstructure.

Subsequent testing established and assumed that this problem could be resolved by governing the respective material properties, by stipulating a maximum HRC delta for resultant microstructure. However; further tests involving alternative material heats and different coil spring OEM's, established that the AISI 4161H material exhibited metallurgical variability when processed / heat treated using similar heat treatment and manufacturing conditions. This variability has driven TechnipFMC to change its current design criteria by reducing the required UTS of the 2.875-inch (73.0mm) material to a minimum of 210 Ksi.

More importantly, the initial findings have established that there is a necessity for both industry and governing bodies to fully understand how to control the variability exhibited within the AISI 4161H material. Therefore, the problem statement and research scope detailed within this thesis is fully justified.

4 LITERATURE REVIEW

4.1 Introductory remarks

This chapter details the results from both an industrial and academic literature review of the material and the respective hot forming processes used to manufacture coil springs for subsea applications. The work detailed within initially establishes the manufacturing methods utilised, followed by a detailed review of the metallurgical processes that have a direct influence on the resultant material properties.

4.2 Method of Manufacture

There are several different methods used to manufacture hot wound coil springs for industrial applications; however, in simplistic terms materials such as AISI 4161H follow the process represented within Figure 4-1.

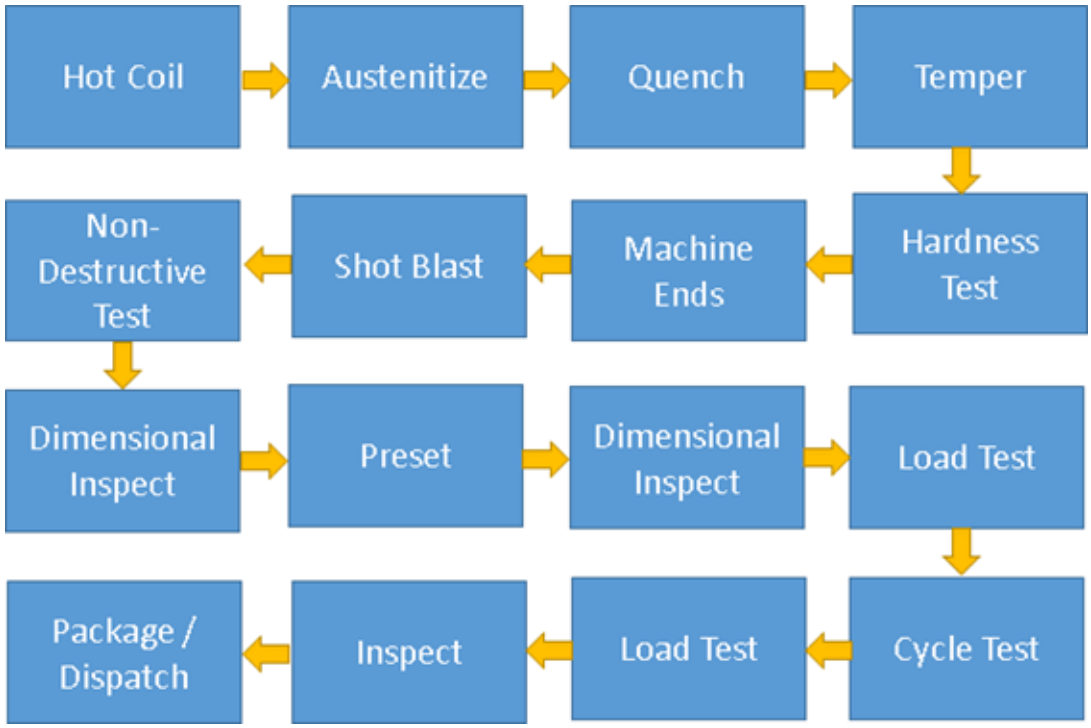

Figure 4-1: Typical Manufacturing Process for a Low Alloy Steel

In general terms, the material is supplied in a bar form, which is subsequently heated in a furnace to a temperature of approximately 1700-1800°F (926-982°C). The

material is then removed manually or automatically ejected onto a mandrel, where the bar is formed into a coil spring - see Figure 4-2.

Figure 4-2: Hot Coiling of Low Alloy Steel

Once formed, the coil spring is immediately quenched by transferring the material into a tank of a specific cooling medium, such as oil. The austenitising temperature range is generally between 1500-1600°F (816-771°C). This process step is then followed by a tempering operation, where the coils are held in a furnace between 750-850°F (399-454°C) for a set duration, which is dependent on the bar size (diameter) and desired resultant HRC and UTS.

The remaining process steps have no direct effect on the part, as these are used as controls to ensure the material meets the desired design intent in terms of return load, surface hardness and dimensional stability. Other than the pre-setting operation, which increases the elastic range of the material beyond the minimum working height (L3 position Figure 2-1); steps 1 to 4 (Figure 4-1) are the key and fundamental processes that influence mechanical / metallurgical properties.

4.3 Coil Spring Material

The raw material used to manufacture coil springs for Oil / Gas subsea applications is specified within ASTM A29 [54], A304 [57], and A689 [58]. In general, the material selected is considered as a high carbon / high strength hot rolled alloy bar, which exhibits excellent through thickness hardenability. When the material is designated with the letter 'H', this notates that the steel grade must satisfy "end-quench hardenability requirements" of ASTM A304 and A689.

The material selected by TechnipFMC is based on the requirements of AISI 4161H [54] [57], except for both the Phosphorus and Sulphur composition, which have been reduced from the current industry requirement of (P-0.035% / S-0.040%) to (P-0.025% & S -0.015%) respectively. This company stance was adopted to ensure a cleaner bar material would be procured, which would reduce the risk of the formation of impurities and subsequent segregation during the raw melting process.

4161H	
Carbon	0.55 - 0.65
Manganese	0.65 - 1.10
Phosphorus, max	0.025
Sulfur, max	0.015
Silicon	0.15 - 0.35
Chromium	0.65 - 0.95
Molybdenum	0.25 - 0.35

Figure 4-3: Material Composition of the AISI 4161H material [5]

4.3.1 Raw Material Manufacture

4.3.1.1 Melting

The raw material is made by the electric arc melting process, which is followed by a separate degassing / refining operation. Dependant on the mill, secondary melting using electro-slag or vacuum re-melting may also be incorporated. The molten material is then subjected to the continuous casting process, where the liquid steel is transferred into a Tundish. Depending on the Continuous Caster type, the Tundish may supply one or multiple strands [6] Reference Figures 4-4 & 4-5.

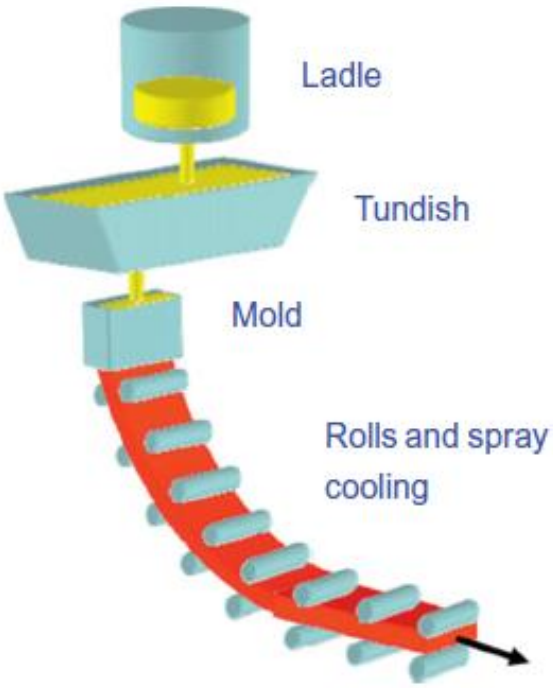

Figure 4-4: Schematic Representation of a One Strand Curved Continuous Casting Process [6]

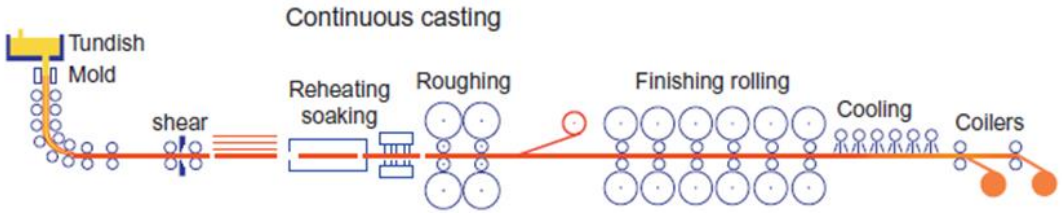

Figure 4-5: Schematic Representation of a Conventional Slab-Caster [6]

Once the material is released from the Tundish, the molten liquid enters a mold, which is water cooled. At this point the solidification of the outer surfaces begins, with secondary water spraying providing adequate cooling to completely solidify the material cross-section. The slow incremented movement of the strand through the rollers ensures uniform cooling and solidification with a high level of repeatability [6]. Dependant on continuous casting setup; the resultant / completed product shall be either a be a slab, billet or bloom- see Figure 4-6.

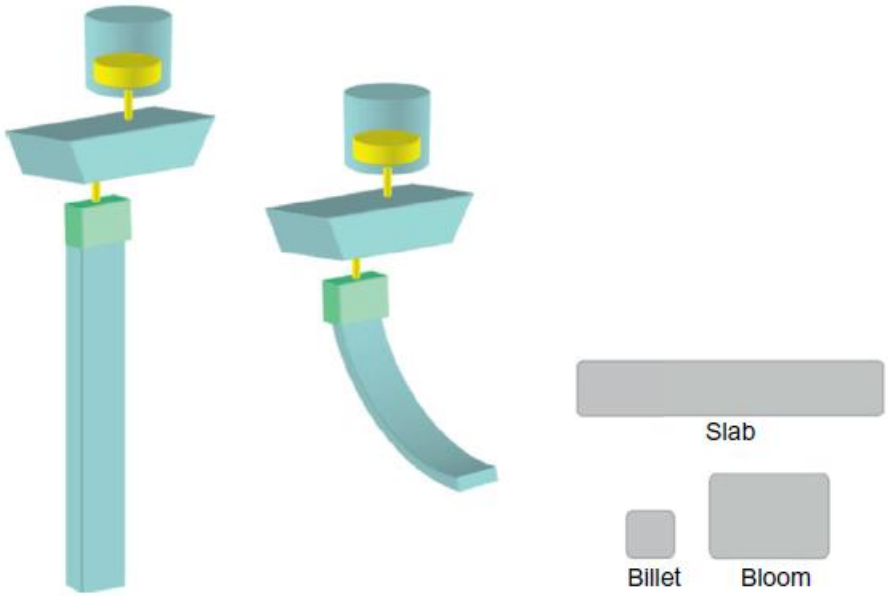

Figure 4-6: Schematic Representation of the Continuous Casting Process [6]

All raw material Mills who supply bar for coil spring manufacture shall utilise the continuous casting process. However, the methodology may differ, with some companies' adopting either a "Static" or "Rotary" casting machine tool.

The main difference between the two processes, is that the Rotary method continually rotates the Strand during the casting process, which helps mix the molten material during the solidification process, and reduces the level of centre-line segregation.

One of the many limitations or considerations of the continuous casting process is the level of segregation, which takes place during the solidification process. This is dependent on the carbon content and alloying elements within the chemical composition. "In the case of steels, the diffusion coefficients of many chemical elements are much higher in ferrite than in austenite, which means that the micro segregation typically is much stronger for high carbon steels, which solidify from liquid to austenite" [6]. Therefore, the work conducted by Louhenkilp [6], highlights the susceptibility of AISI 4161H material, being a high carbon hypo-eutectoid steel.

4.3.2 Hot Working – Rolled

The billet, once produced passes to the Rolling Mill, where the material is hot worked to create the final raw bar that is used for coil spring manufacture.

Hot Working is a process that takes the billet above its recrystallization temperature, and transforms the material into a soft, ductile, low strength condition. This subsequently allows the material to be reduced in section over several hot rolling steps. The advantage of this process, is that the as-cast structure produced during continuous casting, is broken up to form a fine-grained material. However, this is dependent on the amount of hot work and respective reduction ratio subjected to the billet during the rolling process. In summary; the greater the amount of hot work / reduction ratio, the smaller resultant grain size [7].

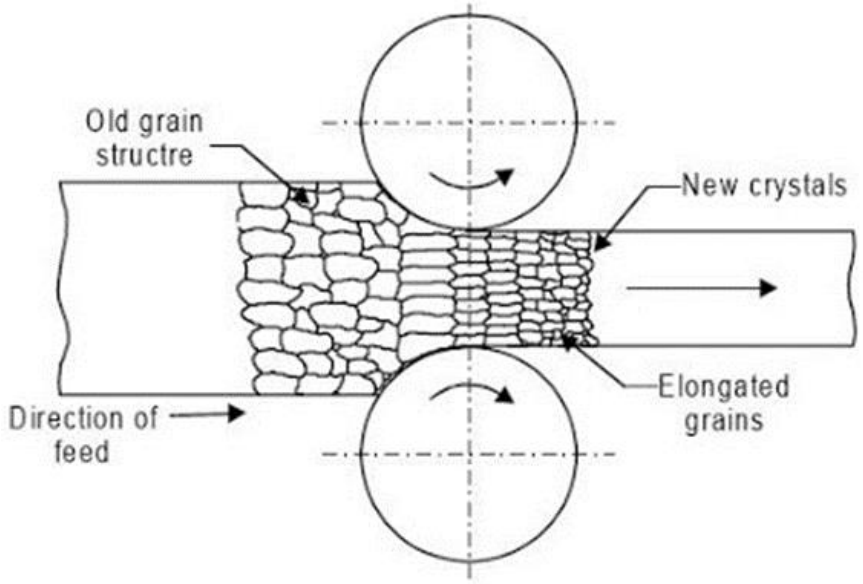

Figure 4-7: Diagram of Hot Rolling Process & resultant recrystallization [7]

In addition, the formation of fine grains is promoted during the melting process, where the Mill will add a minimum of 0.02% Aluminium to the chemical composition of the melt. This is required for the AISI 4161H material, to meet the pre-Austenitic grain size of 5 or finer per the ASTM E112 evaluation technique. Note, the pre-Austenitic grain is formed during the subsequent hot coiling process, where the bar is taken to or above the material recrystallization temperature [54]. The hot rolled process shall deliver the material bar in the Annealed soft condition, at the required diameter, equipped ready for the hot coiling / heat treatment process.

4.4 Hot Coiling / Heat Treatment

The hot coiling operation and subsequent heat treatment processes are the key manufacturing steps that induce the required mechanical and metallurgical properties for the respective design. Heat treatment processes rely on several factors in determining the resultant properties of a specific material type. Materials react based on their chemical composition, sectional thickness / geometry, cooling mediums / furnace environment, and most importantly the time / temperature transformation characteristics of the respective heat treatment operations.

4.4.1 Austenitising

Dependant on the material composition and Carbon content, the resultant microstructure is based on the respective Time Temperature Transformation (TTT) diagram. The TTT diagram or alternatively named Isothermal Transformation Diagram (ITD) is crucial in the heat treatment process, as it clearly defines the critical temperatures of phase transformation and the effect of time on nucleation and growth within the material. The curves also provide the temperatures at which different phases begin and subsequently end. However, ITD's are specific to phase transformations at a constant temperature; where a material is held for a specific time to achieve the resultant phase / microstructure – [8] Reference figure 4-8**.**

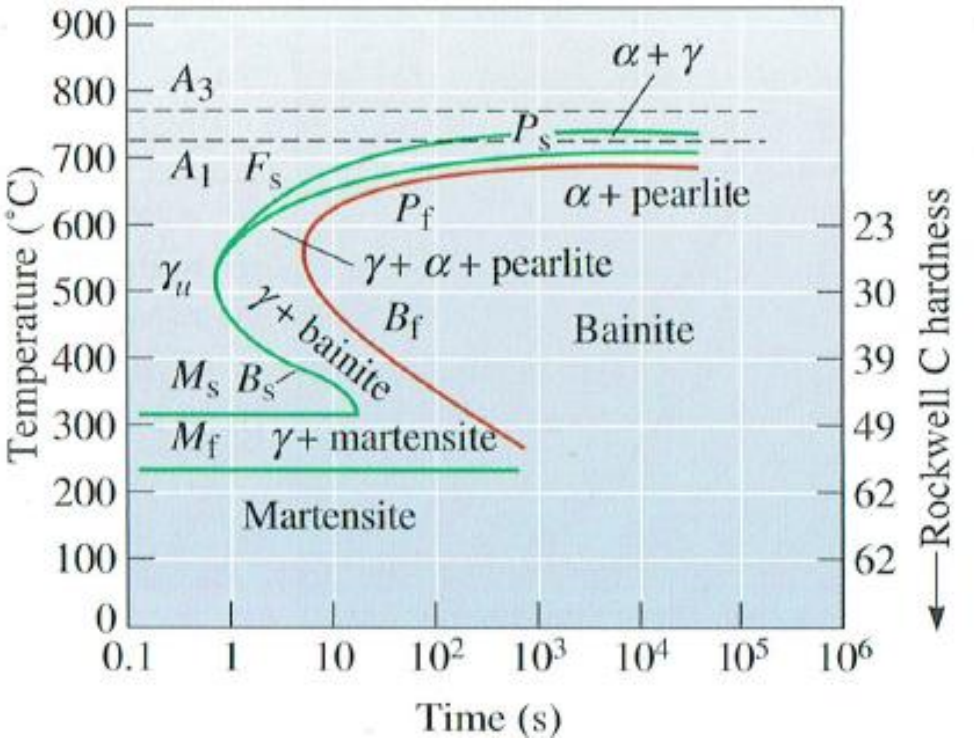

Figure 4-8: TTT Diagram for an AISI 1050 Steel [8]

The key phases and temperatures associated with transformation curves can be defined as [9]:

- A3 temperature – Temperature below which Austenite transforms to Ferrite
- A1 temperature – The minimum temperature above which Austenite forms
- s – phase transformation start
- f – phase transformation finish
- (A) Austenite (ϒ-iron) – Soft medium temperature phase
- (F)Ferrite (α-iron) – Relatively soft low temperature phase
- (P) Pearlite – Lamellar mixture of ferrite & Iron carbides Fe 3C (Cementite)
- (C)Cementite – Iron Carbide / hard metastable phase
- (B)Bainite – Nonlamellar mixture of Ferrite & Cementite
- (M)Martensite – Hard metastable phase formed when rapidly cooled (quenched) from Austenite

The material chemical composition also has a major implication on the respective TTT curve, with specific elements having a direct influence on the A1 & A3 temperatures.

Austenite stabilizing elements such as Manganese and Nickel decrease the A1 temperature; with Ferrite stabilizing elements, such as Chromium, Silicon, Molybdenum and Tungsten increasing the A1 temperature [9].

In practical terms, especially for the heat treatment of spring steels; ITD's do not consider the effect of different cooling rates, which are observed when Annealing, Normalizing or Quenching. Instead reference should be made to Continuous Cooling Transformation (CCT) diagrams, which predict resultant microstructures based on chemical composition and cooling rates. [8] – reference figure 4-9.

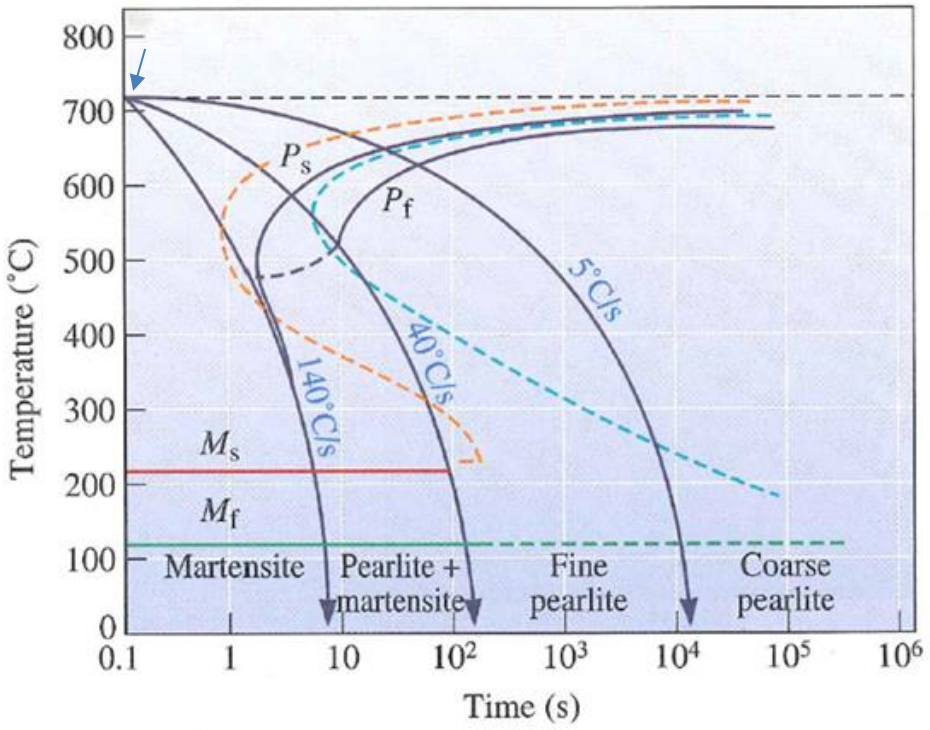

Figure 4-9: CCT Diagram (Solid Lines) compared to the TTT diagram (dashed lines) for an AISI 1080 Steel [8]

The cooling rate has a major influence on the resultant microstructure, especially when cooled from the A1 temperature (depicted by arrow-head figure 4-9). Depending on the rate of cooling, the material will either encroach on or pass through the knee of the curve or indeed cool straight to the Martensite start (Ms) zone. Regardless, different cooling rates, will result in changes to the metallurgical properties of the respective part.

Consideration must also be made to the sectional thickness of the part in question, and the cooling medium used, as they have a direct effect on the material thermal conductivity / cooling rate.

Cooling rates are greatly influenced by the environment, and by the cooling medium used:

- Environment: - furnace cool / air cool / quenched
- Medium: still or circulated air / water or oil (static or agitated)

This is depicted in figure 4-10, which illustrates the effect of cooling in different mediums such as air, oil, and water. The CCT diagram illustrates that the same microstructure can be obtained for a 2mm diameter sample that is cooled in air with a 40mm bar cooled in oil and 50mm bar cooled in water [63].

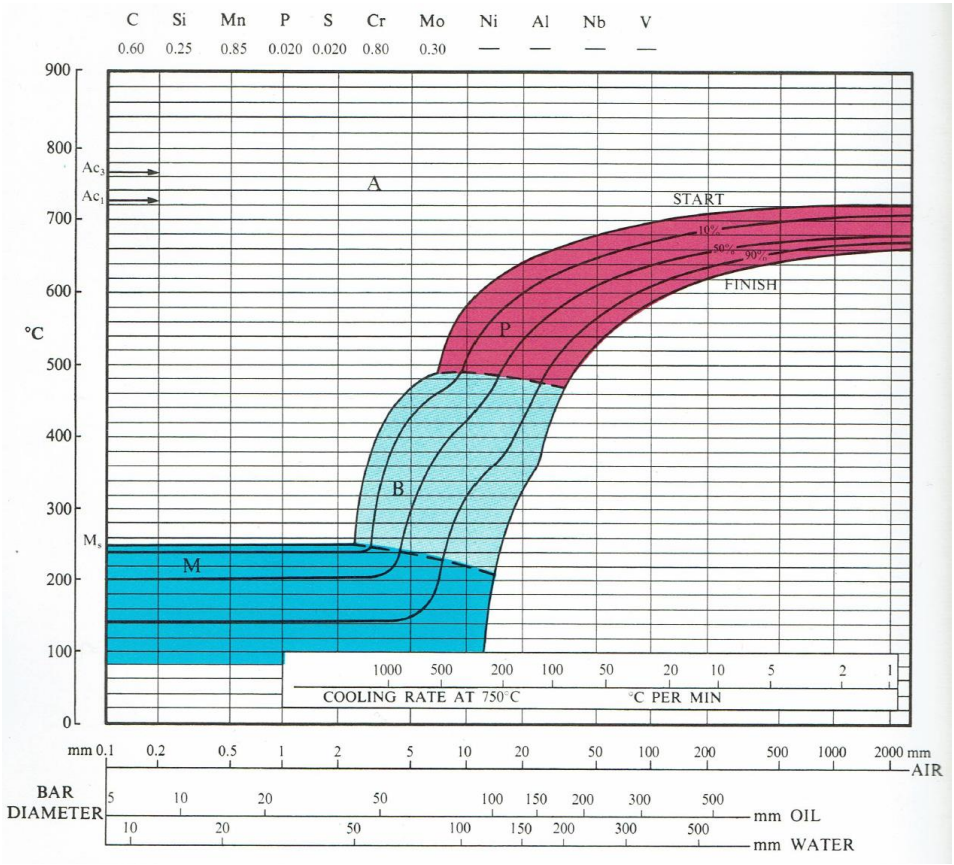

Figure 4-10: CCT Diagram for (AISI 4161H Steel) Austenitised at 850°C (1562°F) [63].

The effect of cooling medium and sectional thickness can also be seen in Figure 4-11, which exhibits the effect of quenching a range of AISI 4130 steel diameter bars (25-

300mm) in both water and oil. The experiment conducted lists the resultant hardness of the bar core for each of the tested bar diameters. Experimental data has shown that the resulting hardness at each of the incremented bar diameters has consistently reduced, when tested at the core location. Also, the test has proven that with the water quenched specimens achieved a greater hardness for each bar diameter when compared to the oil quenched samples.

Regarding the 50mm bar diameter- Figure 4-11; the water quenched bar passes the knee of the CCT curve, where the oil quench sample cuts through the curve resulting in a different microstructure and resultant hardness value [9].

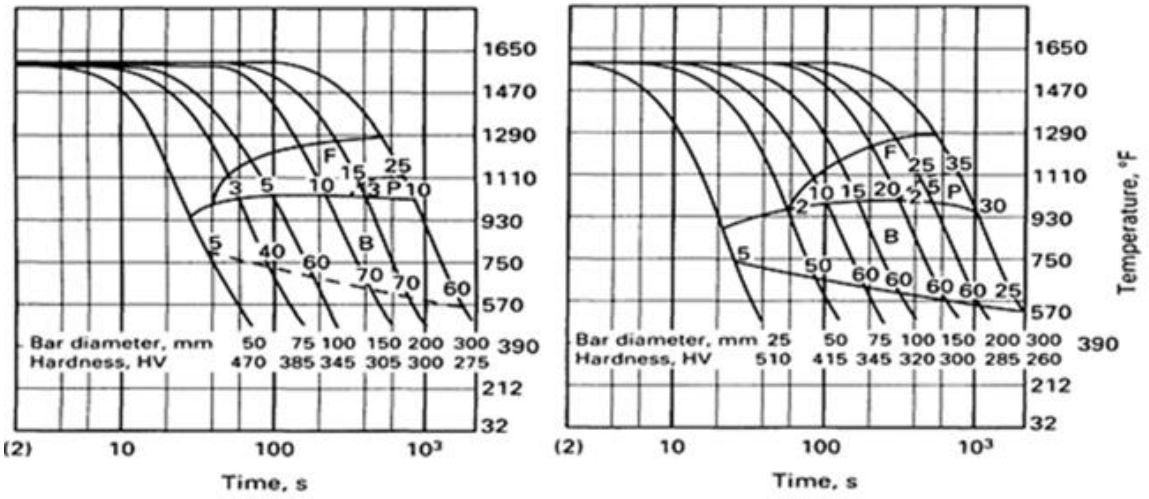

Figure 4-11: CCT Diagrams for AISI 4130 steel (Left Water Quench / Right Oil Quench) [9]

The cooling medium / environment therefore, have a direct influence on the resultant CCT curve, which affects the as-quenched properties (microstructure / hardness) of the material. This is further clarified within Figure 4-12, where a chromium-molybdenum steel, has been cooled using three separate mediums, resulting in different CCT curves for the same material type.

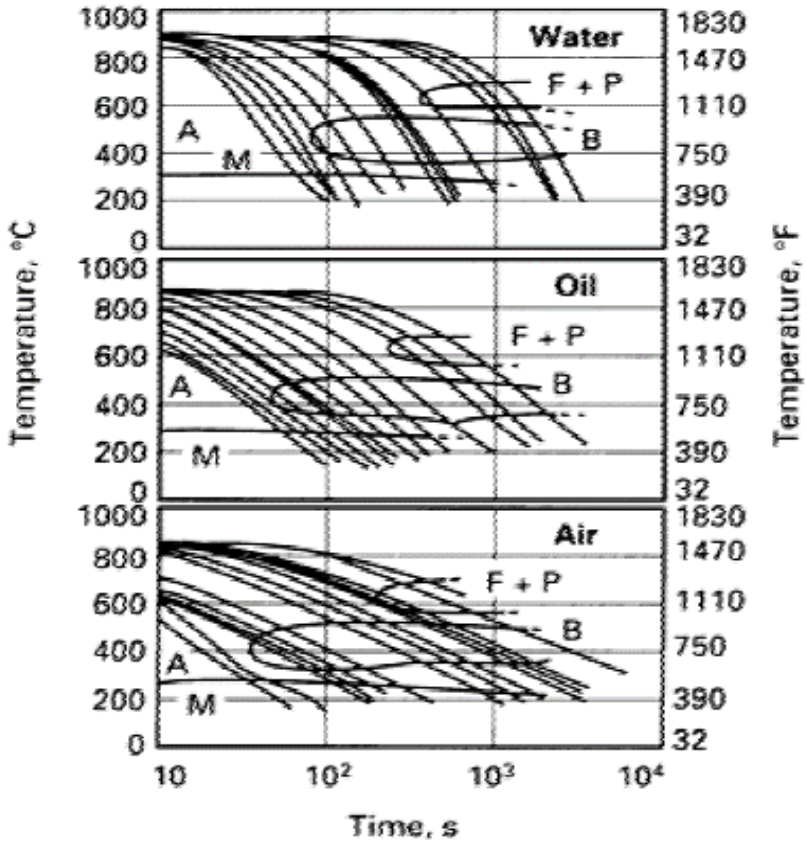

Figure 4-12: CCT Diagrams of a Chromium-Molybdenum Steel Using Simulated Cooling Curves for Water, Oil and Air [9]

The position of the "c-shaped" curves can also change in relation to other factors separate from cooling conditions. Consideration should be given to the hold time during the austenitising operation. “If the hold time in the austenitic range is too short, the C-shaped cooling curves may be shifted to shorter times. This may be due to incomplete carbide dissolution or a smaller grain size after a short austenitising time” [9]. This is demonstrated by Figure 4-13, which represents a shift in curve orientation, when an AISI 4140 steel was austenitised for 6 seconds at 950°C (1740 °F) and 10 minutes at 860°C (1580°F) [9].

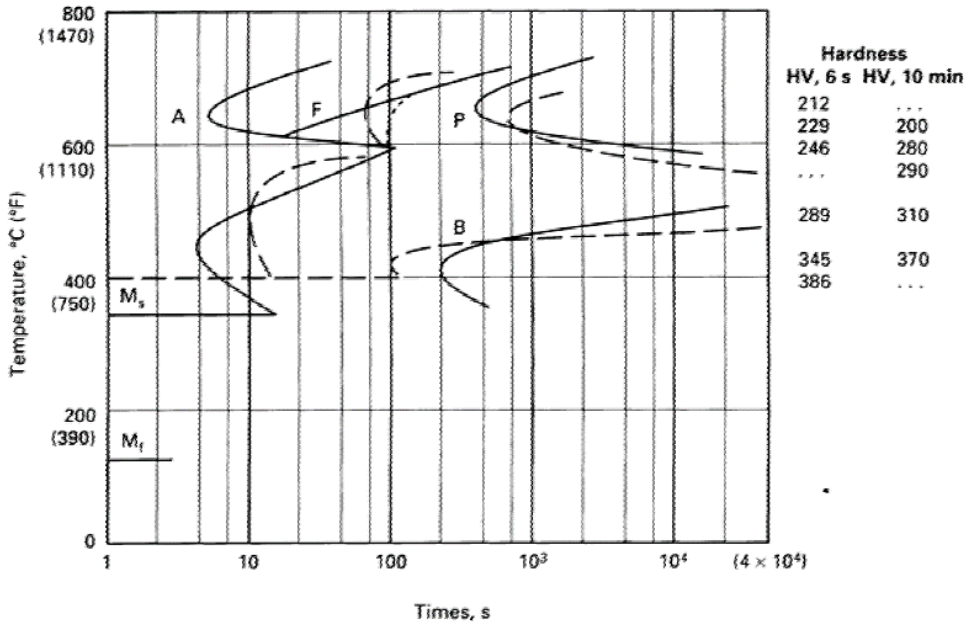

Figure 4-13: AISI 4140 – Solid Line (950°C Austenitise) / Dashed Line 860°C Austenitise) [9]

The analysis of the CCT curves has confirmed that dependant on material grade, faster cooling occurs at the surface compared to the core. Therefore, a transition in material properties is expected, which is dependent on the material thermal conductivity (heat transfer coefficient), thickness, chemical composition and hardenability.

Chemical composition is also key to the formation of the CCT / TTT diagram. Work conducted by Kirkaldy et al [23] [24] [25] determined that the transformation temperatures and respective phases can be determined through the development of experiment and the correlation to empirical formula to create a full CCT / TTT model. Similarly, others have developed formula such as Steven & Haynes [26] and Andrews [27] in determining phase transformation temperatures; such as the Bainite & Martensite start temperatures.

$$Bs\ (°C) = 830 – 270C – 90Mn – 37Ni – 70Cr – 83Mo \text{ [26]}$$

Equation 4-1

$$Ms\ (°C) = 539 – 423C - 30.4Mn - 17.7Ni - 12.1Cr - 11.0Si – 7Mo \text{ [27]}$$

Equation 4-2

This is further clarified within Figure 4-14, which demonstrates the TTT curve for two different material types (chemical composition), which have been plotted using both experimental and calculated data [28]. Regardless whether experimental or calculation generated, the respective diagram moves to the respective left / right as a direct factor of resultant chemical composition.

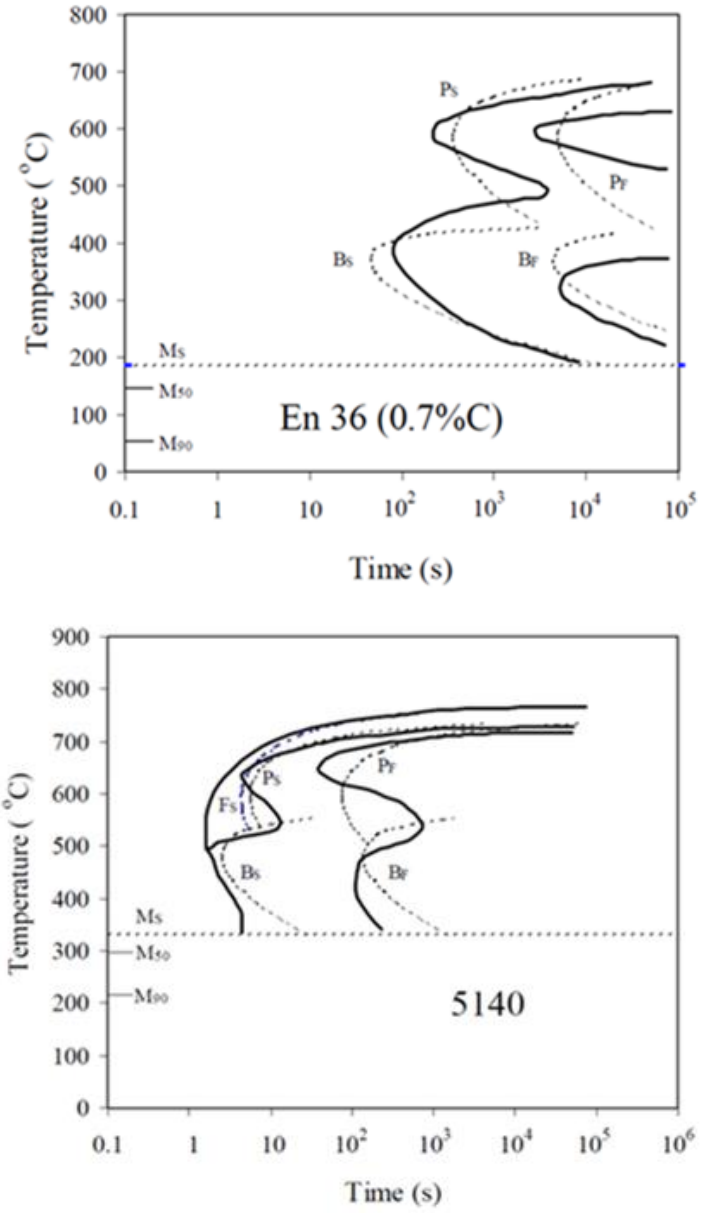

Figure 4-14: Comparison Between Experimental (Bold Lines) & Calculated TTT Diagram (Dashed Lines), Top En36 (Fe-0.7%C-0.35%Mn-0.16%Si-3.24%Ni-0.96%Cr-0.06%Mo (wt%), Bottom 5140 (Fe-0.42%C-0.68%Mn-0.16%Si-0.93%Cr (wt%) [28]

4.4.1.1 Limitations & Considerations - Austenitising

As with all heat treatment processes, there are limitations and certain situations that can yield undesirable metallurgical properties and conditions. Although the CCT and TTT curves clearly define the resultant microstructure under defined cooling conditions, one must also consider other attributes that can have a direct influence of the material, especially for coil spring applications.

Literature has shown that there are number of other factors that can affect the material during quenching, such as:

- Surface condition – level of oxide / scale
- Thermally induced deformation / strain

Surface oxidation is formed during the hot coiling operation, as the bars used to manufacture actuator springs are placed in an un-protected environment, (gas fired furnace) to achieve the desired hot working temperature of 1700-1800°F (927-982°C). The level of oxidation is dependent on the temperature selected and the respective time the bars spend within the furnace. Typically, the level / depth of oxidation shall increase with temperature and time

Research has shown that the depth of scale can have a direct influence on the quenching characteristics of the material [10]. The work conducted by ASM International established that the rate of cooling increased with an oxidation depth up to 0.08mm (0.003in), when compared to a specimen without scale. However, the opposite was achieved with a heavy surface scale of 0.13mm (0.005in), which reduced the cooling characteristics – see Figure 4-15.

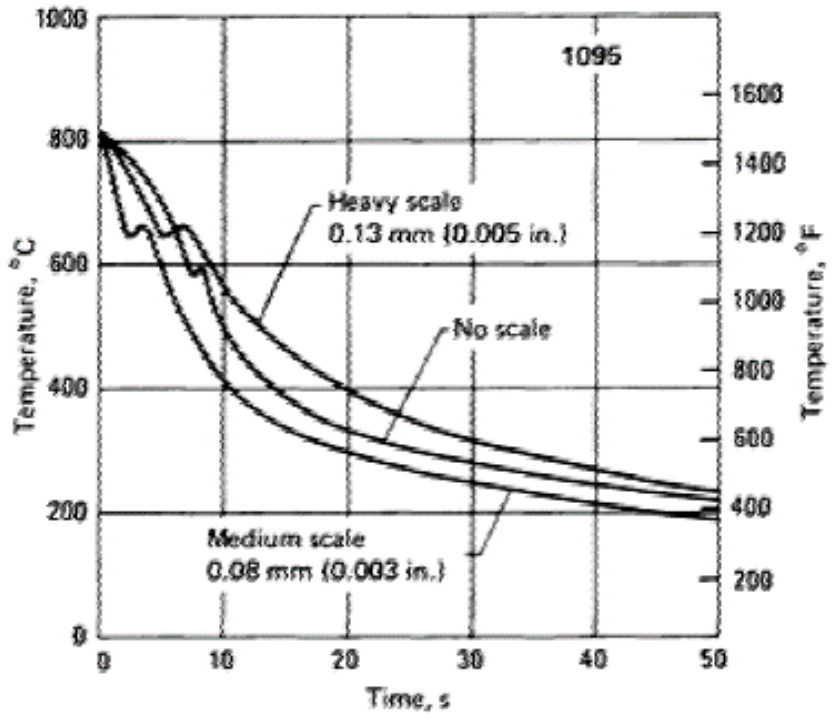

Figure 4-15: Cooling Curves of a 1095 Steel Quenched in Fast Oil [10]

In addition to influencing the cooling rate, oxidation can have a detrimental effect on the coil spring material in the terms of crack formation. The IST, through various metallurgical failure investigations, established that excessive durations within the hot coiling furnace “resulted in oxide penetration between the grains of austenitic structure” [11]. During subsequent quenching, this will result in residual stresses at the grain boundaries inducing the formation of cracks – see Figure 4-16.

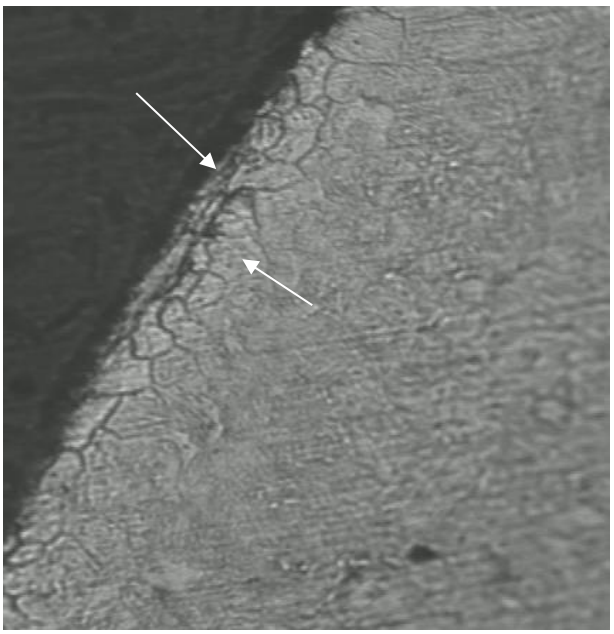

Figure 4-16: Oxide Penetrating Grains at the Surface of a Hot Coiled Spring [11]

The cracking mechanism can also be compounded due to the residual stresses induced during the phase transformation of the material from austenite to martensite. If there is a time delay between the subsequent quenching and tempering operations, the residual stresses can manifest to cracks from the material surface [11] – see Figure 4-17.

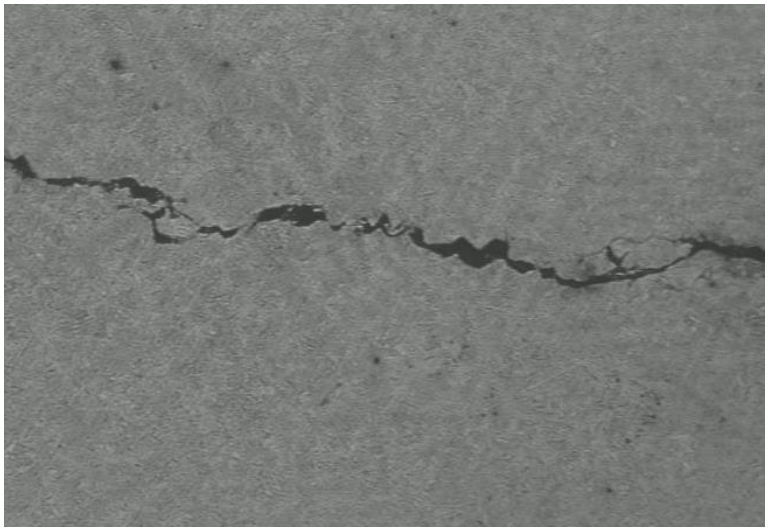

Figure 4-17: Typical Quench Crack from a Coil Spring [11]

Consideration must also be given to the volumetric changes exhibited during the phase transformation and the resultant stresses induced during cooling. In general,

low alloy steels will contract during the quenching process and then subsequently experience linear expansion at room temperature [10]. The rate of which both contraction and expansion takes place is related to the rate of cooling – as shown in Figures 4-18 & 4-19.

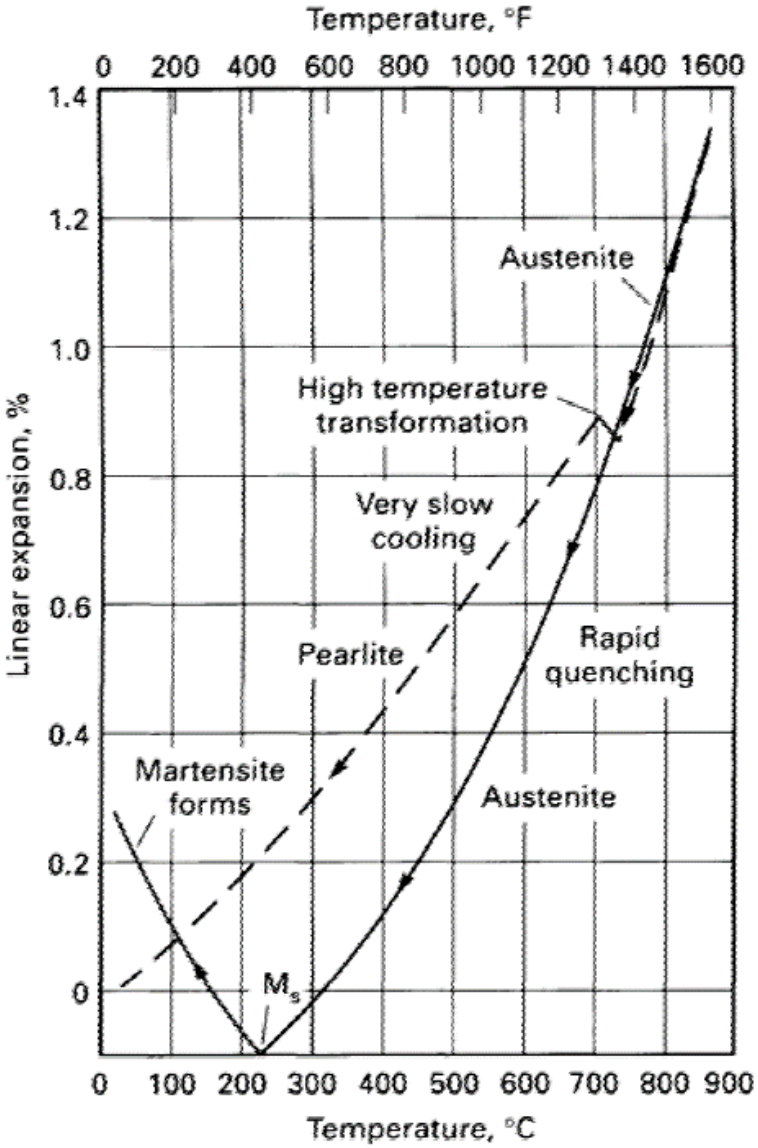

Figure 4-18: Demonstrates the Dimensional Changes Observed Between a Slow & Fast Cooled Material [10]

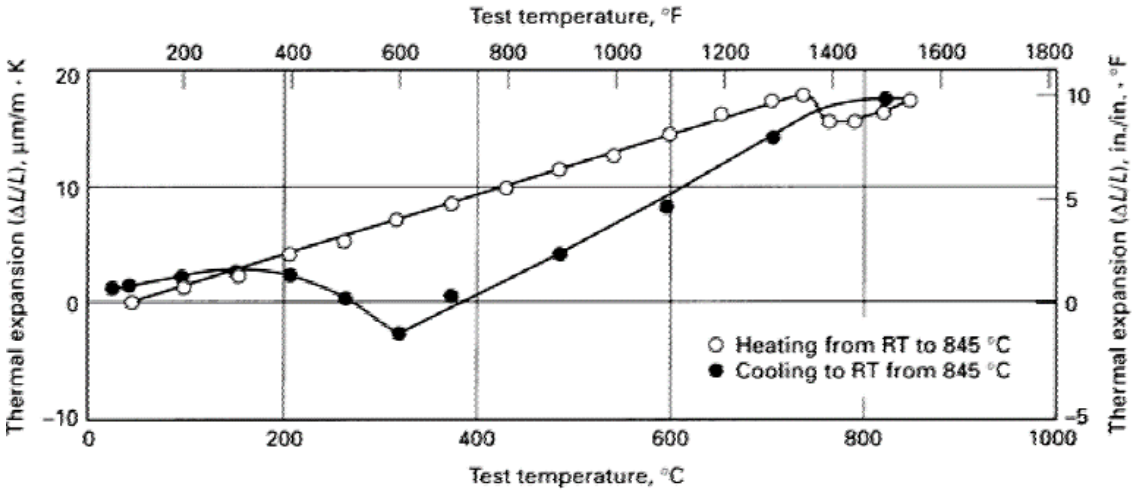

Figure 4-19: Thermal Expansion / Contraction Curve for a 4340 Steel [10]

For coil spring applications, a fast cooling rate and a high carbon content are required to attain the desired metallurgical properties (high strength, high hardness fully martensitic material). However, as demonstrated by Figures 4-18 and 4-20, the faster the cooling rate, the greater degree of linear expansion combined with the resultant higher strain rate associated with the increase in carbon content % [10]. Therefore, there is a potential of crack initiation if the quench rate is too severe.

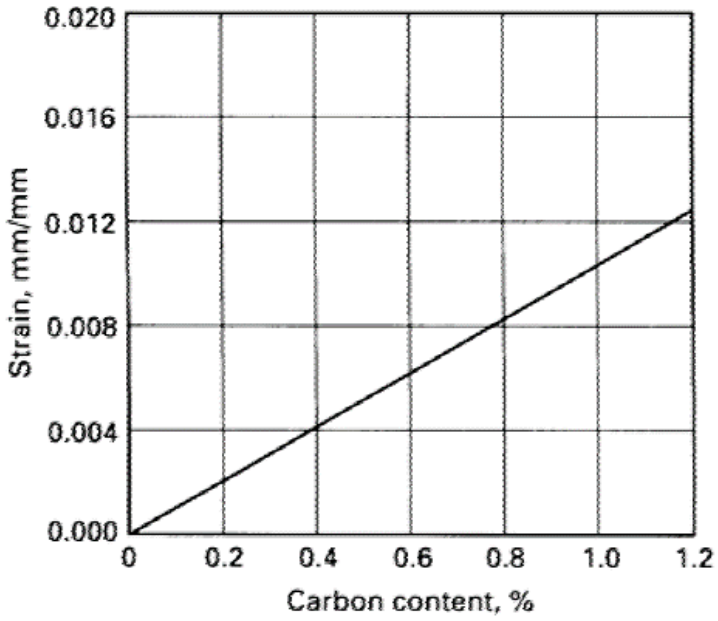

Figure 4-20: Linear Expansion in Steel after Quenching to Produce Martensite [10]

In addition, the quench rate and material hardenability, which is related to chemical composition, will have a direct correlation to the resultant microstructure. If the cooling rate is inadequate for a specific material type, then phases such as retained austenite or ferrite / pearlite could be present. This is undesirable as retained ferrite and pearlite reduces the material strength, whereas retained austenite can lead to embrittlement. [8] [10] [12].

Retained austenite can be determined as “austenite that does not transform to martensite upon quenching” [13]. This respective phase occurs when the steel is not quenched to a temperature low enough to form 100% martensite.

The amount of retained austenite is dependent on several factors, such as [13]:

- Carbon and alloy content (specifically Nickel & Manganese) – these elements increase the stability of austenite, thus increasing the amount of retained austenite upon quenching.
- Quenchant temperature – since the martensitic Mf temperature is below room temperature for steel with >0.3% Carbon, then higher quenchant temperatures, shall result in increased amounts of retained austenite within the structure [13].
- Subsequent heat treatment processes (Tempering) – the duration and tempering temperature shall determine the amount of retained austenite that transforms into martensite.

The presence of retained austenite can also help improve metallurgical / mechanical properties such as [13]:

- Improved fatigue strength - by arresting the crack tips and providing compressive stresses inside the material as it transforms to martensite.
- Increased impact strength - due to its higher ductility of the retained austenite, compared to a fully transformed martensite structure

However, by increasing the content of retained austenite within the structure dimensional stability is lost. This is due to the transformation to martensite, where "martensite, a body centred tetragonal crystal structure, has a larger volume than

the face centred cubic austenite that it replaces "[13]. This results in a localized volume increase of 4-5% within the microstructure, with the martensite (low ductility) phase unable to tolerate the expansional stresses, creating cracks within the material [13] [14].

4.4.2 Tempering

Tempering is a key fundamental process in the manufacture of actuator coil springs, and indeed for any alloy steel that has undergone quenching and the resultant formation of a martensitic microstructure. It is well known fact that martensite is a very hard and brittle phase, with negligible ductility; however, is essential in producing the required strength (UTS) for the respective alloy and application.

The lack of ductility is due to the martensite atomic lattice, especially for steels that exhibit a Carbon content of >0.2%, which exhibit a BCT (Body Centred Tetragonal) formation / structure, formed during rapid cooling from austenite [8]. This lattice formation has no “close-packed slip planes” [8] and is “highly saturated with Carbon” atoms [8], which results in a very brittle material that requires to be tempered.

Tempering is a heat treatment process that promotes diffusion of the carbon atoms within the atomic lattice and the formation of Fe_3C or an alloy carbide in a ferrite matrix [15]. The properties of the tempered steel are primarily determined by the size, shape, composition, and distribution of the carbides that form [15].
This is also known as the “decomposition of martensite [8], which is achieved by heating the material below the lower critical temperature A1, to produce an increase in toughness and ductility, with a reduction in hardness and yield /tensile strength.
Like austenitising, the tempering process conditions and the chemical composition, have a major influence on the resultant mechanical and microstructural properties of the respective material. Considerations should therefore should be given to [15]:

- Tempering temperature and time at temperature
- Cooling rate
- Alloying elements within the material

4.4.2.1 Tempering Temperature / Time

Both tempering temperature and the time at temperature have a direct effect on the resultant metallurgical properties of the material. For alloy steels, the actual temperature at which tempering takes place has more of an impact in terms of the fundamental resultant metallurgical changes, in respect to incremental differences in time – see Figures 4-21 & 4-22.

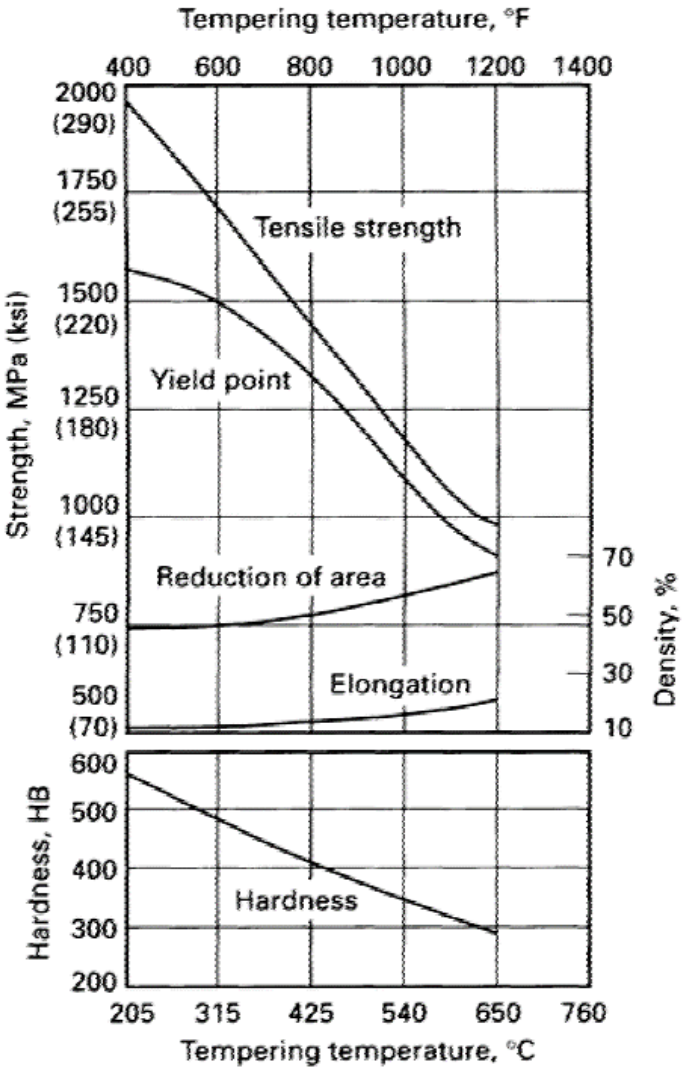

Figure 4-21: Effects of Tempering an Oil Quenched AISI 4340 Steel Bar at Various Temperatures [15]

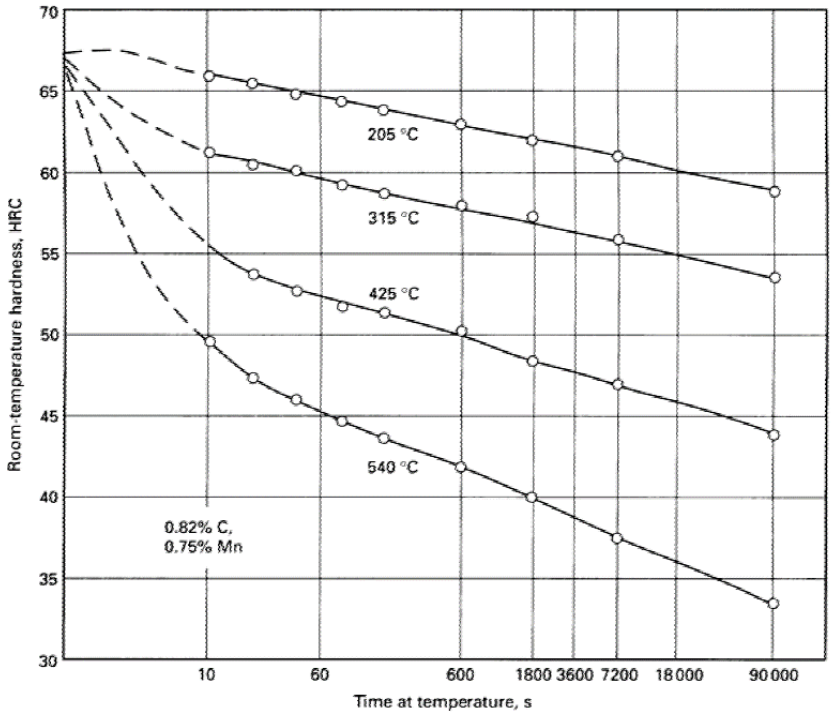

Figure 4-22 Effects of Time at Four Tempering Temperatures on HRC Hardness of a 0.82% Carbon Steel [15]

Figures 4-21 and 4-22, both highlight that higher tempering temperatures increase the gradient of change in terms of hardness, ductility (elongation / reduction of area) and yield / tensile strength. The influence of time at a specified temperature is more apparent as the tempering temperature is increased [15]. This suggests that the rate of diffusion within the material is increasing in conjunction with the formation / precipitation of ferrite and Fe_3C [8]. At low tempering temperatures, the martensite may form two transition phases – a lower carbon martensite and a very fine none equilibrium carbide [8], which will result in a strong brittle material. Whereas at higher temperatures stable ferrite and Fe_3C form, and the steel becomes softer and more ductile [8].

4.4.2.2 Cooling Rate / Alloying Elements

Another consideration is tempered martensite embrittlement, which is directly related to slow cooling rates and excessive dwell times at specific tempering temperatures. Research has shown that when steels are slowly cooled from

temperatures above 575°C (1065°F) or indeed held at long periods between 375°C - 575°C (705°F – 1065°F), precipitation of “compounds containing trace elements” can occur [8]. The long dwell times allow precipitation to take place along the grain boundaries (prior austenitic), reducing the fracture toughness of the material [8] [16]. Figure 4-23 shows the effect of temper embrittlement in relation to different cooling rates from 620°C (1150°F).

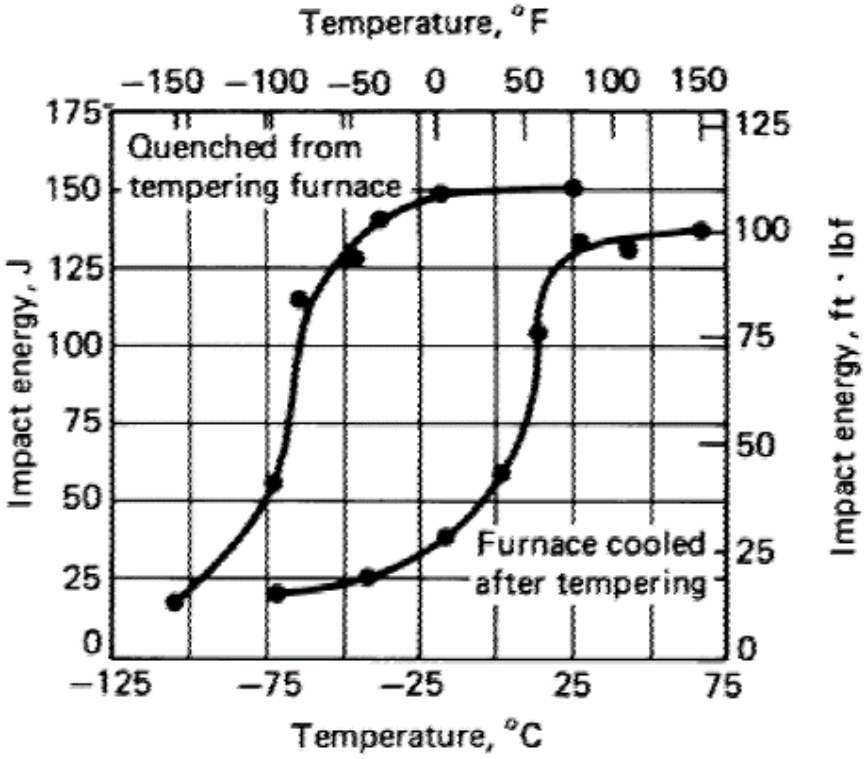

Figure 4-23: Effects of Temper Embrittlement on Notch Toughness for AISI 5140 Steel Hardened & Tempered at 620°C (1150°F) – Oil Quenched V Furnace Cool from the Tempering Temperature [8]

The work conducted K.B. Lee [16], established that intergranular tempered martensite embrittlement; was directly influenced by “the combined action of coarse carbides and impurities at the prior austenite grain boundaries” [16]. This suggests that the alloying elements form segregates during the quenching process, which are precipitated out during the subsequent tempering operation. Therefore, due diligence is required not only with the tempering duration, but with the effects of different alloying elements within the material.

4.5 Considerations of the Material & Hot Forming / Working Processes

Both the hot forming and subsequent heat treatment processes have a major effect on the mechanical and metallurgical properties of both the raw bar material and the fully quenched and tempered coil spring. Influencing factors can be considered as both fixed and variable, in terms of chemical composition, melting practices, hot-working reduction ratio and subsequent heat treatment conditions.

These key variables have an impact on the resultant segregation and microstructural banding evident within the raw material and the fully functional subsea valve product. D'Errico et al [17] stated that "the ultimate quality of steel products is determined from the steelmaking technological cycles and the casting process technologies employed to fabricate raw products". This is of great importance, as the continuous casting process used to create the raw material bar, is known to produce segregation at the centreline location of material billet [17]. In addition, the subsequent hot-working / rolling processes used to form the respective bar, will align the segregation to from elongated bands [17].

This is also confirmed by Penha et al [18] who stated that during "mechanical deformation the dendritic micro-segregation strung out into stringers parallel to the dominant flow direction".

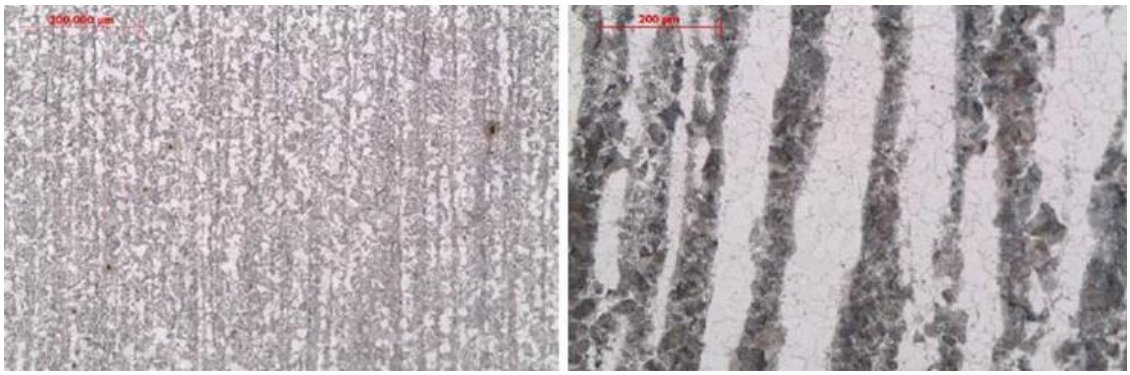

Figure 4-24: Example of Banding Exhibited within a UNI EN 18 CrNiMo Normalized Material

The work conducted by both D'Errico & Penha et al [17] [18], established that the chemical composition of the bands will be different because of the micro-segregation exhibited. Therefore, subsequent heat treatment operations will not only be sensitive

to the bulk material chemistry, but to those of the individual bands throughout the material. This suggests that a banded structure will not exhibit a homogenous microstructure or indeed mechanical properties across the respective cross-section. In fact, “the composition of neither band is equivalent to the bulk chemistry. Therefore, “the bands may respond to the heat treatments in an appropriate manner” [17].

D’Errico et al [17] [18] confirmed that the degree of banding is influenced by several key factors; such as alloying elements, cooling rate, austenitization temperature and prior austenite grain size:

- Alloying elements:
    - “Manganese acts directly on Ar^3 temperature, stabilizing austenite by lowering the Ar^3” [17].
    - “Phosphorus has a very strong tendency to segregate during solidification and may be a factor in the banding process” [17].
    - Manganese, Chromium and Molybdenum “influences the temperatures and compositions during solidification producing an inhomogeneous distribution of alloying elements” [18].

- Cooling rate / Austenitization Temperature
    - Because of the chemical compositional differences, each band will have its own transformation temperature, which will result in an independent TTT / CCT curve for that respective zone. This in conjunction with the cooling rate, will result in the formation of different microstructures within the independent band; such as “martensite & bainite, ferrite & bainite, ferrite & martensite, pearlite & bainite, pearlite & martensite” [18].

- Prior Austenite grain size
    - D’Errico et al [17] established that the dimension of the prior austenite grain had a direct relation to the promotion of banding within the

resultant microstructure. “Increasing the austenitic grain size so that it is greater than the interspacing of segregation, could result in the disappearance of banding”

Krauss [29] has also studied the effect of solidification, segregation and banding within alloy steels. Comparable with the findings D’Errico [17] and Penha et al [18], banding within the resultant microstructure is very much dependant on the hot working process and the diffusion coefficients of the elements within the material.

- Reheating of as-cast products and hot rolling reduce chemical segregation but further microstructural partitioning (often by design in parent austenite of uniform composition), occurs during diffusion-controlled solid-state transformations.
- Hot rolling aligns the interdendritic variations in chemistry in bands parallel to the rolling direction producing alternating regions of high and low concentrations of various solute elements. Substitutional elements with low diffusion coefficients respond most sluggishly to the homogenizing effects of hot work - Reference figure 4-25.

Experimental work reported by Krauss [29], established that the chemical composition of key elements such as Mn, Cr and Ni would vary depending on their respective chemical composition, and effect of their ability to suppress the dissolution of Carbon. Both Mn and Cr lower the activity of C in austenite; resulting in consistent C values across the material sectional thickness -see Figures 4-25 & 4-26. The work also concluded that the micro segregation manifests itself as banding, which can be influenced / reduced by holding the material for long durations at elevated temperatures. However, this will be dependent on the mobility and chemical composition of a given element within the banded zone.

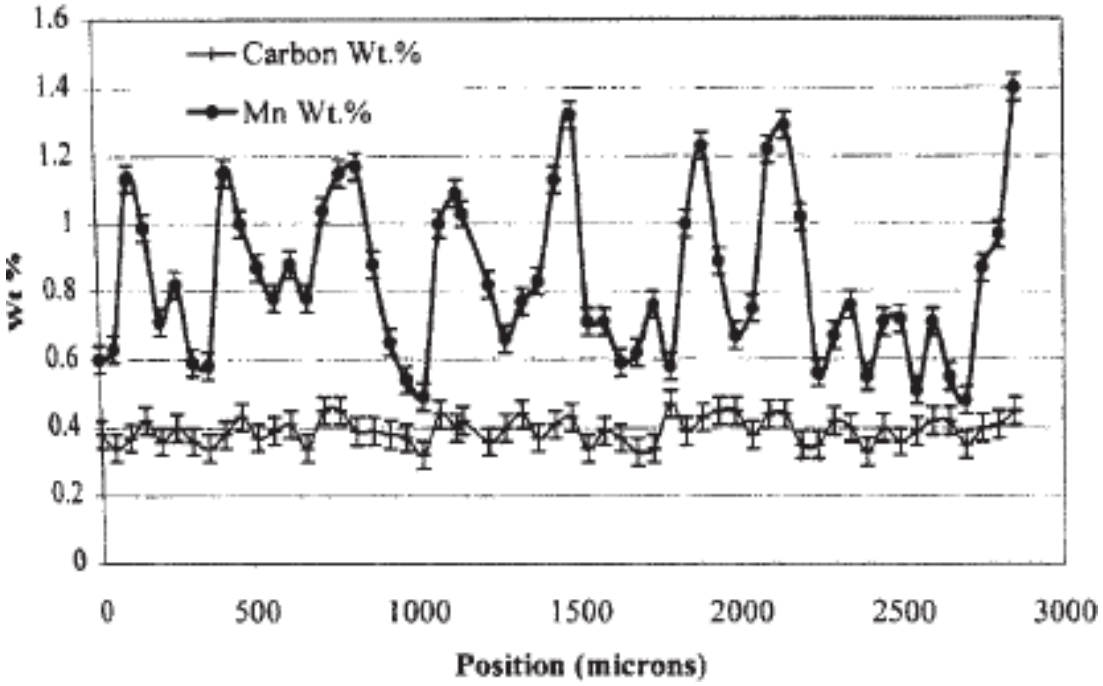

Figure 4-25: Variations of Mn & C across a Quenched & Tempered 96.25mm Diameter 4140 Steel Bar [29]

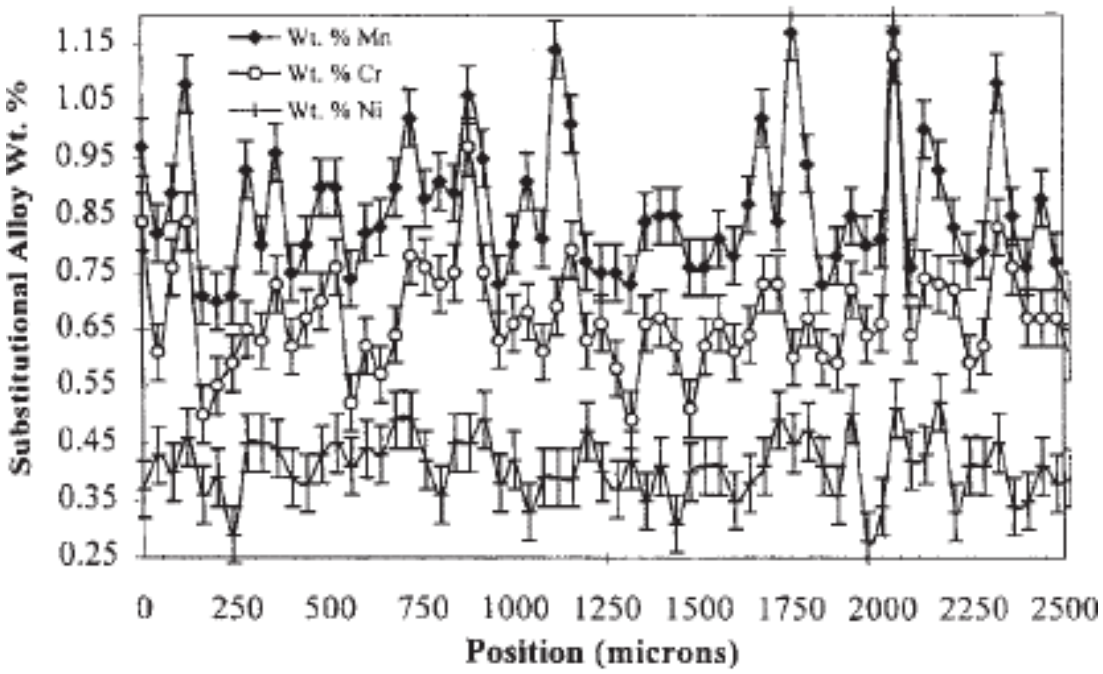

Figure 4-26: Variations in Mn, Cr & Ni Across a Hot Rolled Bar Of 8617h 26.19mm In Diameter [29]

4.6 Summary Remarks

The literature review has established the key operations within the method of manufacture that can affect the mechanical and metallurgical intent of the AISI 4161H coil spring. As identified by industry and academic research, there are four fundamental processes that influence the material properties:

- Raw material melting / hot working
- Coiling
- Austenitising
- Tempering

The literature has shown, contrasting to common understanding that the material is not homogenous in terms of chemical composition. Instead the continuous cast material is prone to centre-line segregation, which when hot rolled can manifest into elongated zones as bands. These bands can exhibit both low and high concentrations of the individual elements stated within the bulk chemistry. This is however dependent on the element and its respective diffusion coefficient, which can influence the mobility of the elements and reaction with Carbon during heat treatment operations.

Chemical composition along with cooling rates / mediums have a major influence on both the TTT and CCT diagram, with specific elements influencing the transformation temperatures along with changing the shape and position of the respective curve. This results in distinct phases within the resultant microstructure, which could impact the mechanical properties of the material.

Considerations should also be made to the times and temperatures selected for both austenitising and tempering operations, as the literature has clearly demonstrated that the material will respond differently for a given heat treatment condition, producing a range of metallurgical properties for one material type.

These key findings substantiate the requirement to conduct a detailed design of experiments to understand the effects of the various heat treatment conditions for the AISI 4161H material.

5 EXPERIMENTAL PROGRAMME

Chapter 5 details the research philosophy and methodology used to determine and characterize the metallurgical properties of the AISI 4161H material at the fundamental and extremities of the heat treatment processing window.

The initial work specifies the scope of the test program and the design of experiment approach taken, to identify the range of test conditions and test methods selected to enable a full understanding of the resulting properties achieved through varied inputs.

For each set of test conditions, the findings are presented along with a summary of the key conclusions from the analysis of the results obtained through experimental study.

5.1 Scope

The scope of the experimental research covers the AISI 4161H material over 3 bar sizes. This is due to the requirement to fully understand the technical issues presented within Chapter 3, and the need to evaluate new innovative designs in terms of material capability. The future philosophy of TechnipFMC is to operate subsea trees with actuated valves at deeper water depths, higher temperatures and higher pressures. This drives the requirement for larger diameter coil springs. To make the experimental research representative, the following bar diameters have been selected:

- 2.875-inch (73mm)
- 3.375-inch (85.7mm)
- 4-0-inch (101.6mm)

Using these standard sizes allows a fuller understanding of the current material utilised, and determines the effect of increasing the bar dimeter to enable a full evaluation / characterization and limitations of the AISI 4161 bar used for coil spring manufacture.

5.2 Methodology

5.2.1 Material / Test Samples / Set -Up

The material used for the experimental research was sourced from Mill 4 under two Heat numbers. However, the 2.875-inch (73mm) trials included the comparison of material supplied by an alternative, namely Mill 1. In all cases, the raw material production route utilised electric arc melting, followed by vacuum degassing / ladle refinement, prior to continuously casting the billet for the subsequent hot rolling operation.

A summary of the respective raw material properties for each heat number is detailed within table 5-1.

Table 5-1: As-Received Raw Material Properties

			Chemistry							Jominy Value				
Bar Size	Raw Material Mill	Heat No.	C	Mn	P	S	Si	Cr	Mo	J5	J10	Austenitic Grain size	Reduction Ratio	Ideal Diameter
2.875 inch	Timken	90307	0.58	0.88	0.009	0.004	0.26	0.68	0.29	61	60	5/finer	23.9 : 1	5.54
3.375 inch	Timken	90307	0.58	0.88	0.009	0.004	0.26	0.68	0.29	61	60	5/finer	15.7 : 1	5.54
4.0 inch	Timken	27231	0.56	0.89	0.011	0.004	0.25	0.68	0.28	62	60	5/finer	12.1 : 1	5.36
2.875 inch	SDI	A141303	0.57	0.85	0.01	0.014	0.25	0.76	0.28	64	64	8	20.3 : 1	5.58

For the purposes of the test program, the material was supplied as a complete 15 metre bar length, in the fully hot rolled and machined (scale free) condition. The test samples were then sectioned from bar length into 11-inch (279.4mm) lengths, to obtain a standardized test specimen dimension for subsequent heat treatment operations. To increase the sensitivity of the program, 3 bar samples were tested for each respective quench and temper condition.

5.2.2 Test Conditions

To fully understand the AISI 4161H material across the 2.875-4.0-inch (73 - 101.6mm) bar diameter range; four (4) heat treat conditions were evaluated:

- As-received (Datum) - hot rolled with no subsequent heat treatment processing.

- Air-cooled - where bars are heated to the OEM hot coiling temperature, and allowed to cool in air to room temperature.
- As-Quenched - where the bars are heated to various austenitising temperatures and quenched in oil.
- Quenched and Tempered - where the bars are exposed to various heat treatment conditions, utilising different austenitising and tempering temperatures.

Throughout the experimental DoE; real time temperature monitoring was employed to establish the heating and cooling rates of the respective bar diameters. This was accomplished by attaching a thermocouple to the respective surface and core of the bar material- reference Figure 5-1. It must be noted that only few test samples for each bar size had core thermocouples attached, however, all bars were subjected to surface temperature measurement. Sample core measurement was employed to determine the differences in the respective heat transfer properties at core and surface of the individual bar sizes.

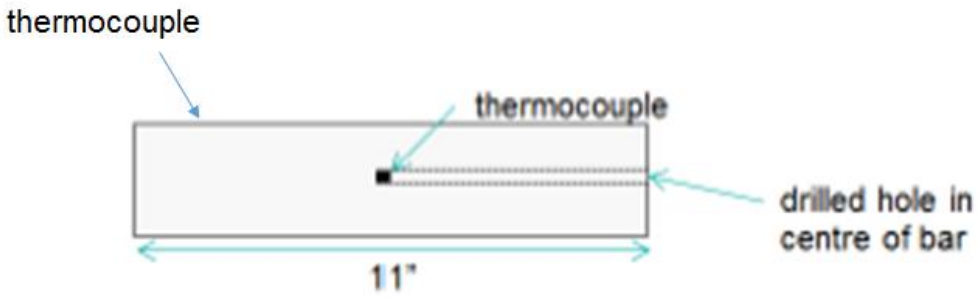

Figure 5-1: Thermocouple location for surface & core temperature monitoring

5.2.3 Test Set-up

To conduct the experimental analysis, and to ensure a high level of repeatability was maintained throughout the testing phase; several pieces of key equipment were standardized. The set-up included the following pieces of standard apparatus:

- Quench Tank - see Figure 5-2
    - Oil Super S quench oil - 521 (reference Appendix D for CoC)

Figure 5-2: Picture of the Quench Tank Utilised for the Experimental Testing

- 2-off Electric furnaces - see Figure 5-3
    - Type: Watlow 942A
    - Controller Type: Honeywell DC2500
    - Multi-point temperature recorder type: Honeywell Multi-trend SX

Figure 5-3: Picture of Furnace Type Utilised for the Experimental Testing

5.2.4 Design of Experiments

The test methodology used for the experimental research is based on a Factorial DoE [51] and Response Surface DoE approach, which was created to reduce the required number of test combinations while maintaining the test integrity, when determining the effect of different heat treatment process inputs (Quench and Temper conditions).

Based on the literature review [10] [15] it is believed that changing the Quench and Tempering temperatures would result in a linear change in properties i.e. with decreasing tempering temperatures it would lead to an increase in hardness and tensile strength. The optimal DoE philosophy for evaluating straight line responses is a Factorial DoE approach, which involves testing for boundary conditions with an option to test at the middle point, to validate the linear effect of changing the input parameters on the resultant output. However, following the testing carried out on 2.875" (73mm) bar, it was found that relationship between process parameters and test results is not linear. Thus for 3.375" (85.7mm) and 4" (101.6mm) bar diameters the Response surface DoE approach was utilised, which involves limited testing at boundary conditions and in-depth testing within the range of process parameters, to better evaluate the impact of changing the conditions within the range.

The DoE was created to ensure that only two variables at any one time were varied, as this was in line with the current practices utilized by the coil spring OEM's.

All other inputs, such as the quench oil type, quench oil temperature, furnace type, bar sample heating / cooling conditions and time at temperature were kept as a constant - Reference Table 5-2.

Table 5-2: Constant DoE Conditions

	Austenitise - Quench				Temper	
Bar Size (inch)	Time at temperature (hours)	Cooling medium	Cooling medium temperature - prior to quench	Max bar temperature out of quench	Time at Temperature (hours)	Cooling medium
2.875	1.5	Oil Super S quench oil - 521	90-130ºF	210ºF	2.5	Air
3.375	2				3	
4.0	2				4	

The variable inputs of the DoE, were created from the use of both JMP [48] & Minitab software [49], which are statistical analysis programs designed to optimize the test

conditions for each respective bar size. These are subsequently detailed within Tables 5-3 through 5-5.

Table 5-3: 2.875-Inch Bar Diameter DoE Test Conditions

Test Piece No's	2.875" bar		
	Test Description	Material	Heat Number
AR - Timken	As-received	Timken	90307
AR - SDI	As-received	SDI	A141303

Test Piece No's	2.875" bar				
	Test Description	Material	Heat Number	Hold Temp	Cooling Medium
T1	Air cool	Timken	90307	1700 F	Air
T2	Air cool	Timken	90307	1800 F	Air
T3	Air cool	SDI	A141303	1700 F	Air
T4	Air cool	SDI	A141303	1800 F	Air

Test Piece No's	2.875" bar						
	Test Description	Material	Heat Number	Hold Temp	Cooling Medium	Quench Temp	Cooling Medium
A1-Q	As-Quenched	Timken	90307	1800 F	Air to 1550 F	1550 F	Oil
B1-Q	As-Quenched	SDI	A141303	1700 F	Air to 1550 F	1550 F	Oil
C1-Q	As-Quenched	Timken	90307	1550 F	N/a	1550 F	Oil
E1-Q	As-Quenched	Timken	90307	1600 F	N/a	1600 F	Oil
G1-Q	As-Quenched	Timken	90307	1500 F	N/a	1500 F	Oil

Test Piece No's	2.875" bar							
	Test Description	Material	Heat Number	Hold Temp	Cooling Medium	Quench Temp	Cooling Medium	Temper Temp
A1a-A3a	Quench & Temper	Timken	90307	1800 F	Air to 1550 F	1550 F	Oil	790 F
B1-B3	Quench & Temper	SDI	A141303	1700 F	Air to 1550 F	1550 F	Oil	790 F
C1-C3	Quench & Temper	Timken	90307	1550 F	N/a	1550 F	Oil	790 F
E1-E3	Quench & Temper	Timken	90307	1600 F	N/a	1600 F	Oil	830 F
F1-F3	Quench & Temper	Timken	90307	1600 F	N/a	1600 F	Oil	750 F
G1-G3	Quench & Temper	Timken	90307	1500 F	N/a	1500 F	Oil	830 F
H1-H3	Quench & Temper	Timken	90307	1500 F	N/a	1500 F	Oil	750 F
I1-I2	Quench & Temper	Timken	90307	1550 F	N/a	1550 F	Oil	750 F
J1-J2	Quench & Temper	Timken	90307	1600 F	N/a	1600 F	Oil	790 F

Table 5-4: 3.375- Inch Bar Diameter DoE Test Conditions

Test Piece No's	3.375" bar		
	Test Description	Material	Heat Number
AR - Timken	As-received	Timken	90307

Test Piece No's	3.375" bar				
	Test Description	Material	Heat Number	Hold Temp	Cooling Medium
AC1	Air cool	Timken	90307	1800 F	Air
AC2	Air cool	Timken	90307	1700 F	Air

Test Piece No's	3.375" bar					
	Test Description	Material	Heat Number	Hold Temp	Quench Temp	Cooling Medium
AQ -1600	As-Quenched	Timken	90307	1600 F	1600 F	Oil
AQ -1585	As-Quenched	Timken	90307	1585 F	1585 F	Oil
AQ - 1550	As-Quenched	Timken	90307	1550 F	1550 F	Oil
AQ - 1515	As-Quenched	Timken	90307	1515 F	1515 F	Oil
AQ - 1500	As-Quenched	Timken	90307	1500 F	1500 F	Oil

Test Piece No's	3.375" bar						
	Test Description	Material	Heat Number	Hold Temp	Quench Temp	Cooling Medium	Temper Temp
I1 & I2	Quench & Temper	Timken	90307	1500 F	1500 F	Oil	790 F
J1 & J2	Quench & Temper	Timken	90307	1600 F	1600 F	Oil	790 F
K1 & K2	Quench & Temper	Timken	90307	1550 F	1550 F	Oil	790 F
K3 & K6	Quench & Temper	Timken	90307	1550 F	1550 F	Oil	750 F
K4 & K5	Quench & Temper	Timken	90307	1550 F	1550 F	Oil	830 F
L1 & L2	Quench & Temper	Timken	90307	1515 F	1515 F	Oil	815 F
L3 & L4	Quench & Temper	Timken	90307	1515 F	1515 F	Oil	765 F
M1 & M3	Quench & Temper	Timken	90307	1585 F	1585 F	Oil	815 F
M2 & M4	Quench & Temper	Timken	90307	1585 F	1585 F	Oil	765 F
N1& N2	Quench & Temper	Timken	90307	1570 F	1570 F	Oil	750 F

Table 5-5: 4.0- Inch Bar Diameter DoE Test Conditions

Test Piece No's	4.0" bar		
	Test Description	Material	Heat Number
AR - Timken	As-received	Timken	90307

Test Piece No's	4.0" bar				
	Test Description	Material	Heat Number	Hold Temp	Cooling Medium
AC1	Air cool	Timken	90307	1800 F	Air

Test Piece No's	4.0" bar					
	Test Description	Material	Heat Number	Hold Temp	Quench Temp	Cooling Medium
AQ -1515	As-Quenched	Timken	90307	1515 F	1515 F	Oil
AQ -1550	As-Quenched	Timken	90307	1550 F	1550 F	Oil
AQ - 1585	As-Quenched	Timken	90307	1585 F	1585 F	Oil

Test Piece No's	4.0" bar						
	Test Description	Material	Heat Number	Hold Temp	Quench Temp	Cooling Medium	Temper Temp
O1 & O2	Quench & Temper	Timken	90307	1550 F	1550 F	Oil	790 F
P1 & P2	Quench & Temper	Timken	90307	1585 F	1585 F	Oil	830 F
Q1 & Q2	Quench & Temper	Timken	90307	1515 F	1515 F	Oil	750 F
R1 & R2	Quench & Temper	Timken	90307	1550 F	1550 F	Oil	850 F
S1 & S2	Quench & Temper	Timken	90307	1515 F	1515 F	Oil	830 F
T1 & T2	Quench & Temper	Timken	90307	1585 F	1585 F	Oil	750 F
U1 & U2	Quench & Temper	Timken	90307	1550 F	1550 F	Oil	730 F

5.2.5 Metallurgical Tests

To fully evaluate the respective test bars, various mechanical and metallurgical tests were conducted on test bars before, during and after the heat treatment. These methods of analysis were considered paramount as they would determine the variability / differences throughout the material section thickness, when exposed to different heat treatment conditions. In addition, they would characterize the different respective bar sizes, and enable a comparison of the resultant properties, identifying the influencing factors that produce metallurgical changes within the AISI 4161 H material. The following tests were therefore selected:

- Surface and Through-Thickness Hardness Testing
    - *Taken on the surface and across a transverse slice of the heat-treated bar*
- Tensile Testing
    - *Conducted at the ¼ & ½ thickness locations (bar size dependent)*
- Banding Analysis
    - *Analysed at 10%, ¼, & ½ thickness locations*
- General Microstructure & Phase Distribution - Longitudinal direction
    - *Analysed at 10%, ¼, & ½ thickness locations*
- SEM EDS analysis
    - *Analysed at 10%, ¼, & ½ thickness locations*

With any DoE approach, it is important to remove any systematic errors that can occur by conducting the respective test runs in sequence. To avoid this, a randomized methodology was taken. This is demonstrated within Table 5-6, which summarizes the random test sequence and respective test regime adopted for the 2.875-inch bar (73mm) size. Note, that this experimental philosophy was employed for all bar sizes.

Table 5-6: Test Sequence and Heat Treatment DOE for 2.875-Inch Bar

Operation Sequence	Operation Detail	No. of Test Pieces	Test Piece(s)	Temp. (°F)	Time (hrs.)	Temp. before Quench (°F)	Cooling Medium	Oil Temp. Before Quench (°F)	Max Bar Temp. out of Quench (°F)
1	Rockwell Hardness Test	24	A1 - H3						
2	Hot Working/ Austenise/ Quenching	3	A1 - A3	1800	2	1550	Oil	90 - 130	210
3	Rockwell Hardness Test	3	A1 - A3						
4	Tempering	3	A1 - A3	790	3		Air		
5	Rockwell Hardness Test	3	A1 - A3						
6	Hot Working/ Austenise/ Quenching	3	B1 - B3	1700	1.5	1550	Oil	90 - 130	210
7	Rockwell Hardness Test	3	B1 - B3						
8	Tempering	3	B1 - B3	790	3		Air		
9	Rockwell Hardness Test	3	B1 - B3						
10	Austenise / Quenching	3	D1 - D3	1550	1.5		Oil	90 - 130	210
11	Rockwell Hardness Test	3	D1 - D3						
12	Tempering	3	D1 - D3	790	3		Air		
13	Rockwell Hardness Test	3	D1 - D3						
14	Austenise / Quenching	1	E1	1600	2		Oil	90 - 130	210
15	Rockwell Hardness Test	1	E1						
16	Tempering	1	E1	830	3		Air		
17	Rockwell Hardness Test	1	E1						
18	Austenise / Quenching	1	G1	1500	2		Oil	90 - 130	210
19	Rockwell Hardness Test	1	G1						
20	Tempering	1	G1	830	3		Air		
21	Rockwell Hardness Test	1	G1						
22	Austenise / Quenching	1	E2	1600	2		Oil	90 - 130	210
23	Rockwell Hardness Test	1	E2						
24	Tempering	1	E2	830	3		Air		
25	Rockwell Hardness Test	1	E2						

Operation Sequence	Operation Detail	No. of Test Pieces	Test Piece(s)	Temp. (°F)	Time (hrs.)	Temp. before Quench (°F)	Cooling Medium	Oil Temp. Before Quench (°F)	Max Bar Temp. out of Quench (°F)
26	Austenise / Quenching	1	C1	1550	2		Oil	90 - 130	210
27	Rockwell Hardness Test	1	C1						
28	Tempering	1	C1	790	3		Air		
29	Rockwell Hardness Test	1	C1						
30	Austenise / Quenching	1	F1	1600	2		Oil	90 - 130	210
31	Rockwell Hardness Test	1	F1						
32	Tempering	1	F1	750	3		Air		
33	Rockwell Hardness Test	1	F1						
34	Austenise / Quenching	1	E3	1600	2		Oil	90 - 130	210
35	Rockwell Hardness Test	1	E3						
36	Tempering	1	E3	830	3		Air		
37	Rockwell Hardness Test	1	E3						
38	Austenise / Quenching	1	C2	1550	2		Oil	90 - 130	210
39	Rockwell Hardness Test	1	C2						
40	Tempering	1	C2	790	3		Air		
41	Rockwell Hardness Test	1	C2						
42	Austenise / Quenching	1	C3	1550	2		Oil	90 - 130	210
43	Rockwell Hardness Test	1	C3						
44	Tempering	1	C3	790	3		Air		
45	Rockwell Hardness Test	1	C3						
46	Austenise / Quenching	1	G2	1500	2		Oil	90 - 130	210
47	Rockwell Hardness Test	1	G2						
48	Tempering	1	G2	830	3		Air		
49	Rockwell Hardness Test	1	G2						

Operation Sequence	Operation Detail	No. of Test Pieces	Test Piece(s)	Temp. (°F)	Time (hrs.)	Temp. before Quench (°F)	Cooling Medium	Oil Temp. Before Quench (°F)	Max Bar Temp. out of Quench (°F)
50	Austenise / Quenching	1	H1	1500	2		Oil	90 - 130	210
51	Rockwell Hardness Test	1	H1						
52	Tempering	1	H1	750	3		Air		
53	Rockwell Hardness Test	1	H1						
54	Austenise / Quenching	1	H2	1500	2		Oil	90 - 130	210
55	Rockwell Hardness Test	1	H2						
56	Tempering	1	H2	750	3		Air		
57	Rockwell Hardness Test	1	H2						
58	Austenise / Quenching	1	F2	1600	2		Oil	90 - 130	210
59	Rockwell Hardness Test	1	F2						
60	Tempering	1	F2	750	3		Air		
61	Rockwell Hardness Test	1	F2						
62	Austenise / Quenching	1	F3	1600	2		Oil	90 - 130	210
63	Rockwell Hardness Test	1	F3						
64	Tempering	1	F3	750	3		Air		
65	Rockwell Hardness Test	1	F3						
66	Austenise / Quenching	1	G3	1500	2		Oil	90 - 130	210
67	Rockwell Hardness Test	1	G3						
68	Tempering	1	G3	830	3		Air		
69	Rockwell Hardness Test	1	G3						
70	Austenise / Quenching	1	H3	1500	2		Oil	90 - 130	210
71	Rockwell Hardness Test	1	H3						
72	Tempering	1	H3	750	3		Air		
73	Rockwell Hardness Test	1	H3						

Operation Sequence	Operation Detail	No. of Test Pieces	Test Piece(s)	Temp. (°F)	Time (hrs.)	Temp. before Quench (°F)	Cooling Medium	Oil Temp. Before Quench (°F)	Max Bar Temp. out of Quench (°F)
74	Tensile Test and Rockwell Hardness Test on tensile ends	24	A1 - H3						
75	Through Thickness Hardness	24	A1 - H3						
76	Banding Assessment at 10% dia. below surface, Mid Radius and Centre	8	A1, B1, C1, D1, E1, F1, G1, H1						

End of Table 5-6.

To ensure a prominent level of repeatability was achieved, the heat-treated bars were sectioned and prepared using a standard approach. This was to ensure the test samples were extracted from the same place for each respective test any that any subsequent end-quench effects would be eliminated. Therefore, no specimen used for analysis was taken from a zone 1.5 inches (38mm) from either end of the bar - reference Figure 5-4.

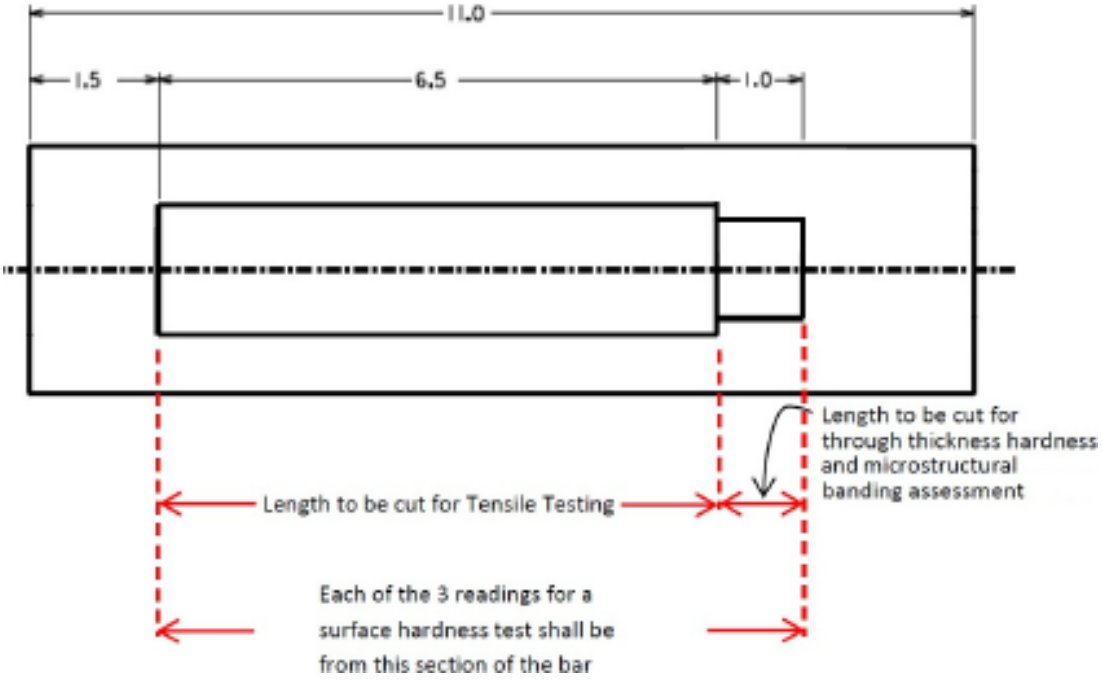

Figure 5-4: Test Bar Drawing Detailing Sample Test Locations

5.3 Results

The results of the DoE testing have been collated into the individual metallurgical test types, which detail the respective values for each bar diameter and heat treatment condition. A comparison is also made across the bar range, with a summary made at the end of each test result section.

Where possible, the use of Minitab [49] has been employed as an analysis tool, to help determine specific trends, and create plots of the resultant values obtained throughout the DoE. This methodology is key in determining the limitations of the material and establishing the optimized conditions that can be achieved for the respective bar diameters and heat treatment conditions. Minitab is a tool that considers the inputs of the DoE, both individually and compounded together; and the effect on the output, which is the (measured material property such as hardness & UTS).

5.3.1 Tensile Testing

Tensile testing was conducted on the Quench and Tempered DoE samples only. Other heat treatment conditions, such as As-Quenched were not considered as the final coil spring product is in the fully heat-treated condition.

The specimens were taken in the longitudinal direction per Figure 5-4, and tested to the requirements of ASTM A370 [60].

The test results list the values for the core location for the 2.875-inch (73mm) test bars, and the mid-radius & core for the 3.375 (85.7mm) & 4.0-inch (101.6mm) samples. The main reason for the additional tests, was due to the low core UTS values achieved for both the 3.375 (85.7mm) & 4-inch (101.6mm) bars, which necessitated the need to test these respective bar sizes at the ¼T position. The test results for the respective bar sizes are detailed within Table 5-7 through Table 5-9.

Table 5-7: Tensile Test Results for the 2.875-Inch Diameter Bar

Bar size	ID	Material	Heat Temp°F	Quench Temp°F	Temper Temp°F	Core yield - Psi	Core UTS - Psi	Core El%	Core RoA%
2.875	A1a	Timken	1800	1550	790	175000	207000	10.4	29.1
2.875	A2a	Timken	1800	1550	790	187500	217000	8.7	24
2.875	A3a	Timken	1800	1550	790	193500	221000	10	28.3
2.875	B1	SDI	1700	1550	790	171900	207000	7.9	17.8
2.875	B2	SDI	1700	1550	790	170200	205000	7.3	22.6
2.875	B3	SDI	1700	1550	790	181300	217000	4.8	10.1
2.875	C1	Timken	1550	1550	790	185800	221000	9.7	27.2
2.875	C2	Timken	1550	1550	790	180900	215000	10	26.9
2.875	C3	Timken	1550	1550	790	179600	213000	11	30.9
2.875	E1	Timken	1600	1600	830	158400	191800	13.7	35.9
2.875	E2	Timken	1600	1600	830	168800	200000	13.5	37.1
2.875	E3	Timken	1600	1600	830	162100	193600	11.2	31.5
2.875	F1	Timken	1600	1600	750	170800	207000	11.5	35.1
2.875	F2	Timken	1600	1600	750	173600	209000	10.4	29.6
2.875	F3	Timken	1600	1600	750	170400	207000	12.1	35.7
2.875	G1	Timken	1500	1500	830	146500	183400	12.7	36.4
2.875	G2	Timken	1500	1500	830	162400	196800	10.8	29.2
2.875	G3	Timken	1500	1500	830	153700	185700	11.2	29.2
2.875	H1	Timken	1500	1500	750	155500	195200	11.3	28.1
2.875	H2	Timken	1500	1500	750	152000	198600	9.8	27.3
2.875	H3	Timken	1500	1500	750	150800	192900	11.1	29.6
2.875	I1	Timken	1550	1550	750	188400	221000	10.8	33.8
2.875	I2	Timken	1550	1550	750	185400	214000	10.2	31.5
2.875	J1	Timken	1600	1600	790	183700	214000	10.4	28.6
2.875	J2	Timken	1600	1600	790	173500	206000	9.4	27.1

Table 5-8: Tensile Test Results for the 3.375-Inch Diameter Bar

Bar size	ID	Material	Heat Temp°F	Quench Temp°F	Temper Temp°F	Core yield - Psi	Core UTS - Psi	Core El%	Core RoA%	0.25T yield - Psi	0.25T UTS - Psi	0.25T El%	0.25T RoA%
3.375	I1	Timken	1500	1500	790	146300	184900	10.5	27.8	149200	184200	14.2	41.1
3.375	I2	Timken	1500	1500	790	153400	192900	10.6	28.3	157800	192700	14	43
3.375	J1	Timken	1600	1600	790	141400	188500	10.5	29.4	156500	191700	13.6	41.1
3.375	J2	Timken	1600	1600	790	134200	175800	12.9	37	157400	190400	12.4	41.4
3.375	K1	Timken	1550	1550	790	148300	187800	11.3	31.2	169800	199700	14.2	39.2
3.375	K2	Timken	1550	1550	790	139200	182500	12	34.6	163300	195500	13	41
3.375	K4	Timken	1550	1550	830	158700	189600	12	33.6	186400	208000	13	42.3
3.375	K5	Timken	1550	1550	830	148600	185300	12.3	37.1	175500	203000	13	42
3.375	K3	Timken	1550	1550	750	157600	199300	9.3	24.6	179200	211000	13.1	42.2
3.375	K6	Timken	1550	1550	750	157900	202000	9	23	172800	207000	11	39
3.375	L1	Timken	1515	1515	815	153500	189800	10.8	28.2	176000	202000	13.3	38.8
3.375	L2	Timken	1515	1515	815	151700	186400	12	30	163000	191900	13.3	43.8
3.375	L3	Timken	1515	1515	765	139000	185100	11.7	31.4	155800	193800	14.2	41.4
3.375	L4	Timken	1515	1515	765	156300	199400	10.2	25.3	159400	198000	12	41
3.375	M1	Timken	1585	1585	815	141300	182000	12	37	155800	190700	13	43
3.375	M3	Timken	1585	1585	815	147400	182100	12.8	34.2	161200	191000	13.3	44.1
3.375	M2	Timken	1585	1585	765	151100	194700	12	35	173800	208000	12	41
3.375	M4	Timken	1585	1585	765	156800	196800	13	34	157000	194600	12.9	42
3.375	N1	Timken	1570	1570	750	162900	199800	9.7	23.4	174600	209000	12.4	39
3.375	N2	Timken	1570	1570	750	137600	180200	13.9	37.3	155800	192200	13.6	42.6

Table 5-9: Tensile Test Results for the 4.0-Inch Diameter Bar

Bar size	ID	Material	Heat Temp°F	Quench Temp°F	Temper Temp°F	Core yield - Psi	Core UTS - Psi	Core El%	Core RoA%	0.25T yield - Psi	0.25T UTS - Psi	0.25T El%	0.25T RoA%
4	O1	Timken	1550	1550	790	154600	190600	11.5	29.6	157400	192700	13.6	38.6
4	O2	Timken	1550	1550	790	143800	180700	13.6	35.2	148400	184400	13.9	42.2
4	P1	Timken	1585	1585	830	150000	182200	10.9	29.7	159700	190100	13.1	39.6
4	P2	Timken	1585	1585	830	138500	174600	12	35	147800	182100	14	44
4	Q1	Timken	1515	1515	750	143900	185900	11	30	161300	201000	14	38
4	Q2	Timken	1515	1515	750	141000	185700	10	27	150200	188900	13	41
4	R1	Timken	1550	1550	850	147000	178800	12	33	156400	185800	13	41
4	R2	Timken	1550	1550	850	157900	187800	13.2	41.1	155500	185800	12.9	35.2
4	S1	Timken	1515	1515	830	137800	173500	12	35	147000	180700	16	44
4	S2	Timken	1515	1515	830	140500	175600	12	35	153400	185100	13	39
4	T1	Timken	1585	1585	750	143500	189000	10.8	30.9	148300	190700	12.3	40.1
4	T2	Timken	1585	1585	750	146100	186900	11.2	29.8	150600	189100	13.6	42.5
4	U1	Timken	1550	1550	730	149200	181000	13	34	162200	191000	14	41
4	U2	Timken	1550	1550	730	143900	186800	11	31.2	154900	193300	15	41.5

5.3.2 Tensile Results - DoE Analysis and Optimisation Study

To determine the effects of the different heat treatment conditions for each experimental bar size, the tensile results detailed within Tables 5-7 to 5-9 were analysed using Minitab. The initial analysis scope was to determine the optimum heat treatment conditions from the DoE that would achieve the desired mechanical properties for the coil spring design.

To determine the optimum conditions, precise response values were used as inputs to the model. These were based on the current company requirements and expected resultant values for the respective bar size:

- Ultimate tensile strength: 210Ksi minimum
- Elongation percentage: 7% minimum
- Reduction of area percentage: 25% minimum
- Hardness Brinell: 421-469 HBW

In addition, to the generation of the respective plots, Minitab creates an empirical formula, which details the mechanical property output (Yield, UTS, El%, RoA% and HBW), for a specific Quench & Temper condition. This is based on the results achieved through the DoE creation and testing. The values for each output (e.g. UTS) have a specific formula, which includes coefficient constants and factors; which when compounded and added together give the actual mechanical property values for that specific heat treatment condition; as described in Figure 5-5.

Term	Coefficient
Constant	1603560
Quench	-477.62
Temper	-2544.64
Quench*Quench	-0.225624
Temper*Temper	0.118056
Quench*Temper	1.47321

Formula UTS =
1603560 + (-477.62*Quench Temp) + (-2544.64*Temper Temp)
+ (-0.225624*(Quench Temp * Quench Temp)
+(0.118056*(Temper Temp*Temper Temp) +
(1.47321*(Quench Temp*Temper Temp)

If you select 1550°F Quench temperature & 790°F Temper temperature:
UTS = 188546 psi

Figure 5-5: Worked Example - Determining Mechanical Properities as a Function of Heat Treatment Conditions

The results generated from the 2.875-inch (73mm) bar study have established that the design requirements have been met at the ½T core position, with optimization plot demonstrating that the minimum 210 Ksi requirement has been exceeded, with all other properties being satisfied. This model has also highlighted that the optimum mechanicals have been achieved at a respective Quench and Temper temperature of 1564°F & 751°F - see Figure 5-6.

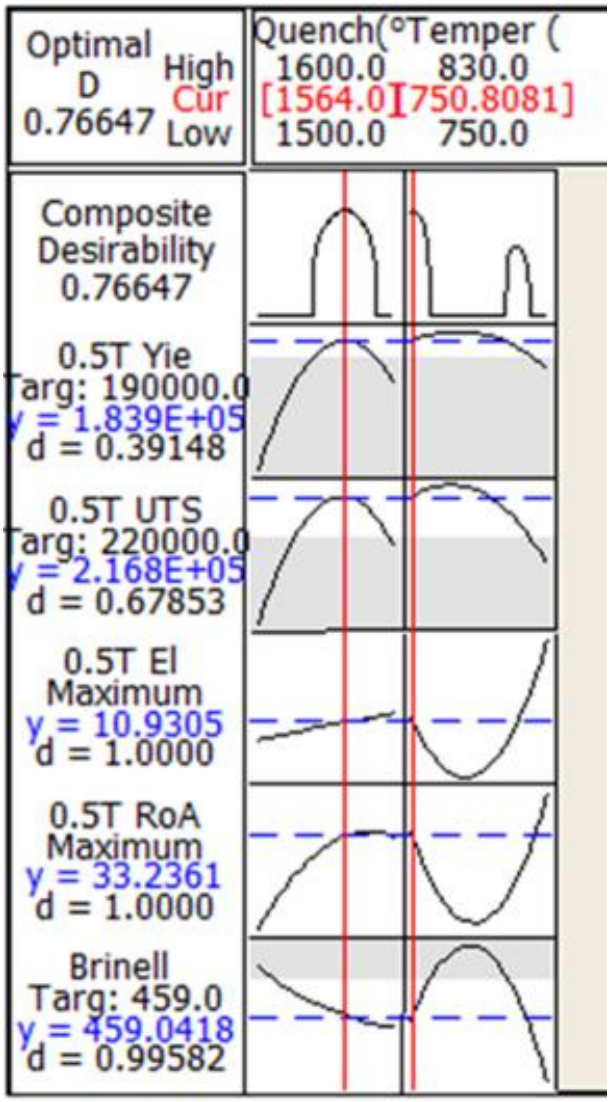

2.875-inch ½T - All mechanical values	
Brinell HBN	459
Yield Psi	183900
UTS Psi	216800
Yield / UTS ratio	0.85
El%	10.9
RoA%	33.2
Optimum Quench Temp °F	1564
Optimum Temper Temp °F	751

Figure 5-6: Optimization Plot for 2.875-Inch Bar at the ¼T Location

The optimization plots for the 3.375-inch (85.7mm) bar have established that the desired engineering UTS requirement of 210,000psi cannot be met - see Figure 5-7 (red arrows). This is evident from the detailed plot, where values of 191,000 and 203,800psi were achieved for the respective ½T and ¼T positions. The results have also established that over the DoE quench and temper range, there is a marked difference in the achievable maximum yield and UTS from the ¼T to ½T core position.

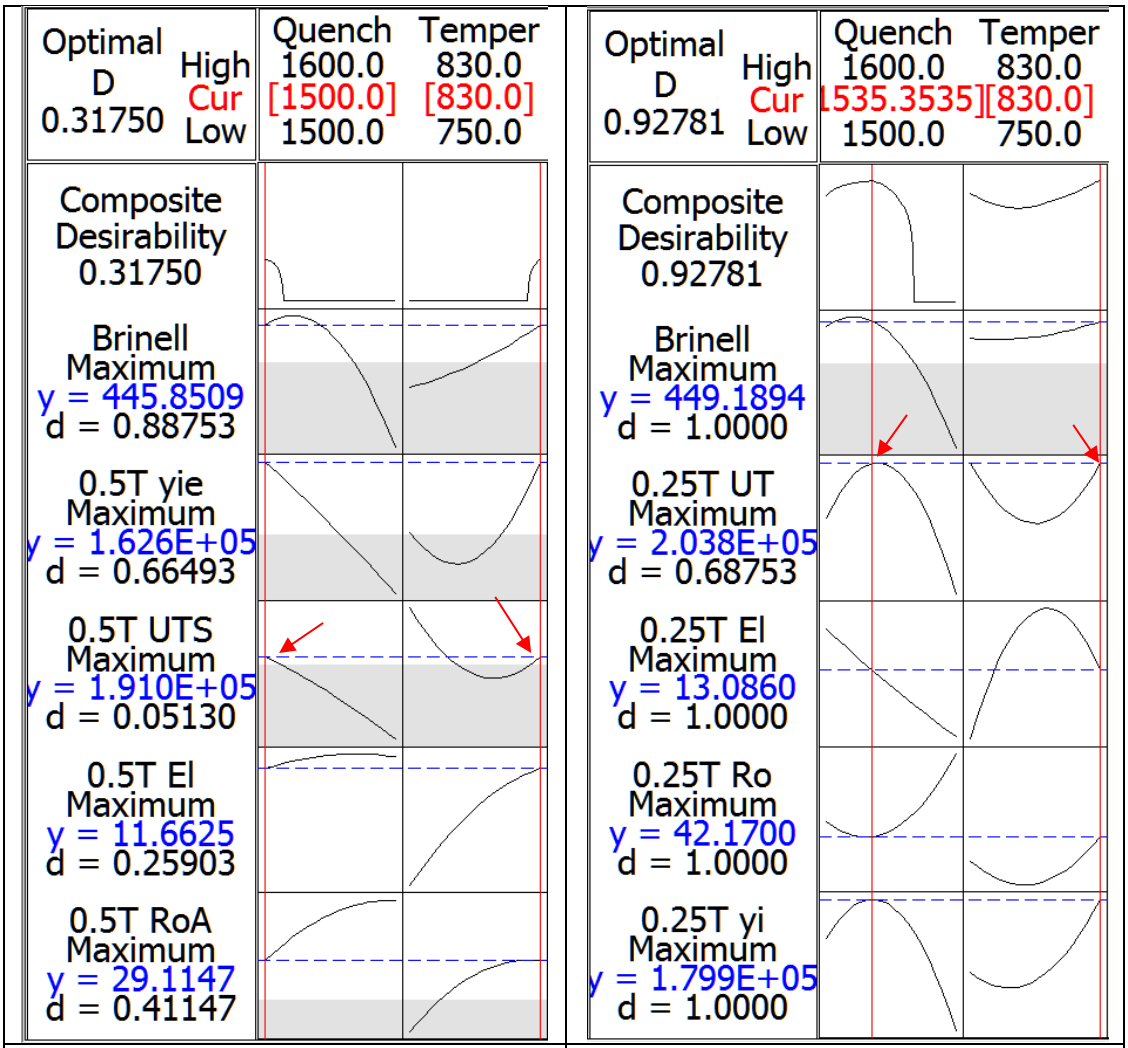

3.375-inch ½T - All mechanical values		3.375-inch ¼T - All mechanical values	
Summary		Summary	
Brinell HBN	445	Brinell HBN	449
Yield Psi	162600	Yield Psi	179900
UTS Psi	191000	UTS Psi	203800
Yield / UTS ratio	0.85	Yield / UTS ratio	0.88
El%	11.7	El%	13.1
RoA%	29.1	RoA%	42.2
Optimum Quench Temp °F	1500	Optimum Quench Temp °F	1535
Optimum Temper Temp °F	830	Optimum Temper Temp °F	830

Figure 5-7: Optimization Plot for 3.375-inch bar at both the ½ & ¼T locations

Comparing the 3.375-inch (85.7mm) results, the optimization plots for the 4.0-inch (101.6mm) bar, do not produce values that meet the minimum UTS requirement. In addition, the Yield / UTS ratio has reduced, from an average of 0.87 to 0.80. This means that the difference between the yield and UTS has increased as the respective bar diameter has changed from 3.375 (85.7mm) - 4.0 inches (101.6mm). This would suggest that the sectional thickness and through thickness metallurgical properties have a direct influence on the response to the respective heat treatment conditions - see Figure 5-8.

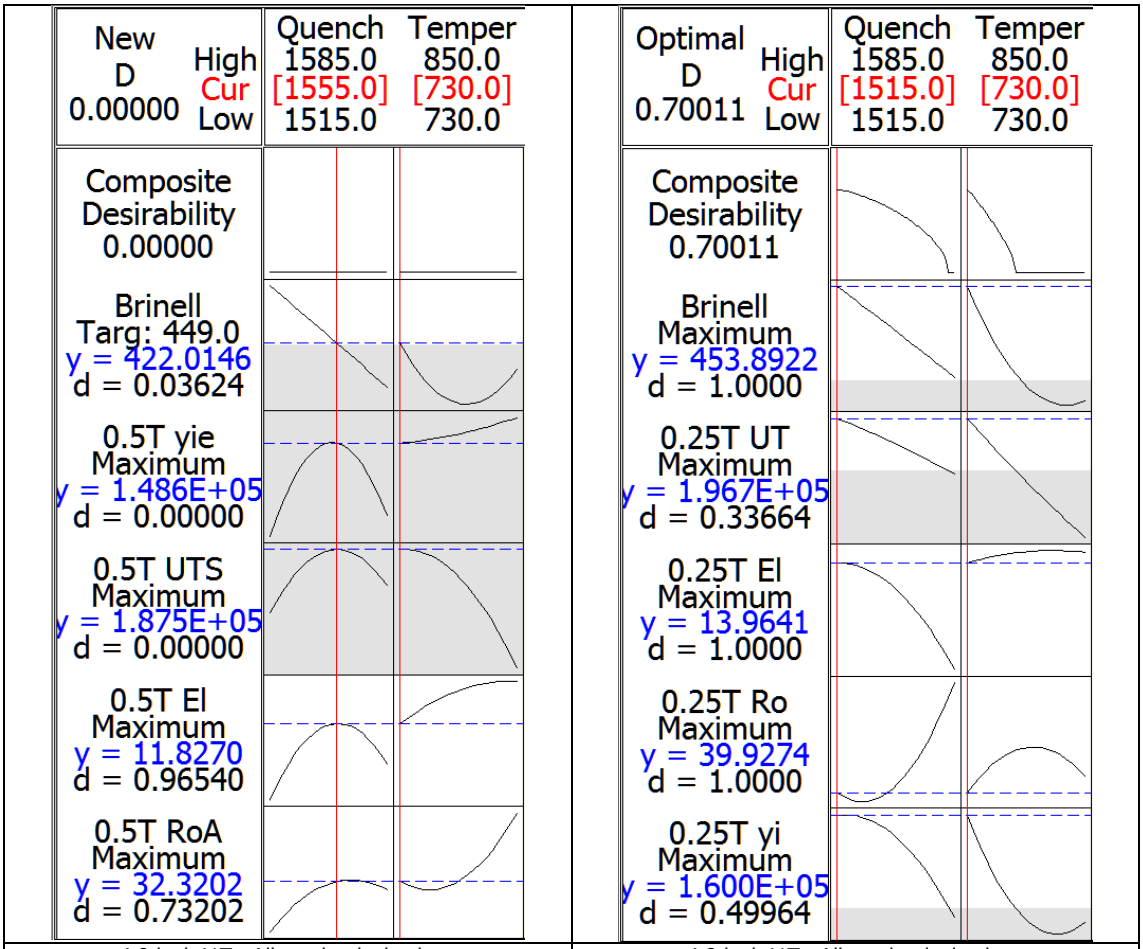

4.0-inch ½T - All mechanical values		4.0-inch ¼T - All mechanical values	
Summary		Summary	
Brinell HBN	422	Brinell HBN	454
Yield Psi	148600	Yield Psi	160000
UTS Psi	187500	UTS Psi	196700
Yield / UTS ratio	0.79	Yield / UTS ratio	0.81
El%	11.8	El%	14.0
RoA%	32.3	RoA%	39.9
Optimum Quench Temp °F	1555	Optimum Quench Temp °F	1515
Optimum Temper Temp °F	730	Optimum Temper Temp °F	730

Figure 5-8: Optimization Plot for 4.0 -inch bar at both the ½ & ¼T locations

5.3.3 Tensile Trends / Analysis - UTS & Yield

In addition to determining the optimized conditions, the results were analysed to determine the effect of the different heat treatment conditions across the full bar range. This involved assessing the effect of both the quench and temper conditions combined; and as individual inputs.

The results from the DoE, have confirmed that both the UTS and Yield reduce when the bar diameter increases form 2.875 - 4.0-inch (73 - 101.6mm). This trend is applicable for both the ½T-core & ¼T positions. It is also apparent that greater mechanical properties are achieved at the ¼T location - see Figure 5-9 and Figure 5-10.

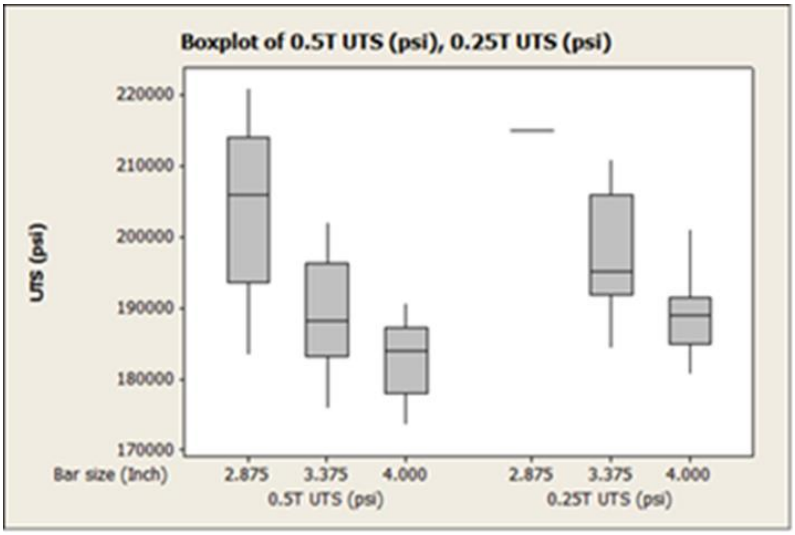

Figure 5-9: Boxplot of UTS values versus bar diameter at ½ and ¼T locations

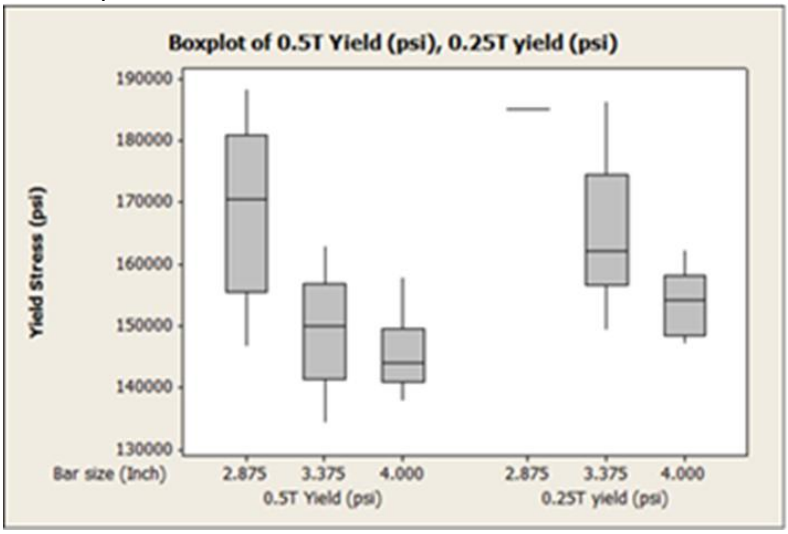

Figure 5-10: Boxplot of Yield values versus bar diameter at ½ and ¼T locations

The median result, (horizontal line) within each boxplot (Figure 5-9 and Figure 5-10), has shown that a higher UTS / Yield delta exists, from the 2.875-inch (73mm) values to that of the 3.375" & 4-inch results. Whereas the delta between the respective 3.375" (85.7mm) and 4.0" (101.6mm) bars is much less. This is further confirmed when comparison is made between the mean values taken from all the tensile results. This is demonstrated within Table 5-10.

Table 5-10: Average Tensile Results

Location	Bar Dia. [inch]	Yield [psi]	UTS [psi]	Elongation [%]	Reduction of Area [%]
0.5T	2.875	170832	205000	10.9	30.6
0.5T	3.375	149160	189245	11.4	31.1
0.5T	4.000	145550	182793	11.7	32.6
0.25T	3.375	165015	197720	13.1	41.5
0.25T	4.000	153793	188621	13.7	40.6

5.3.3.1 Quench

The analysis has also confirmed that the Quench temperature has a direct influence on the resultant mechanical values achieved for each bar size. Although the same trend in terms of UTS / Yield reduction exists across the material, the resultant values increase / decrease in respect to the quench temperature selected. This is confirmed within Figures 5-11 to 5-16, which demonstrates how the mechanical properties for a given bar thickness (½ & ¼T) and quench temperature changes.

An example is given by taking the 3.375-inch (85.7mm) bar at the ¼T position. The respective median UTS changes from approximately 195,000 Psi - 204,000 Psi - 192000 Psi, across the respective temperatures of 1515, 1550 & 1585°F - see Figures 5-11 to 5-16.

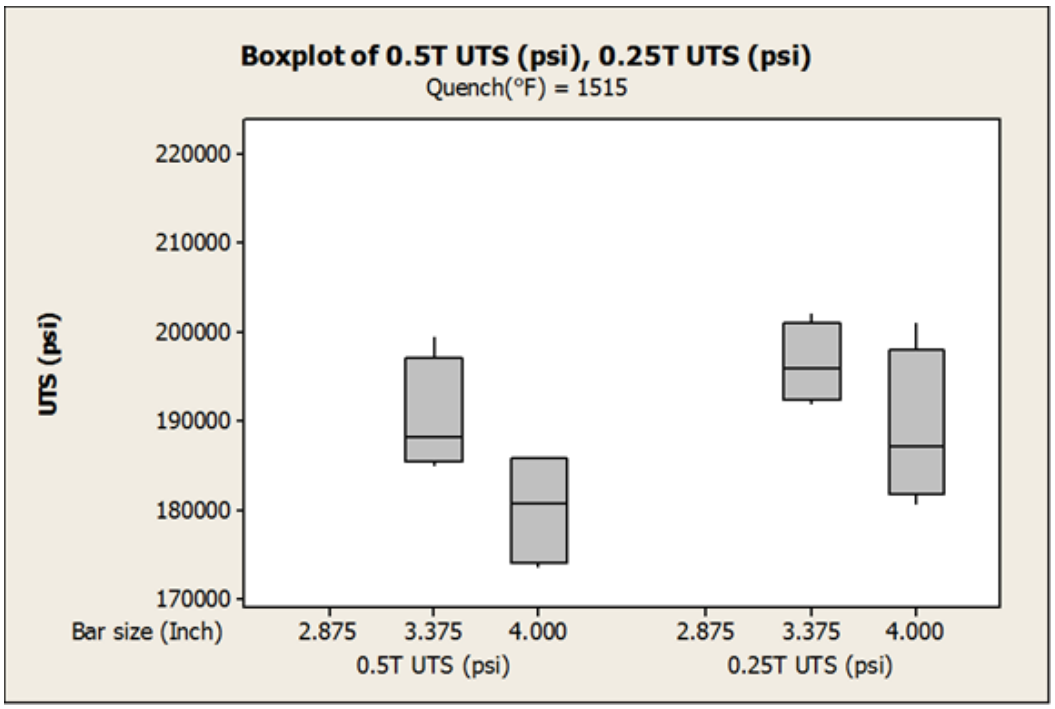

Figure 5-11: Boxplot of UTS for 3.375 & 4.0-inch bars Quenched at 1515°F

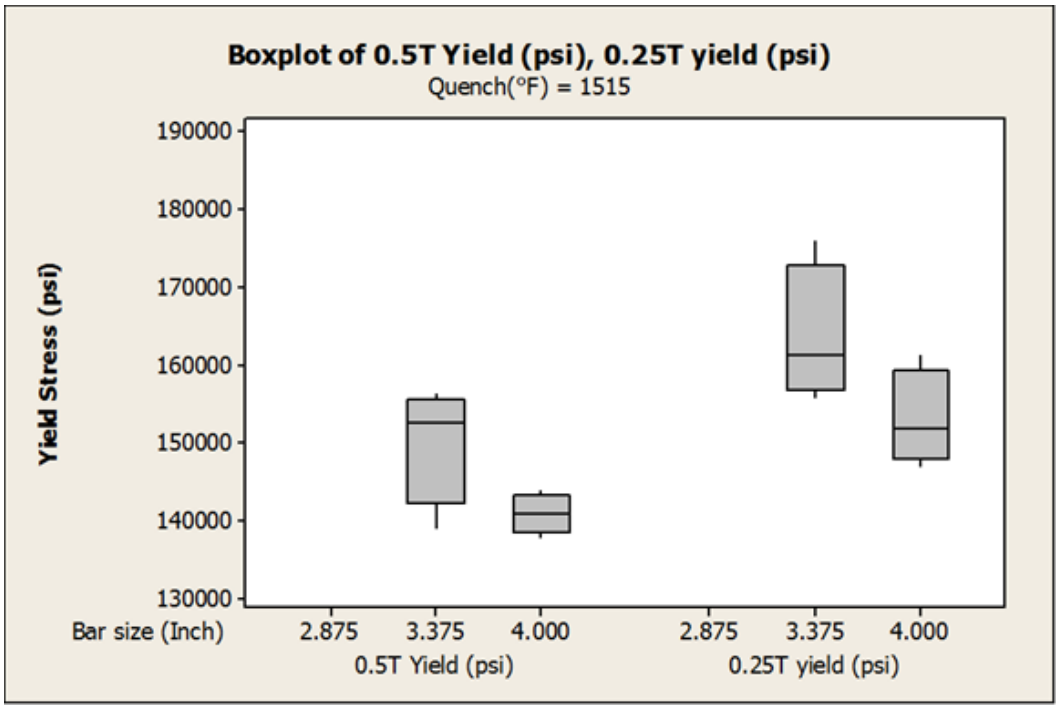

Figure 5-12 Boxplot of Yield for 3.375 & 4.0-inch bars Quenched at 1515°F

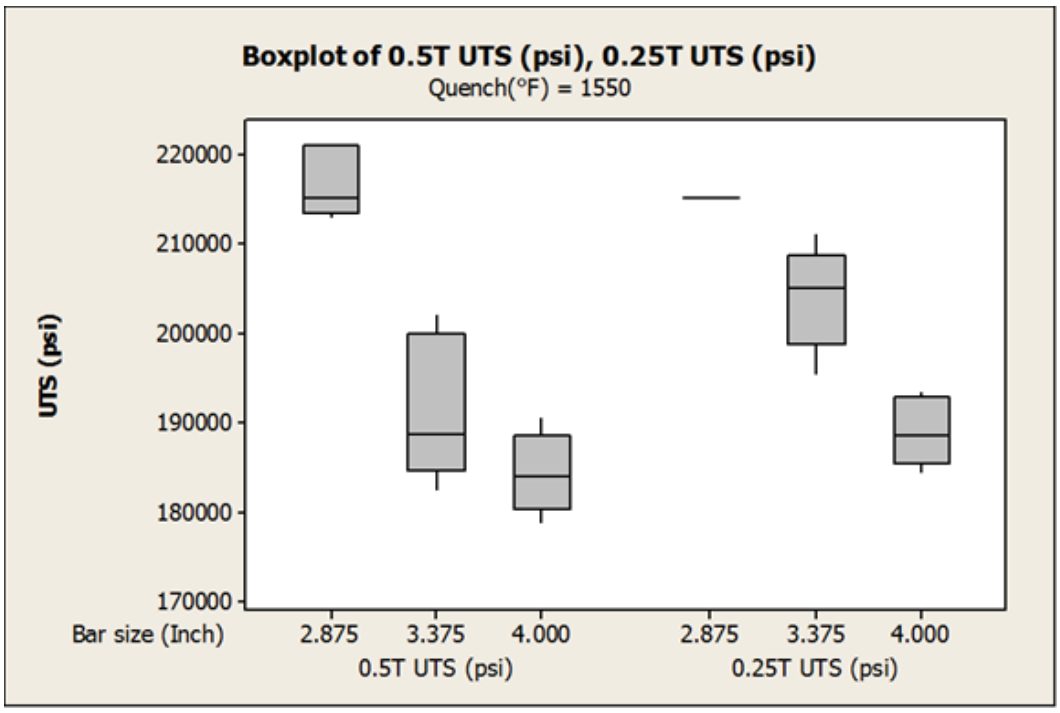

Figure 5-13: Boxplot of UTS for all bars Quenched at 1550°F

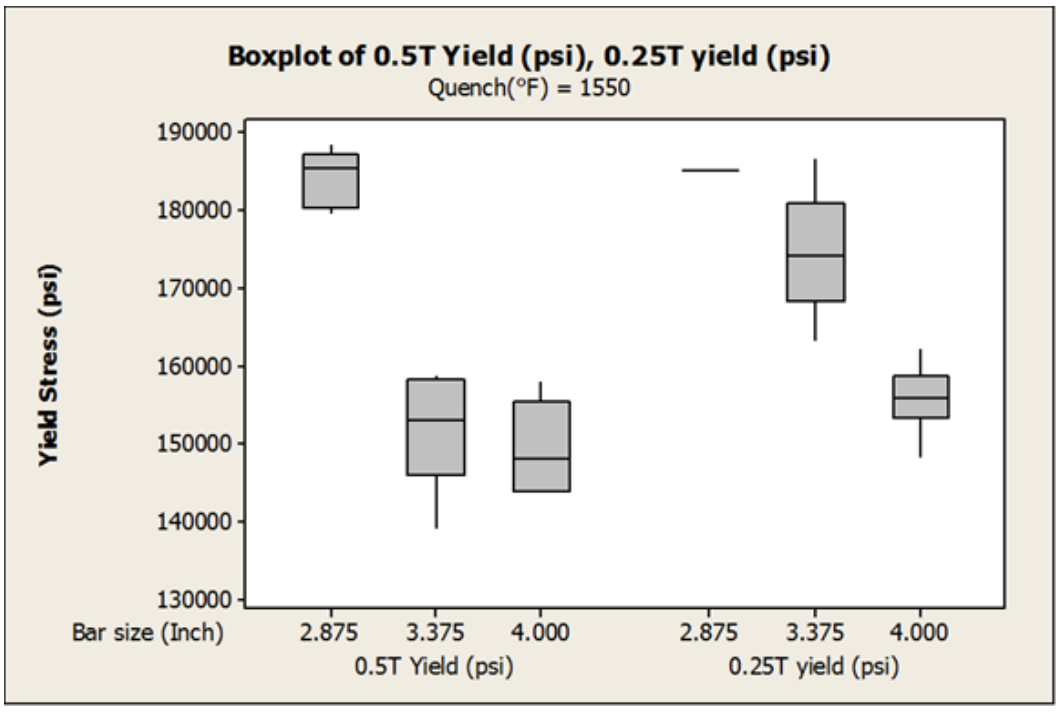

Figure 5-14: Boxplot of Yield for all bars Quenched at 1550°F

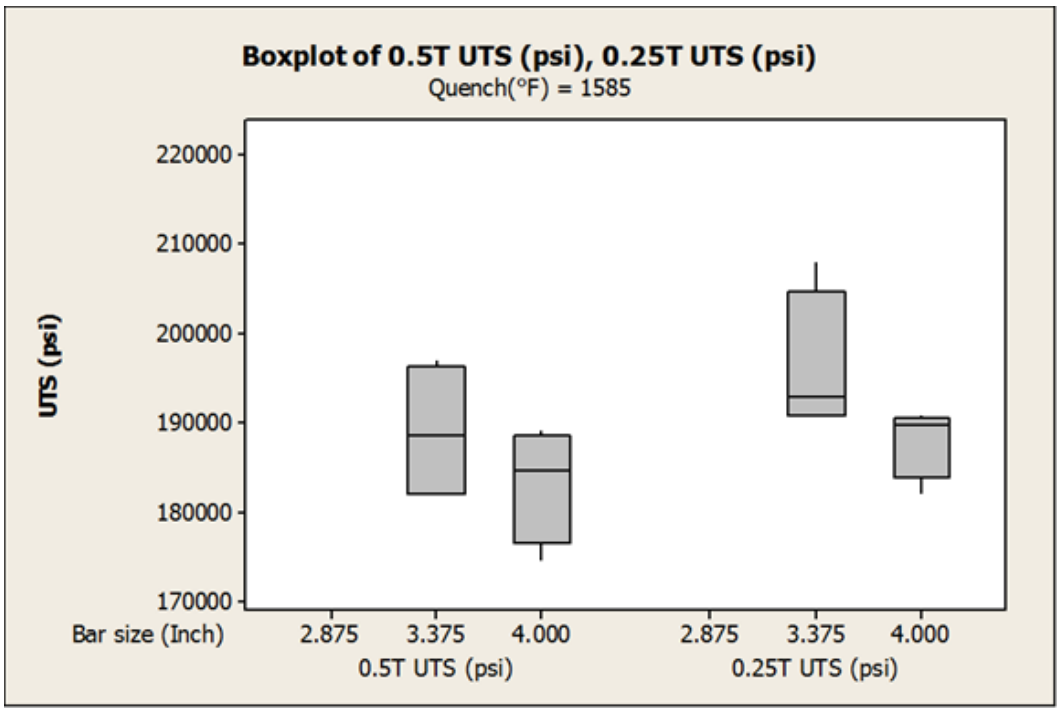

Figure 5-15: Boxplot of UTS for 3.375 & 4.0-inch bars Quenched at 1585°F

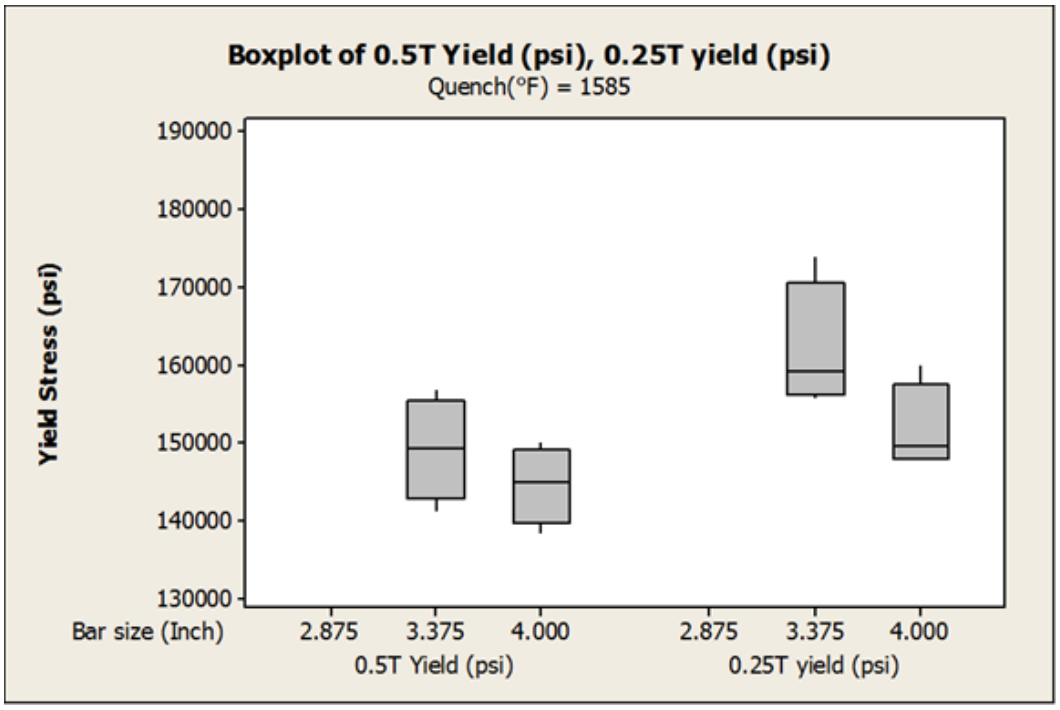

Figure 5-16: Boxplot of Yield for 3.375 & 4.0-inch bars Quenched at 1585°F

The Minitab analysis has also identified that an optimum quench temperature of 1550°F, achieved the highest UTS / Yield values across all the bar sizes and at the respective ¼T & ½T locations, see Figures 5-17 to 5-20. It must be noted however, that the 1550°F optimum temperature is for UTS / Yield only, which will change when trying to satisfy all the mechanical property requirements as detailed within Section 5.3.2 - full optimization plots.

In addition, the ½T core plot has demonstrated that the 2.875-inch bar has responded to a greater extent over the quench temperature range. This is demonstrated by the deep bell type curve exhibited within Figures 5-17 and 5-19. The 3.375-inch bar results however, are less affected in terms of UTS / Yield change across the respective temperature range, with the 4.0-inch exhibiting a subtle difference, with the least effect driven by changes in quench temperature.

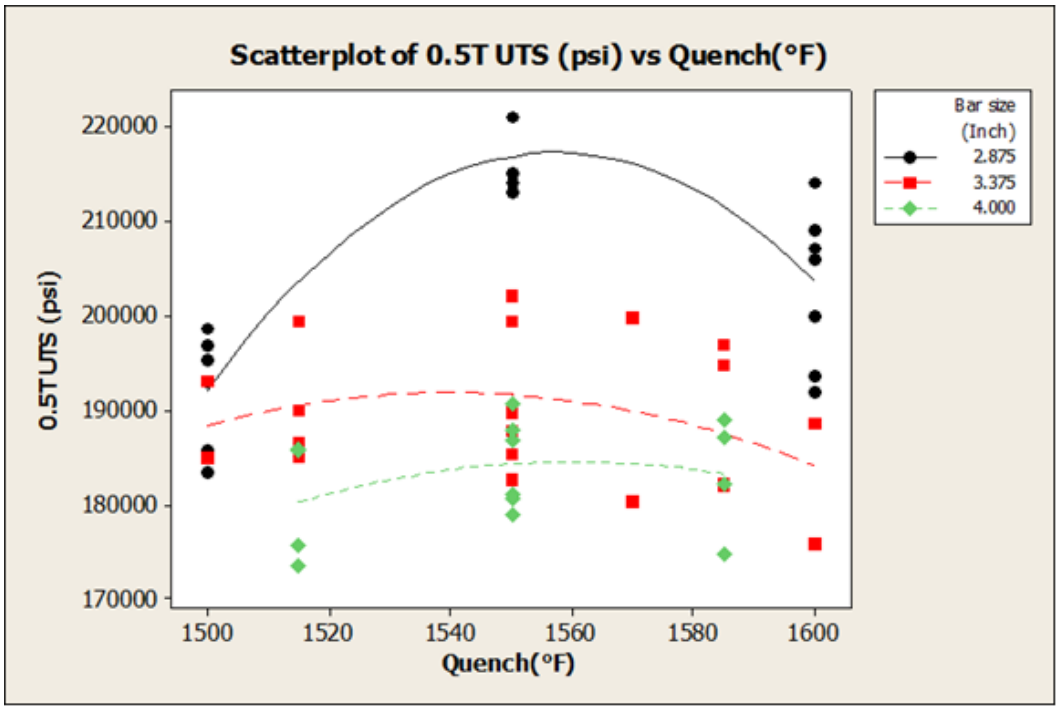

Figure 5-17: Quadratic Analysis Plot of Quench Temperature v UTS values at ½T

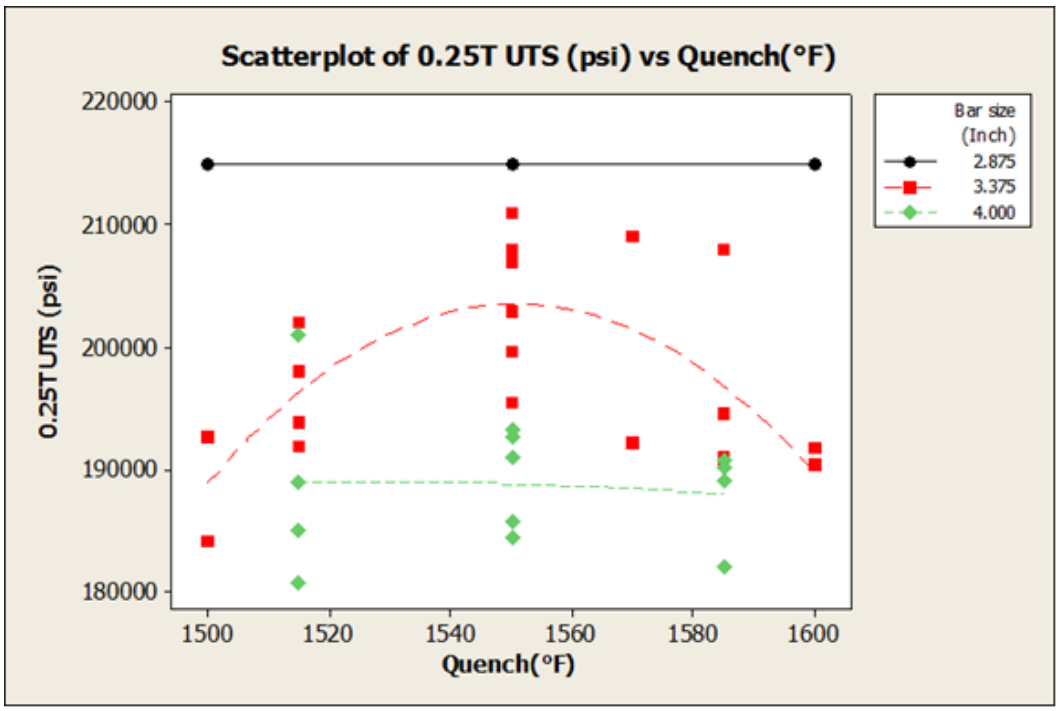

Figure 5-18: Quadratic Analysis Plot of Quench Temperature v UTS values at ¼T

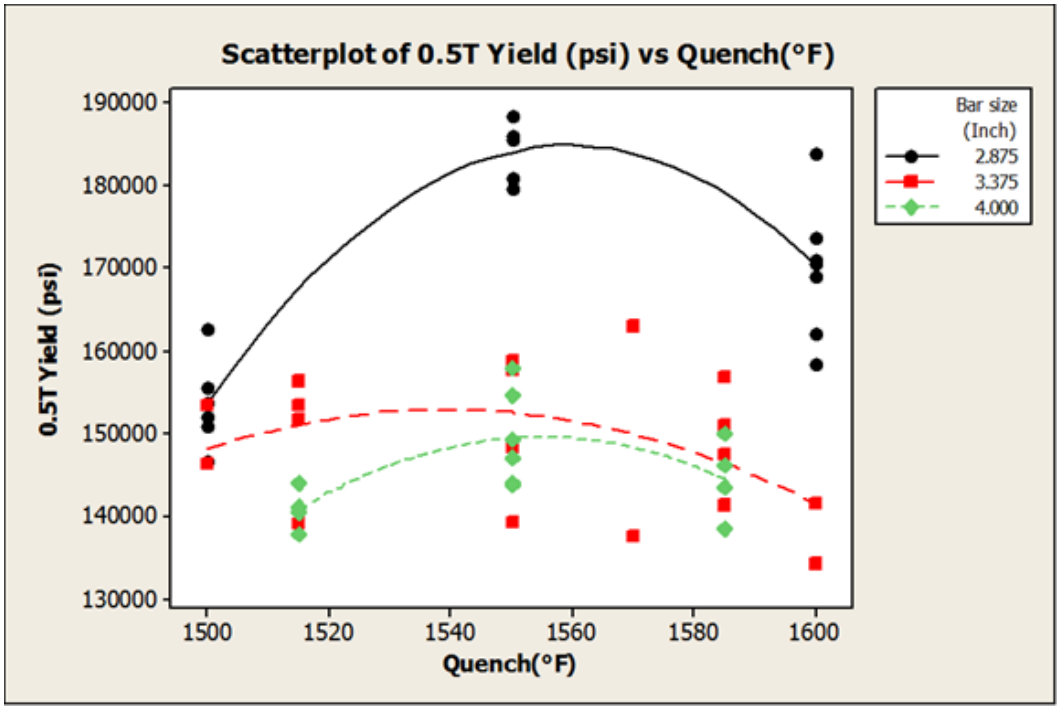

Figure 5-19: Quadratic Analysis Plot of Quench Temperature v Yield values at ½T

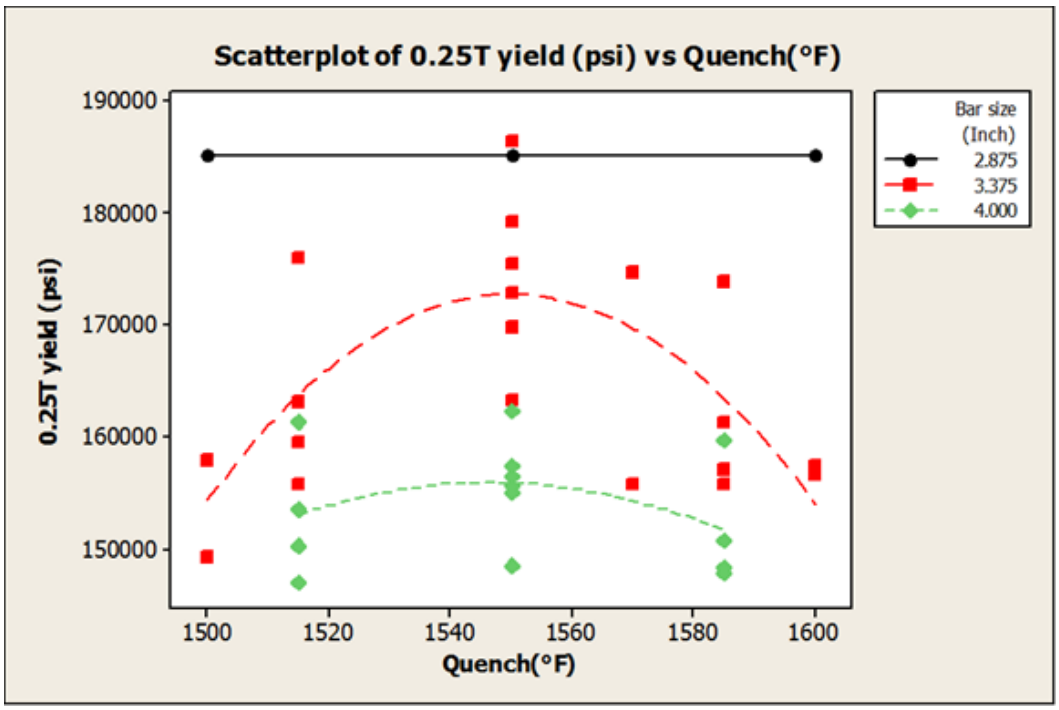

Figure 5-20: Quadratic Analysis Plot of Quench Temperature v Yield values at ¼T

The same can be said about the ¼T results, except for the 3.375-inch plot. 1550°F is the optimum temperature; however, the shape of the 3.375-inch plot is more of a bell curve compared to that achieved at the ½T - core results. This suggests that the quench temperature has an impact on the UTS / Yield results up to the ¼T location; which reduces as the sectional thickness increases towards the core location.

5.3.3.2 Temper

The analysis of the results detailed within Tables 5-7 to 5-9 confirmed that the Temper temperature has a direct influence on the resultant mechanical values achieved for each bar size. This is demonstrated within the boxplots presented within Figures 5-21 to 5-26.

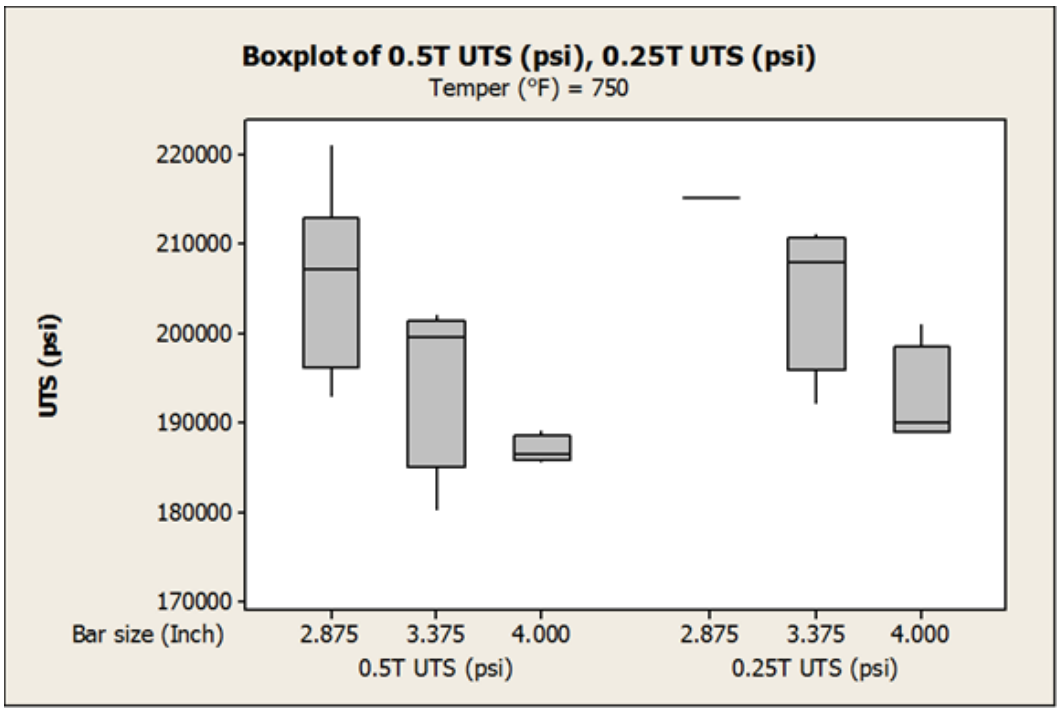

Figure 5-21: Boxplot of UTS for all bar sizes Tempered at 750°F

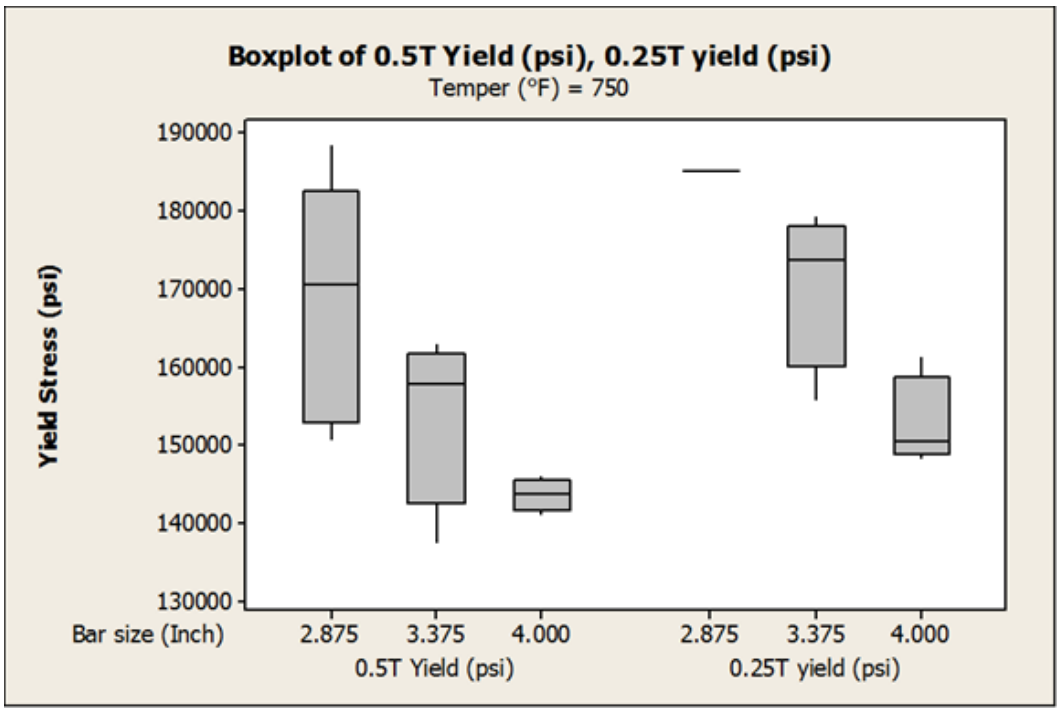

Figure 5-22: Boxplot of Yield for all bar sizes Tempered at 750°F

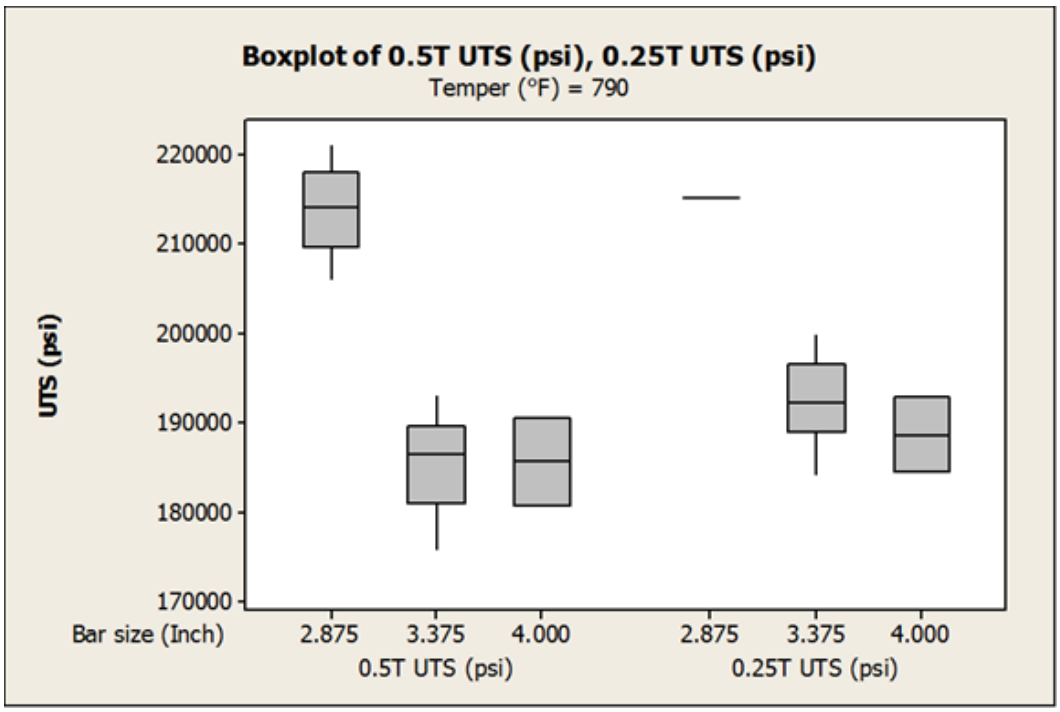

Figure 5-23: Boxplot of UTS for all bar sizes Tempered at 790°F

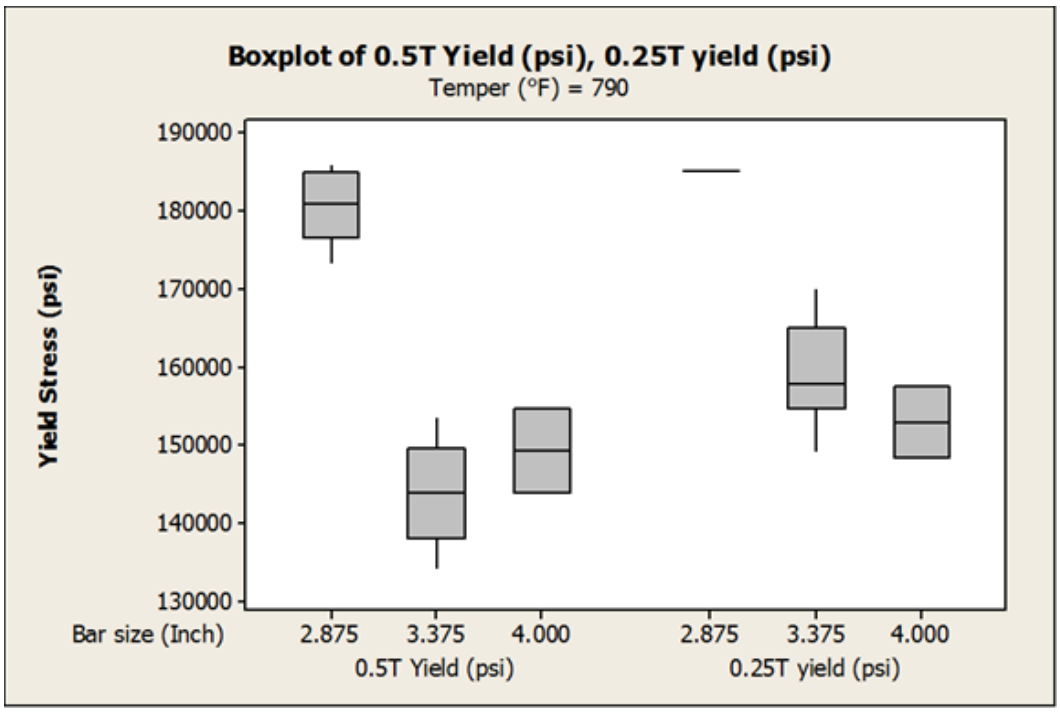

Figure 5-24: Boxplot of Yield for all bar sizes Tempered at 790°F

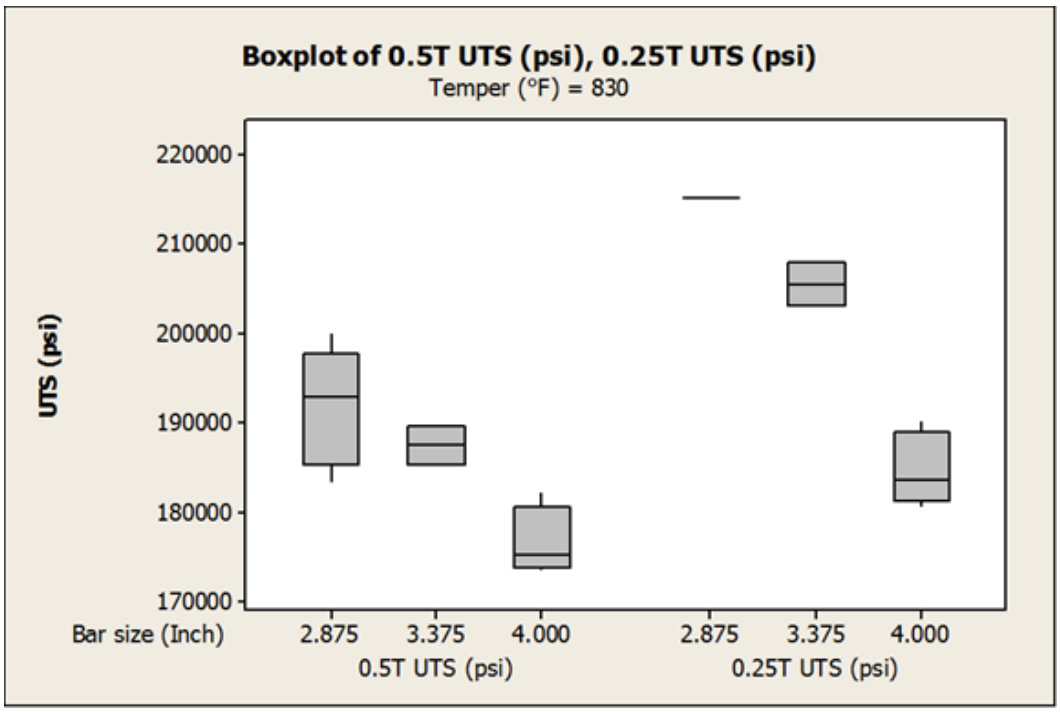

Figure 5-25: Boxplot of UTS for all bar sizes Tempered at 830°F

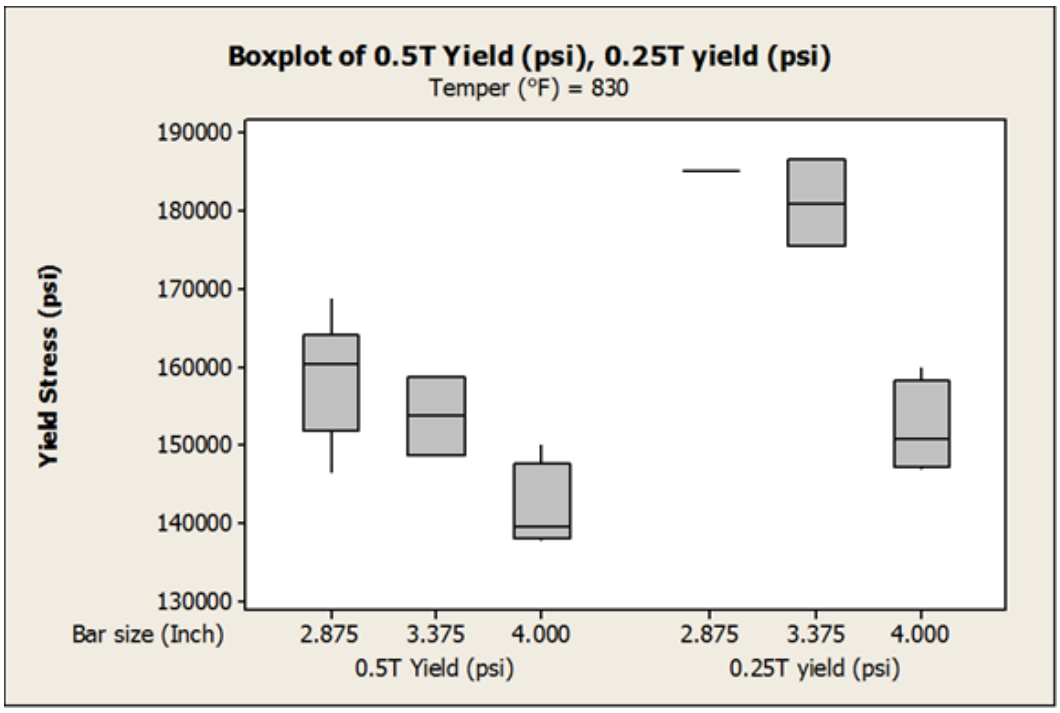

Figure 5-26: Boxplot of Yield for all bar sizes Tempered at 830°F

Compared to the quench analysis results; the tempering temperature has a direct influence on the UTS & Yield properties. In all cases (bar diameter) the resultant values increase form the ½T to ¼T location, regardless of the Tempering temperature selected - see Figures 5-21 to 5-26.

However, the Tempering temperature relationship with the resultant mechanical properties differs across the bar range, especially with the 2.875-inch material at ½T location. This is depicted by Figures 5-27 & 5-28, which reveal a quadratic bell curve produced from the DoE results. Distinct from the other bar sizes, the 2.875-inch material exhibited an optimum UTS / Yield at 790°F, which is at the mid-Tempering temperature - see Figures 5-27 & 5-28.

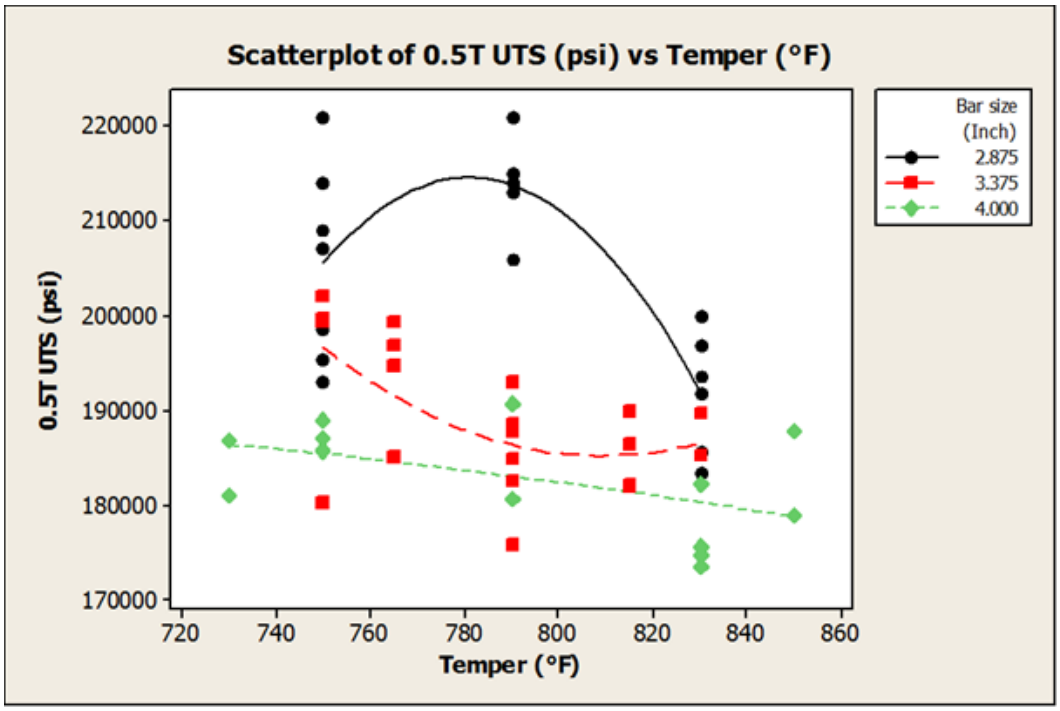

Figure 5-27: Scatterplot of Tempering temperature v UTS at ½T

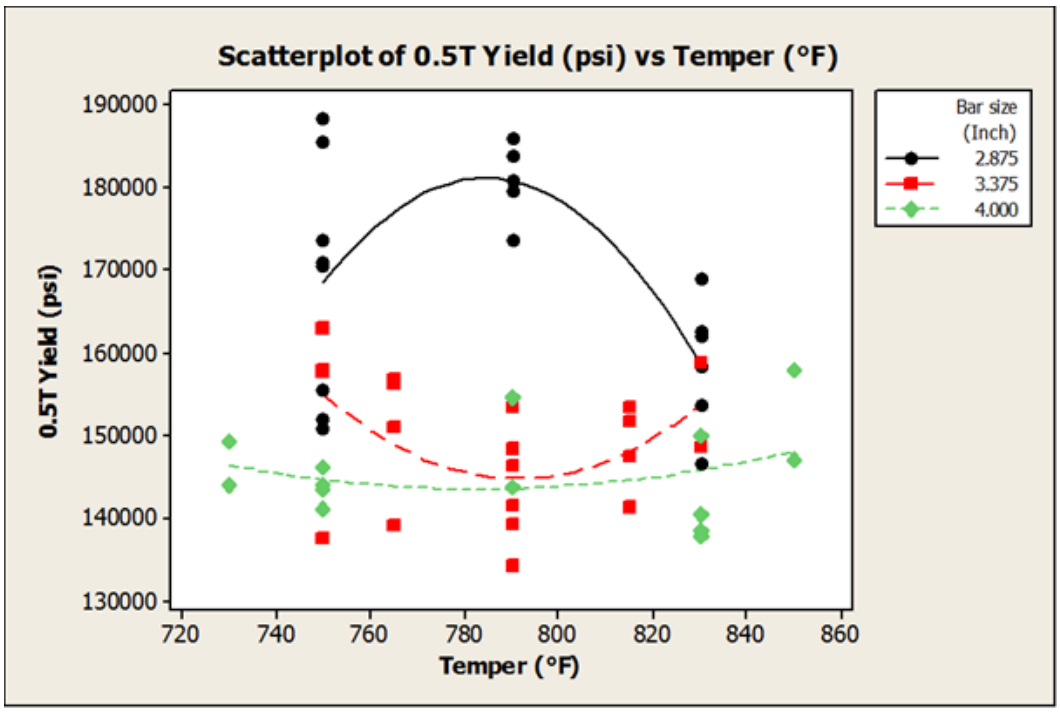

Figure 5-28: Scatterplot of Tempering temperature v Yield at ½T

The 3.375-inch bar results followed an opposing trend, with the results tracking an inverted curve, with the lowest mechanical properties produced at the mid temperature. However, the severity of the heat treatment response was more apparent at the ¼T location with maximum values achieved at either end of the tempering temperature range - see Figures 5-29 and 5-30.

The 4.0-inch results were responsive to the various temper conditions, however the resultant values changed subtly over a linear transition across the exposed temperature range - see Figures 5-27 to 5-30.

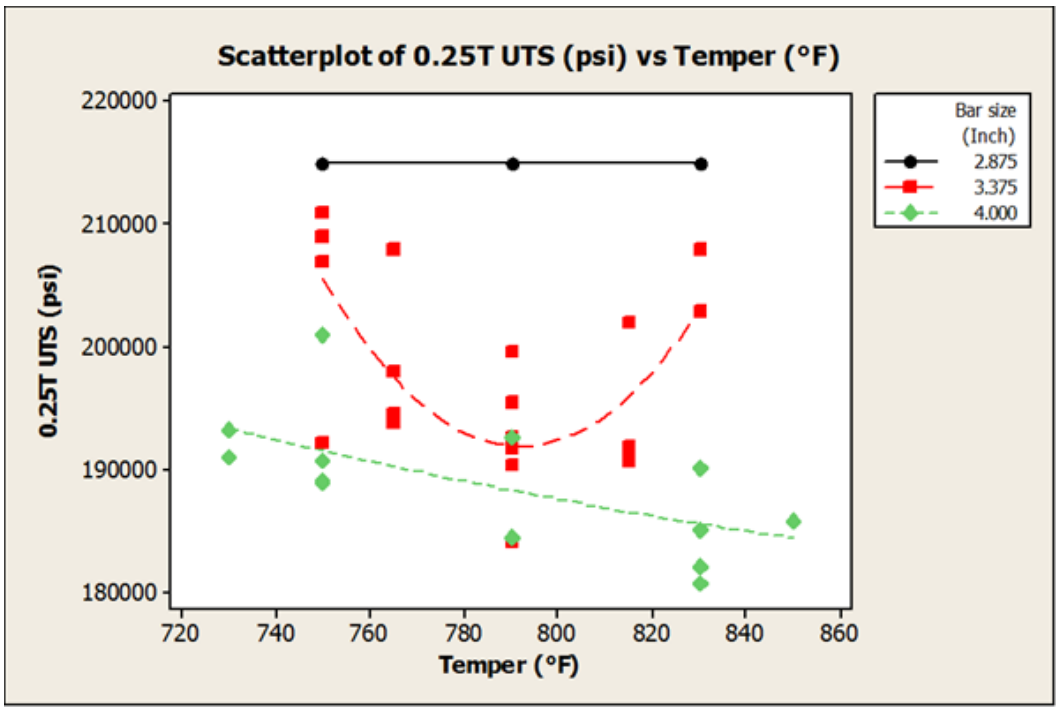

Figure 5-29: Scatterplot of Tempering temperature v UTS at ¼T

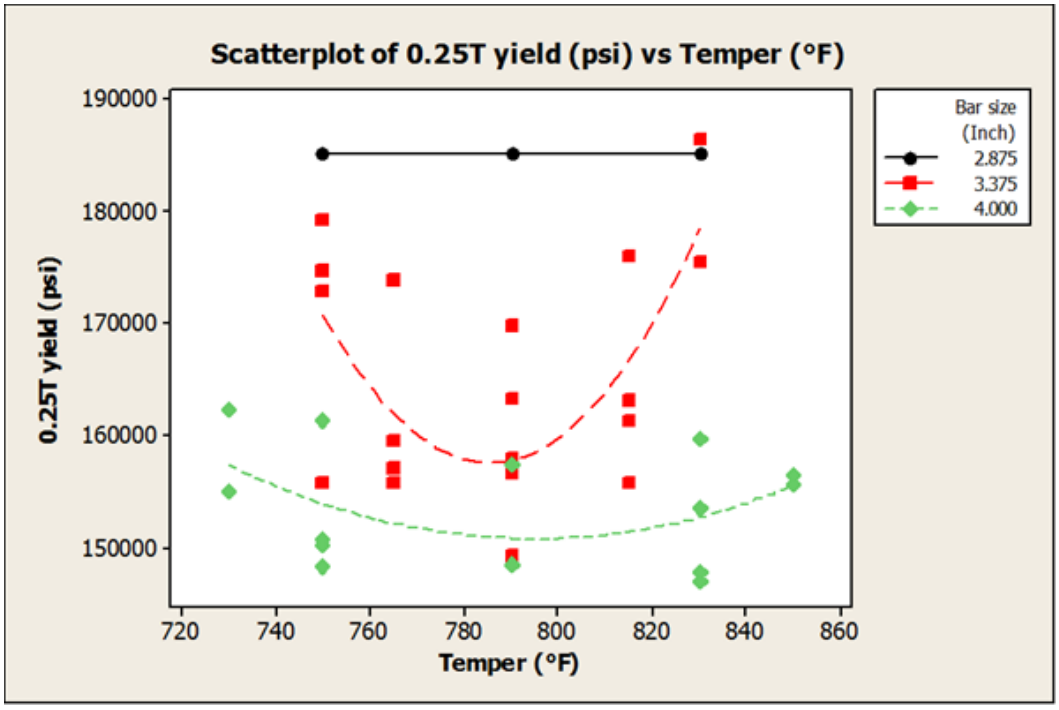

Figure 5-30: Scatterplot of Tempering temperature v Yield at ¼T

5.3.4 Tensile Testing Summary

The DoE has enabled a true understanding of the achievable mechanical properties for the AISI 4161H material over a bar diameter range of 2.875 (73mm) to 4.0-inches (101.6mm).

This information is paramount for both current and future designs, because:

- The maximum diameter used for subsea applications to date has been 2.875-inches.
- There is a requirement to understand if larger diameter coil springs can deliver the required load / stress values for higher pressure / temperature applications.
    - This information is needed for actuator design purposes, due to the increased drag force associated with larger bore valves (friction to overcome between the gate / seat).
- Industry standards dictate that the maximum stress level of the coil spring should be 56% of the UTS.
    - Therefore, any reduction in tensile strength for a given design, will result in an increase in the resultant stress level, which requires the respective coil spring design to be changed to meet industry requirements.

To date, TechnipFMC design standards, have set the required mechanical property requirements to 210Ksi minimum & 421-469 HBN (45-49HRC) respectively. This governance is for the material in the final heat-treated condition (Quenched and Tempered), and covers bar / coils springs up to a diameter of 2.875-inches. However, the DoE has enabled a full understanding of the mechanical properties up to and including 4-inches.

The results throughout the analysis phase have been assessed by the means of Minitab software, which has allowed the generation of material property values.

In summary, the DoE has established the following findings:

- In all cases the resultant UTS / Yield values are greater at the ¼T mid-radius location compared to the ½T core.
- The UTS / Yield strength reduces as the bar diameter increases from 2.875 - 4.0 inches. This was applicable for all heat treatment conditions assessed.
- Both the quench and tempering temperature have a direct influence on the resultant mechanical properties. This is the case as individual inputs and as both processes combined.
- Each bar size has an optimum set of heat treatment conditions, (Quench and Temper temperature), which will produce the maximum mechanical property values at the specific through thickness location - Reference Table 5-11.

Table 5-11: Maximum Achievable Mechanical Properties - Optimization Conditions

Bar Size - inch	Location	UTS Psi	Yield Psi	RoA %	El%	HBN	Quench °F	Temper °F
2.875	½T - Core	2168000	183900	33.2	10.9	459	1564	751
3.375	½T - Core	191000	162600	29.1	11.7	445	1500	830
3.375	¼T - Mid-radius	203800	179900	42.2	13.1	449	1535	830
4	½T - Core	187500	148600	32.3	11.8	422	1555	730
4	¼T - Mid-radius	196700	160000	39.9	14.0	454	1515	730

- The average mechanical properties in terms of UTS / Yield, across all heat treatment conditions have been identified. As expected the resultant values are less than the optimized conditions - Reference Table 5-12.

Table 5-12: Average Tensile Properties for all DoE Heat Treatment Conditions

Bar Size - inch	Location	UTS Psi	Yield Psi	RoA %	El%
2.875	½T - Core	205000	170832	30.6	10.9
3.375	½T - Core	189245	149160	31.1	11.4
3.375	¼T - Mid-radius	197720	165015	41.5	13.1
4	½T - Core	182793	145550	32.6	11.7
4	¼T - Mid-radius	188621	153793	40.6	13.7

Although the optimization plots have established the maximum achievable set of mechanical properties, the operating window is narrow in terms of process control (one temperature input for both quench & temper operations). Therefore, an

understanding of the consistency of the resultant values in a shop floor environment must be considered, as the manufacturing processes utilise manual intervention when transferring parts from the furnace to the quench tank. This along with the average results achieved, requires the OEM to have an operating window that consistently produces a minimum UTS and hardness value required by TechnipFMC. To deal with these considerations, a series of Heat Treatment Contour / Surface plots have been created. This identifies the operating window for a given mechanical property target (e.g. UTS / HBN). These are presented within Figure 5-31 to Figure 5-35, and summarized within Table 5-13.

Table 5-13: Target Properties for Each Bar Size V Heat Treatment Operating Window

Bar Size - inch	Location	UTS Psi	Yield Psi	RoA %	El%	HBN	Quench Range °F	Temper Range °F
2.875	½T - Core	210000	180000	25.0	7.0	421	1532 - 1590	(750 -763) & (806 - 820)
3.375	½T - Core	190000	152000	25.0	7.0	429	1518 - 1580	750 -778
3.375	¼T - Mid-radius	190000	152000	25.0	7.0	429	1500 - 1580	750 - 830
4	½T - Core	175000	140000	25.0	7.0	421	1515 - 1558	730 - 755
4	¼T - Mid-radius	190000	152000	25.0	7.0	421	1515 - 1558	730 - 755

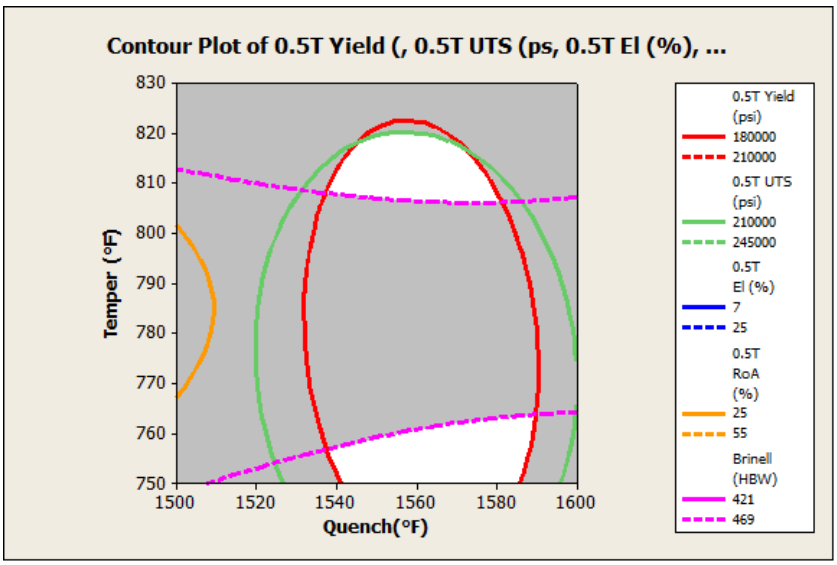

Contour Plot - Heat Treatment window to achieve 210Ksi UTS & 421 HBN (45 HRC) Hardness

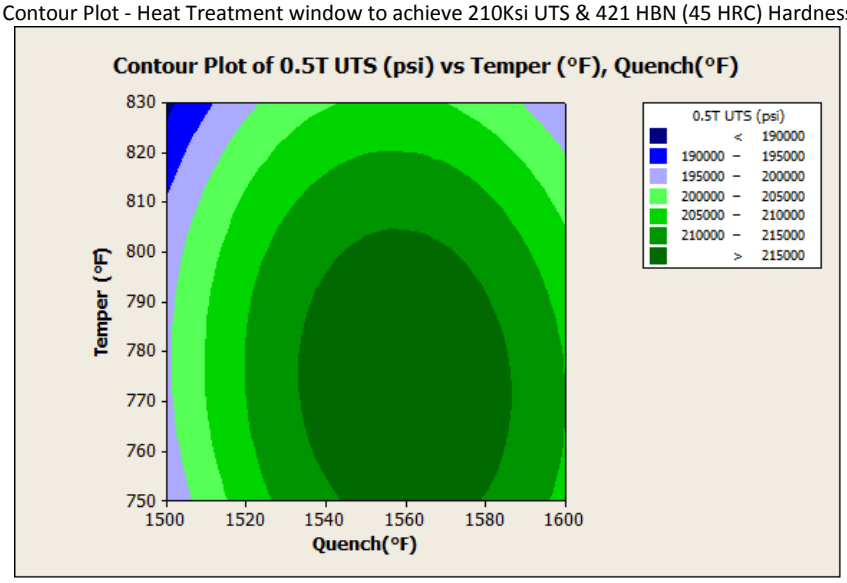

Contour Plot - Heat Treatment window to achieve a specific UTS value

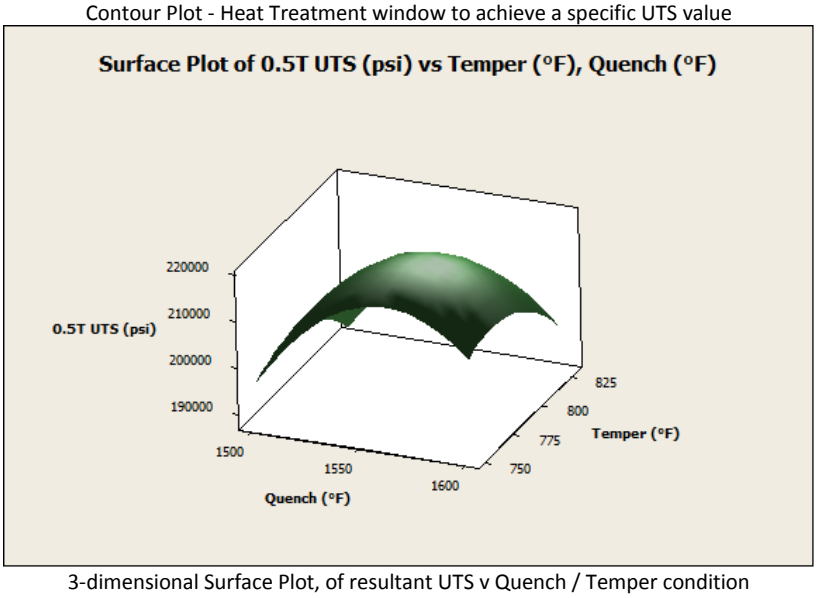

3-dimensional Surface Plot, of resultant UTS v Quench / Temper condition

Figure 5-31: 2.875-inch bar ½T Core: Heat Treatment Contour / Surface Plots

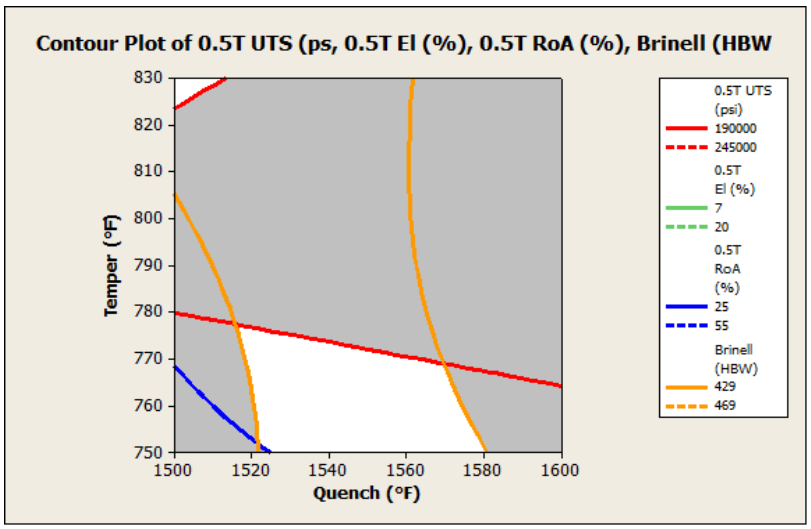

Contour Plot - Heat Treatment window to achieve 190Ksi UTS & 429 HBN (46 HRC) Hardness

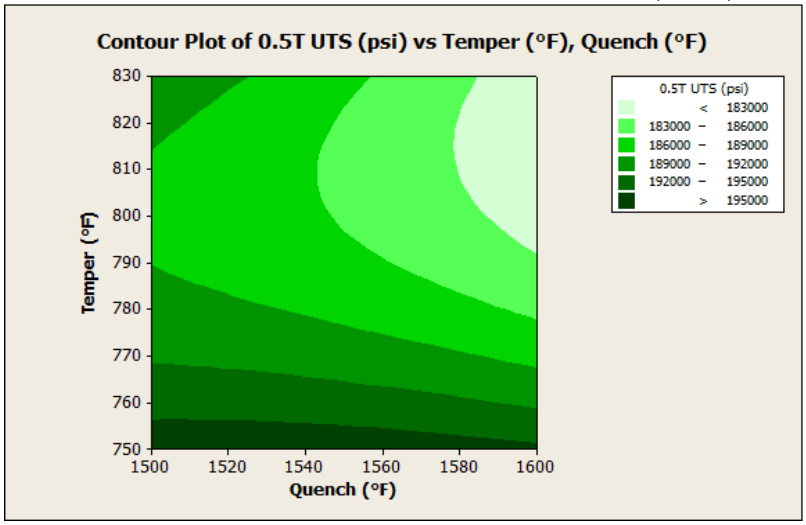

Contour Plot - Heat Treatment window to achieve a specific UTS value

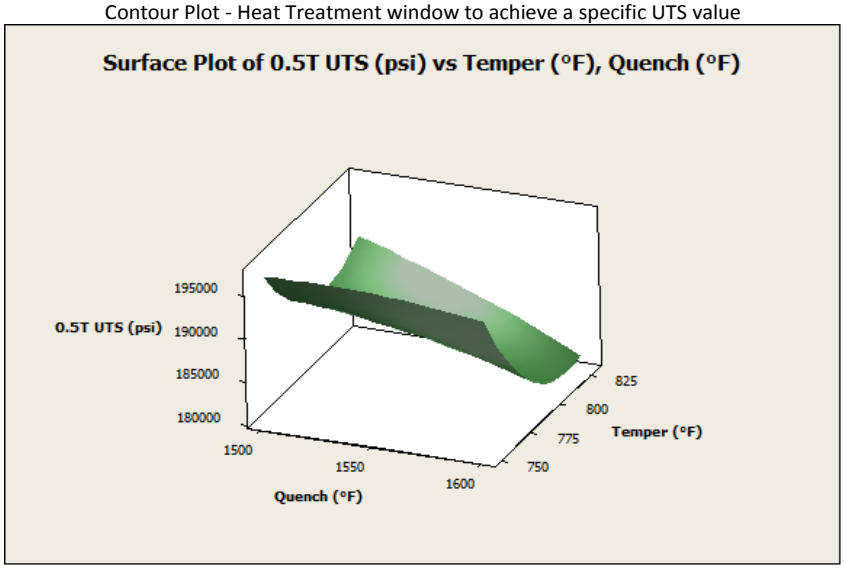

3-dimensional Surface Plot, of resultant UTS v Quench / Temper condition

Figure 5-32: 3.375-inch bar ½T Core: Heat Treatment Contour / Surface Plots

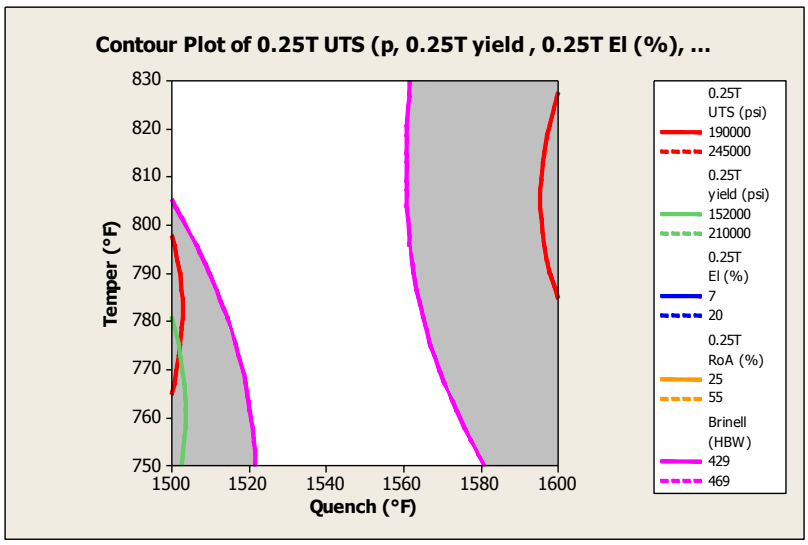

Contour Plot - Heat Treatment window to achieve 190Ksi UTS & 429 HBN (46 HRC) Hardness

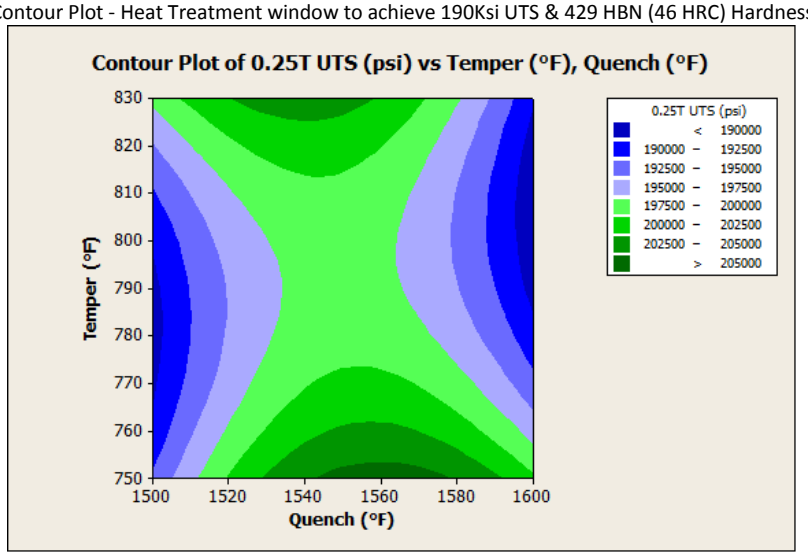

Contour Plot - Heat Treatment window to achieve a specific UTS value

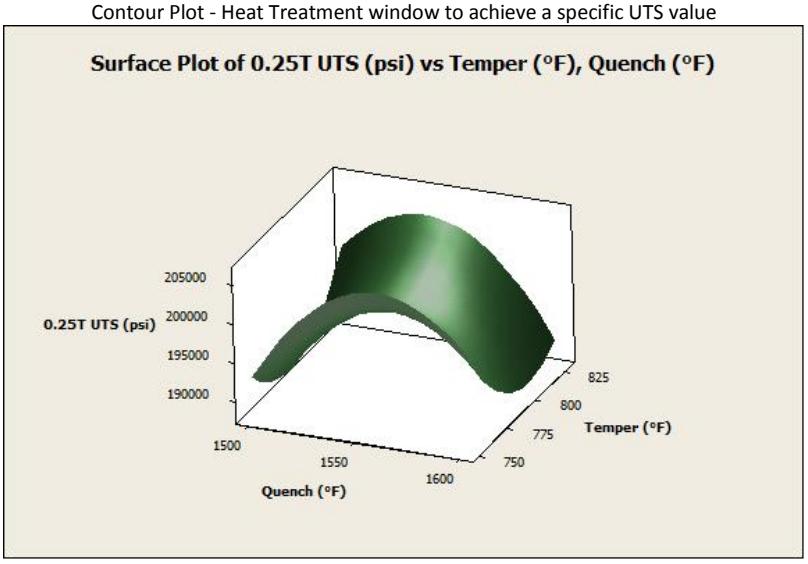

3-dimensional Surface Plot, of resultant UTS v Quench / Temper condition

Figure 5-33: 3.375-inch bar ¼T: Heat Treatment Contour / Surface Plots

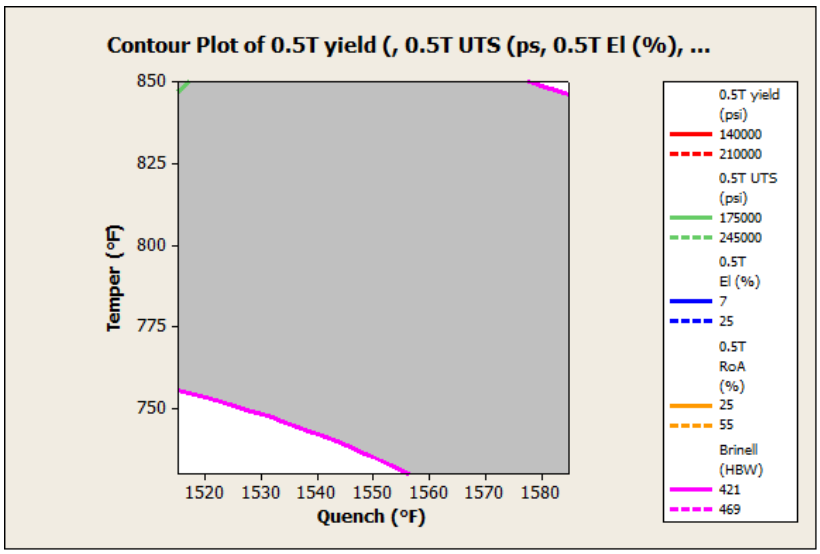

Contour Plot - Heat Treatment window to achieve 175Ksi UTS & 421 HBN (45 HRC) Hardness

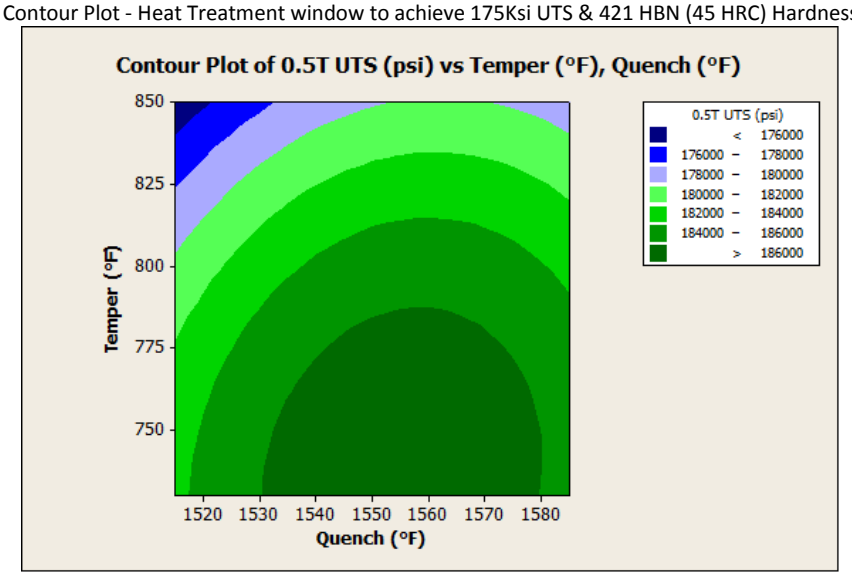

Contour Plot - Heat Treatment window to achieve a specific UTS value

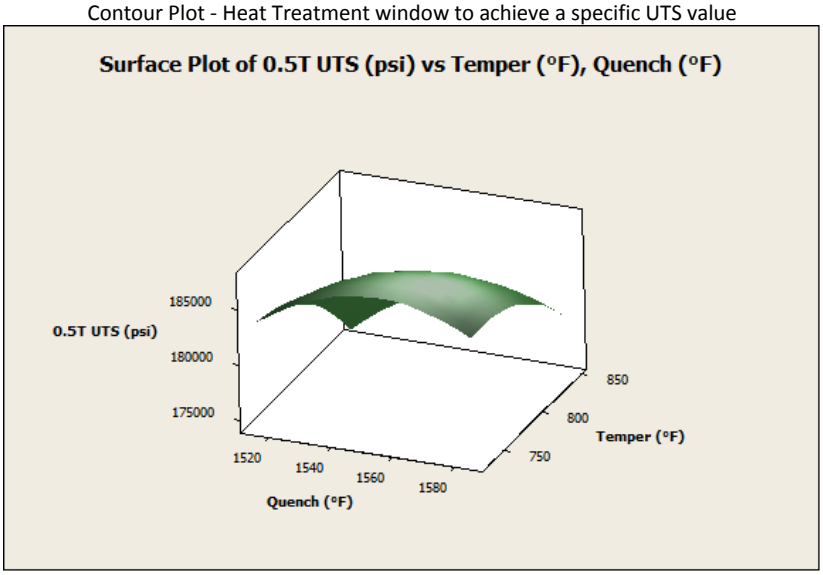

3-dimensional Surface Plot, of resultant UTS v Quench / Temper condition

Figure 5-34: 4.0-inch bar ½T Core: Heat Treatment Contour / Surface Plots

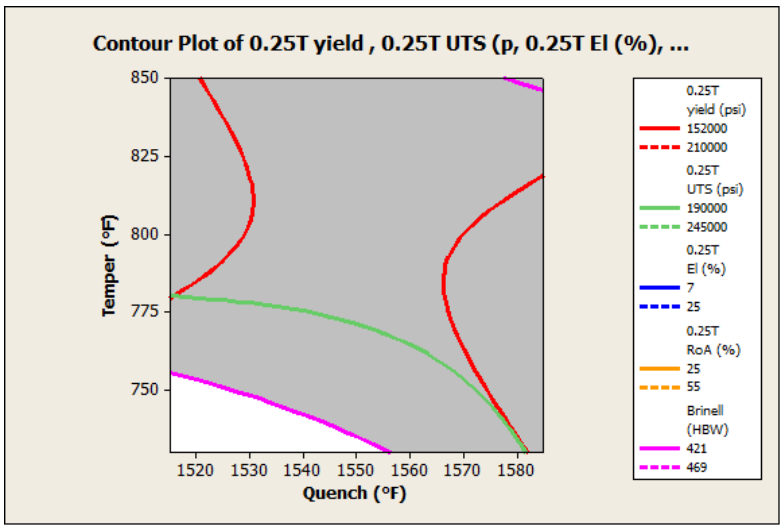

Contour Plot - Heat Treatment window to achieve 190Ksi UTS & 421 HBN (45 HRC) Hardness

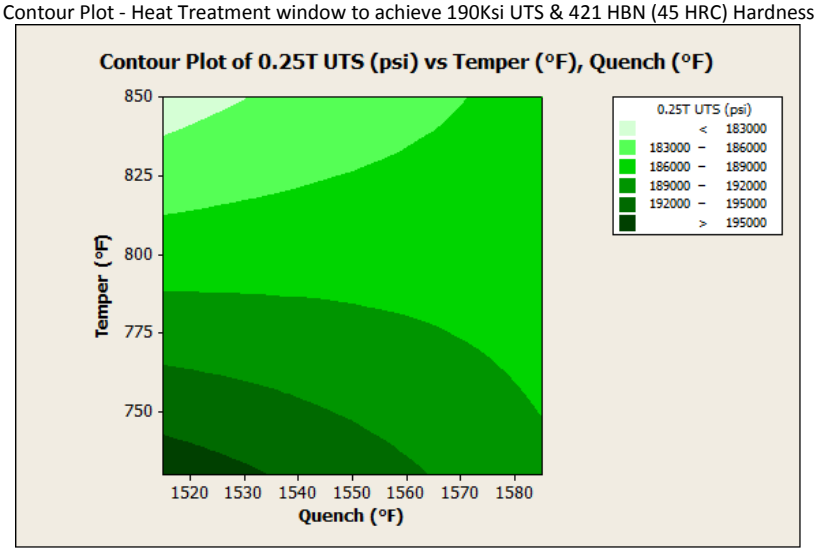

Contour Plot - Heat Treatment window to achieve a specific UTS value

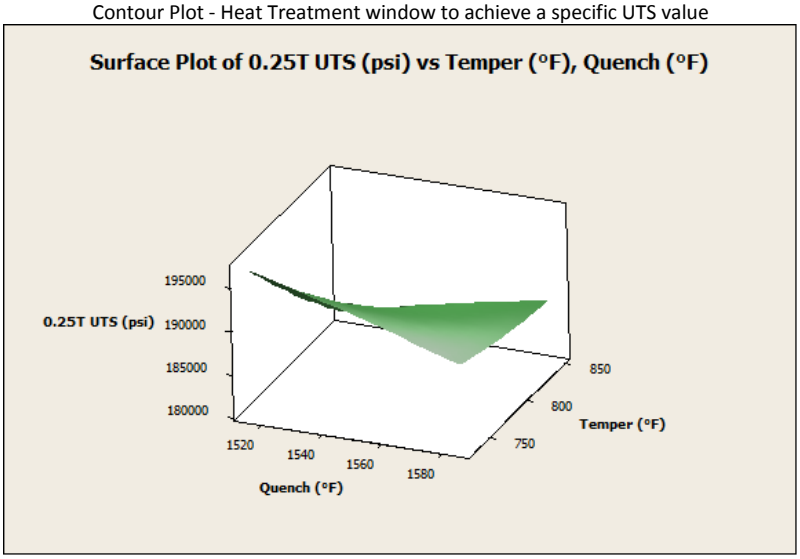

3-dimensional Surface Plot, of resultant UTS v Quench / Temper condition

Figure 5-35: 4.0-inch bar ¼T: Heat Treatment Contour / Surface Plots

The Contour / Surface Plots have identified the UTS values over the complete heat treatment range for each bar type & respective location. This along with the optimization model and empirical formula, enable a satisfactory level of predictability when heat treating the AISI 4161H material over the 2.875 - 4.0-inch bar range.

Appendix C details the residual plots for the optimisation diagrams shown in Figure 5-31 through Figure 5-35.

Optimisation has enabled a governance to be set for current and future actuator designs, with the following minimum UTS values being set for each respective bar size:

- 2.875 inch (73mm) - 210 Ksi UTS
- 3.375 inch (85.7mm) - 190 Ksi UTS
- 4.0 inch (101.6mm) - 190 Ksi UTS

These UTS values should be stipulated for the ¼T (mid-radius) position only for 3.375" and 4" bar. The 2.875" bar can achieve the required values throughout the cross-section.

5.3.5 Hardness Test Analysis

Hardness testing is a key part of the experimental work, as it is a fundamental output of the DoE in terms of how the material behaves / responses to different heat treatment conditions. Therefore, to ensure a full understanding of the various AISI 4161H material; hardness testing was conducted on both the surface and through thickness section of each bar exposed to the DoE.

The surface hardness tests were conducted along the length of the bar at 3 equidistant spaced locations - Reference Figure 5-4.

To ensure an accurate result was obtained, the test zone was subjected to light mechanical grinding to remove any surface oxide present post the respective heat treatment operation. Both HBN & HRC indentations (three off each) were made at each specified zone.

Through-thickness hardness testing was conducted in the transverse direction, with 5 HRC indentations being taken at the following locations - see Figure 5-36

- Sub-surface X2
- Mid-radius X2
- Core

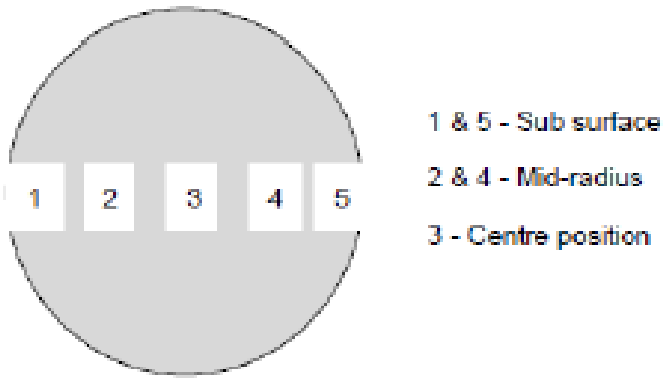

Figure 5-36: Through-Thickness Hardness Test Locations

5.3.5.1 Surface Hardness

Surface hardness measurement is important, as this is the method utilized by the coil spring OEM to control the heat treatment process. It is also part of TechnipFMC design requirements, which states "the resultant average hardness shall be 45 - 49 HRC (421 - 469 HBW) in the fully quenched and tempered condition".

The DoE has established the resultant values in the fully heat treated (Quench & Tempered) condition; in addition to the As-Cooled and As-Quenched form. The results are detailed within Tables 5-14 to 5-16.

Table 5-14: 2.875-Inch Surface Hardness Results

Bar size	Condition	ID	Material	Heat	Cool medium	Quench	Temper	HRC	Brinell
2.875	Air cool	T1	Timken	1700	Air	na	na	31.5	not taken
2.875	Air cool	T2	Timken	1800	Air	na	na	31.1	not taken
2.875	Quench	E1**	Timken	1600	Oil	1600	na	55.7	601
2.875	Quench	A1**	Timken	1800	Oil	1550	na	60.8	653
2.875	Quench	C1**	Timken	1550	Oil	1550	na	62.7	653
2.875	Quench	G1**	Timken	1500	Oil	1500	na	57.6	578
2.875	Q & T	A1a	Timken	1800	Oil	1550	790	46.2	not taken
2.875	Q & T	A2a	Timken	1800	Oil	1550	790	46.8	not taken
2.875	Q & T	A3a	Timken	1800	Oil	1550	790	46.9	not taken
2.875	Q & T	C1	Timken	1550	Oil	1550	790	48.2	477.0
2.875	Q & T	C2	Timken	1550	Oil	1550	790	49.1	495.0
2.875	Q & T	C3	Timken	1550	Oil	1550	790	49.4	477.0
2.875	Q & T	E1	Timken	1600	Oil	1600	830	45.8	461.0
2.875	Q & T	E2	Timken	1600	Oil	1600	830	44.2	444.0
2.875	Q & T	E3	Timken	1600	Oil	1600	830	43	429.0
2.875	Q & T	F1	Timken	1600	Oil	1600	750	41	472.0
2.875	Q & T	F2	Timken	1600	Oil	1600	750	45	446.0
2.875	Q & T	F3	Timken	1600	Oil	1600	750	46.8	459.0
2.875	Q & T	G1	Timken	1500	Oil	1500	830	42.7	435.0
2.875	Q & T	G2	Timken	1500	Oil	1500	830	47	456.0
2.875	Q & T	G3	Timken	1500	Oil	1500	830	46.2	440.0
2.875	Q & T	H1	Timken	1500	Oil	1500	750	48.1	473.0
2.875	Q & T	H2	Timken	1500	Oil	1500	750	46.6	466.0
2.875	Q & T	H3	Timken	1500	Oil	1500	750	48.3	478.0
2.875	Q & T	I1	Timken	1550	Oil	1550	750	47.6	455.0
2.875	Q & T	I2	Timken	1550	Oil	1550	750	45.1	450.0
2.875	Q & T	J1	Timken	1600	Oil	1600	790	47.8	461.0
2.875	Q & T	J2	Timken	1600	Oil	1600	790	48.4	477.0

Table 5-15: 3.375-Inch Surface Hardness Results

Bar size	Condition	ID	Material	Heat	Cool medium	Quench	Temper	HRC	Brinell
3.375	Air cool	AC1	Timken	1800	Air	na	na	31.2	299.0
3.375	Air cool	AC2	Timken	1700	Air	na	na	30.4	299.0
3.375	Quench	AQ1600	Timken	1600	Oil	1600	na	not taken	601.0
3.375	Quench	AQ1585	Timken	1585	Oil	1585	na	not taken	653.0
3.375	Quench	AQ1550	Timken	1550	Oil	1550	na	not taken	644.0
3.375	Quench	AQ1515	Timken	1515	Oil	1515	na	not taken	629.0
3.375	Quench	AQ1500	Timken	1500	Oil	1500	na	not taken	644.0
3.375	Q & T	**I1**	Timken	1500	Oil	1500	790	45.4	388.0
3.375	Q & T	**I2**	Timken	1500	Oil	1500	790	47.6	429.0
3.375	Q & T	**J1**	Timken	1600	Oil	1600	790	41.6	366.0
3.375	Q & T	**J2**	Timken	1600	Oil	1600	790	42.7	392.0
3.375	Q & T	**K1**	Timken	1550	Oil	1550	790	44	419.0
3.375	Q & T	**K2**	Timken	1550	Oil	1550	790	45	434.0
3.375	Q & T	**K3**	Timken	1550	Oil	1550	750	46.3	455.0
3.375	Q & T	**K4**	Timken	1550	Oil	1550	830	46.8	444.0
3.375	Q & T	**K5**	Timken	1550	Oil	1550	830	46.5	444.0
3.375	Q & T	**K6**	Timken	1550	Oil	1550	750	45.8	450.0
3.375	Q & T	**L1**	Timken	1515	Oil	1515	815	43.2	461.0
3.375	Q & T	**L2**	Timken	1515	Oil	1515	815	45.4	439.0
3.375	Q & T	**L3**	Timken	1515	Oil	1515	765	43.7	423.0
3.375	Q & T	**L4**	Timken	1515	Oil	1515	765	46.6	450.0
3.375	Q & T	**M1**	Timken	1585	Oil	1585	815	43.2	397.0
3.375	Q & T	**M2**	Timken	1585	Oil	1585	765	44.4	444.0
3.375	Q & T	**M3**	Timken	1585	Oil	1585	815	40.3	388.0
3.375	Q & T	**M4**	Timken	1585	Oil	1585	765	47.3	444.0
3.375	Q & T	**N1**	Timken	1570	Oil	1570	750	44.5	397.0
3.375	Q & T	**N2**	Timken	1570	Oil	1570	750	44.5	415.0

Table 5-16: 4.0-Inch Surface Hardness Results

Bar size	Condition	ID	Material	Heat	Cool medium	Quench	Temper	HRC	Brinell
4	Air cool	AC1	Timken	1800	Air	na	na	32.1	298.0
4	Quench	AQ1515	Timken	1515	Oil	1515	na	60.5	610.0
4	Quench	AQ1550	Timken	1550	Oil	1550	na	57.8	570.0
4	Quench	AQ1585	Timken	1585	Oil	1585	na	58.7	601.0
4	Q & T	O1	Timken	1550	Oil	1550	790	46.2	415.0
4	Q & T	O2	Timken	1550	Oil	1550	790	41.7	363.0
4	Q & T	P1	Timken	1585	Oil	1585	830	41.9	415.0
4	Q & T	P2	Timken	1585	Oil	1585	830	41.9	388.0
4	Q & T	Q1	Timken	1515	Oil	1515	750	49	439.0
4	Q & T	Q2	Timken	1515	Oil	1515	750	45.7	425.0
4	Q & T	R1	Timken	1550	Oil	1550	850	44.4	406.0
4	Q & T	R2	Timken	1550	Oil	1550	850	42.7	415.0
4	Q & T	S1	Timken	1515	Oil	1515	830	40.4	359.0
4	Q & T	S2	Timken	1515	Oil	1515	830	43.2	392.0
4	Q & T	T1	Timken	1585	Oil	1585	750	44.3	392.0
4	Q & T	T2	Timken	1585	Oil	1585	750	43.4	392.0
4	Q & T	U1	Timken	1550	Oil	1550	730	45.2	415.0
4	Q & T	U2	Timken	1550	Oil	1550	730	47.9	425.0

5.3.5.2 Surface Hardness Analysis

The resultant surface values have shown a direct trend with respect to the heat treatment condition and bar diameter. In all cases the highest values are achieved in the As-Quenched condition, followed by Quench and Temper, with the Air-Cooled treated surface producing the lowest values – see Figures 5-37 to 5-39.

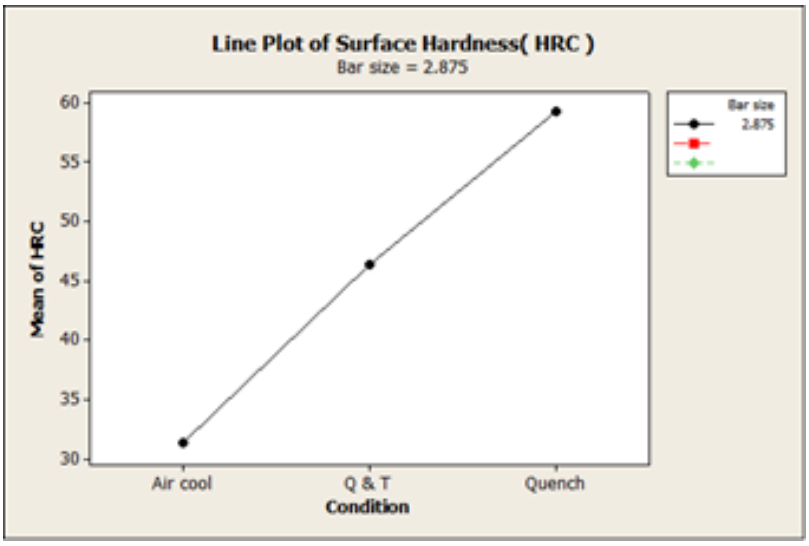

Figure 5-37: 2.875-inch average surface hardness (HRC) plot across all heat treatment conditions

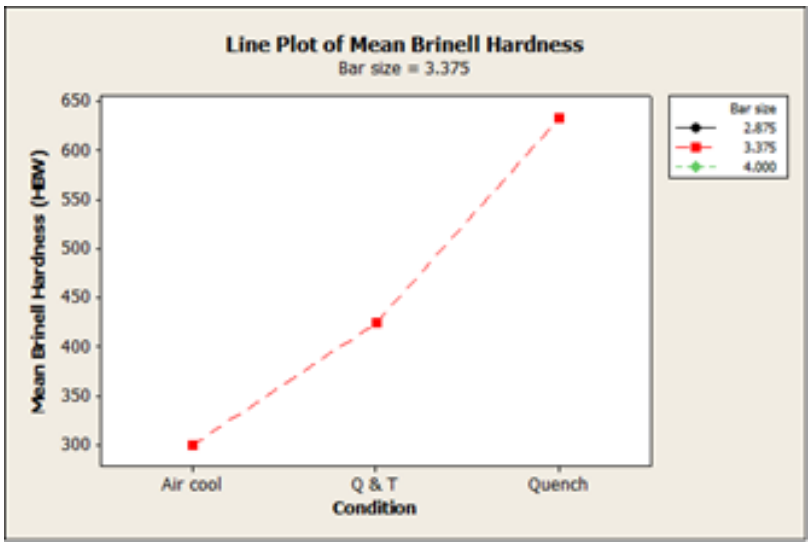

Figure 5-38: 3.375-inch average surface hardness (HBW) plot across all heat treatment conditions

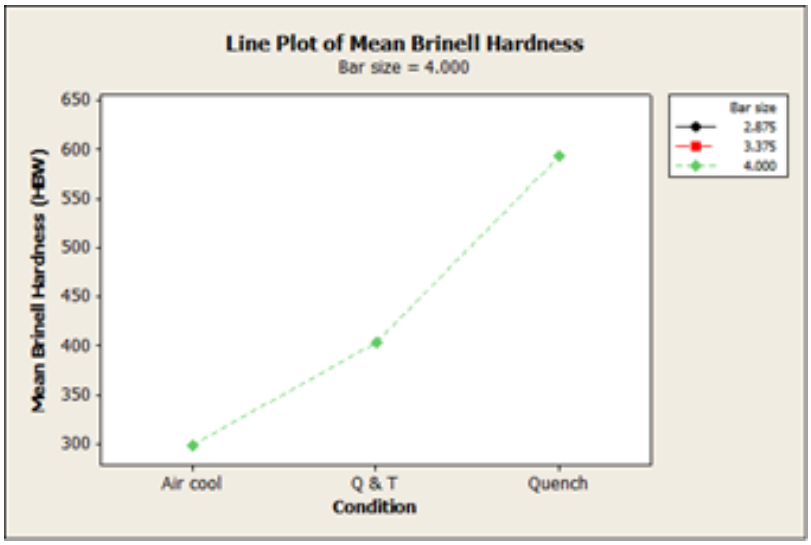

Figure 5-39: 4.0-inch average surface hardness (HBW) plot across all heat treatment conditions

The main point for consideration is the resultant surface values that were achieved in the quench & temper condition. As per TechnipFMC desired design criteria, the required Brinell hardness must be within the limits of (421 - 469 HBW). However, the average results achieved (reference Figure 5-40) for each bar size were:

- 2.875" (73mm) - 461 HBW,
- 3.375" (85.7mm) - 424 HBW,
- 4.0"(101.6mm) - 403 HBW.

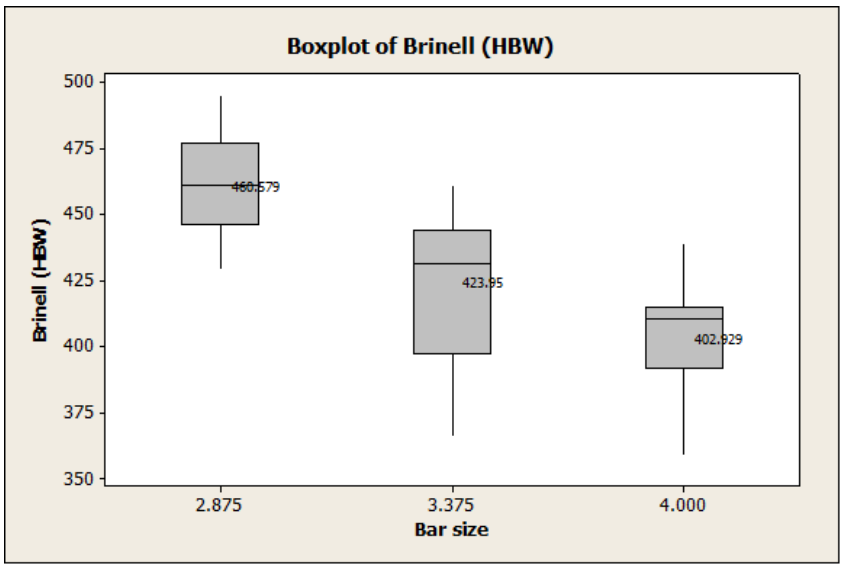

Figure 5-40: Box plot of average HBW hardness results for Quench / Temper conditions - all bar sizes

The results of the surface hardness analysis have shown that the 2.875-inch bar has the capability of being heat treated to the desired engineering requirement, with the 3.375-inch bar marginally meeting the 421 HBW minimum. However, certain heat treatment conditions, as used on the 3.375-inch bar yielded values up to 461 HBW, which suggests the design intent in terms of surface hardness can be met, but only over a tighter heat treatment operating process window. As for the 4.0-inch tests, only one parameter set (Q and T) exceeded the 421 HBW minimum, which suggests this respective bar size will consistently struggle to meet the design requirement currently set by the respective company standards.

5.3.6 Through-Thickness Hardness (HRC)

Through thickness hardness measurement is important, in that it determines how well the material responds to the respective heat treatment conditions. The AISI 4161H grade material has been selected due to its chemical composition and its level of hardenability required for coil spring application.

Although through-thickness hardness is not a company requirement, the DoE has recognized that there is a need to understand the resultant hardness values across each of the respective bar sizes and heat treatment conditions.

The results from the through-thickness testing for is detailed within Tables 5-17 to 5-19.

Table 5-17: 2.875-Inch Through-Thickness Hardness Results

Bar size	Condition	ID	Material	Heat	Cool medium	Quench	Temper	Sub Surface	Mid-Radius	Core	Mid-Radius	Sub Surface	Ave HRC
2.875	Air cool	T1	Timken	1700	Air	na	na	30.9	31.4	38.8	31.2	30.9	32.6
2.875	Air cool	T2	Timken	1800	Air	na	na	28.7	30.2	34.7	29.7	29.4	30.5
2.875	Quench	E1	Timken	1600	Oil	1600	na	57.4	57.1	55.1	58.1	59.1	57.4
2.875	Quench	A1	Timken	1800	Oil	1550	na	59.8	59.5	59.5	58.9	58.4	59.2
2.875	Quench	C1	Timken	1550	Oil	1550	na	59.3	58.3	56	58.9	59.2	58.3
2.875	Quench	G1	Timken	1500	Oil	1500	na	58.8	58	57	57.6	59.5	58.2
2.875	Q & T	A1a	Timken	1800	Oil	1550	790	46.3	46.3	43	44.7	46.2	45.3
2.875	Q & T	A2a	Timken	1800	Oil	1550	790	46.3	46	43.7	43.7	44.6	44.9
2.875	Q & T	A3a	Timken	1800	Oil	1550	790	46.3	46.7	45.6	46.9	47.4	46.6
2.875	Q & T	C1	Timken	1550	Oil	1550	790	44.9	44.1	46.5	46.5	46.6	45.7
2.875	Q & T	C2	Timken	1550	Oil	1550	790	46.8	47.4	47.8	48.1	48.7	47.8
2.875	Q & T	C3	Timken	1550	Oil	1550	790	45.3	45.7	45.8	46	47.7	46.1
2.875	Q & T	E1	Timken	1600	Oil	1600	830	43.1	43.6	40.8	44.2	42.6	42.9
2.875	Q & T	E2	Timken	1600	Oil	1600	830	44.5	44.6	41.6	45.3	45.1	44.2
2.875	Q & T	E3	Timken	1600	Oil	1600	830	47	44.6	43.7	44.7	44.9	45.0
2.875	Q & T	F1	Timken	1600	Oil	1600	750	42.8	42.1	40.1	40.9	40.7	41.3
2.875	Q & T	F2	Timken	1600	Oil	1600	750	46.1	45.6	44.9	45.1	46	45.5
2.875	Q & T	F3	Timken	1600	Oil	1600	750	49	48	46.7	46.2	47.5	47.5
2.875	Q & T	G1	Timken	1500	Oil	1500	830	42.8	43.3	40.7	42.3	43.3	42.5
2.875	Q & T	G2	Timken	1500	Oil	1500	830	44.6	43.7	42.6	43.5	45.1	43.9
2.875	Q & T	G3	Timken	1500	Oil	1500	830	45.6	44.4	43	43.9	45.2	44.4
2.875	Q & T	H1	Timken	1500	Oil	1500	750	45.4	44.2	42.4	44.1	45.6	44.3
2.875	Q & T	H2	Timken	1500	Oil	1500	750	45.8	45.7	43.6	44.6	46.3	45.2
2.875	Q & T	H3	Timken	1500	Oil	1500	750	46.5	45.6	43.6	45	46.4	45.4
2.875	Q & T	I1	Timken	1550	Oil	1550	750	48	48.1	47.2	47.8	49.1	48.0
2.875	Q & T	I2	Timken	1550	Oil	1550	750	48.6	48.5	48.1	48	48.3	48.3
2.875	Q & T	J1	Timken	1600	Oil	1600	790	47.5	47.2	47.1	46.7	46.9	47.1
2.875	Q & T	J2	Timken	1600	Oil	1600	790	49.2	48.6	48.4	48.9	48.9	48.8

Table 5-18: 3.375-Inch Through-Thickness Hardness Results

Bar size	Condition	ID	Material	Heat	Cool medium	Quench	Temper	Sub Surface	Mid-Radius	Core	Mid-Radius	Sub Surface	Ave HRC
3.375	As-recived	AS	Timken	na	na	na	na	27	29	28	29	27	28.0
3.375	Air cool	AC1	Timken	1800	Air	na	na	29	28.8	30.9	28.9	29.8	29.5
3.375	Air cool	AC2	Timken	1700	Air	na	na	29.6	29.9	30.1	31.1	29.5	30.0
3.375	Quench	AQ1500	Timken	1500	Oil	1500	na	51	47	40	49	51	47.6
3.375	Quench	AQ1515	Timken	1515	Oil	1515	na	58	56	51	55	58	55.6
3.375	Quench	AQ1550	Timken	1550	Oil	1550	na	55	51	50	52	55	52.6
3.375	Quench	AQ1585	Timken	1585	Oil	1585	na	57	58	51	57	57	56.0
3.375	Quench	AQ1600	Timken	1600	Oil	1600	na	54	54	50	55	56	53.8
3.375	Q & T	I1	Timken	1500	Oil	1500	790	44	42.4	42.1	44.6	44	43.4
3.375	Q & T	I2	Timken	1500	Oil	1500	790	43.1	42.6	41.2	40.5	44.2	42.4
3.375	Q & T	J1	Timken	1600	Oil	1600	790	40.2	39.2	39	40.1	41.5	40.0
3.375	Q & T	J2	Timken	1600	Oil	1600	790	36.6	37.4	38.9	38.9	38.7	38.1
3.375	Q & T	K1	Timken	1550	Oil	1550	790	44.1	43.9	44.6	43.3	45.1	44.2
3.375	Q & T	K2	Timken	1550	Oil	1550	790	45.3	45.7	46.3	44.2	43.6	45.0
3.375	Q & T	K3	Timken	1550	Oil	1550	750	46.1	44.8	43.8	43.5	45.8	44.8
3.375	Q & T	K4	Timken	1550	Oil	1550	830	43.6	43	43.7	43.4	43	43.4
3.375	Q & T	K5	Timken	1550	Oil	1550	830	45	44.6	42.5	41.9	44.4	43.7
3.375	Q & T	K6	Timken	1550	Oil	1550	750	46.1	44.2	43.9	44.7	46.8	45.1
3.375	Q & T	L1	Timken	1515	Oil	1515	815	46	44.2	46.9	43.6	44.4	45.0
3.375	Q & T	L2	Timken	1515	Oil	1515	815	45.5	45.3	44.3	45.6	44.6	45.1
3.375	Q & T	L3	Timken	1515	Oil	1515	765	44.1	43.2	43	41.9	44.9	43.4
3.375	Q & T	L4	Timken	1515	Oil	1515	765	46	43.9	44.6	44.5	46.6	45.1
3.375	Q & T	M1	Timken	1585	Oil	1585	815	38.1	38.6	38	39.5	41.7	39.2
3.375	Q & T	M2	Timken	1585	Oil	1585	765	43.3	41.8	41.8	42.2	44.6	42.7
3.375	Q & T	M3	Timken	1585	Oil	1585	815	39.5	39.5	42.6	36.6	38.3	39.3
3.375	Q & T	M4	Timken	1585	Oil	1585	765	42.1	42	40.7	39.3	39.5	40.7
3.375	Q & T	N1	Timken	1570	Oil	1570	750	46.1	45.5	43.1	42.5	44.4	44.3
3.375	Q & T	N2	Timken	1570	Oil	1570	750	41.5	42.1	39.6	41.6	39.1	40.8

Table 5-19: 4.0-Inch Through-Thickness Hardness Results

Bar size	Condition	ID	Material	Heat	Cool medium	Quench	Temper	Sub Surface	Mid-Radius	Core	Mid-Radius	Sub Surface	Ave HRC
4	As-recived	AS	Timken	na	na	na	na	27	31	27	29	25	27.8
4	Air cool	AC1	Timken	1800	Air	na	na	30.3	31.2	30.2	32.2	30.6	30.9
4	Quench	AQ1515	Timken	1515	Oil	1515	na	52	43	46	49	54	48.8
4	Quench	AQ1550	Timken	1550	Oil	1550	na	50	46	44	44	54	47.6
4	Quench	AQ1585	Timken	1585	Oil	1585	na	52	50	44	52	54	50.4
4	Q & T	O1	Timken	1550	Oil	1550	790	37.1	37.7	38.2	38.4	36.1	37.5
4	Q & T	O2	Timken	1550	Oil	1550	790	37.6	37.1	40.7	37.6	37.1	38.0
4	Q & T	P1	Timken	1585	Oil	1585	830	39.3	39	40.4	40.6	39.6	39.8
4	Q & T	P2	Timken	1585	Oil	1585	830	37.9	37.2	39.1	37.8	37.1	37.8
4	Q & T	Q1	Timken	1515	Oil	1515	750	44.7	43	42.5	43.5	43.9	43.5
4	Q & T	Q2	Timken	1515	Oil	1515	750	39.3	37.3	38.7	37.9	40.1	38.7
4	Q & T	R1	Timken	1550	Oil	1550	850	42	41.3	38.4	39	38.2	39.8
4	Q & T	R2	Timken	1550	Oil	1550	850	37.8	37.3	38.1	38.5	39.5	38.2
4	Q & T	S1	Timken	1515	Oil	1515	830	39.3	40.3	40.2	39.5	40.4	39.9
4	Q & T	S2	Timken	1515	Oil	1515	830	39.2	37.5	38.9	38.8	37.2	38.3
4	Q & T	T1	Timken	1585	Oil	1585	750	39	39.4	38.5	38.5	37.4	38.6
4	Q & T	T2	Timken	1585	Oil	1585	750	37.5	37.7	39.6	37.1	38.2	38.0
4	Q & T	U1	Timken	1550	Oil	1550	730	39.6	37.9	39.7	39.1	40.3	39.3
4	Q & T	U2	Timken	1550	Oil	1550	730	39.8	40.1	39.4	40.8	40.1	40.0

5.3.6.1 Through-thickness Analysis - Average values

The DoE has shown there is a marked difference in the average through-thickness hardness between each of the respective heat treatment conditions. As expected, the As-Quenched values are highest, followed by the Quenched and Tempered condition, with the Air-Cooled yielding the lowest results. It is also apparent that the Air-Cooled results for each bar size are almost identical in terms of average HRC values achieved - Reference Table 5-20 & Figure 5-41.

Table 5-20: Average Through-Thickness Results for Each Bar Type V Heat Treatment Condition

Bar Dia. [inch]	Average HRC Air Cool	Average HRC Quench	Average HRC Quench & Temper
2.875	31.6	58.3	45.5
3.375	29.8	53.1	42.8
4.000	30.9	48.9	39.1

There is also a trend between the respective bar sizes, with the 2.875-inch yielding the highest HRC values for both the As-Quenched and Quenched & Tempered conditions. The average values for both the 3.375 & 4-inch reduce, with the 4-inch diameter bar producing the lowest values - reference Figure 5-41.

In addition, the average through-thickness results for each location (sub surface / mid-radius / core), have demonstrated that the core generally produces the lowest resultant HRC value, with the sub surface yielding the highest hardness - see Table 5-21 & Figure 5-41.

Table 5-21: Average HRC values for each through-thickness position across the bar for - As Quenched & Quench & Temper Conditions

Bar size	Condition	Sub surface	Mid-radius	Core	Mid-radius	Sub surface
2.875	Quench	58.9	58.2	56.9	58.4	59.1
3.375	Quench	55	53.2	48.4	53.6	55.4
4	Quench	51.3	46.3	44.7	48.3	54

Bar size	Condition	Sub surface	Mid-radius	Core	Mid-radius	Sub surface
2.875	Q & T	46	45.6	44.4	45.3	46.1
3.375	Q & T	43.3	42.7	42.5	42.1	43.3
4	Q & T	39.3	38.8	39.5	39.1	38.9

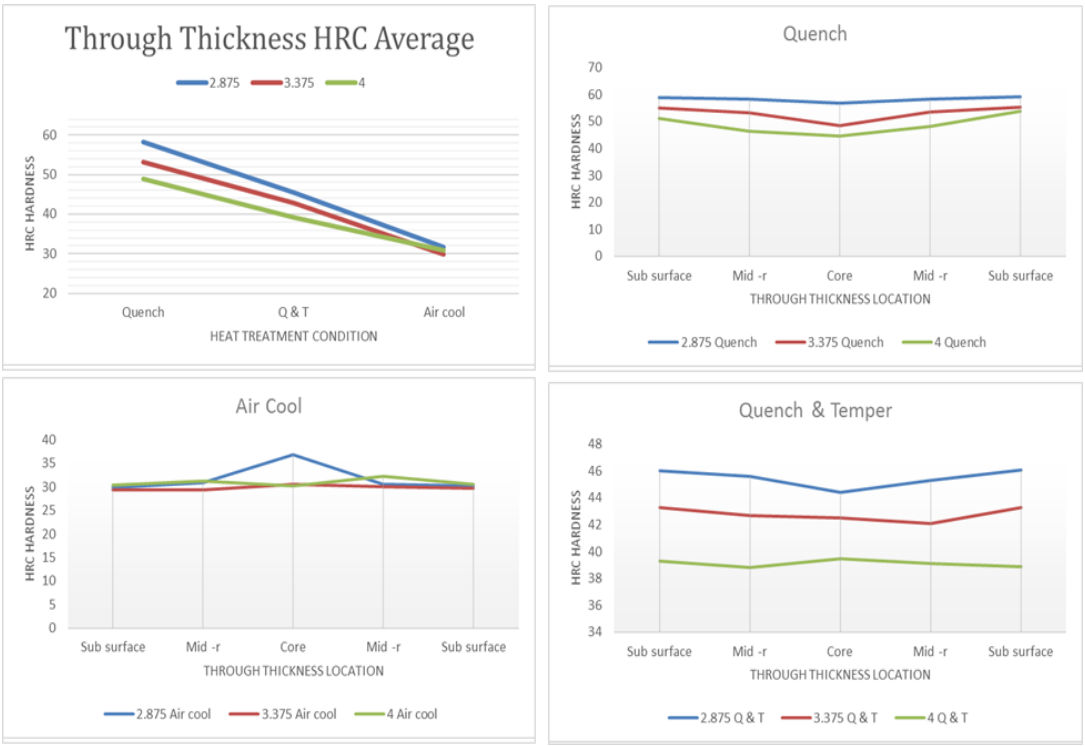

Figure 5-41: Through-Thickness Average HRC versus Heat Treatment Conditions (all bar sizes)

5.3.6.2 Through-thickness Analysis - Heat Treatment Conditions

Like the tensile results of the respective bars, the heat treatment conditions have a major impact on the resultant through-thickness hardness properties. This is apparent when you specifically look at the core values, where the material hardenability is generally at its lowest - Reference Figures 5-42 to 5-47.

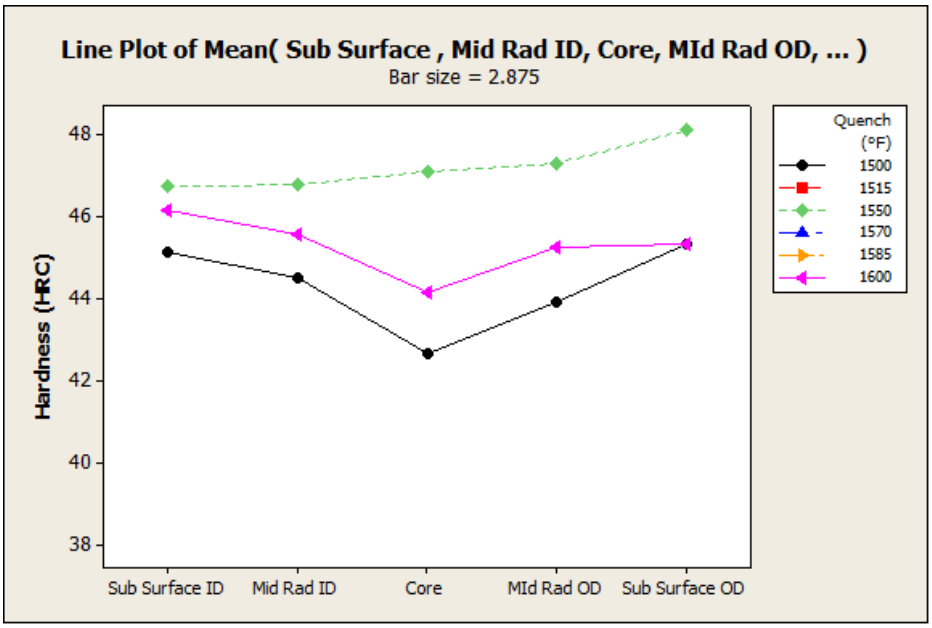

Figure 5-42: HRC versus Quench temperature, for 2.875-inch bar

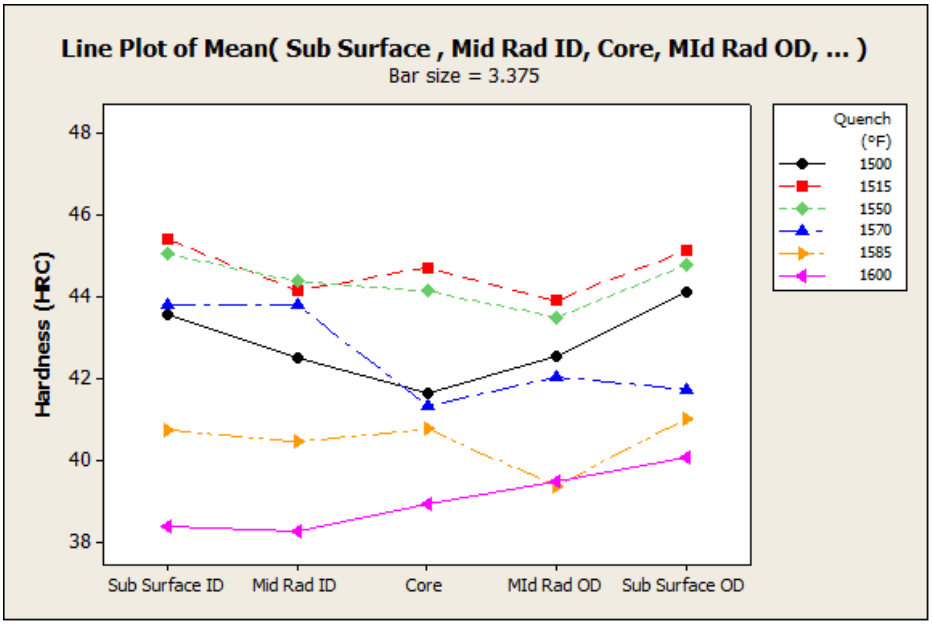

Figure 5-43: HRC versus Quench temperature, for 3.375-inch bar

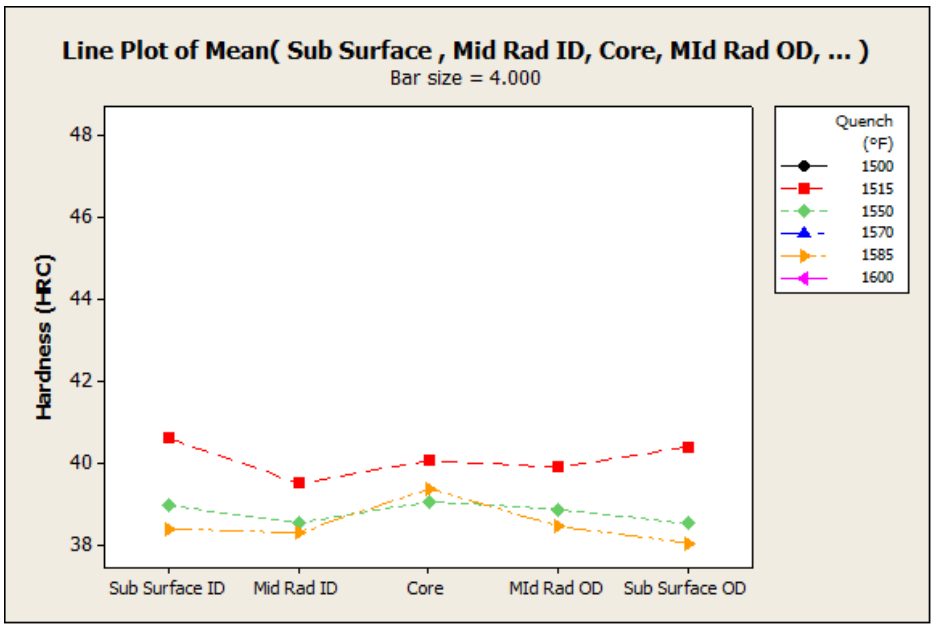

Figure 5-44: HRC versus Quench temperature, for 4.0-inch bar

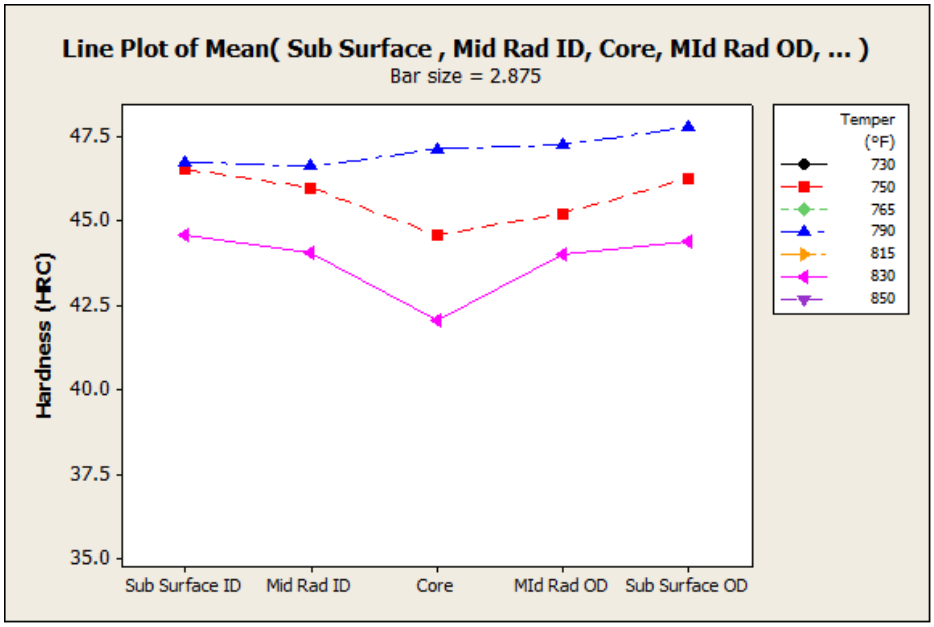

Figure 5-45: HRC versus Temper temperature, for 2.875-inch bar

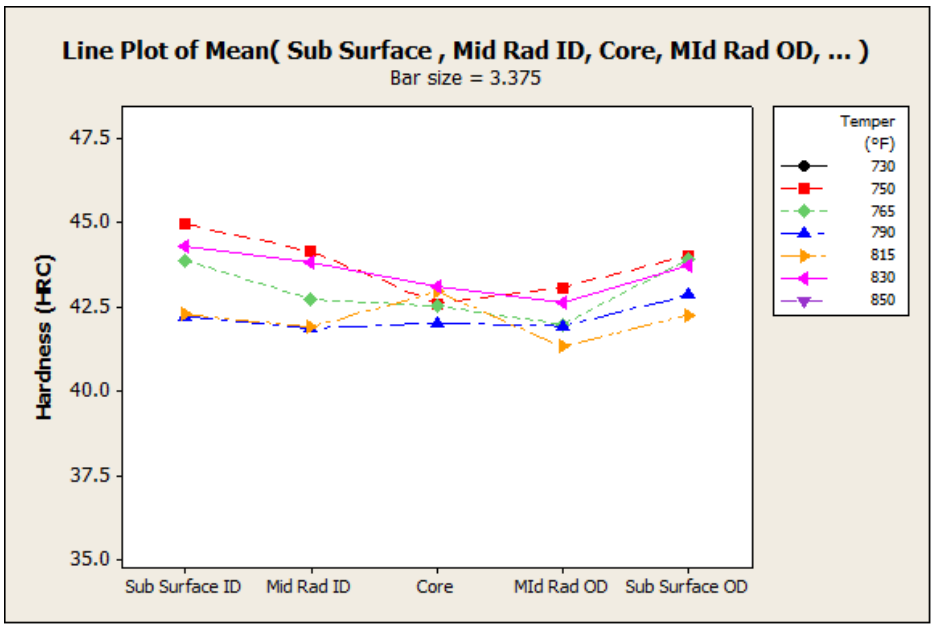

Figure 5-46: HRC versus Temper temperature, for 3.375-inch bar

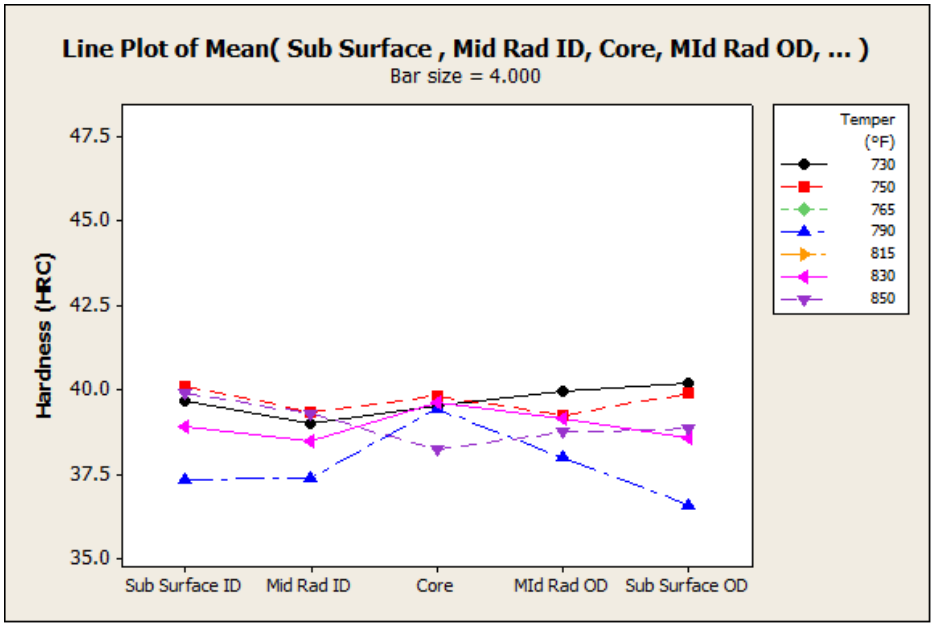

Figure 5-47: HRC versus Temper temperature, for 4.0-inch bar

The charts detailed within Figures 5-42 to 5-44, have demonstrated that the quench temperature has the greatest influence on the resultant through-thickness values. This is specifically apparent with both the 2.875 & 3.375-inch bars, which exhibit the greatest hardness delta across the evaluated quench temperature range.

Although the tempering temperature has an influence on the HRC values, it is apparent that the effect is less compared to the quenching operation. The results

within Figures 5-45 to 5-47 illustrate that the hardness values delta across the respective temperatures is reduced. In addition, the 4-inch bar exhibits the greatest level of uniformity across the bar sectional thickness with regards both the quench and tempering operations.

The combined results (Figure 5-48 through Figure 5-50) have also demonstrated that there is an optimum temperature range (Quench and Temper) for each bar type, which yields the highest set of core HRC values. The following assumptions are made:

- 2.875-inch (1550°F Quench @ 750 - 790°F Temper)
- 3.375-inch (1515°F - 1550°F Quench @ 790 - 815°F Temper)
- 4.0-inch (1515°F Quench @ 750°F Temper

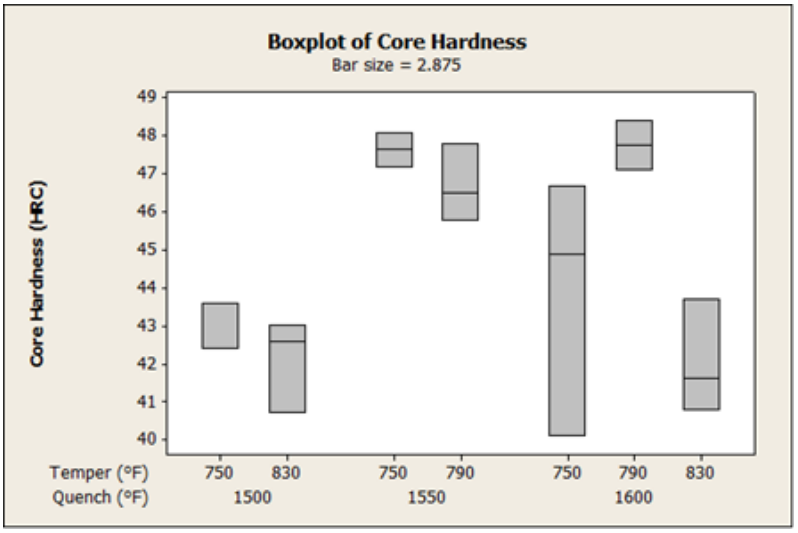

Figure 5-48: 2.875-inch bar box plot - average core HRC versus Quench and Temper conditions

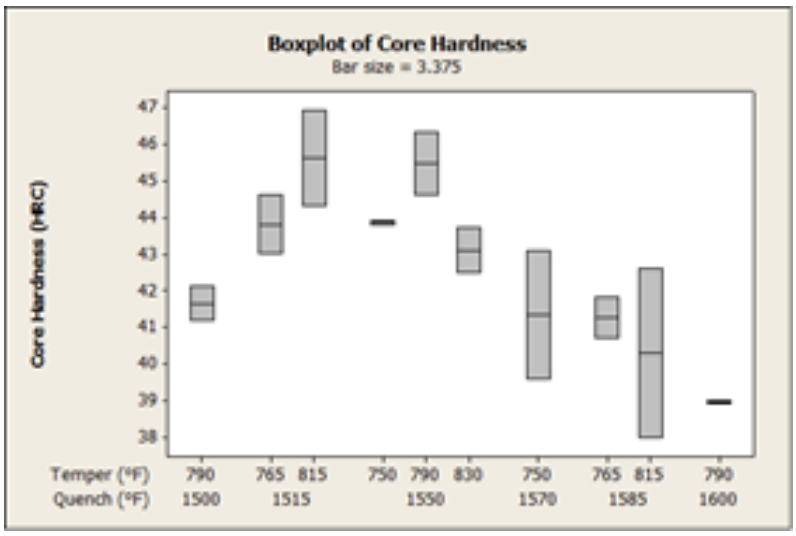

Figure 5-49: 3.375-inch bar box plot - average core HRC versus Quench and Temper conditions

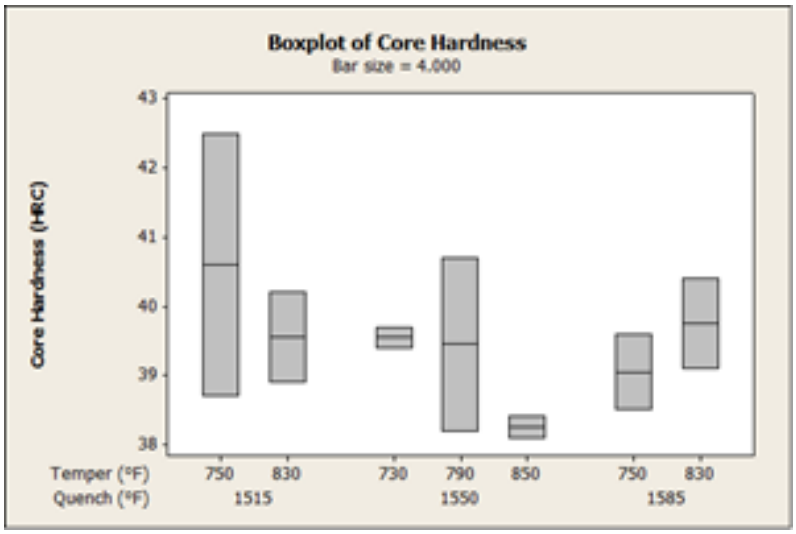

Figure 5-50: 4.0-inch bar box plot - average core HRC versus Quench and Temper conditions

5.3.7 Hardenability

As per the requirements of M20905 & ASTM A304 (Method D); the hardenability of the AISI 4161H material must meet the minimum hardness values of 60 & 59 HRC at the respective J5 & J10 locations - Reference Figure 5-51. These values are based on an end-quench test specified within ASTM A255, which measures the resultant HRC value at a set distance from the water quenched end (ASTM A255). As per Table 5-1, all raw material bars (2.875 - 4.0-inch diameter) met this requirement.

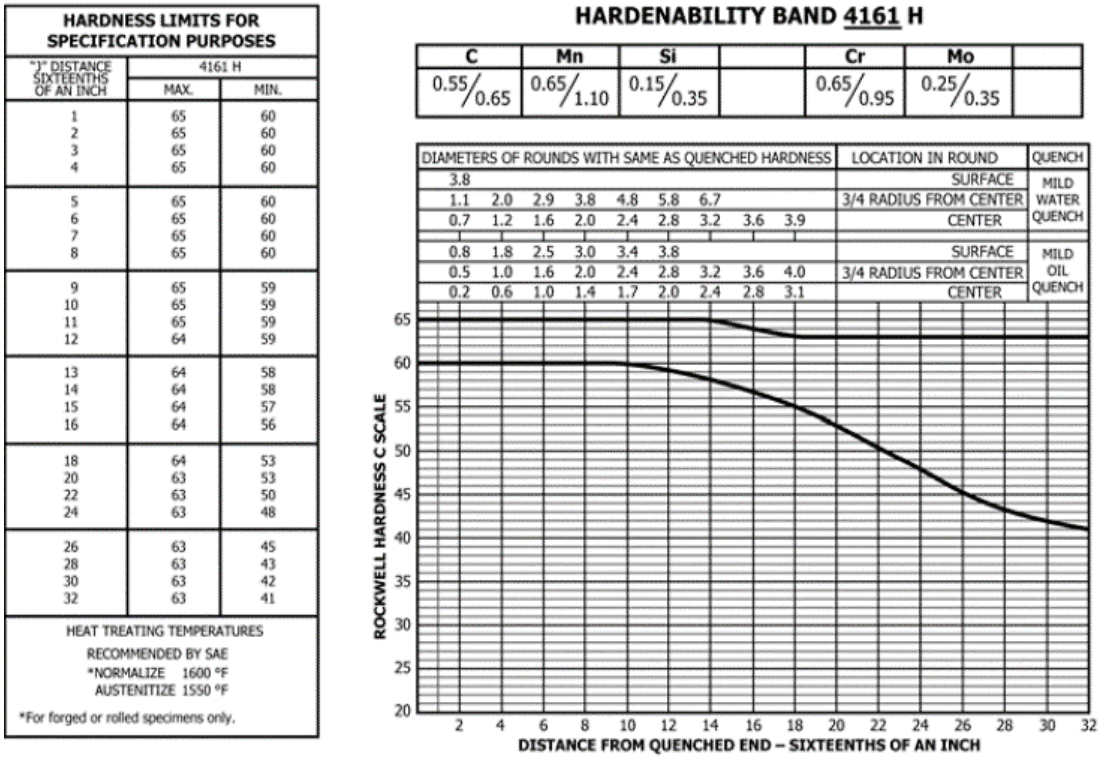

HARDNESS LIMITS FOR SPECIFICATION PURPOSES

"J" DISTANCE SIXTEENTHS OF AN INCH	4161 H MAX.	4161 H MIN.
1	65	60
2	65	60
3	65	60
4	65	60
5	65	60
6	65	60
7	65	60
8	65	60
9	65	59
10	65	59
11	65	59
12	64	59
13	64	58
14	64	58
15	64	57
16	64	56
18	64	53
20	63	53
22	63	50
24	63	48
26	63	45
28	63	43
30	63	42
32	63	41

HEAT TREATING TEMPERATURES
RECOMMENDED BY SAE
*NORMALIZE 1600 °F
AUSTENITIZE 1550 °F
*For forged or rolled specimens only.

Figure 5-51: Hardenability Band for AISI 4161H [56]

However, as per ASTM A125, there is a requirement that the core hardness shall be 50 HRC minimum in the as-quenched condition. The DoE results have demonstrated that over the complete as-quenched temperature range, the following average core values were achieved - reference Figure 5-52:

- 2.875-inch - 56.9 HRC
- 3.375-inch - 48.4 HRC
- 4.0-inch - 44.7 HRC

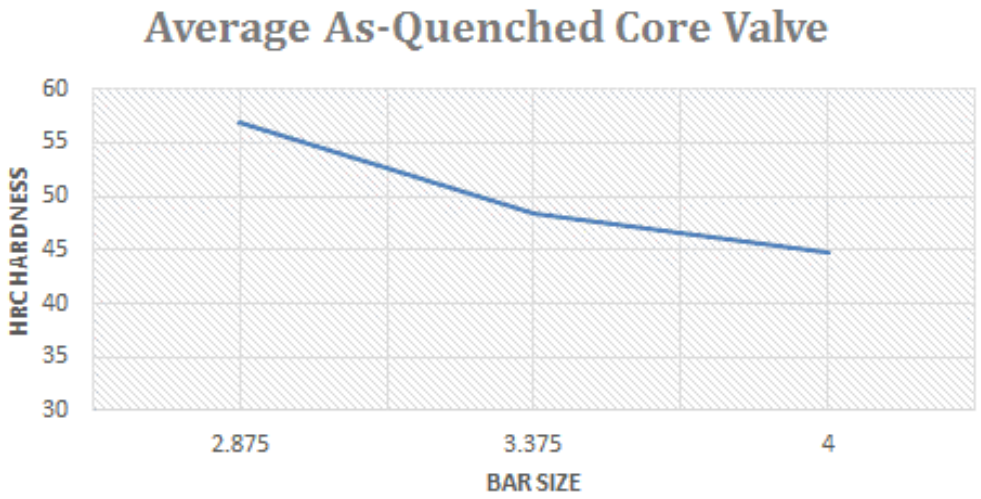

Figure 5-52: Average As-Quenched Core Hardness for All Bar Sizes

Although these respective results suggest that the ASTM A125 requirement cannot be met for both the 3.375 & 4.0-inch bars; the values specified by the end quench test plot (Figure 5-51) state the opposite. The AISI 4161 plot, specifies that < 50 HRC values can be achieved for the respective core position:

- 2.875-inch (24 sixteenths/inch - rounded up) = 48 HRC minimum
- 3.375-inch (28 sixteenths/inch - rounded up) = 43 HRC minimum
- 4.0-inch (32 sixteenths/inch) = 41 HRC minimum

This experimental core hardness suggests that there is a conflict between both coil spring convening standards ASTM A125 & ASTM A304, where ASTM A125 does not state a limit to bar diameter; beyond which, alloy steel bars conforming to Specification A689 are not capable of achieving the core hardenability requirement. Engineers therefore need to consider whether a core value <50 HRC is an area of concern, considering that the tensile properties are based on the ¼T mid-radius location. The impact of having a softer core on coil spring functionality is detailed in Section 7.1, Effects on Material Variability on the Coil Spring Functionality.

5.3.8 Hardness Testing Summary

The DoE has established the surface and through-thickness hardness properties of three bar sizes, across various heat treatment conditions. Both hardness attributes are important, as they are required by either internal or industry requirements:

- M20905 - Q &T condition; surface hardness shall be 45 - 49 HRC (421 - 469 HBW).
- ASTM A125 - Core As-Quenched hardness shall be 50 HRC minimum.

The surface and through-thickness results have exhibited a similar trend, with the heat treatment condition governing the values recorded. In all cases the As-Quenched conditions produced the greatest value with the As-cooled yielding the lowest set of results. The results have shown that the 2.875-inch bar will meet both TechnipFMC and industry requirements; however, the 3.375 & 4.0-inch material do not fully comply - see Table 5-22.

Table 5-22: Summary of key findings - Surface / Core Hardness

Bar Size	Ave Surface Hardness (Q & T) condition	TechnipFMC requirement of Q01019	As-Quenched Ave Core Hardness	ASTM A 125 requirement
2.875 inch	461 HBW	421 - 469 HBW	56.9	50 HRC minimum
3.375 inch	424 HBW		48.4	
4.0 inch	403 HBW		44.7	

The DoE has shown that the 3.375-inch bar meets the minimum surface requirements however, this can only be achieved over a tighter operating window in terms of heat treatment conditions. With regards the 4.0-inch material the results show that the minimum 421 HBW surface requirement is not met.

The hardenability of the material reduces with an increase in bar diameter / cross sectional thickness. This was evident in both the As-Quenched & Quenched / Tempered conditions, with the resultant HRC properties decreasing as the bar diameter was increased from 2.875 - 4.0-inches. The main concern with regards hardenability was the ASTM 125 requirement; "that a minimum of 50 HRC must be achieved at the core location in the As-Quenched condition". Both the 3.375 & 4.0-inch bars failed to meet this value, however as per ASTM A304 and the respective AISI 4161H hardenability band, the material is expected to yield lower values at the core thickness location, which is 43 & 41 HRC respectively. This would suggest that the values detailed within Table 5-22 are acceptable.

Therefore, further clarification is required by TechnipFMC engineering, coil spring OEM's and the industry governing bodies to determine, which specification should take precedence and which resultant value should be set as the minimum requirement.

The DoE results have shown that the:

- Quenching temperature has the greatest influence on the through-thickness hardness. This was mainly apparent across the 2.875 & 3.375-inch bar sizes, where there was a recognized hardness shift, with the increase / decrease in the respective Quenching temperature. The 4.0-inch material however, exhibited more of an incremental change in terms of resultant HRC values and the response to different heat treatment temperatures.
- Tempering operation has had an impact on the resultant through-thickness hardness properties, however the DoE has shown the changes in temperature have had a lower impact compared to the Quench temperature. The results have concluded that the responsiveness to temperature change reduces as the bar diameter has increased.

5.3.9 Banding

The work conducted prior to the DoE, (Chapter 3), had shown that the material used for coil spring application was not homogenous in terms of metallurgical properties. This was mainly related to the microstructural banding exhibited within the resultant microstructure, which had shown to produce a hardness delta between the material matrix and the adjacent band.

The work also established that there was a level variability between the raw material supplied from different Mills; and across coil springs manufactured from different heats. Because of these findings, and the relationship with reduced tensile properties, TechnipFMC Engineering placed a limit of 5 HRC on the hardness delta (difference in HRC between the band and matrix - M20905). Therefore, to fully understand the effect of banding within the AISI 4161H material, a DoE approach was taken.

5.3.9.1 Banding DoE

The DoE detailed within Section 5.2.3, has enabled the direct analysis of the banded microstructure across different heat treatment conditions and across the different respective bar sizes. This approach has allowed the evaluation of the resultant metallurgical properties in the As-Cooled, As-Quenched & Quenched & Tempered conditions within the key zones of bar sectional thickness - see Figure 5-53.

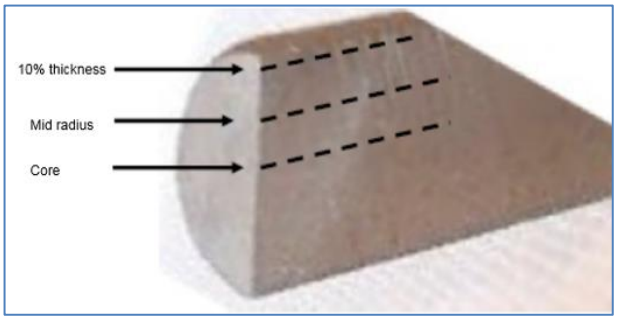

Figure 5-53: Longitudinal micro-section locations

To fully characterize the banding and its respective effect in metallurgical properties, the following testing has been completed:

- Micro Hardness Measurement - Knoop (converted to HRC) & Vickers
- SEM EDAX analysis
- Microstructural Evaluation

5.3.9.2 Micro Hardness Assessment

To determine the hardness delta across the 3 zones, Knoop and / or Vickers micro hardness measurement was completed in both the matrix & banded zones. The results were recorded as individual values, and averaged to determine the differences between the two microstructural phases. For the purposes of analyses, the values identified as "Dark" correspond to the matrix, with "Light" corresponding to the respective adjacent band. The results for each bar size and heat treatment condition are detailed within Tables 5-23 to 5-25.

Table 5-23: 2.875-inch micro hardness results

Bar size	Condition	ID	Material	Heat °F	Cool medium	Quench °F	Temper °F	10% Diameter Ave delta	10 % Diameter Dark Ave	10% Diameter Light Ave	Mid radius Ave delta	Mid radius Dark Ave	Mid radius Light Ave	Centre Ave delta	Centre Dark Ave	Centre Light Ave
2.875	Air cool	T1	Timken	1700	Air	na	na	12.8	34.4	47.2	23.4	34.2	57.6	27.2	34.4	61.6
2.875	Air cool	T2	Timken	1800	Air	na	na	12.6	34.2	46.8	16.4	34.2	50.6	26.4	31.8	58.2
2.875	Quench	E1**	Timken	1600	Oil	1600	na	141	772	913	345	543	888	358	570	928
2.875	Quench	A1**	Timken	1800	Oil	1550	na	74	759	833	491	407	898	429	483	912
2.875	Quench	C1**	Timken	1550	Oil	1550	na	51	724	775	236	575	811	423	435	858
2.875	Quench	G1**	Timken	1500	Oil	1500	na	265	540	805	373	417	790	340	412	752
2.875	Q & T	A1a	Timken	1800	Oil	1550	790	1.6	47.8	49.4	1.3	45.8	47.1	7.2	41.6	48.8
2.875	Q & T	A2a	Timken	1800	Oil	1550	790	0.2	50.2	50.4	1.2	50	51.2	0.8	49.4	48.6
2.875	Q & T	A3a	Timken	1800	Oil	1550	790	0.8	47.8	48.6	0.8	47.8	48.6	8.7	40.2	48.9
2.875	Q & T	C1	Timken	1550	Oil	1550	790	1.8	48.8	50.6	3.2	46.4	49.6	3.6	48.4	52
2.875	Q & T	C2	Timken	1550	Oil	1550	790	4	45.2	49.2	5.6	44.8	50.4	10.2	40.4	50.6
2.875	Q & T	C3	Timken	1550	Oil	1550	790	4	43.8	47.8	4	46.6	50.6	6.4	44.4	50.8
2.875	Q & T	E1	Timken	1600	Oil	1600	830	3.2	43.2	46.4	3.6	44.4	48	1.2	48.6	49.8
2.875	Q & T	E2	Timken	1600	Oil	1600	830	3.4	44.4	47.8	6.6	41.2	47.8	11.8	37.8	49.6
2.875	Q & T	E3	Timken	1600	Oil	1600	830	2.6	46.6	49.2	6.2	43.8	50	12	41	53
2.875	Q & T	F1	Timken	1600	Oil	1600	750	2.6	46.4	49	8.8	41	49.8	12.6	40.2	52.8
2.875	Q & T	F2	Timken	1600	Oil	1600	750	3.2	49.4	52.6	11	42.4	53.4	14.2	41.6	55.8
2.875	Q & T	F3	Timken	1600	Oil	1600	750	0.4	50.2	50.6	8.8	42.6	51.4	12	41	53
2.875	Q & T	G1	Timken	1500	Oil	1500	830	3.4	42.6	46	7.8	40.8	48.6	12.4	36.2	48.6
2.875	Q & T	G2	Timken	1500	Oil	1500	830	3.4	43.4	46.8	13.2	37	50.2	12	38.6	50.6
2.875	Q & T	G3	Timken	1500	Oil	1500	830	1.6	47.8	49.4	8.4	41.2	49.6	4.8	44	48.8
2.875	Q & T	H1	Timken	1500	Oil	1500	750	5.2	44.4	49.6	6.4	44.6	51	11.6	40.2	51.8
2.875	Q & T	H2	Timken	1500	Oil	1500	750	3.4	49.8	53.2	9.8	42.6	52.4	9.6	44.6	54.2
2.875	Q & T	H3	Timken	1500	Oil	1500	750	4.4	47.8	52.2	8.4	43.6	52	13.8	40.4	54.2
2.875	Q & T	I1	Timken	1550	Oil	1550	750	3.4	46.8	50.2	7.2	43.2	50.4	7.6	42.2	49.8
2.875	Q & T	I2	Timken	1550	Oil	1550	750	4.8	42.6	47.4	4	45.8	49.8	10.8	41	51.8
2.875	Q & T	J1	Timken	1600	Oil	1600	790	2.8	46.8	49.6	6	44.2	50.2	5.8	44.4	50.2
2.875	Q & T	J2	Timken	1600	Oil	1600	790	3.8	47	50.8	5.6	45	50.6	8.8	40.8	49.6

All results converted from Knoop Hardness to HRC, except Quench condition = HV 0.3 Kg

Table 5-24: 3.375-inch micro hardness results

Bar size	Condition	ID	Material	Heat °F	Cool medium	Quench °F	Temper °F	10% Diameter Ave delta	10 % Diameter Dark Ave	10% Diameter Light Ave	Mid radius Ave delta	Mid radius Dark Ave	Mid radius Light Ave	Centre Ave delta	Centre Dark Ave	Centre Light Ave
3.375	Air cool	AC1	Timken	1800	Air	na	na	9.4	28.8	38.2	6	35	41	20	39.2	59.2
3.375	Air cool	AC2	Timken	1700	Air	na	na	8.4	31	39.4	14.2	33.2	47.4	18.4	37.8	56.2
3.375	Quench	1500	Timken	1500	Oil	1500	na	103	525	628	139	380	519	215	333	548
3.375	Quench	1515	Timken	1515	Oil	1515	na	57	565	622	143	482	625	243	396	639
3.375	Quench	1550	Timken	1550	Oil	1550	na	263	442	705	250	360	610	199	358	557
3.375	Quench	1585	Timken	1585	Oil	1585	na	197	515	712	245	462	707	322	404	726
3.375	Quench	1600	Timken	1600	Oil	1600	na	128	522	650	176	480	656	253	366	619
3.375	Q & T	I1	Timken	1500	Oil	1500	790	5.8	41.8	47.6	8.6	39.6	48.2	11	39	50
3.375	Q & T	I2	Timken	1500	Oil	1500	790	8	44	52	7.2	43.6	50.8	13.8	38.2	52
3.375	Q & T	J1	Timken	1600	Oil	1600	790	4.6	43.4	48	8.2	40.4	48.6	11.6	39.2	50.8
3.375	Q & T	J2	Timken	1600	Oil	1600	790	6.6	41.4	48	10	40.2	50.2	16.2	34.6	50.8
3.375	Q & T	K1	Timken	1550	Oil	1550	790	6.2	42.6	48.8	9.8	38.8	48.6	15.2	35	50.2
3.375	Q & T	K2	Timken	1550	Oil	1550	790	2.6	44.8	47.4	4.2	43.6	47.8	10	37.8	47.8
3.375	Q & T	K3	Timken	1550	Oil	1550	750	3.8	45.4	49.2	3.4	45.2	48.6	8.8	41.6	50.4
3.375	Q & T	K4	Timken	1550	Oil	1550	830	5.6	41.6	47.2	11.2	37.2	48.4	11.2	39	50.2
3.375	Q & T	K5	Timken	1550	Oil	1550	830	3	45.2	48.2	5.2	42.6	47.8	12.6	36.4	49
3.375	Q & T	K6	Timken	1550	Oil	1550	750	0.8	49	49.8	9	42.2	51.2	8.4	40	48.4
3.375	Q & T	L1	Timken	1515	Oil	1515	815	2.4	46.2	48.6	7.8	41.6	49.4	9.8	40.4	50.2
3.375	Q & T	L2	Timken	1515	Oil	1515	815	2	44.8	46.8	6.2	41	47.2	10.6	37.8	48.4
3.375	Q & T	L3	Timken	1515	Oil	1515	765	6.8	44.6	51.4	14.8	36.4	51.2	8.8	41.2	50
3.375	Q & T	L4	Timken	1515	Oil	1515	765	5	44.4	49.4	7.6	42.6	50.2	12.8	39	51.8
3.375	Q & T	M1	Timken	1585	Oil	1585	815	5.8	41	46.8	10	40.2	50.2	14.6	37	51.6
3.375	Q & T	M2	Timken	1585	Oil	1585	765	5.4	44	49.4	5	44.8	49.8	13.6	38.2	51.8
3.375	Q & T	M3	Timken	1585	Oil	1585	815	1.4	42	43.4	4.2	41	45.2	9.6	37.6	47.2
3.375	Q & T	M4	Timken	1585	Oil	1585	765	9.6	41	50.6	10.6	39.6	50.2	12.6	38	50.6
3.375	Q & T	N1	Timken	1570	Oil	1570	750	5.8	44.6	50.4	5.8	45.8	51.6	15.2	38.4	53.6
3.375	Q & T	N2	Timken	1570	Oil	1570	750	9.8	41	50.8	8.8	40.8	49.6	13.4	37.8	51.2

All results converted from Knoop Hardness to HRC, except Quench condition = HV 0.3 Kg

Table 5-25: 4.000-inch Micro Hardness Results

Bar size	Condition	ID	Material	Heat °F	Cool medium	Quench °F	Temper °F	10% Diameter Ave delta	10 % Diameter Dark Ave	10% Diameter Light Ave	Mid radius Ave delta	Mid radius Dark Ave	Mid radius Light Ave	Centre Ave delta	Centre Dark Ave	Centre Light Ave
4	Air cool	AC1	Timken	1800	Air	na	na	1.2	37.6	36.4	11	34	45	22.8	34.8	57.6
4	Quench	1515	Timken	1515	Oil	1515	na	282	432	714	282	390	672	225	362	587
4	Quench	1550	Timken	1550	Oil	1550	na	222	379	601	268	392	660	255	344	599
4	Quench	1585	Timken	1585	Oil	1585	na	152	529	681	124	511	635	220	396	616
4	Q & T	O1	Timken	1550	Oil	1550	790	8.2	40.6	48.8	10.2	38.2	48.4	11	39.8	50.8
4	Q & T	P1	Timken	1585	Oil	1585	830	6.2	38.2	44.4	9.8	37.4	47.2	13	35.6	48.6
4	Q & T	Q1	Timken	1515	Oil	1515	750	7.6	42.6	50.2	9.8	41.6	51.4	15	37.4	52.4
4	Q & T	R1	Timken	1550	Oil	1550	850	3.2	41.6	44.8	10.8	38	48.8	13.4	36.8	50.2
4	Q & T	S1	Timken	1515	Oil	1515	830	6.2	39	45.2	11.4	38.2	49.6	12	37.6	49.6
4	Q & T	T1	Timken	1585	Oil	1585	750	5.8	43.4	49.2	10	42.2	52.2	14.4	35.8	50.2
4	Q & T	U1	Timken	1550	Oil	1550	730	4.2	39.4	43.6	8.4	41	49.4	11	38.4	49.4

All results converted from Knoop Hardness to HRC, except Quench condition = HV 0.3 Kg

5.3.9.3 Micro Hardness Assessment - Analysis Summary

The analysis from the DoE has established there is a hardness delta between the distinct phases (band /matrix) within the microstructure. It is also apparent that the delta changes across the respective bar sectional thickness, which is greatly influenced by different heat treatment conditions.

When considering all the bar size results together (2.875 - 4.0 inches), in both the Air Cooled & Quench / Tempered conditions, an increasing hardness delta trend exists from the surface location to the core - see Figure 5-54. This is further clarified when studying the resultant values for the individual bar sizes themselves - reference Figure 5-55, which confirms that by increasing the respective bar size the hardness delta increases from the surface to core.

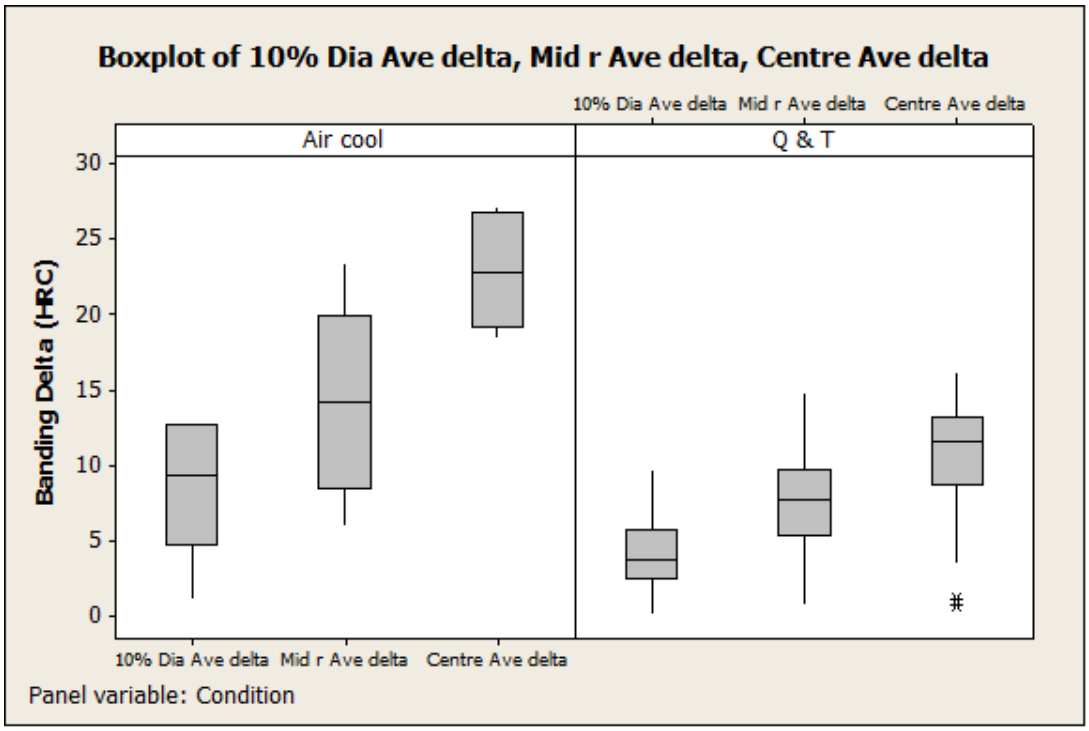

Figure 5-54: Box plot Hardness Delta values for the 3 bar sizes - Air cool versus Q & T Conditions

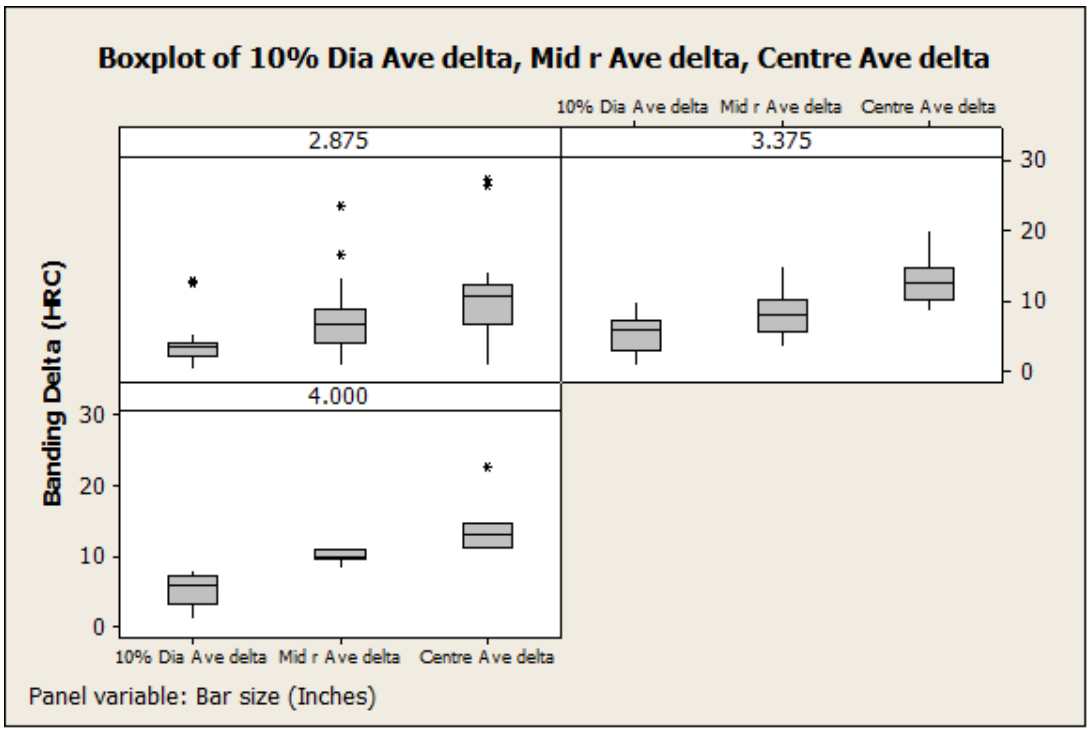

Figure 5-55: Box plot of Hardness Delta for the Individual Bar Sizes

To establish the effect of actual sectional thickness against the resultant hardness delta, the values recorded at each respective distance were plotted for the Quench / Temper conditions. The purpose of this approach, was to consider each of the 3 bars as one, and to determine the effect over the complete distance (compounded) from the surface to the core - Reference Figure 5-56 & Table 5-26.

Table 5-26: Distances where the Hardness Delta was measured for Each Bar Dia.

Location	2.875"	3.375"	4.000"
10% thickness	0.2875 inches	0.337 inches	0.4 inches
Mid-radius	0.72 inches	0.84 inches	1.0 inches
Core / center	1.44 inches	1.68 inches	2.0 inches

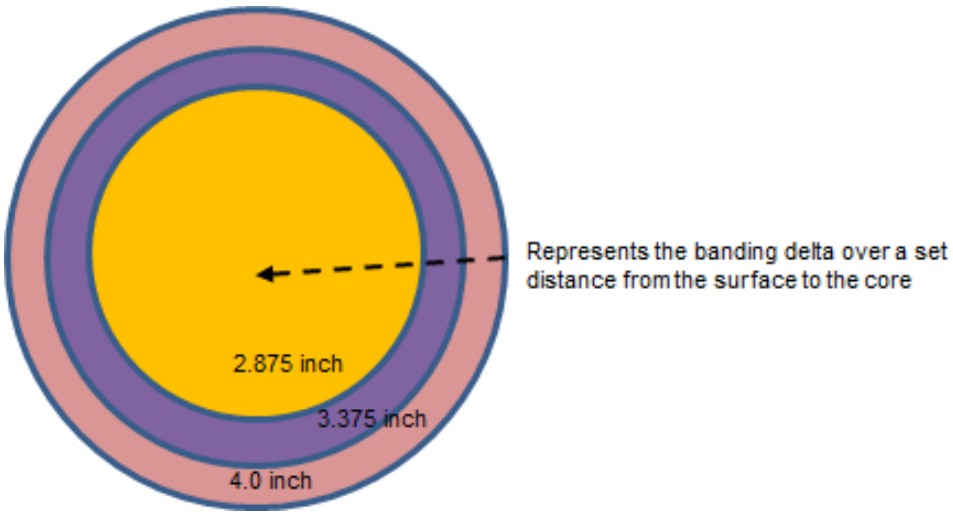

Figure 5-56: Diagram of 3 Bars Compounded Together for Analysis Purposes (based on Table 5-26)

By representing the results as one bar, it enables a better understanding of how the the delta (hardness difference between the matrix & band) in the fully heat treated condition (Quench / Temper) is increasing from the surface to the core. This verifies that a change in bar diameter, will have a direct influence on the resulting hardness delta between the matrix and band - Reference Figure 5-57.

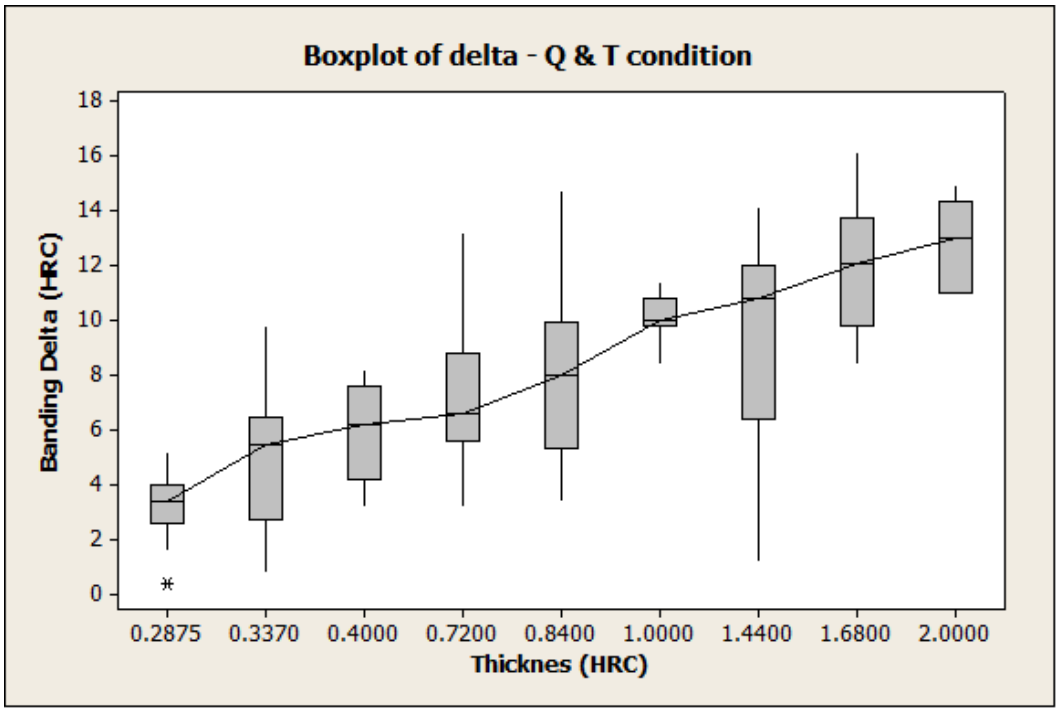

Figure 5-57: Boxplot of the Hardness Delta versus distance for all 3 bar sizes

In addition to evaluating the Quench / Temper process as one combined heat treatment condition; the results have been assessed on an individual basis, with the effects of each respective operation being considered. This has been completed by comparing the Quench & Temper heat treatment temperatures against the resultant hardness delta achieved across the total bar sectional thickness - Reference Table 5-26, Figure 5-58, and Figure 5-59.

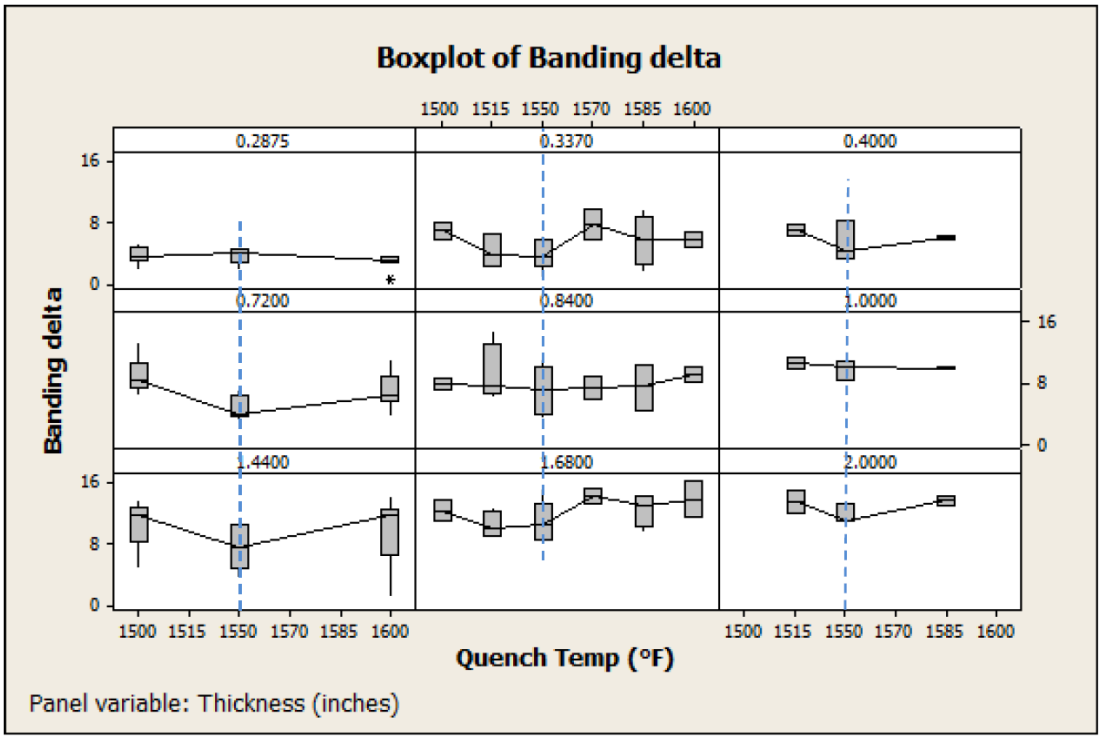

Figure 5-58: Hardness Delta versus Sectional Thickness at Specific Quench Temperatures

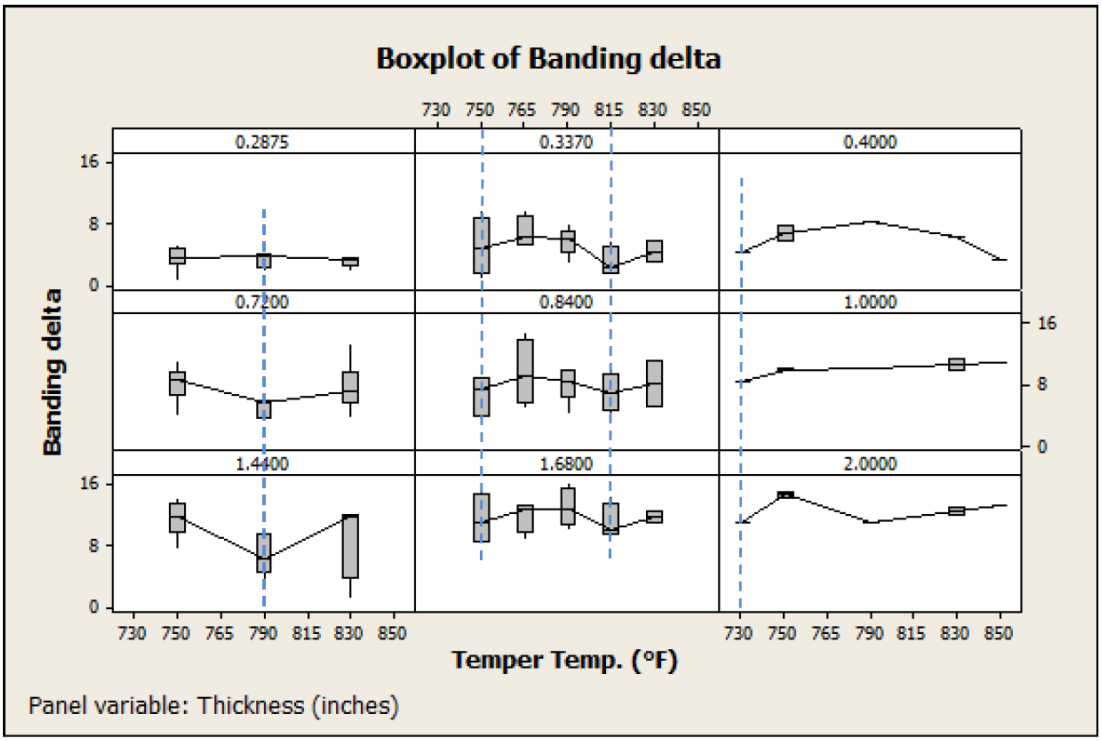

Figure 5-59: Hardness Delta versus Sectional Thickness at Specific Tempering temperatures

The boxplot of the quench results - Figure 5-58, demonstrates that the Austenitise / Quench temperature has an effect in terms of the hardness delta within the microstructure. Within each sectional thickness point, the hardness delta various depending of the Quench temperature selected. Also, the results have shown that a Quench temperature of 1550°F produces the lowest delta value for all respective bar sizes.

A similar effect is also applicable for the temper boxplot reference Figure 5-59, where a shift in hardness within the microstructure exists with a change in process temperature. The tempering temperature effect is not the same for each bar size, as the lowest HRC delta was experienced at different respective values.

- 790°F @ 2.875-inch diameter
- 750°F & 815°F @ 3.375-inch diameter
- 730°F @ 4.0-inch diameter

5.3.9.3.1 Matrix versus Band

The micro hardness assessment has clearly established that a delta does exist across the respective bar sectional thickness. However, it is key to understand what phase within the microstructure is changing to create the hardness difference, and whether this is influenced by different heat treatment operations.

The results from the DoE, detailed within Tables 5-23 to 5-25 have been summarized within Table 5-27. These are the average delta values for each heat treatment condition, and the average values for each respective microstructural phase (dark - matrix / light - band) within the bar cross-section.

Table 5-27: Summary of Average Hardness Delta for each Heat Treatment condition

Bar size	condition	10% dark	10% light	Bar size	condition	mid rad dark	mid rad light	Bar size	condition	core dark	core light
2.875	Air cool	34.3	47	2.875	Air cool	34.2	54.1	2.875	Air cool	33.1	59.9
3.375	Air cool	29.9	38.8	3.375	Air cool	34.1	44.2	3.375	Air cool	38.5	57.7
4	Air cool	37.6	36.4	4	Air cool	34	45	4	Air cool	34.8	57.6
Bar size	condition	10% dark	10% light	Bar size	condition	mid rad dark	mid rad light	Bar size	condition	core dark	core light
2.875	Quench	61.4	62.9	2.875	Quench	65.8	62.6	2.875	Quench	53.2	64.3
Bar size	condition	10% dark	10% light	Bar size	condition	mid rad dark	mid rad light	Bar size	condition	core dark	core light
2.875	Q & T	46.5	49.4	2.875	Q & T	43.9	50.1	2.875	Q & T	42.1	51.1
3.375	Q & T	43.6	48.7	3.375	Q & T	41.4	49.2	3.375	Q & T	38.3	50.3
4	Q & T	40.7	46.6	4	Q & T	39.5	49.6	4	Q & T	37.3	50.2

The results clearly show that across the three heat treatment conditions, the matrix is the key phase, which is changing. This is primarily apparent with the Quench and Temper results, which show a uniform band hardness across the 3 measured locations (10%, mid-radius & core) e.g. 2.875 - 49.4, 50.1 & 51.1 HRC respectively. However, the matrix for the same locations, yield values of 46.5, 43.9 & 42.1 HRC - see Table 5-27.

This is also shown in Figure 5-60, which presents the hardness trend for each microstructural zone (matrix / band) across all the bars at a set distance from the surface. The resultant boxplots at the Quench / Temper conditions display a hardness decline within the material matrix, as the bar thickness is increased. On the other hand, the band values are considered more consistent across the section; with an approximate straight line exhibited throughout the median values - see Figure 5-60.

The boxplots in Figure 5-60, also reiterate the delta trend shown in Figure 5-57, with an increase in resultant values over the sectional thickness, which is due to the differences of the hardness values between the matrix and band phases.

In addition, the matrix is the phase, which is changing more in terms of resultant hardness, over the different heat treatment conditions. This is shown in the 2.875-inch bar results, at the mid-radius position, where the matrix location yielded values of 34.2, 65.8 & 43.9 across different conditions, compared to 54.1, 62.6 & 50.1 for the band - see Table 5-27.

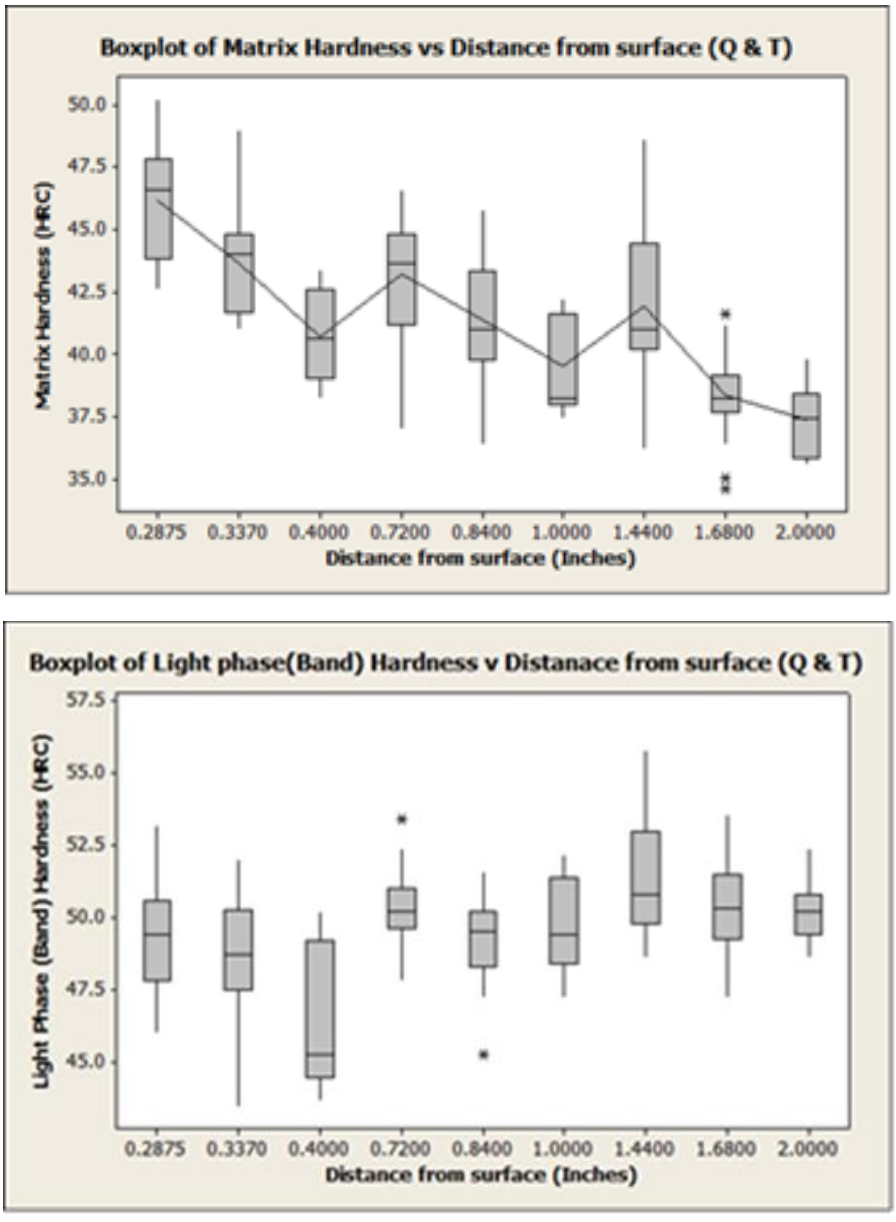

Figure 5-60: Boxplots of Matrix & Band Hardness versus Distance from surface

5.3.9.4 Heat Treatment Response

The DoE has established that the hardness delta, and indeed the hardness of each phase within the microstructure (Matrix / Band), is influenced by the type of heat treatment process. This is summarized within Figure 5-61, which shows the influence of changing the heat treatment conditions at the core location.

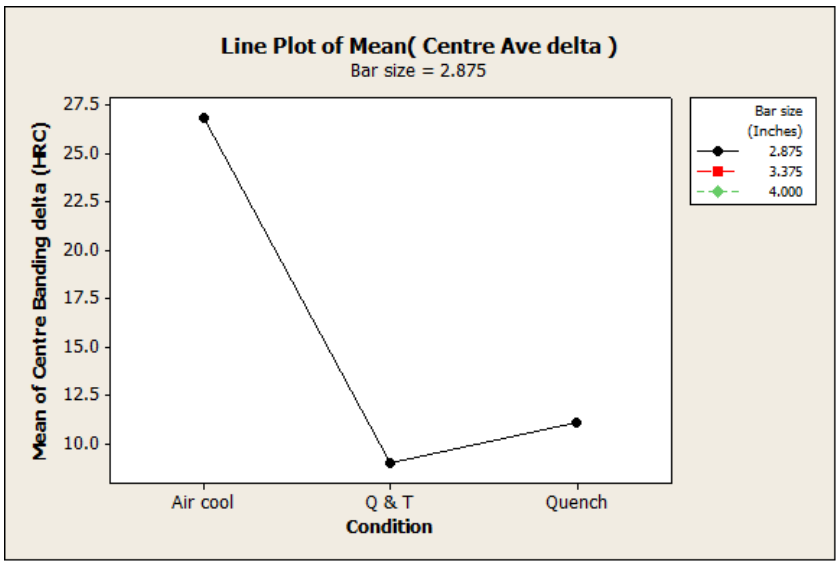

Figure 5-61: Average Core Hardness Delta Hardness for 2.875-Inch Bar - All Heat Treatment Conditions

The graph shown in Figure 5-61 exhibits a significant delta change within the microstructure once the material is quenched; and then further after the bar is subjected to the Quench and Temper process. The effect of the hardness delta is compounded by bar size, in addition to the subjected heat treatment operation. This is confirmed within Figure 5-62, which compares the resultant HRC delta at three locations across each respective bar range (2.875 - 4.0 inches).

The line plots referenced within Figure 5-62, reiterate the point that in the Quenched and Tempered condition, the hardness delta increases with bar diameter (reference red dashed line). In addition, the delta has shown to increase from the surface to the core, which verifies the data set presented within Figure 5-57.

The plots clearly establish that the 2.875-inch bar has had the greatest response to the heat treatment conditions. This is shown by the significant hardness shift / reduction at each respective location, specifically for the smallest bar size (2.875-inch purple arrow).

The 3.375 & 4.0-inch material have both responded to heat treatment; however, when comparisons are made against the Air cooled (Normalized) & Q and T conditions, the shift change is reduced, especially with the mid-radius position, which exhibits a minimal shift in hardness delta. In addition, the 3.375 & 4.0-inch material yield similar hardness delta reductions at both the mid-radius and core locations - Reference Figure 5-62.

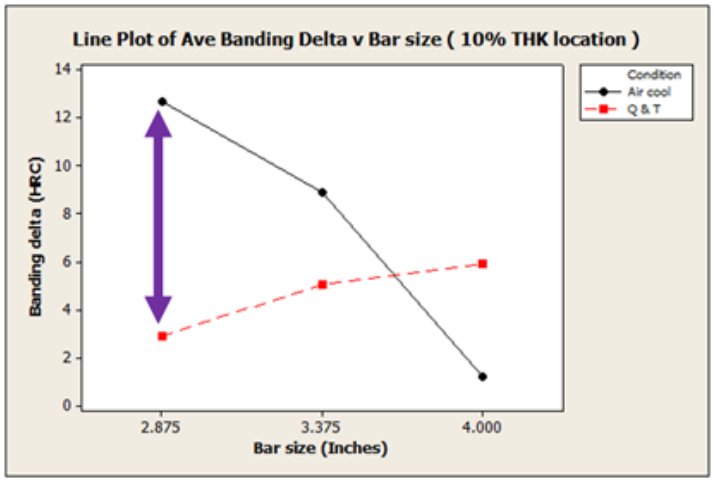

Line Plot for the 10% thickness location - Bar size v banding delta

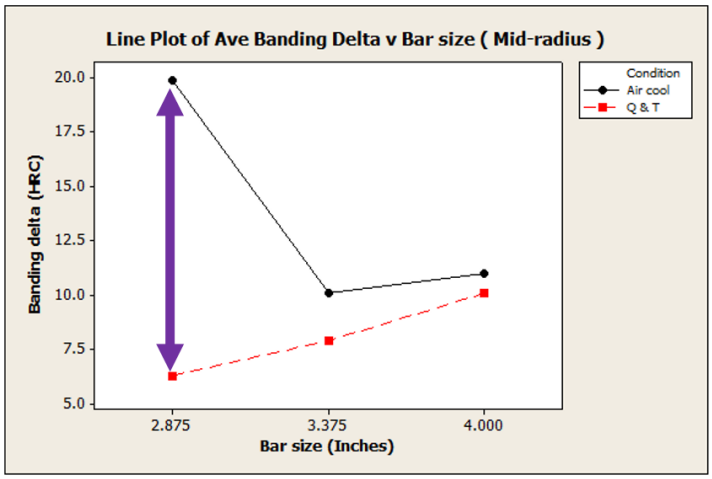

Line Plot for the Mid-radius location - Bar size v banding delta

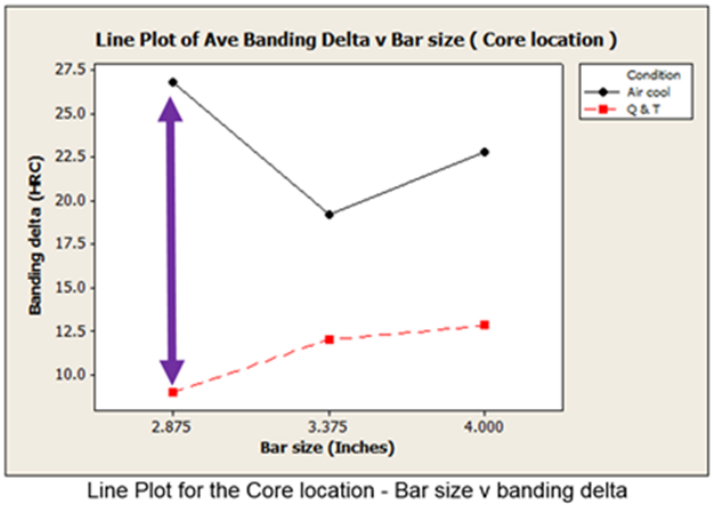

Line Plot for the Core location - Bar size v banding delta

Figure 5-62: Hardness Delta vs. Bar Size

5.3.9.5 Hardness Delta - Air Cooled

The results from the Air Cool heat treatment DoE, have confirmed that the hardness delta increases from the 10% surface thickness location through to the bar core. This trend is applicable for all bar sizes, with the 2.875-inch material yielding the greatest delta across the respective locations - Reference Table 5-28.

The range of the hardness delta also varies with the bar size:

- 2.875-inch: 12.7 - 26.8 HRC
- 3.375-inch: 8.9 - 19.2 HRC
- 4.0-inch: 1.2 - 22.8 HRC

In addition, the results have confirmed that the 3.375 and 4.0-inch bars produced a similar resultant hardness delta at the respective mid-radius & core positions - Reference Table 5-28.

Table 5-28: Air Cool - Average Hardness Delta for Each Bar Size

bar size	condition	10% delta ave - HRC		bar size	condition	mid rad delta ave - HRC		bar size	condition	core delta ave - HRC
2.875	Air cool	12.7		2.875	Air cool	19.9		2.875	Air cool	26.8
3.375	Air cool	8.9		3.375	Air cool	10.1		3.375	Air cool	19.2
4	Air cool	1.2		4	Air cool	11		4	Air cool	22.8

5.3.9.6 Hardness Delta - As Quenched

In the As-Quenched condition, the results have shown a similar trend with regards the hardness delta across the respective bar sectional thickness, with near surface values producing the lowest values, compared to the core, which exhibited the highest difference between the matrix and adjacent band - Reference Table 5-29.

Table 5-29: As-Quenched - Average Hardness Delta for Each Bar Size

bar size	condition	10% delta ave - HV 0.2Kg		bar size	condition	mid rad delta ave - HV 0.2Kg		bar size	condition	core delta ave - HV 0.2 Kg
2.875	Quench	133		2.875	Quench	358		2.875	Quench	386
3.375	Quench	149		3.375	Quench	191		3.375	Quench	247
4	Quench	219		4	Quench	225		4	Quench	234

5.3.9.7 Hardness Delta - Quenched & Tempered

The Quench / Tempered condition is very important in that it fully defines the material properties for the application and service environment of the respective coil spring. The results have been summarized within Table 5-30 & Figure 5-63.

It is evident that the delta increases from the surface to the core; with a trend of increased HRC across the evaluated bar sizes, 2.875 - 4.0 inches.

It is also apparent that over the large number of heat treatment trials /inputs, the average delta was greater than the current TechnipFMC specification (M20905) requirement of ≤ 5 HRC. This was the case for all locations, except the 10% thickness value for 2.875-inch bar, which achieved a delta of 2.9 HRC.

Table 5-30: Q & T - Average Hardness Delta for Each Bar Size

bar size	condition	10% delta ave - HRC		bar size	condition	mid rad delta ave - HRC		bar size	condition	core delta ave - HRC
2.875	Q & T	2.9		2.875	Q & T	6.3		2.875	Q & T	9
3.375	Q & T	5.1		3.375	Q & T	7.9		3.375	Q & T	12
4	Q & T	5.9		4	Q & T	10.1		4	Q & T	12.8

The graphs detailed within Figure 5-63 show that the hardness of the material in the band is greater than that of the matrix in all cases. In each individual graph, the position of the data point along the x axis is arbitrary ordered by sample number.

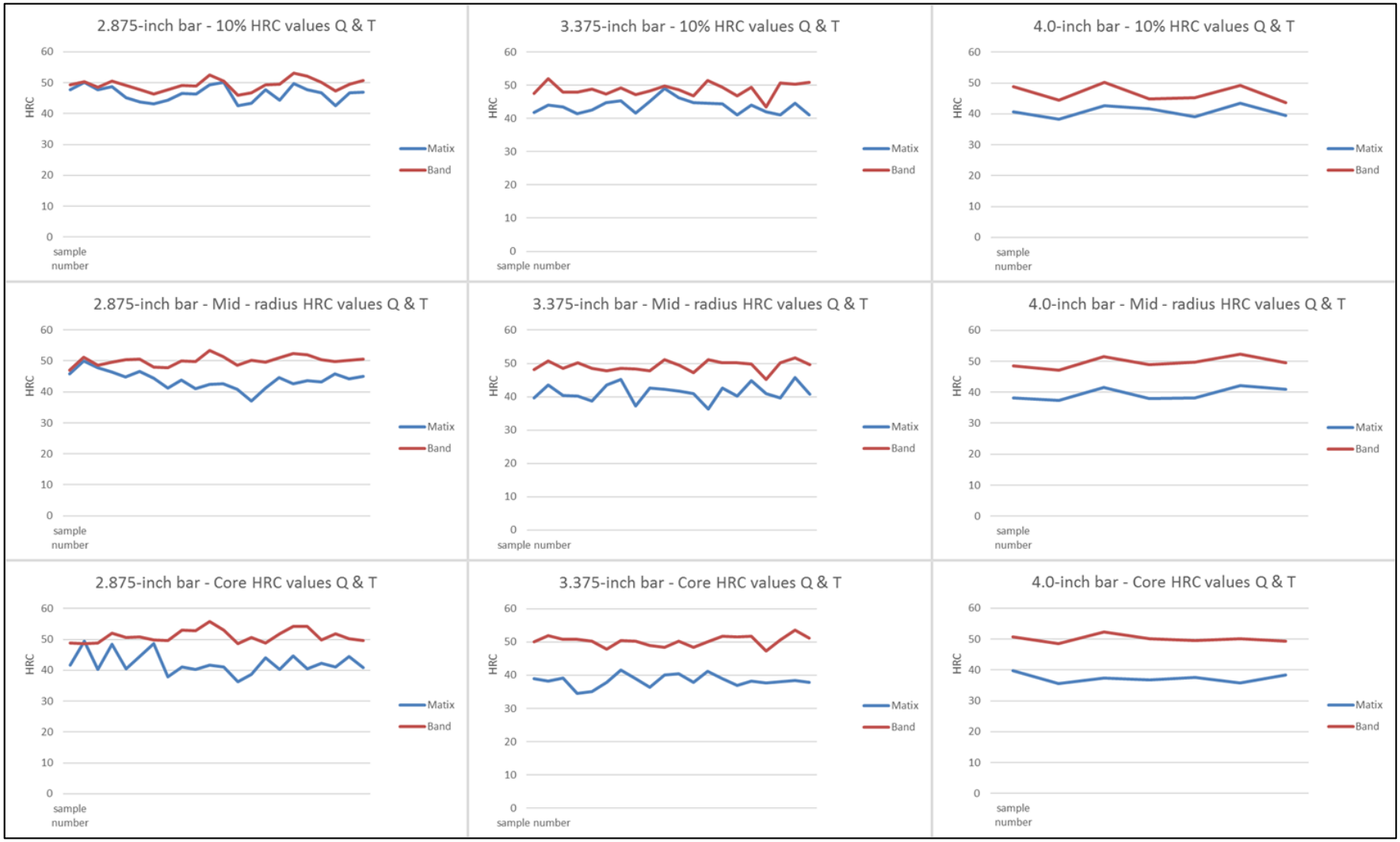

Figure 5-63: Graphical View of the Q & T Hardness Results for the Band v Matrix - All Bar Sizes

5.3.9.8 Micro Hardness Assessment Summary

The micro hardness assessment has enabled a full understanding of the effects of banding within the microstructure. The DoE has clearly established that:

- A hardness delta exists between the different phases within the microstructure (matrix / bands).
    - It is apparent this delta will increase, from the surface location through to the core, irrespective of the bar diameter.
- In the fully heat-treated condition (Q & T), there is a clear trend that the hardness delta will continue to increase through the sectional thickness of the material.
    - This was demonstrated within Figure 5-57, where the results of the three bars were combined as one 4-inch section; where the resultant values increased from approximately 3 to 13 HRC over a 2-inch radius.
- There is one predominant phase, which is changing during the heat treatment operations, and is thus responsible for creating the HRC delta.
    - The DoE has established that the matrix is the phase, which is more susceptible to heat treatment response and resultant hardness changes, compared to the band, which produces more consistent / stable results.
- The hardness delta within the microstructure is directly influenced by the respective heat treatment process.
    - Within all bar sizes, the hardness delta changed when exposed to the Air Cooled (Normalized), As-Quenched & Quench / Temper conditions. This was demonstrated by the 2.875-inch bar core location, which yielded results of 26.8 HRC, 11.1 HRC & 9.0 HRC when heat treated through these respective conditions.
- The Quench and Temper condition, as an individual data set, has shown that different Austenitizing and Tempering temperatures can affect the HRC delta between the matrix and band.

    - This is apparent for each location across the material sectional thickness - Reference Figure 5-58 and Figure 5-59.
    - All bars tested, regardless of thickness yielded the lowest HRC delta at an Austenitize temperature of 1550°F
- Each bar size has an optimum Tempering temperature / range, which will produce the lowest delta between the matrix and band.
- The bar diameter has a major influence on the change of the HRC delta.
    - Results have shown that the 2.875-inch bar responded to greatest extent than the other material sizes. This was due to the reduction in the HRC delta exhibited by the smaller diameter bar, when exposed to the various heat treatment conditions - Reference Figure 5-62.
- The current TechnipFMC (M20905) material specification requirements (HRC delta of ≤ 5 HRC) can only be consistently met at the 10% location for 2.875-inch bar only. All other 2.875-inch locations & larger bar sizes (3.375 / 4.0-inch) failed to meet the material specification requirement.
    - Therefore, this material process control cannot be used to verify the acceptance and design quality needed for coil spring applications.

5.3.9.9 SEM EDAX analysis

The analysis completed within the micro-hardness assessment, has clearly demonstrated that the coil spring material is not homogenous across the complete bar cross-section. It has also shown that the matrix and the banded zones, exhibit differences in resultant hardness, which can affect the material metallurgical properties.

To understand why a hardness delta exists within each bar size, an in-depth evaluation was undertaken. This involved conducting SEM EDAX analysis across the AISI 4161H material matrix & banded zones, in each of the heat-treated conditions specified within the DoE. In the same way to the micro-hardness evaluation; measurements were taken at three locations for each respective heat treatment condition: 10%-thickness, Mid-radius, and Core; these locations are detailed in Figure 5-53.

Although the chemical composition of the AISI 4161H material consists of seven (7) elements, reference Table 5-31; the SEM EDAX analysis was set up to accurately determine the respective values for Si, Cr, Mn and Mo only. This was due to the analysis reliability for the detection of Carbon, Sulfur and Phosphorous when using EDAX for quantitative measurements. In addition, these elements are conventionally analysed using more repeatable techniques.

Table 5-31: Chemical compositional requirements of the AISI 4161H material

4161H	
Carbon	0.55 - 0.65
Manganese	0.65 - 1.10
Phosphorus, max	0.025
Sulfur, max	0.015
Silicon	0.15 - 0.35
Chromium	0.65 - 0.95
Molybdenum	0.25 - 0.35

The analysis method in all cases involved taking the chemical composition along the respective zone (band / matrix) within the microstructure at the specified position across the longitudinal section of the analysed bar. Examples of the analysis and respective results are demonstrated within Figure 5-64 and Figure 5-65.

To gain a better understanding of the chemical composition results for each respective phase within the microstructure, it was decided to adopt an analytical technique that would determine the effect of the variability exhibited between the two microstructural phases (band / matrix) for each heat treatment condition. For this purpose, the Ideal Diameter calculation per the requirements of ASTM A255 [56] was selected. ASTM A255 utilizes a compound calculation and different multiplying factors for each respective element percentage. The method considers that each element has a different influencing factor in terms of material hardenability (more / less).

	Mid - radius Band							Core Band			
Measure	Si	Cr	Mn	Mo			Measure	Si	Cr	Mn	Mo
1	0.31	0.9	1.25	0.65			1	0.39	1.21	1.49	0.87
2	0.33	0.96	1.21	0.61			2	0.45	1.21	1.43	0.91
3	0.38	0.96	1.12	0.55			3	0.41	1.19	1.41	0.81
4	0.35	0.95	1.17	0.63			4	0.4	1.1	1.4	0.88
5	0.3	0.97	1.23	0.55			5	0.42	0.98	1.31	0.8
mean	0.34	0.95	1.2	0.6			mean	0.41	1.14	1.41	0.86
STD deviation	0.03	0.03	0.05	0.05			STD deviation	0.02	0.1	0.06	0.05
max	0.38	0.97	1.25	0.65			max	0.45	1.21	1.49	0.91
min	0.3	0.9	1.12	0.55			min	0.39	0.98	1.31	0.8

Figure 5-64: SEM EDAX analysis for the 3.375-inch bar, which was quenched at 1500°F and tempered at 790°F

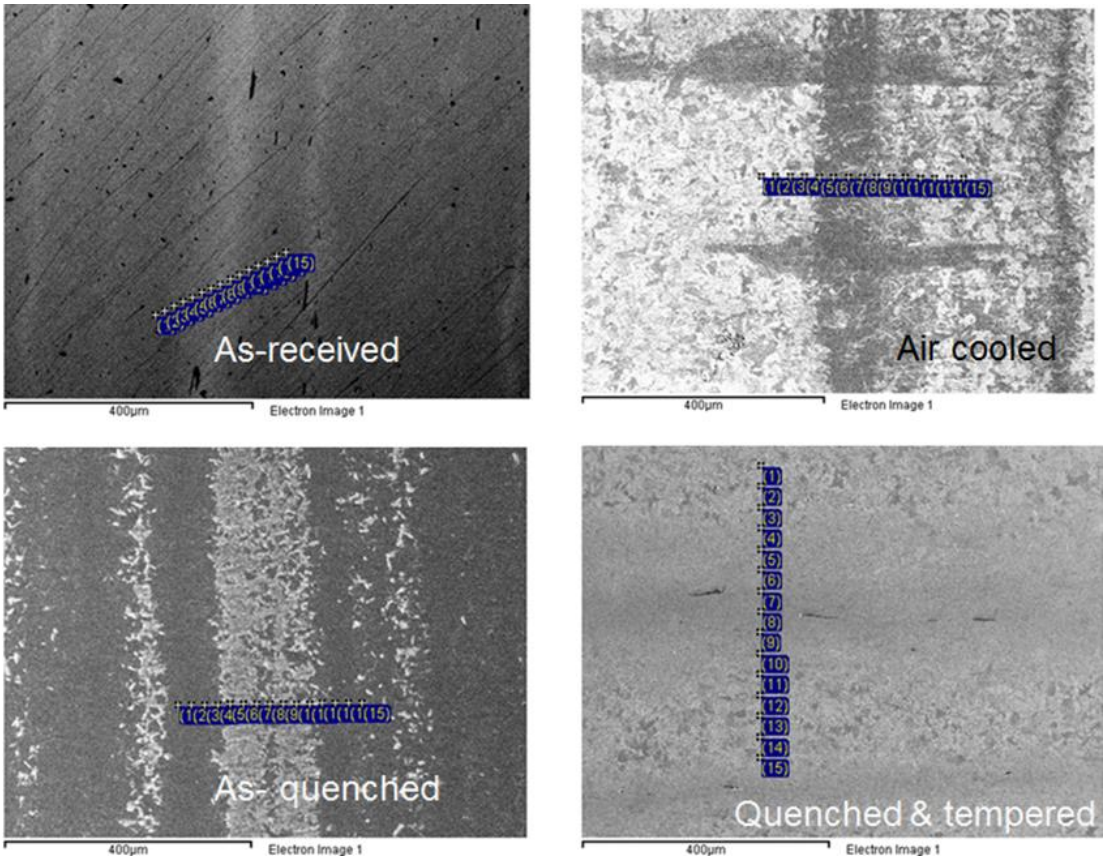

Figure 5-65: Example of SEM EDAX Analysis Locations for the Four (4) Conditions Evaluated

5.3.9.10 SEM EDAX Analysis - Phase Hardenability Results

Per the requirements of ASTM A255, the chemical composition for each microstructural phase was used to determine the respective Ideal Diameter value for the zone analysed. The compound formula adopted by A255, takes each element individually and applies a multiplying factor. This is dependent on the element and its effect on through-thickness properties (hardenability); with some elements having a greater effect than others - Reference Figure 5-66.

% Alloy	Carbon-Grain Size 7	Mn	Si	Ni	Cr	Mo	Cu	V	Zr
0.01	0.005	1.033	1.007	1.004	1.022	1.03	1.00	1.02	1.02
0.02	0.011	1.067	1.014	1.007	1.043	1.06	1.01	1.03	1.05
0.03	0.016	1.100	1.021	1.011	1.065	1.09	1.01	1.05	1.07
0.04	0.022	1.133	1.028	1.015	1.086	1.12	1.01	1.07	1.10
0.05	0.027	1.167	1.035	1.018	1.108	1.15	1.02	1.09	1.12

Figure 5-66: Example of ASTM A255 Multiplying factors for individual elements [56]

The calculation also takes into consideration the carbon values and respective material grain size. Therefore, for the purposes of the DI determination, the C% from the material CoC was utilized, along with a pre-austenitic grain size of 7, "which is assumed, since most steels with hardenability control are melted to a fine grain practice" [56]. Figure 5-67 demonstrates an example of the formula used to determine the DI for both the band and matrix, with Figure 5-68 displaying and extract from the DoE result spread sheet.

Element	%	Multiplying Factor
Carbon	0.22	0.119
Manganese	0.80	3.667
Silicon	0.18	1.126
Nickel	0.10	1.036
Chromium	0.43	1.929
Molybdenum	0.25	1.75
Copper	0.10	1.04
Vanadium	0.05	1.09

where:

DI = 0.119 × 3.667 × 1.126 × 1.036 × 1.929 × 1.75 × 1.04 × 1.09 = 1.95 in.

Figure 5-67: Example of Ideal Diameter calculation taken from ASTM A255

Sample	Position	Measure	C- G size 7	C	Si	A255 - F	Cr	A255 - F	Mn	A255 - F	Mo	A255 - F	Ideal Diameter
AC1	Mid-radius	Band	0.258	0.58	0.38	1.266	1.06	3.29	1.23	5.153	0.77	2.65	14.67
AC1	Mid-radius	Matrix	0.258	0.58	0.29	1.203	0.64	2.382	0.8	3.667	0.32	1.96	5.31

Figure 5-68: Extract from the 3.375-inch bar DI results - Air Cool condition at the mid-radius position

The results from the DI calculation are summarized within Table 5-32, which lists the resultant values for all heat treatment conditions conducted within the DoE.

Table 5-32: DI results for all DoE test conditions

		Ideal Diameter						Core		Mid-radius		10%	
Bar Size	Condition	ID	Material	Heat °F	Cool medium	Quench °F	Temper °F	Band	Matrix	Band	Matrix	Band	Matrix
2.875	As received	AR	SDI	Na	Na	Na	Na	29.55	10.65	12.22	6.32	5.07	5.82
2.875	As received	AR	Timken	Na	Na	Na	Na	44.89	7.57	14.92	6.59	7.57	6.85
2.875	Air Cool	T1	Timken	1700	Air	Na	Na	20.73	7.38	8.46	6.90	6.02	6.02
2.875	Air Cool	T2	Timken	1800	Air	Na	Na	13.45	4.33	13.10	5.77	9.76	6.65
2.875	Air Cool	T3	SDI	1700	Air	Na	Na	14.93	4.73	14.10	7.00	11.61	7.17
2.875	Air Cool	T4	SDI	1800	Air	Na	Na	18.36	7.84	8.66	5.77	8.77	5.43
2.875	Quench	A1a	Timken	1800	Oil	1550	Na	9.01	5.86	11.38	5.45	4.98	4.26
2.875	Quench	B1	Timken	1700	Oil	1550	Na	8.03	3.47	9.87	4.66	6.62	5.35
2.875	Quench	C1	Timken	1550	Oil	1550	Na	6.16	3.81	8.90	4.42	5.89	5.89
2.875	Quench	E1	Timken	1600	Oil	1600	Na	8.17	5.11	10.90	5.46	5.63	5.63
2.875	Quench	G1	Timken	1500	Oil	1500	Na	17.34	4.37	7.04	4.03	6.74	4.81
2.875	Quench / Temper	A1a	Timken	1800	Oil	1550	790	15.43	3.39	13.32	5.92	6.60	6.60
2.875	Quench / Temper	B1	SDI	1700	Oil	1550	790	27.00	7.06	11.73	3.86	4.01	5.68
2.875	Quench / Temper	C3	Timken	1550	Oil	1550	790	11.27	5.54	9.16	4.72	5.79	5.79
2.875	Quench / Temper	E3	Timken	1600	Oil	1600	830	11.09	4.23	5.44	4.53	7.37	7.37
2.875	Quench / Temper	F1	Timken	1600	Oil	1600	750	8.33	3.70	10.76	5.82	6.80	6.80
2.875	Quench / Temper	G1	Timken	1500	Oil	1500	830	13.27	4.31	16.47	6.43	6.99	6.99
2.875	Quench / Temper	H3	Timken	1500	Oil	1500	750	16.40	4.29	10.88	3.76	5.04	6.17
2.875	Quench / Temper	I2	Timken	1550	Oil	1550	750	5.56	4.59	7.96	7.96	8.36	6.19
2.875	Quench / Temper	J2	Timken	1600	Oil	1600	790	13.50	4.37	14.19	3.70	7.38	7.38

		Ideal Diameter						Core		Mid-radius		10%	
Bar Size	Condition	ID	Material	Heat °F	Cool medium	Quench °F	Temper °F	Band	Matrix	Band	Matrix	Band	Matrix
3.375	As received	AR	Timken	Na	Na	Na	Na	23.31	3.15	10.29	5.96	3.88	3.36
3.375	Air Cool	AC1	Timken	1800	Air	Na	Na	25.96	7.52	18.00	5.31	9.36	6.99
3.375	Air Cool	AC2	Timken	1700	Air	Na	Na	16.28	7.73	17.37	6.32	10.55	6.12
3.375	Quench	AQ1500	Timken	1500	Oil	1500	Na	7.74	2.77	7.92	3.06	6.54	3.51
3.375	Quench	AQ1515	Timken	1515	Oil	1515	Na	17.42	2.72	7.42	2.88	3.96	4.70
3.375	Quench	AQ1550	Timken	1550	Oil	1550	Na	20.41	2.72	12.89	3.04	9.84	3.84
3.375	Quench	AQ1585	Timken	1585	Oil	1585	Na	15.49	2.92	7.96	3.23	10.75	2.74
3.375	Quench	AQ1600	Timken	1600	Oil	1600	Na	9.41	4.41	5.17	2.81	7.21	3.16
3.375	Quench / Temper	I1	Timken	1500	Oil	1500	790	24.78	4.62	13.65	5.86	9.20	6.48
3.375	Quench / Temper	L4	Timken	1515	Oil	1515	765	32.89	5.45	12.54	4.39	8.35	6.04
3.375	Quench / Temper	L2	Timken	1515	Oil	1515	815	28.64	5.52	13.10	5.35	10.09	5.52
3.375	Quench / Temper	K3	Timken	1550	Oil	1550	750	15.23	4.76	13.40	6.90	11.16	4.72
3.375	Quench / Temper	K6	Timken	1550	Oil	1550	750	22.41	5.23	15.48	6.75	12.50	6.47
3.375	Quench / Temper	K1	Timken	1550	Oil	1550	790	12.78	4.47	15.83	4.55	9.70	4.71
3.375	Quench / Temper	K4	Timken	1550	Oil	1550	830	18.37	4.32	14.65	6.41	10.87	6.06
3.375	Quench / Temper	N2	Timken	1570	Oil	1570	750	20.17	4.25	12.06	5.60	9.95	6.43
3.375	Quench / Temper	M4	Timken	1585	Oil	1585	765	18.12	4.89	10.19	4.52	10.00	6.31
3.375	Quench / Temper	M3	Timken	1585	Oil	1585	815	24.53	4.23	18.44	4.66	10.74	6.64
3.375	Quench / Temper	J1	Timken	1600	Oil	1600	790	25.53	5.09	9.83	5.51	12.77	5.77

		Ideal Diameter						Core		Mid-radius		10%	
Bar Size	Condition	ID	Material	Heat °F	Cool medium	Quench °F	Temper °F	Band	Matrix	Band	Matrix	Band	Matrix
4	As received	AR	Timken	Na	Na	Na	Na	21.05	2.77	4.81	3.15	4.18	3.92
4	Air Cool	AC1	Timken	1800	Air	Na	Na	26.99	10.65	22.86	5.97	7.68	7.76
4	Quench	AQ1515	Timken	1515	Oil	1515	Na	16.31	2.61	8.88	3.06	3.78	3.34
4	Quench	AQ1550	Timken	1550	Oil	1550	Na	28.94	3.19	4.19	2.94	6.28	3.58
4	Quench	AQ1585	Timken	1585	Oil	1585	Na	12.26	3.03	3.96	2.93	3.98	3.09
4	Quench / Temper	Q1	Timken	1515	Oil	1515	750	26.60	5.47	12.94	3.51	10.61	4.89
4	Quench / Temper	S1	Timken	1515	Oil	1515	830	23.20	5.01	13.52	6.08	9.66	6.38
4	Quench / Temper	U1	Timken	1550	Oil	1550	730	20.62	4.85	16.89	6.08	9.62	6.35
4	Quench / Temper	O1	Timken	1550	Oil	1550	790	17.28	3.67	13.14	4.56	11.26	6.87
4	Quench / Temper	R1	Timken	1550	Oil	1550	850	26.47	4.99	12.08	4.62	10.10	6.43
4	Quench / Temper	T1	Timken	1585	Oil	1585	750	12.83	4.69	12.40	5.79	11.76	5.90
4	Quench / Temper	P1	Timken	1585	Oil	1585	830	21.72	4.57	15.43	5.25	12.20	5.24

To interpret the results in more detail, the respective values have been analysed, as individual heat treatment groups and as a combination of heat treatment conditions for each respective bar type / size. The results have therefore been extrapolated from Table 5-32 into a more meaningful comparison, as depicted by Tables 5-33 & 5-34.

Table 5-33: Average DI Values for Each Heat Treatment Condition V bar size

Average As-received DI										
	Core		Mid-radius		10%			Average	As-received	DI delta
Bar size	Band	Matrix	Band	Matrix	Band	Matrix	Bar size	Core	Mid-radius	10%
2.875	37.22	9.11	13.57	6.45	6.32	6.34	2.875	28.11	7.12	0.00
3.375	23.31	3.15	10.29	5.96	3.88	3.36	3.375	20.16	4.33	0.52
4	21.05	2.77	4.81	3.15	4.18	3.92	4	18.28	1.66	0.26

Average Air Cool DI										
	Core		Mid-radius		10%			Average	Air Cooled	DI delta
Bar size	Band	Matrix	Band	Matrix	Band	Matrix	Bar size	Core	Mid-radius	10%
2.875	16.87	6.07	11.08	6.36	9.04	6.32	2.875	10.80	4.72	2.72
3.375	21.12	7.62	17.68	5.82	9.96	6.55	3.375	13.5	11.86	3.41
4	26.99	10.65	22.86	5.97	7.68	7.76	4	16.34	16.89	0.08

Average As-quenched DI										
	Core		Mid-radius		10%			Average	As-quenched	DI delta
Bar size	Band	Matrix	Band	Matrix	Band	Matrix	Bar size	Core	Mid-radius	10%
2.875	9.74	4.53	9.62	4.80	5.97	5.19	2.875	5.21	4.82	0.78
3.375	14.09	3.11	8.28	3	7.66	3.59	3.375	10.98	5.28	4.07
4	19.17	2.94	5.68	2.97	4.68	3.34	4	16.23	2.71	1.34

Average Q & T DI										
	Core		Mid-radius		10%			Average	Q & T	DI Delta
	Band	Matrix	Band	Matrix	Band	Matrix		Core	Mid-radius	10%
2.875	13.54	4.61	11.10	5.19	6.48	6.55	2.875	8.93	5.91	0.07
3.375	22.13	4.8	13.56	5.5	10.49	5.92	3.375	17.33	8.06	4.57
4	21.25	4.75	13.77	5.13	10.74	6.01	4	16.50	8.64	4.73

Table 5-34: Average DI Values for each bar size versus all Heat Treatment Conditions

	Average ideal diameter values for each condition					
	Core		Mid-radius		10%	
2.875-inch bar	Band	Matrix	Band	Matrix	Band	Matrix
As received	37.22	9.11	13.57	6.45	6.32	6.34
Air Cool	16.87	6.07	11.08	6.36	9.04	6.32
Quench	9.74	4.53	9.62	4.80	5.97	5.19
Quench / Temper	13.54	4.61	11.10	5.19	6.48	6.55

	Average ideal diameter values for each condition					
	Core		Mid-radius		10%	
3.375-inch bar	Band	Matrix	Band	Matrix	Band	Matrix
As received	23.31	3.15	10.29	5.96	3.88	3.36
Air Cool	21.12	7.62	17.68	5.82	9.96	6.55
Quench	14.09	3.11	8.28	3.00	7.66	3.59
Quench / Temper	22.13	4.80	13.56	5.50	10.49	5.92

	Average ideal diameter values for each condition					
	Core		Mid-radius		10%	
4.0-inch bar	Band	Matrix	Band	Matrix	Band	Matrix
As received	21.05	2.77	4.81	3.15	4.18	3.92
Air cool	26.99	10.65	22.86	5.97	7.68	7.76
As quenched	19.17	2.94	5.68	2.97	4.68	3.34
Quench & Temper	21.25	4.75	13.77	5.13	10.74	6.01

The results within Table 5-33 have clearly shown that the band and matrix have different DI values. This is apparent for each heat treatment condition, and for each bar size and respective position across the analysed sample (core, mid-radius & 10% thickness).

The as-received results, which represent the 3 bar sizes in the hot rolled datum condition, have shown that the microstructural band phase located at the core, exhibits the greatest DI value and resultant chemical composition. It is also clear that the band phase DI reduces from the core through the mid-radius position to the surface location (10% thickness). This trend is apparent for all bar sizes; with 2.875-inch exhibiting the greatest DI followed by the 3.375 and 4.0 respectively - see Table 5-33 and Figure 5-69.

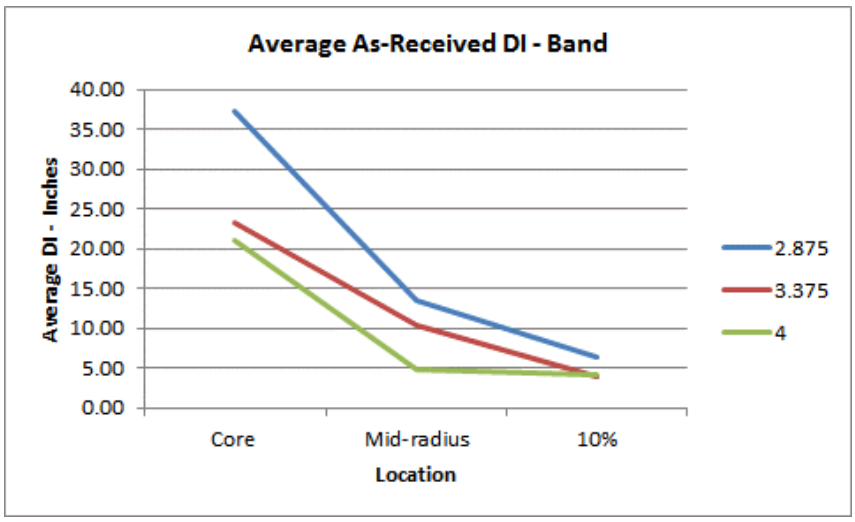

Figure 5-69: Average DI for the Band Phase in the As-Received Condition

The matrix in the as-received condition follows a similar trend to the band phase, with the highest DI achieved with the 2.875-inch bar. However, the resultant values across the section for all bar types, is more consistent, especially the 3.375 and 4.000-inch results - see Table 5-33 and Figure 5-70.

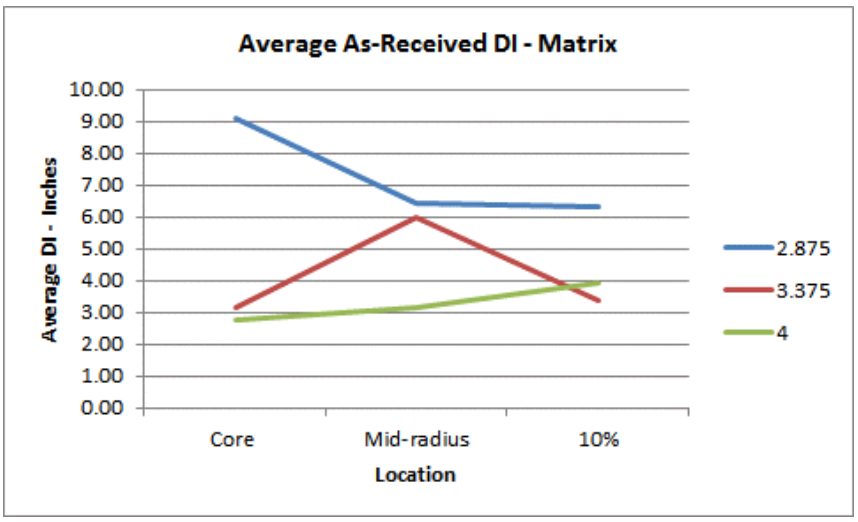

Figure 5-70: Average DI for the Matrix Phase in the As-Received Condition

The results have also demonstrated that the delta in DI for the band and matrix, various considerably across the bar sectional thickness. All three bar sizes follow the same trend, with a large delta in chemical composition present at the core. This is followed by a major reduction in DI delta at the mid-radius location; with no or little chemical compositional difference variance between each respective phase at the 10% zone - Reference Table 5-33 & Figure 5-71.

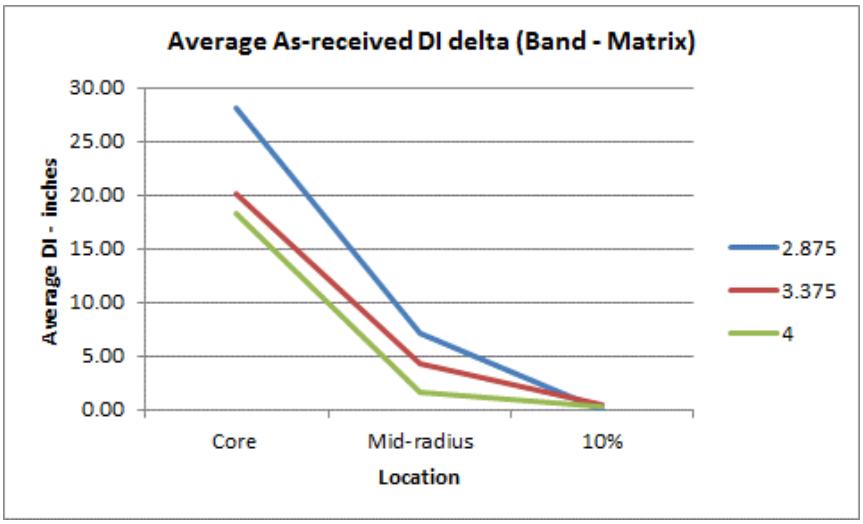

Figure 5-71: Average DI Delta (Band - Matrix) in the As-Received Condition

These results clearly demonstrate that in the as-received condition, the band phase is predominantly rich in chemistry compared to the adjacent matrix, which will vary dependant on bar diameter and location across the respective section.

The air-cooled results presented within Table 5-33 begin to show the effect of heat treating the datum as-received material. As stated within Section 5.2.2, the as-cooled test methodology, represents normalising the material at the OEM hot coiling temperature. The effect of this heat treatment step / process is demonstrated within Figure 5-72 and 5-73.

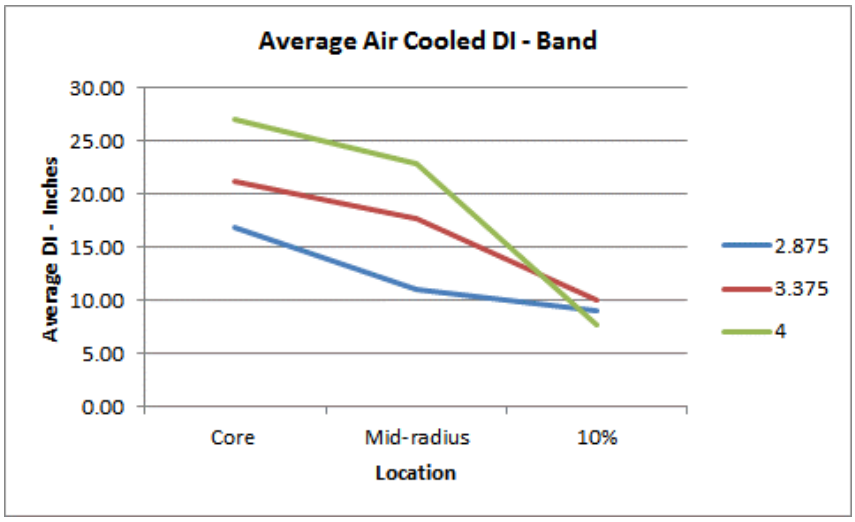

Figure 5-72: Average DI for the Band Phase in the As-cooled condition

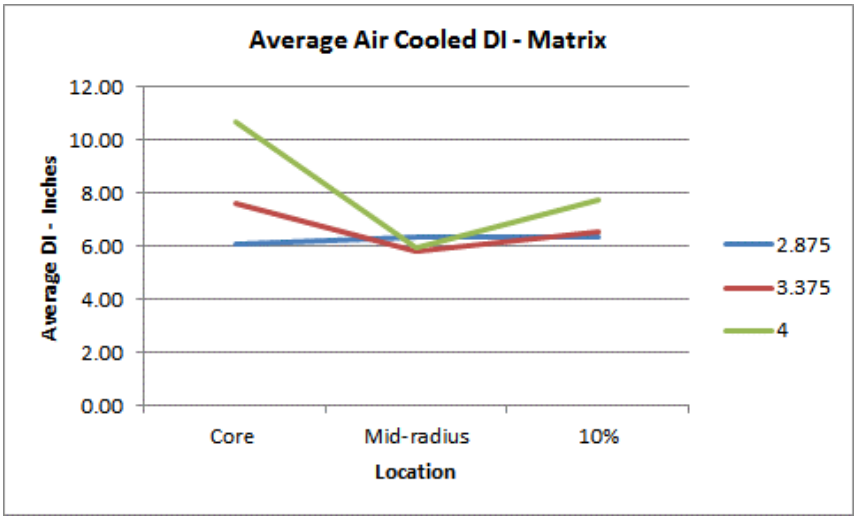

Figure 5-73: Average DI for the Matrix Phase in the As-cooled condition

The results have shown that like the as-received condition, the DI for the band phase, is highest at the core, which reduces over the remaining bar section from mid-radius to the 10% thickness position. However, the chemical composition / DI is greatest with the 4.0-inch bar, reducing to the lowest values with the 2.875-inch material. This

is opposite to what was exhibited by the as-received datum analysis. The 2.875-inch bar core location has responded to the greatest extent to the subsequent heat treatment, by the observed difference in DI reduction from 37.22 to 16.87 inches. On the other hand, the 3.375 and 4.0-inch material DI for the banded zone has increased, especially the core and mid-radius locations.

As for the matrix, in the air-cooled condition, all bar sizes exhibit comparable results with minimal change across the analysed bar sections (core, mid-radius and core) - reference Table 5-33 & Figure 5-73.

The DI delta between the band and matrix phases, reduces from the core to mid-radius location for the 2.875-inch material. However, the larger bars, exhibit a more consistent chemical composition delta between the two phases, from the core to mid-radius; prior to all three bars producing minimum differences at the 10% thickness location - reference Figure 5-74.

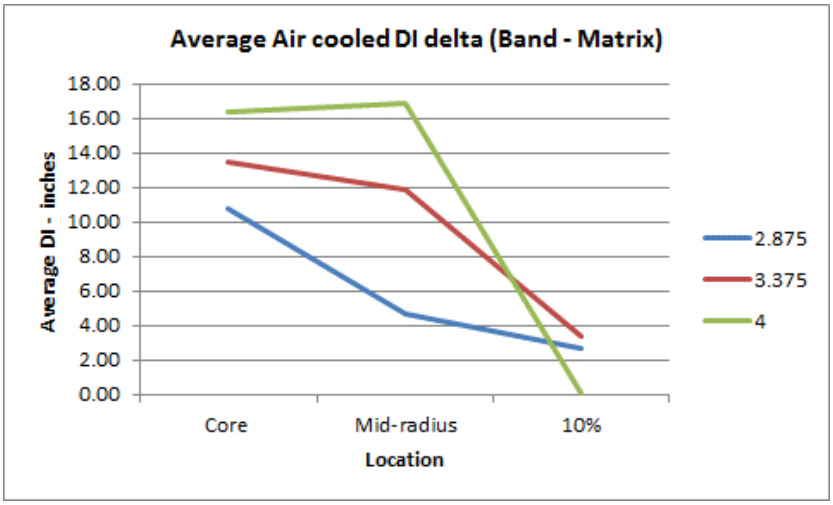

Figure 5-74: Average DI Delta (Band - Matrix) in the As-cooled condition

The as-quenched results are representative of a production environment; where material is taken from the as-received condition to the austenitizing temperature and quenched in oil. Like the previously analysed 'as cooled' condition, the DI values are greatest at the core band position, with the 4.0-inch material exhibiting the greatest chemical composition, and the 2.875-inch with the lowest value. In addition, the respective DI band phase results reduce over the bar cross-section from the core to the near surface location - see Figure 5-75 and 5-76.

With regards to the heat treatment response, the 2.875-inch material has reacted to the greatest extent with the band phase DI reducing from 37.22 to 9.74 - inches. This is a direct result of the quenching operation - see Table 5-33.

The matrix phase however, exhibited consistent values across the microstructure cross section. This was apparent for all bar sizes, with a subtle increase in DI values achieved for the 2.875-inch material. As for the DI delta between the two phases, the lowest difference was achieved for as-quenched treatment compared to the other conditions - see Figure 5-77 & Table 5.33.

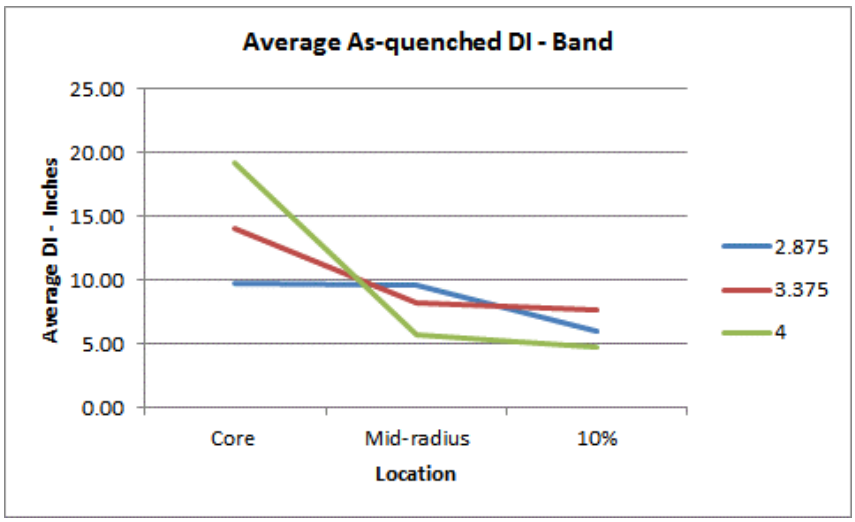

Figure 5-75: Average DI for the Band Phase in the As-quenched condition

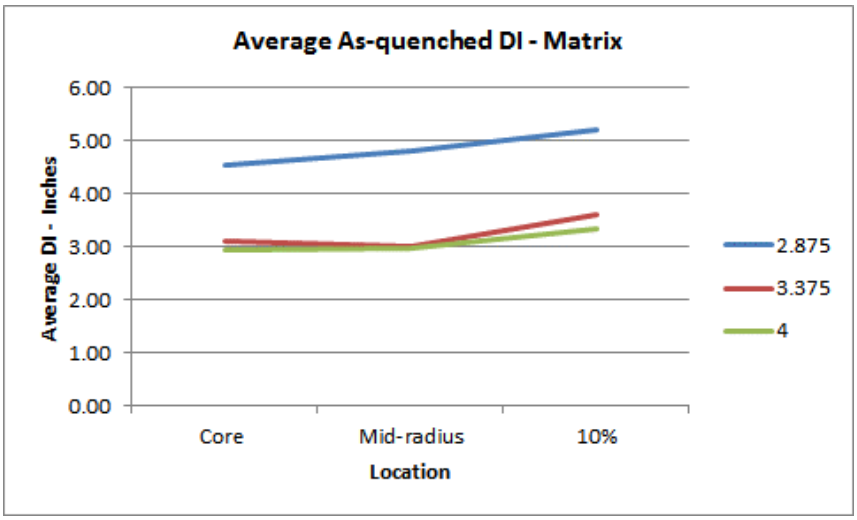

Figure 5-76: Average DI for the Matrix Phase in the As-quenched condition

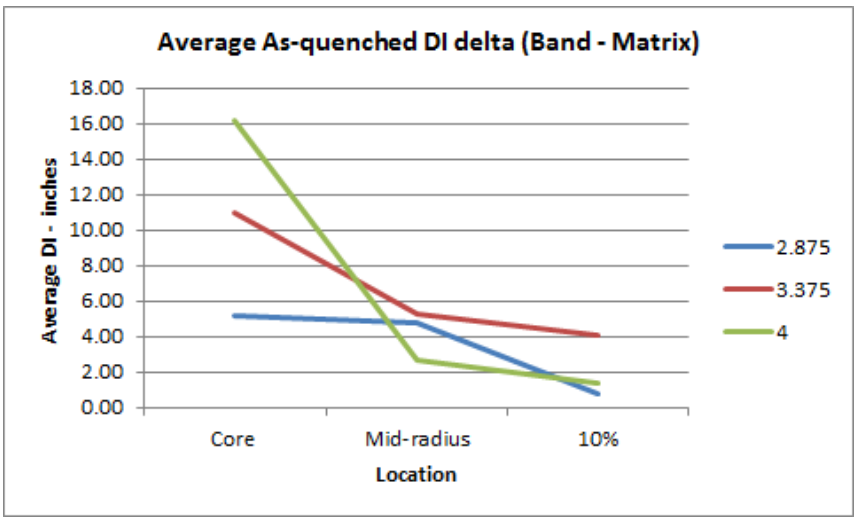

Figure 5-77: Average DI Delta (Band - Matrix) in the As-quenched condition

The final test condition analysed was the effect of the quench and tempering process on the resulting microstructure. This represents the final condition of the coil spring components prior to operating within a subsea valve. In addition, the quench and temper condition is the industry standard that all OEM's supply parts too.

Table 5-33 and Figure 5-78, summarize the results of DI of the band phase across the respective bars cross sectional thickness. Like the air-cooled & as-quenched values, the ideal diameter reduces from the core to the surface. The 2.875-inch bar however, has produced the lowest DI values, with both the 3.375 & 4.0-inch material exhibiting almost identical results. As for the matrix, all bars follow a similar trend with a subtle increase in DI values from the core to the respective 10% location. The matrix across all locations can be considered as uniform in terms of chemical composition, as the maximum variance between any core position and 10% location was 1.94 inches DI (2.875 core - 10% / 6.55 - 4.61), Figure 5-79.

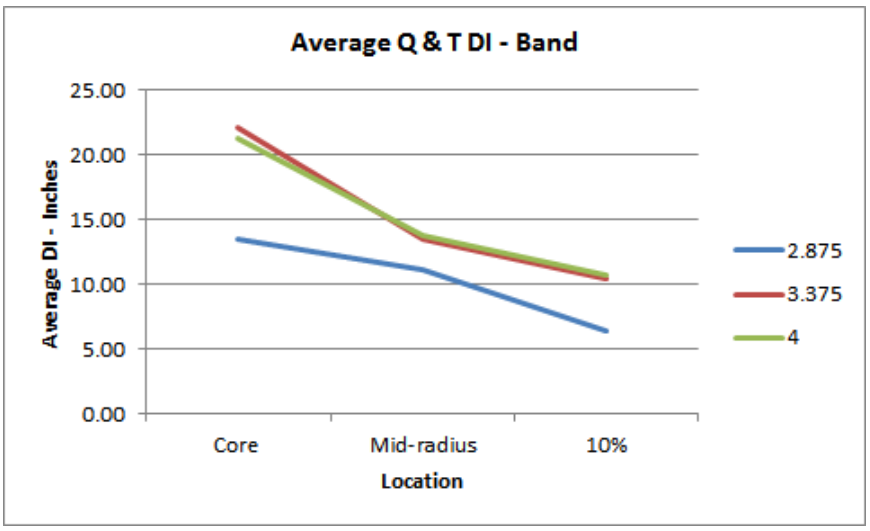

Figure 5-78: Average DI for the Band Phase in the Quenched and Tempered Condition

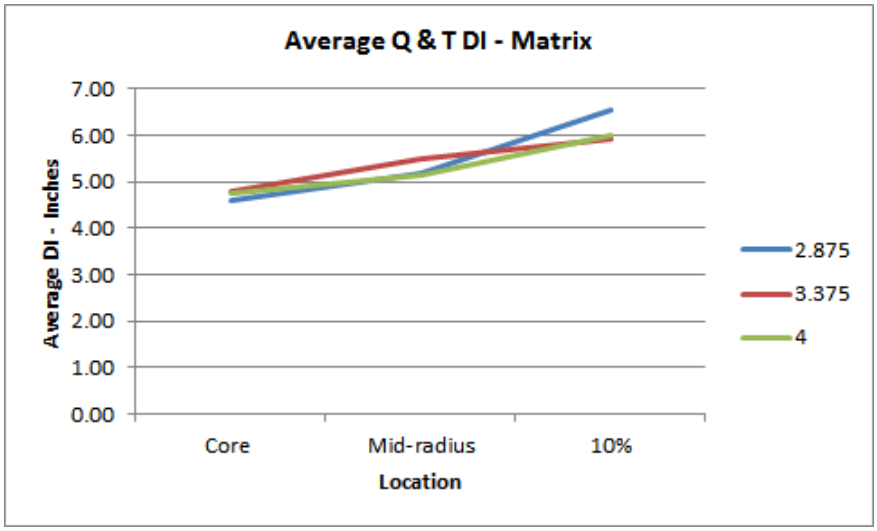

Figure 5-79: Average DI for the Matrix Phase in the Quenched and Tempered Condition

The phase delta, followed the same trend as the band only analysis results, with both the 3.375 & 4.0-inch material producing equivalent results. Yet again the 2.875-inch bar exhibited the lowest ideal diameter delta between the band and matrix phases across all cross-sectional positions - see Figure 5-80.

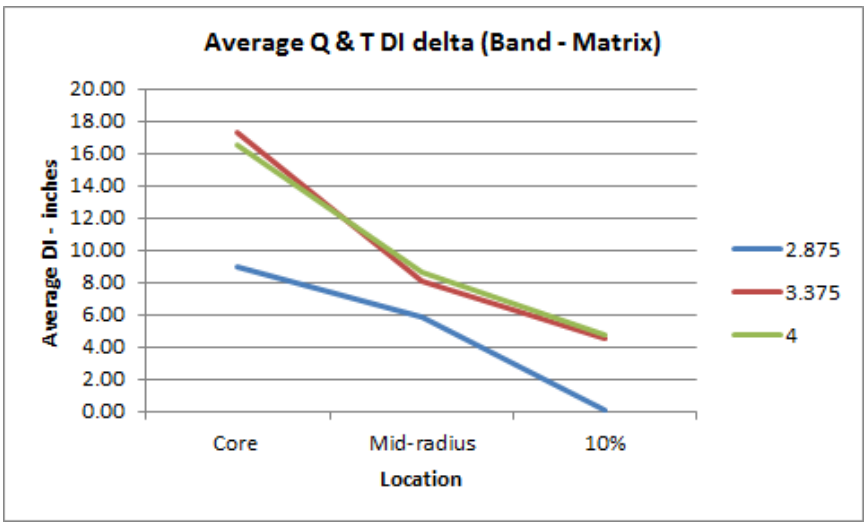

Figure 5-80: Average DI Delta (Band - Matrix) in the Quenched & Tempered Condition

5.3.9.11 SEM EDAX Analysis Summary

The SEM EDAX analysis study has enabled a better understanding of the effect of microstructural variability exhibited across the analysed bar range of 2.875 - 4.0 inches. This experimental approach has allowed the comparison of different heat treatment conditions, and how their effect can influence the resulting chemical composition within both the band and matrix phases present throughout the microstructure. The DoE has clearly established that:

- The chemical composition in terms of individual elements and as an Ideal Diameter (DI), varies across the bar from the core to the 10% thickness location. This is applicable for the band phase and all heat treatment conditions including the As-received material. In all cases the microstructural band phase at the core location, exhibits the richest chemistry and greatest respective DI values. This is summarized within Table 5-35, which demonstrates an example of the respective chemical composition and DI values achieved for the Quench & Temper conditions for the 3.375-inch bar.

Table 5-35: SEM EDAX analysis for the 3.375-inch bar (Quenched at 1500°F / Tempered at 790°F

Band					
Location	Si%	Cr%	Mn%	Mo%	DI - inches
Core	0.41	1.14	1.41	0.86	24.78
Mid-radius	0.34	0.95	1.2	0.6	13.65
10%	0.36	0.85	1.07	0.4	9.2
Matrix					
Location	Si%	Cr%	Mn%	Mo%	DI - inches
Core	0.29	0.64	0.81	0.23	4.62
Mid-radius	0.3	0.69	0.89	0.3	5.86
10%	0.29	0.73	0.96	0.31	6.58

- Overall the matrix has exhibited some to minimal change over the heat treatment conditions, compared to that experienced by the banded zones. Based on the raw material chemistry and TechnipFMC requirements (Reference Table 5-31), the AISI 4161H material should yield an Ideal Diameter of approximately 6.25 inches (based on mean values). This is similar to what was achieved under the Quench & Temper conditions across all bar sizes (average of 5.38 - taken from Table 5-33).
- The Ideal Diameter delta between the two analysed phases (band & matrix) is the greatest at the core, which subsequently reduces as you move towards the surface of the material - Reference Figure 5-81.
- The heat treatment processes have shown to have a major influence on the resultant ideal diameter and chemical composition of the analysed material. The experimental approach has demonstrated that the as-received material in the hot rolled condition can change significantly when exposed to different processes such as Air Cool (Normalize), Quench (Austenitize) and Quench & Temper - Reference Figure 5-81. This is however dependent on the bar diameter:
    - The analysis of the As-received material found the smaller 2.875-inch bar to exhibit the greatest DI values across all locations, followed by the 3.375 & 4.0-inch respectively.

- The Air-cooled (Normalizing) treatment, has had the opposite effect on the material to the datum As-received condition. This has resulted in the 4.0-inch bar producing the highest DI values (band zone) which, reduces by bar diameter to the lowest values experienced by the 2.875-inch material. The 2.875 material within the banded zone has reduced significantly especially at the core location, with the other 2 bar sizes increasing in DI across the core and mid-radius locations.
- The As-Quenched process produced the greatest effect in terms of changing / reducing the resultant DI values, especially at the core locations for each bar type. This was mainly apparent for the 2.875-inch bar, which reduced from 37.22 to 9.74 within the respective banded zone.
- The Quench & Temper treatment produced similar values for both the band and matrix phases for the 3.375 & 4.0-inch bars. However, the 2.875-inch material produced significantly lower DI results for the band phase across the complete cross section.

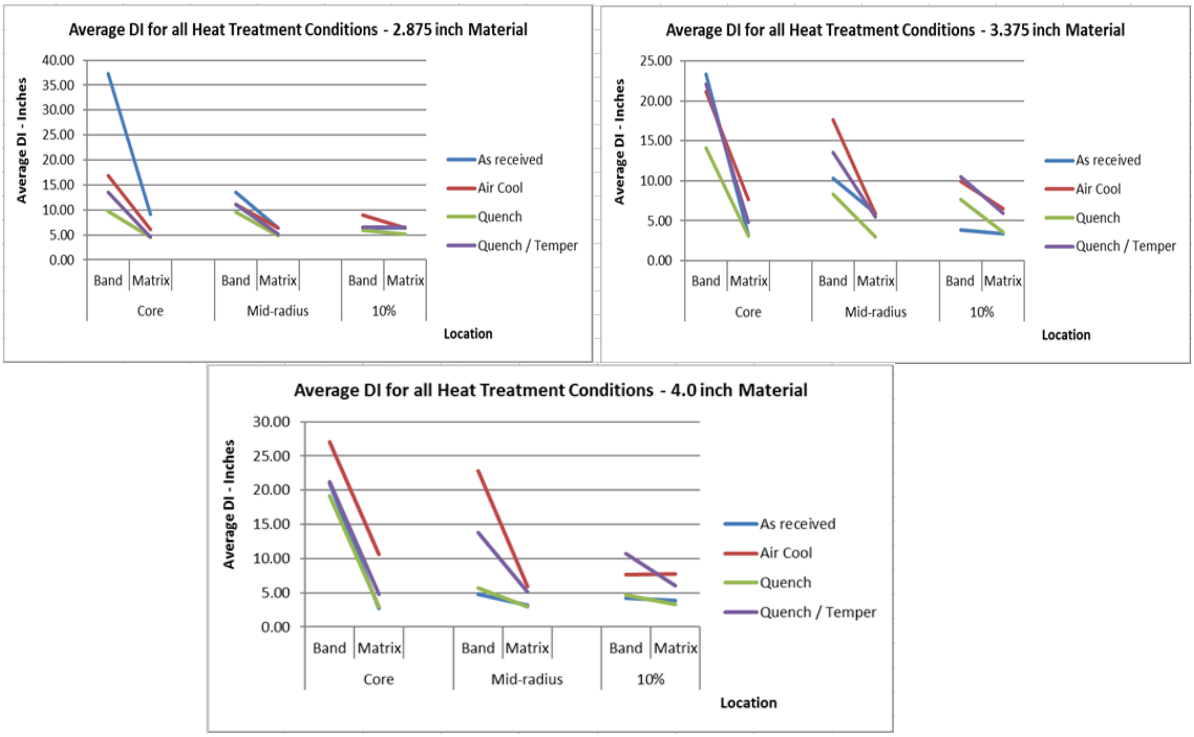

Figure 5-81: Summary of DI values for all heat treatment conditions

The SEM EDAX analysis has demonstrated that the datum material microstructural properties in terms of chemical composition is influenced by the respective heat treatment operation. It has also established that the 2.875-inch material is more responsive to heat treatment in terms of resultant DI values, and that each process has an influence on the mobility of the individual elements across the respective bar cross-sectional thickness. This is fundamental in the understanding on how the microstructure responds at different locations when exposed to different heat treatment temperatures and subsequently cooling conditions. The DI of the band is the phase that is changing considerably when exposed to different heat treatment conditions relative to the subtle differences found with the matrix. These key findings demonstrate that the material is indeed not homogenous, but a duplex of different levels of banding and matrix, which can be changed / altered through different thermal operations / conditions.

5.3.9.12 Microstructural Evaluation

The final stage of the material characterization and understanding, is the microstructural assessment of the samples produced by the DoE, under the different respective heat treatment conditions. Both Chapters 3 & 5, have fully established that the resultant microstructure of the AISI 4161H material is not homogenous, but one of a duplex composition, with two predominant phases throughout the cross-sectional thickness (band & matrix). These phases exhibit different metallurgical properties in terms of hardness and chemical composition / Ideal Diameter; which are greatly influenced by exposure to different types of thermal processing / heat treatment.

Therefore, there is a need to understand what effect different conditions, bar sizes and chemical composition variability have on the resultant microstructures.

5.3.9.13 Methodology

To complete this task, a standard methodology was taken to characterize the microstructures observed. All samples from the DoE were sectioned in the longitudinal direction (see Figure 5-53), and polished using standard metallurgical

techniques to a mirror finish. They were then subsequently etched using Nital (2% solution of Nitric Acid & Methanol) to reveal the resultant microstructure. A standard field of view was also utilised for the analysis, with either an X50 or X200 magnification selected. See Figure 5-82 which shows the metallurgical preparation equipment used.

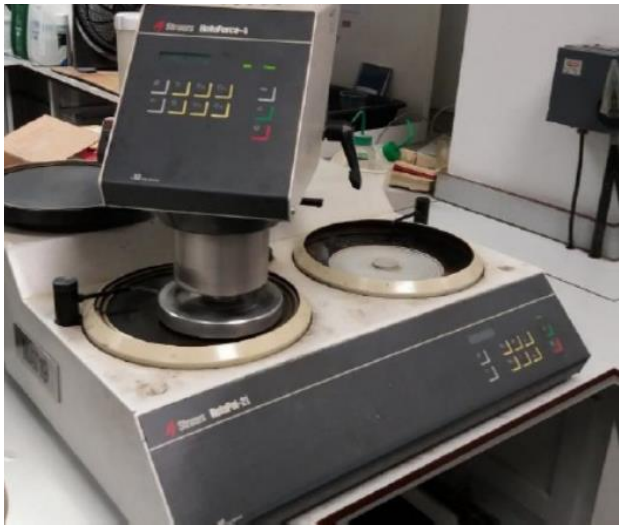

Figure 5-82: Metallurgical polished equipment used for sample preparation

To characterize the microstructure, in terms of the relationship between band & matrix, several key features were measured across the mid-radius and core locations of the DoE samples at a magnification of X50:

- No of bands / individual band widths / minimum and maximum band width / total band width across the field of view / % of bands & matrix within the microstructure.

For this stage in the microstructural analysis, all 3 heat treatment conditions were evaluated (Air Cool / As Quenched/ Quenched & Tempered). It must be noted however, that the 10% location was not analysed for this part of the evaluation strategy, as the previous analysis (micro-hardness & SEM EDAX) established minimum differences in their resultant properties between the band & matrix phases. Also, the bands at the 10% location were not as distinguishable, when compared to the other analysed zones. Figure 5-83 shows a typical quench and temper microstructure exhibited for the 3.375-inch bar material.

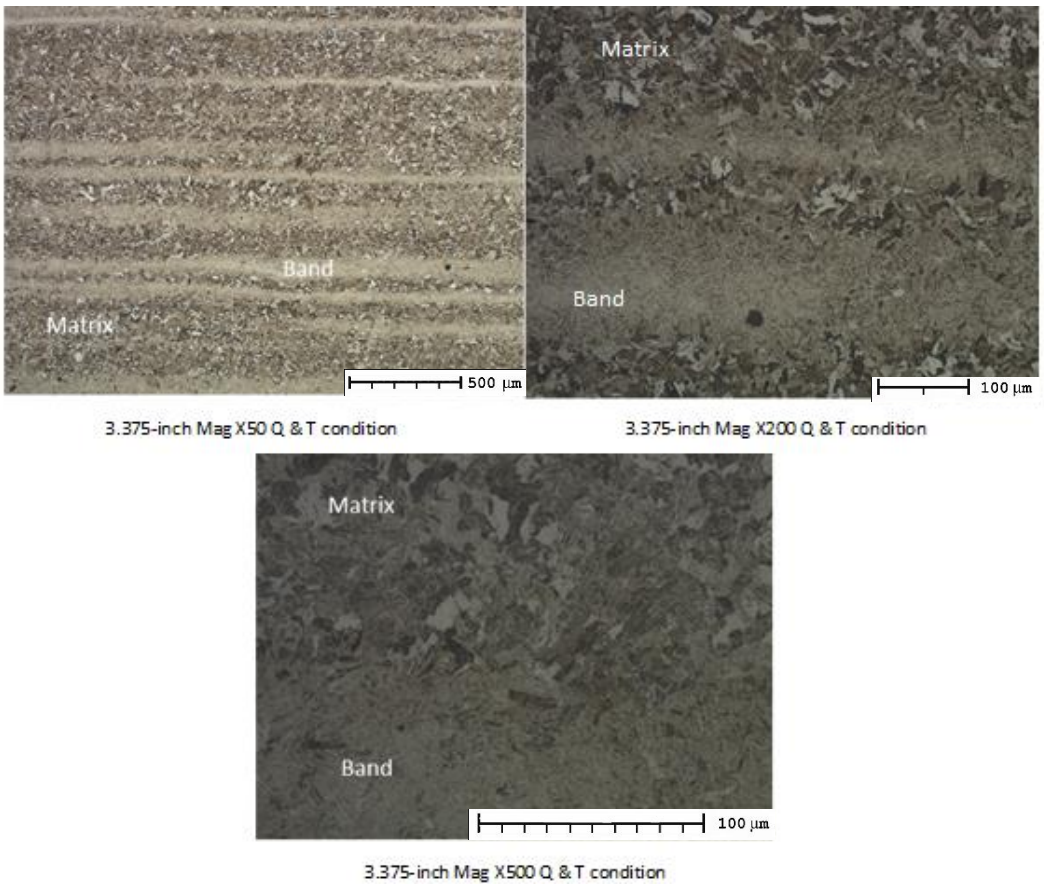

Figure 5-83: Example of Quench and Temper microstructure from the 3.375-inch material (Band - Single Phase) / (Matrix - Dual Phase)

The second stage of the analysis was to identify the microstructure within both the band and matrix phases. Image analysis was adopted for this purpose, specifically for the evaluation of the matrix, which had been identified as exhibiting a dual phase structure. This band however, contained a single phase, which did not necessitate the need for image analysis.

The image analysis program utilised for evaluation purposes of the matrix was Adobe Photoshop CC 2014. This was considered the most appropriate option, as the system featured a robust phase contrast technology that could differentiate between subtle differences of the resultant etched microstructure. However, prior to selecting this system, Photoshop's capabilities were compared to an alternative program also used for image analysis ("Imagic"). Both programs were initially substantiated to establish the level of repeatability when viewing several different images at the same settings.

Adobe Photoshop produced the greatest level of reproducibility and was hence selected.

Figure 5-84 demonstrates the program phase contrast threshold screen used to obtain the optimum and standardise settings, which was used throughout the analysis phase.

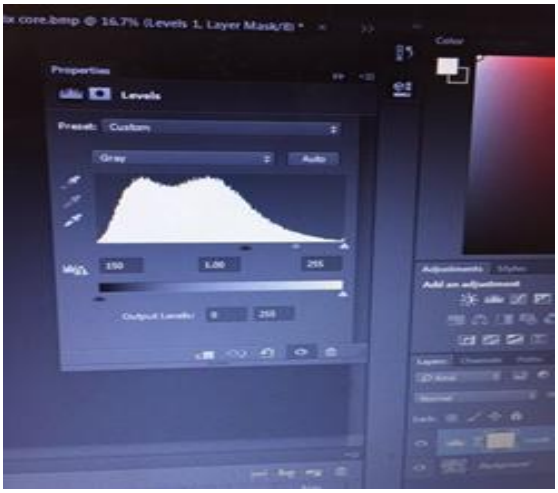

Figure 5-84: Screenshot of the Phase Contrast Software

An example of the phase contrast system in operation is displayed within Figure 5-85, which exhibits the Quenched & Tempered matrix in the etched condition (left). The image is then subjected to the phase contrast software, which depicts the white / grey phase of the dual matrix (right).

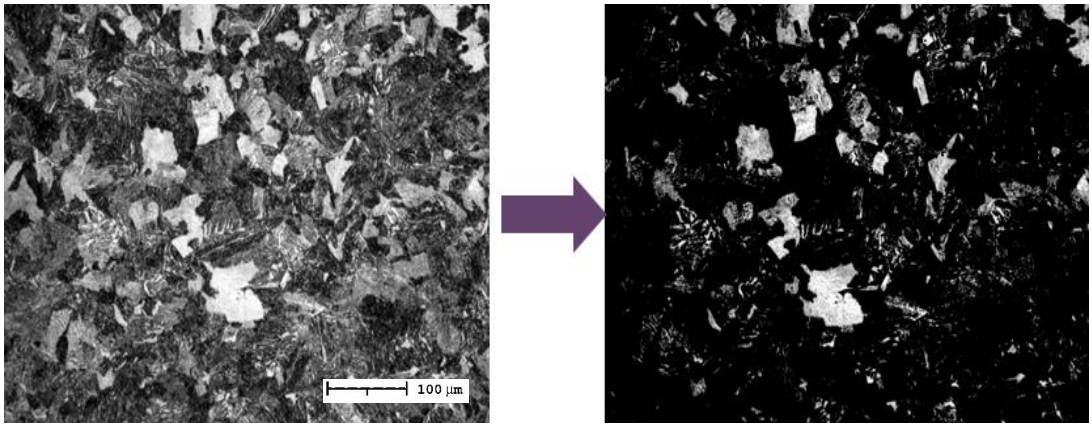

Figure 5-85: Example of the Phase Contrast Analysis Photomicrographs / Etched Quenched and Tempered Matrix Viewed Under White Light (Left) & by Image Analysis (Right)

5.3.9.14 Microstructural Evaluation Results

The results of the microstructural evaluation have been presented in a table format, which represent the effect of the different heat treatment conditions for the analysed individual bar sizes. These are detailed within Tables 5-36 to 5-38.

Table 5-36: 2.875-inch bar Microstructural Assessment Results

	Air Cool						Air Cool					
Sample No.	Mid radius No. of Martensite bands	Mid radius max band width µm	Mid radius min band width µm	Mid radius total band width µm	Mid radius % Martensite band	Mid radius % Matrix	Core No of Martensite bands	Core max band width µm	Core min band width µm	Core total band width µm	Core % Martensite band	Core % Matrix
T1 - T1700	4	89	43	257	15	85	5	225	61	568	33	67
T2 - T1800	5	75	32	339	20	80	6	186	57	625	36	64
T3-SDI 1700	6	100	43	476	27	73	6	317	46	707	41	59
T4-SDI 1800	4	127	32	341	20	80	6	289	36	578	33	67
Average	5	98	38	353	20	80	6	254	50	619	36	64
	Quench						Quench					
Sample No.	Mid radius No. of Martensite bands	Mid radius max band width µm	Mid radius min band width µm	Mid radius total band width µm	Mid radius % Martensite band	Mid radius % Matrix	Core No of Martensite bands	Core max band width µm	Core min band width µm	Core total band width µm	Core % Martensite band	Core % Matrix
A1a	6	392	69	1181	68	32	5	435	68	974	56	44
B1	6	164	93	774	45	55	7	193	64	839	48	52
C1	8	200	43	728	42	58	5	353	89	842	49	51
E1	5	307	89	849	49	51	6	253	75	909	53	47
G1	7	217	50	921	53	47	7	198	69	758	44	56
Average	6	256	69	891	51	49	6	286	73	864	50	50

							Quench and Temper							
Sample No	10% value	White / Grey Phase %	Mid radius value	White / Grey Phase %	Core	White / Grey Phase %	Mid radius No. of Martensite bands	Mid radius max band width µm	Mid radius min band width µm	Mid radius total band width µm	Mid radius % Martensite band	Mid radius% Matrix	Mid radius Total White / Grey Phase %	Mid radius Total Martensite %
A1a	165209	3.3	571427	11.3	677155	13.4	5	441	48	908	52	48	5.4	94.6
B1	314722	6.2	563369	11.2	559995	11.1	8	136	32	469	27	73	8.2	91.8
C3	177646	3.5	675843	13.4	691372	13.7	6	203	64	795	46	54	7.3	92.7
E3	185720	3.7	746035	14.8	723309	14.4	7	120	56	658	38	62	9.2	90.8
F1	213049	4.2	348302	6.9	340793	6.8	6	214	54	694	40	60	4.1	95.9
G1	279219	5.5	544992	10.8	1165284	23.1	5	137	56	545	31	69	7.4	92.6
H3	268775	5.3	381735	7.6	686137	13.6	8	168	40	640	37	63	4.8	95.2
I2	330617	6.6	488549	9.7	452346	9.0	7	216	27	899	52	48	4.7	95.3
J2	158172	3.1	252726	5.0	329912	6.5	6	305	58	756	44	56	2.8	97.2
Average		4.6		10.1		12.4	6	216	48	707	41	59	6	94

							Quench and Temper							
Sample No	10% value	White / Grey Phase %	Mid radius value	White / Grey Phase %	Core	White / Grey Phase %	Core No of Martensite bands	Core max band width µm	Core min band width µm	Core total band width µm	Core % Martensite band	Core % Matrix	Core Total White / Grey Phase %	Core Total Martensite %
A1a	165209	3.3	571427	11.3	677155	13.4	5	200	56	722	42	58	7.8	92.2
B1	314722	6.2	563369	11.2	559995	11.1	6	114	37	430	25	75	8.4	91.6
C3	177646	3.5	675843	13.4	691372	13.7	7	307	21	562	32	68	9.3	90.7
E3	185720	3.7	746035	14.8	723309	14.4	7	160	42	518	30	70	10.1	89.9
F1	213049	4.2	348302	6.9	340793	6.8	6	224	34	763	44	56	3.8	96.2
G1	279219	5.5	544992	10.8	1165284	23.1	6	262	24	464	27	73	16.9	83.1
H3	268775	5.3	381735	7.6	686137	13.6	6	115	40	409	24	76	10.4	89.6
I2	330617	6.6	488549	9.7	452346	9.0	5	240	53	605	35	65	5.8	94.2
J2	158172	3.1	252726	5.0	329912	6.5	6	147	51	597	34	66	4.3	95.7
Average		4.6		10.1		12.4	6	197	40	563	33	67	9	91

The results detailed within Table 5-36, have confirmed that under all heat treatment conditions, the resultant microstructure has exhibited a dual phase, consisting of a band & matrix. For analysis purposes, the percentage of each phase at the mid-radius and core have been quantified.

It is evident that in the As-Cooled condition (Normalised), the number of bands within the resultant microstructure are at their lowest, with values of 20 & 36% exhibited. In addition, the ratio of bands to matrix changes from the respective thickness position across the bar, with the percentage of the band phase increasing from the mid-radius to the core - Reference Table 5-36. The dimensions of the band are also affected in terms of the apparent width, with greater values achieved at the core compared to the mid-radius position (average maximum core band width 254µm versus mid radius maximum width 98µm) - see Figure 5-86.

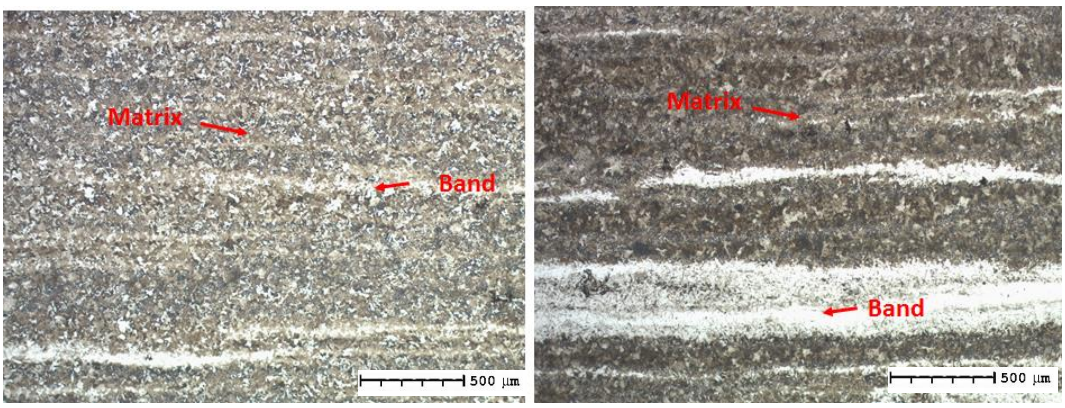

Figure 5-86: Example of the 2.875-Inch Bar Microstructure in the As-Cooled Condition (Left Mid-Radius / Right Core) Mag x50

The phase distribution changes with regards the As-Quenched heat treatment operation; with the band to matrix ratio transforming to an average of a 50:50 relationship, across all test locations and temperature ranges evaluated. - see Table 5-36. The maximum band size widths are also similar, with respective values of 392 & 435 µm achieved at the mid-radius & core locations - see Figure 5-87.

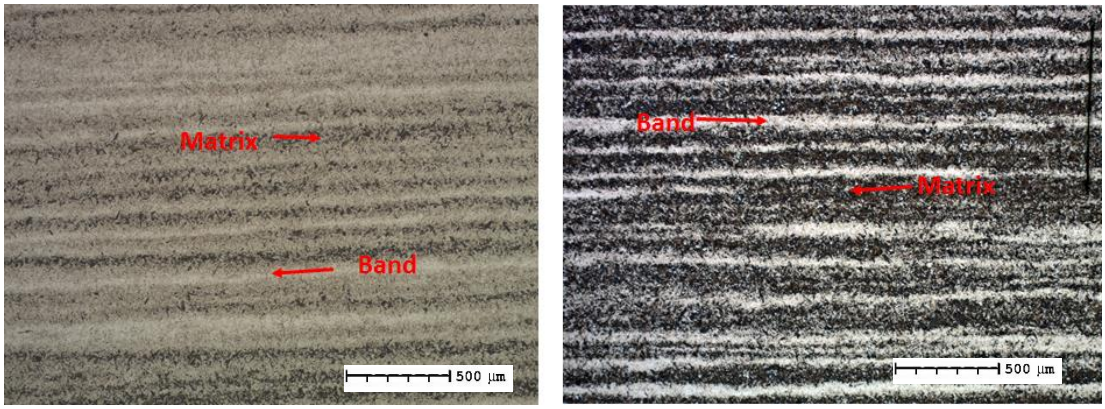

Figure 5-87: Example of the 2.875-Inch Bar Microstructure in the As-Quenched Condition (Left Mid-Radius / Right Core) Mag X50

As for the Quenched and Temper condition, the phase distribution is different compared to both the As-Cooled & As-Quenched treatments. This an important finding, as coil springs are subjected to individual Quenching & Tempering operations during typical manufacturing by the OEM.

It is evident from the results that the equilibrium As-Quenched phase distribution (50:50 band / matrix) changes to an increase in the matrix phase with a subsequent reduction in the apparent band percentage. This is the same for both the mid-radius

and core locations however, the matrix phase distribution is greatest at the core position (average 67% core versus average 59% mid-radius) - see Table 5-36, Figure 5-88, Figure 5-89, and Figure 5-90.

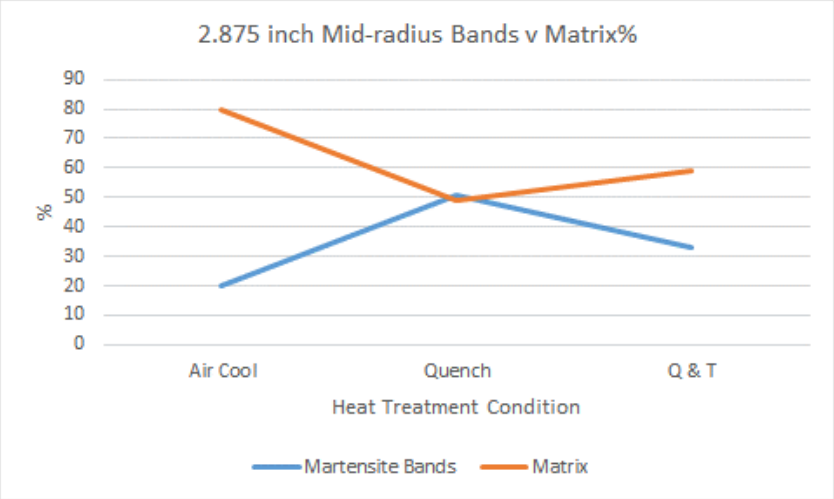

Figure 5-88: 2.875-inch Mid-radius position - Band versus Matrix distribution for all heat treatment conditions

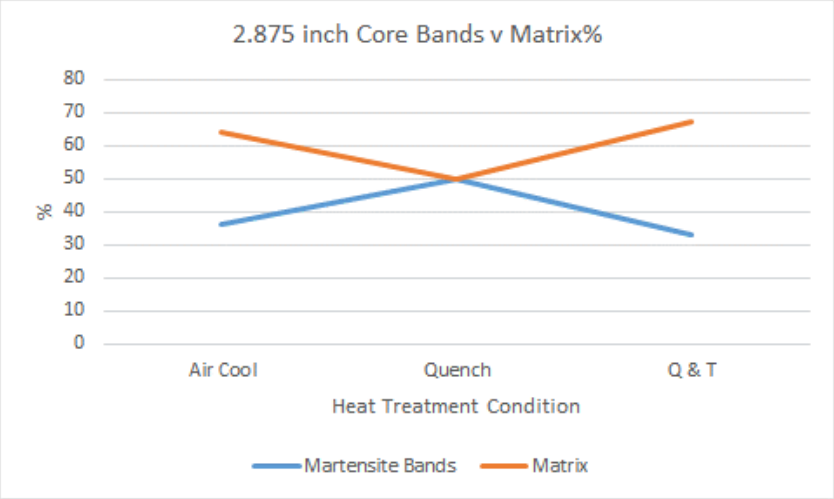

Figure 5-89: 2.875-inch Core position - Band versus Matrix distribution for all heat treatment conditions

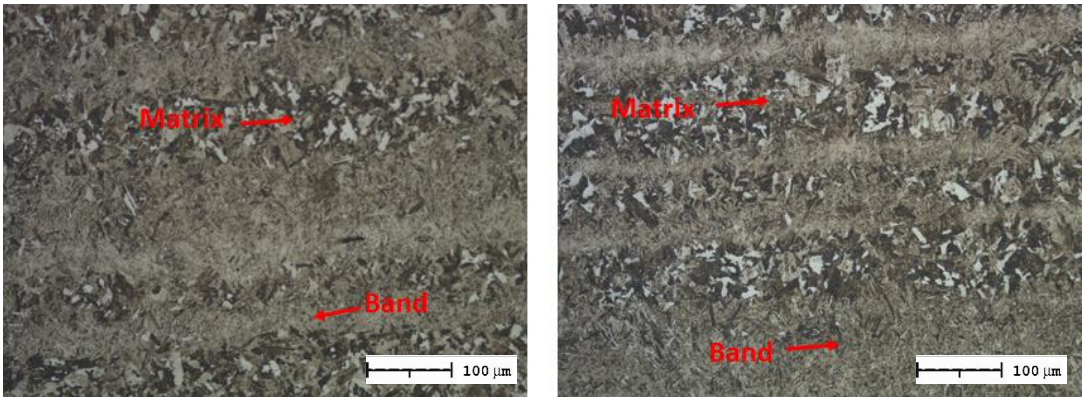

Figure 5-90: Example of the 2.875-Inch Bar Microstructure in the Quenched & Tempered Condition (Left Mid-Radius / Right Core) Mag X200

Another key finding, which has been consistent throughout the testing phase of the DoE, is that the heat treatment conditions have a major influence on the resultant material properties. Figure 5-88 and Figure 5-89 demonstrate that the distribution of the band to the matrix changes significantly by exposing the material to different hot working conditions.

In conjunction with differences exhibited for the Q and T band versus matrix distribution, the image analysis study has established that the matrix and band contain different microstructures. The bands exhibit a fully martensitic structure, with the matrix producing a mixture of both Martensite and a white grey phase, identified as Bainite - see Figure 5-91.

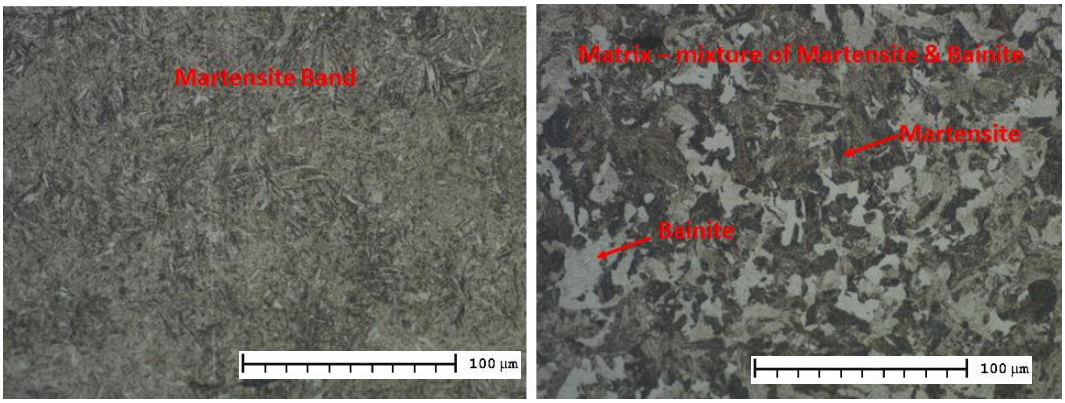

Figure 5-91: Example of the Identified Microstructures in the Q & T Condition, Mag X500

The results shown within Table 5-36, have established that the matrix various in terms of the amount of resultant Bainite% across the respective bar thickness; with average values of 4.6%, 10.1% & 12.4% achieved for the respective 10%, mid-radius and core locations. This therefore influences the overall amount of tempered Martensite produced across the bar and for each Q and T condition - see Table 5-36. To understand the effects on the amount of Martensite within the resultant microstructure; comparison was made to the Ultimate Tensile Properties achieved within Table 5-7 for the 2.875-inch bar. The premise of this study was to determine whether the results followed a specific trend and whether the microstructure could influence the respective mechanical properties.

With reference to Figure 5-92; an increase in the proportion of Martensite equates to a direct increase in resultant UTS.

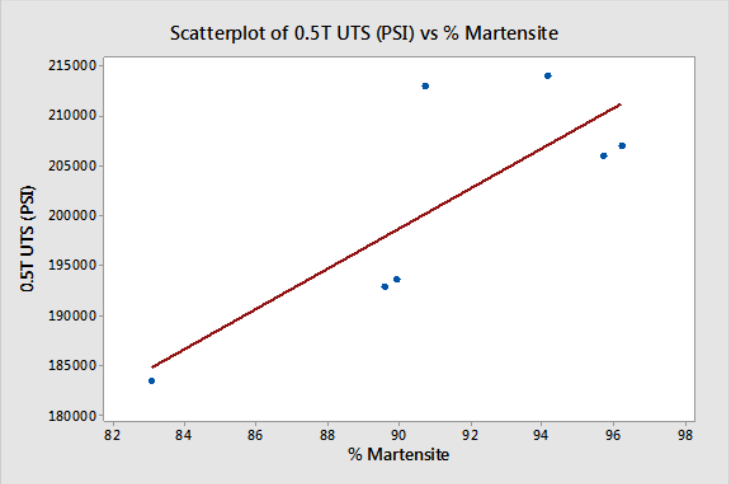

Figure 5-92: 2.875-inch bar - UTS v % Martensite at the Core Location

It is also apparent that different heat treatment conditions influence the amount of Martensite exhibited within the microstructure. The boxplots presented within Figures 5-93 and 5-94 represent the %Martensite achieved for the respective DoE quench & temper temperatures for the 2.875-inch bar. These results clearly identify that the greatest amount of Martensite was achieved at a quench temperature of 1600°F and tempering range of 750°F.

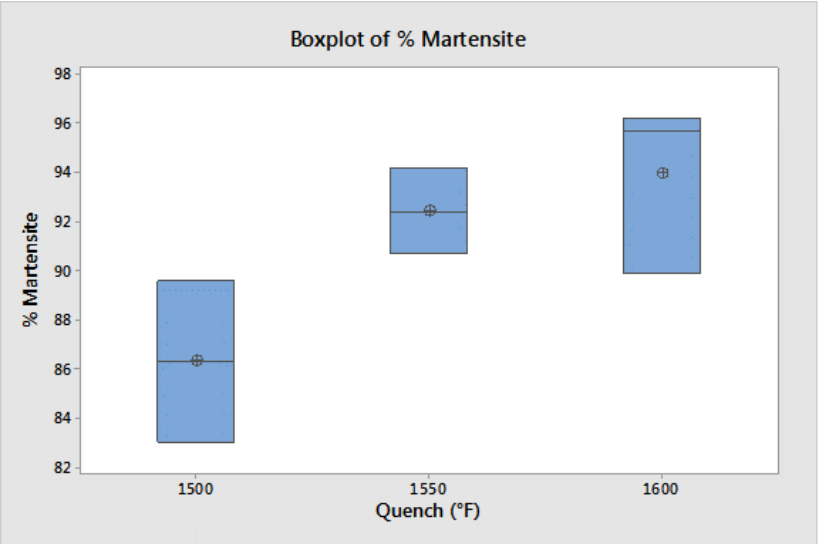

Figure 5-93: 2.875-inch bar Boxplot of %Martensite at the DoE Quench Temperatures

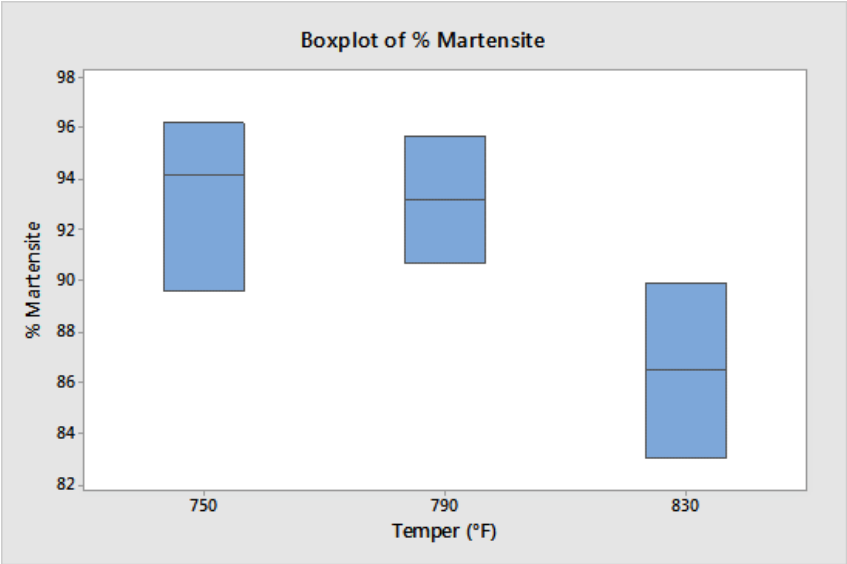

Figure 5-94: 2.875-inch bar Boxplot of %Martensite at the DoE Temper Temperatures

The results for the 3.375-inch bar results are detailed within Table 5-37. They have confirmed that the As-Cooled (Normalised) condition produces the lowest number of bands within the microstructure. This is the same as the 2.875-inch results, which also exhibited this trend, in addition to having larger band widths at the core compared to the mid-radius (Core 285µm maximum width, compared to the mid-radius maximum of 118µm) see Figure 5-95.

The phase distribution changes with regards the As-Quenched heat treatment operation; with the band to matrix ratio transforming to a more homogenous percentage distribution (Band to Matrix: mid-radius 53% / 47% - Core 47% / 53%). These results also demonstrate that the core location exhibits a higher percentage of matrix phase along with a greater maximum band width when compared to the mid-radius position - see Figure 5-96.

Table 5-37: 3.375-inch bar Microstructural Assessment Results

	Air Cool						Air Cool					
Sample No.	Mid radius No. of Martensite bands	Mid radius max band width µm	Mid radius min band width µm	Mid radius total band width µm	Mid radius % Martensite band	Mid radius% Matrix	Core No. of Martensite bands	Core max band width µm	Core min band width µm	Core total band width µm	Core % Martensite band	Core % Matrix
1700AC	8	97	48	506	29	71	7	196	50	642	37	63
1800AC	4	118	47	307	18	82	7	285	39	789	46	54
Average	6	108	48	407	23	77	7	241	45	716	41	59

	Quench						Quench					
Sample No.	Mid radius No. of Martensite bands	Mid radius max band width µm	Mid radius min band width µm	Mid radius total band width µm	Mid radius % Martensite band	Mid radius% Matrix	Core No. of Martensite bands	Core max band width µm	Core min band width µm	Core total band width µm	Core % Martensite band	Core % Matrix
1500	7	289	61	824	48	52	5	339	53	784	45	55
1515	8	228	64	942	54	46	8	239	53	881	51	49
1550	9	153	39	732	42	58	5	196	50	575	33	67
1585	9	221	43	981	57	43	7	207	71	981	57	43
1600	8	257	64	1077	62	38	9	129	50	807	47	53
Average	8	230	54	911	53	47	7	222	55	805	47	53

							Quench & Temper							
Sample No	10% value	Bainite Phase %	Mid radi value	Bainite Phase %	Core	Bainite Phase %	Mid radius No. of Martensite bands	Mid radius max band width µm	Mid radius min band width µm	Mid radius total band width µm	Mid radius % Martensite band	Mid radius% Matrix	Mid radius Total White / Grey Phase %	Mid radius Total Martensite %
I1	309271	6.1	365298	7.2	425806	8.5	6	158	53	572	33	67	4.9	95.1
J1	338935	6.7	484063	9.6	728915	14.5	9	195	32	746	43	57	5.5	94.5
K1	284945	5.7	289689	5.7	622792	12.4	8	189	45	764	44	56	3.2	96.8
K3	211643	4.2	377133	7.5	455658	9.0	7	139	61	666	38	62	4.6	95.4
K4	72201	1.4	152970	3.0	171765	3.4	5	233	70	592	34	66	2.0	98.0
K6	100482	2.0	130334	2.6	382647	7.6	4	352	96	659	38	62	1.6	98.4
L2	165824	3.3	435610	8.6	453321	9.0	9	115	40	694	40	60	5.2	94.8
L4	223532	4.4	352876	7.0	369186	7.3	7	181	35	654	38	62	4.4	95.6
M3	78917	1.6	230271	4.6	488341	9.7	6	219	53	665	38	62	2.8	97.2
M4	164000	3.3	281478	5.6	397630	7.9	9	176	53	829	48	52	2.9	97.1
N2	152895	3.0	172079	3.4	417735	8.3	10	198	29	928	54	46	1.6	98.4
Average		3.8		5.9		8.9	7	196	52	706	41	59	4	96

							Quench & Temper							
Sample No	10% value	Bainite Phase %	Mid radi value	Bainite Phase %	Core	Bainite Phase %	Core No. of Martensite bands	Core max band width µm	Core min band width µm	Core total band width µm	Core % Martensite band	Core % Matrix	Core Total White / Grey Phase %	Core Total Martensite %
I1	309271	6.1	365298	7.2	425806	8.5	6	171	54	483	28	72	6.1	93.9
J1	338935	6.7	484063	9.6	728915	14.5	6	216	48	562	32	68	9.8	90.2
K1	284945	5.7	289689	5.7	622792	12.4	5	163	58	594	34	66	8.1	91.9
K3	211643	4.2	377133	7.5	455658	9.0	5	187	59	534	31	69	6.3	93.7
K4	72201	1.4	152970	3.0	171765	3.4	2	784	134	918	53	47	1.6	98.4
K6	100482	2.0	130334	2.6	382647	7.6	5	377	45	651	38	62	4.7	95.3
L2	165824	3.3	435610	8.6	453321	9.0	5	136	48	492	28	72	6.4	93.6
L4	223532	4.4	352876	7.0	369186	7.3	8	127	29	667	39	61	4.5	95.5
M3	78917	1.6	230271	4.6	488341	9.7	6	262	29	514	30	70	6.8	93.2
M4	164000	3.3	281478	5.6	397630	7.9	6	166	45	606	35	65	5.1	94.9
N2	152895	3.0	172079	3.4	417735	8.3	5	272	42	745	43	57	4.7	95.3
Average		3.8		5.9		8.9	5	260	54	615	36	64	6	94

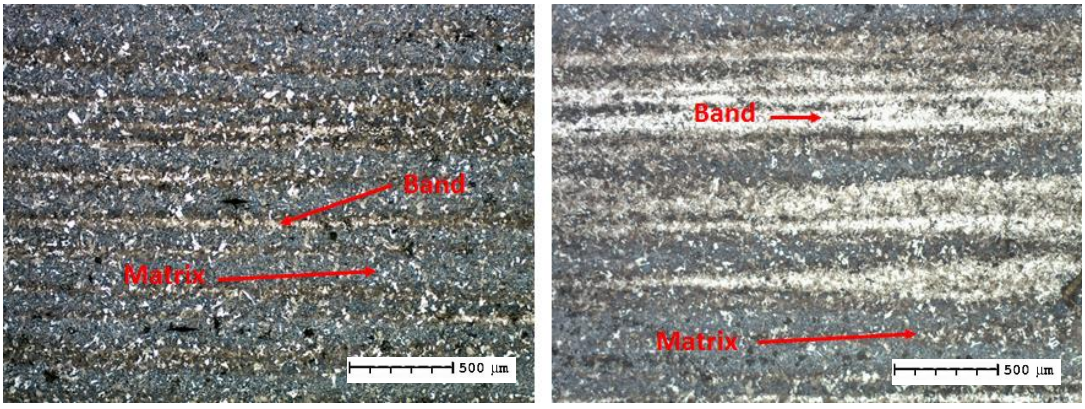

Figure 5-95: Example of the 3.375-Inch Bar Microstructure in the As-Cooled Condition (Left Mid-Radius / Right Core) Mag X50

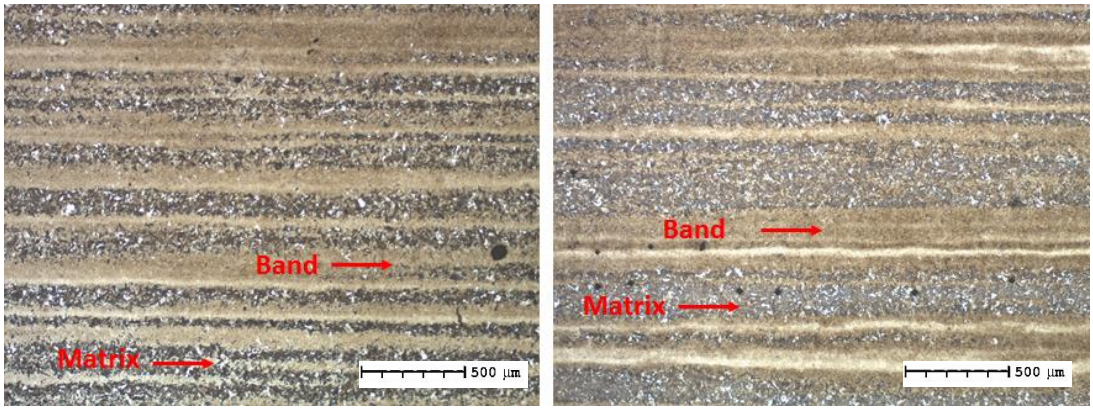

Figure 5-96: Example of the 3.375-Inch Bar Microstructure in the As-Quenched Condition (Left Mid-Radius / Right Core) Mag X50

As for the Quenched and Temper condition, the phase distribution is different compared to both the As-Cooled & As-Quenched treatments. Like the 2.875-inch results, the near equilibrium As-Quenched phase distribution changes to an increase in the matrix phase with a subsequent reduction in the apparent band percentage. This is the same for both the mid-radius and core locations however, the matrix phase distribution is greatest at the core position (average 64% core v average 59% mid-radius) - see Table 5-37, Figure 5-97, Figure 5-98, and Figure 5-99.

Again, it is apparent that the phase distribution changes in respective to the exposure to different heat treatment conditions. This is demonstrated within Figure 5-97 and Figure 5-98.

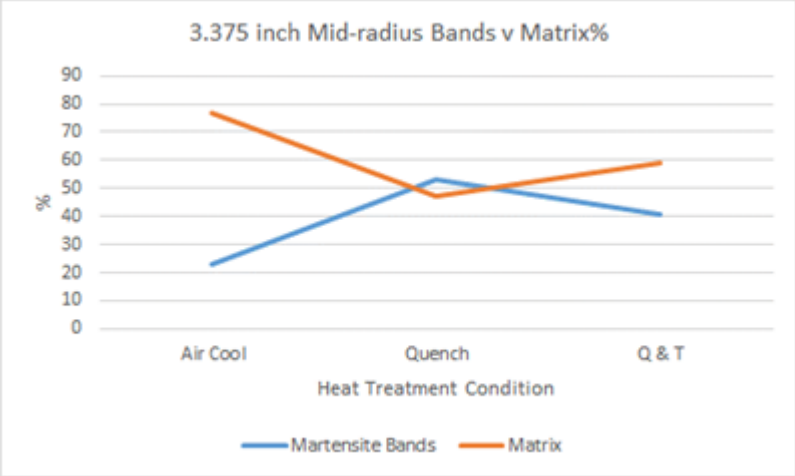

Figure 5-97: 3.375-Inch Mid-radius position - Band versus Matrix distribution for all heat treatment conditions

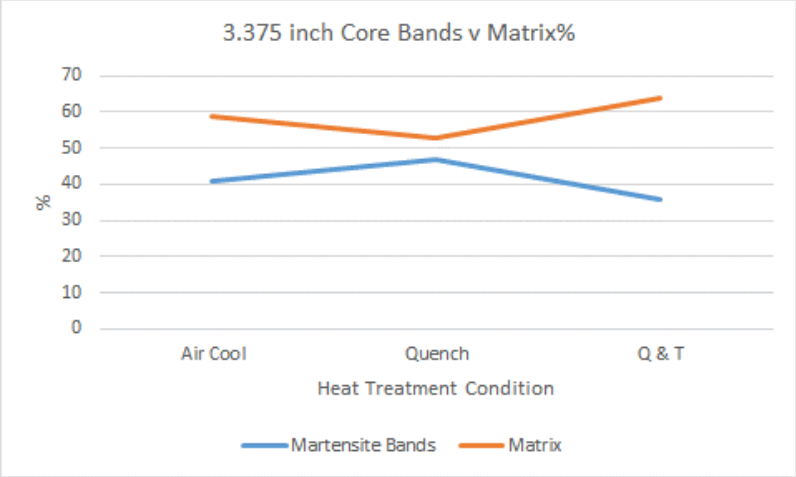

Figure 5-98: 3.375-Inch Core position - Band versus Matrix distribution for all heat treatment conditions

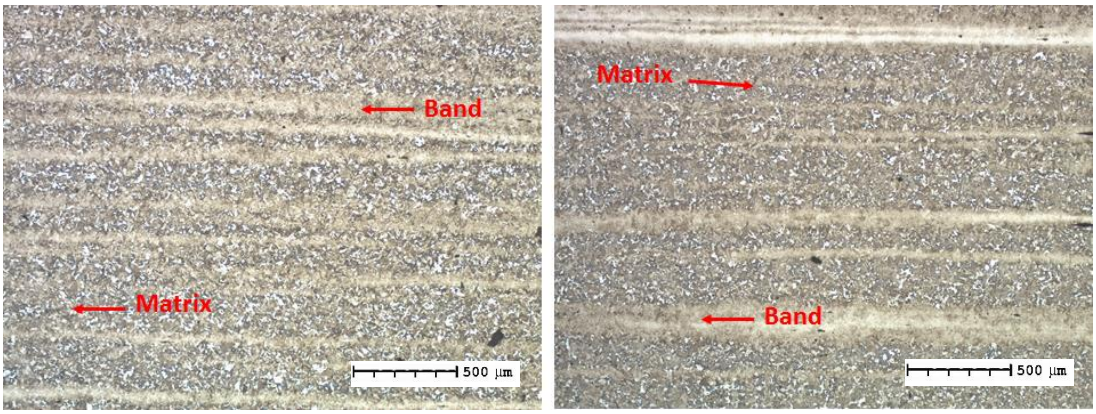

Figure 5-99: Example of the 3.375-Inch Bar Microstructure in the Quenched & Tempered Condition (Left Mid-Radius / Right Core) Mag X50

The microstructure of both phases (band and matrix) were confirmed to be that exhibited by the 2.875-inch material in the quench & tempered condition (Martensite - Band / Bainite & Martensite - Matrix), reference Figure 5-100.

Image analysis also established that the matrix phase contained different levels of Bainite throughout the bar cross-section, with values of 3.8%, 5.9% & 8.9% achieved at the respective 10%, mid-radius & core locations. These values were subsequently used to determine the total % of Martensite for each Q & T heat treatment condition, reference Table 5-37, Figure 5-100 through Figure 5-103.

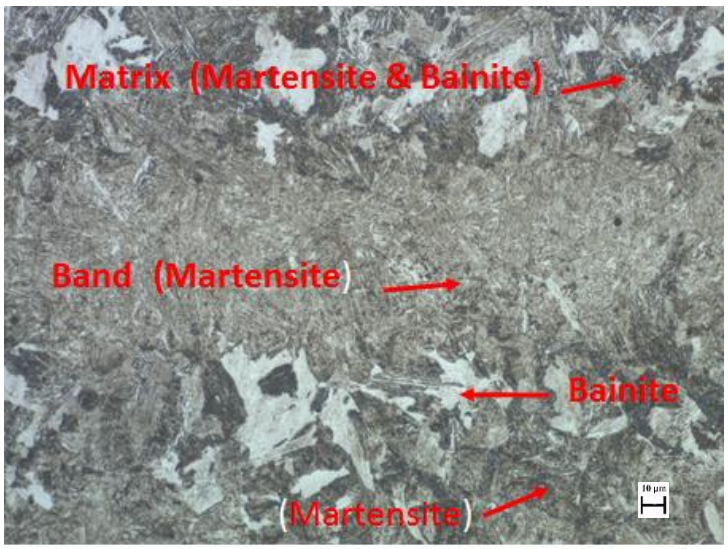

Figure 5-100: Example of the Identified Microstructure in the Q & T Condition (Martensite Band / Bainite & Martensite Matrix) Mag X500

Like the values achieved for the 2.875-inch material, both the ¼ & ½T locations for the 3.375-inch bar exhibited a trend where an increase in UTS was achieved with an increase in the amount of Martensite. Figure 5-101 also identifies that the amount of Martensite is greater at the mid-radius position, which results in higher resultant UTS values.

Another key point for consideration is the gradient of the scatterplot curves changes from the mid-radius to core position, which indicates that the sectional thickness influences the tensile properties. This is further backed up when comparison is made to Figure 5-92 (2.875-inch), which exhibits a step gradient for the smaller bar diameter.

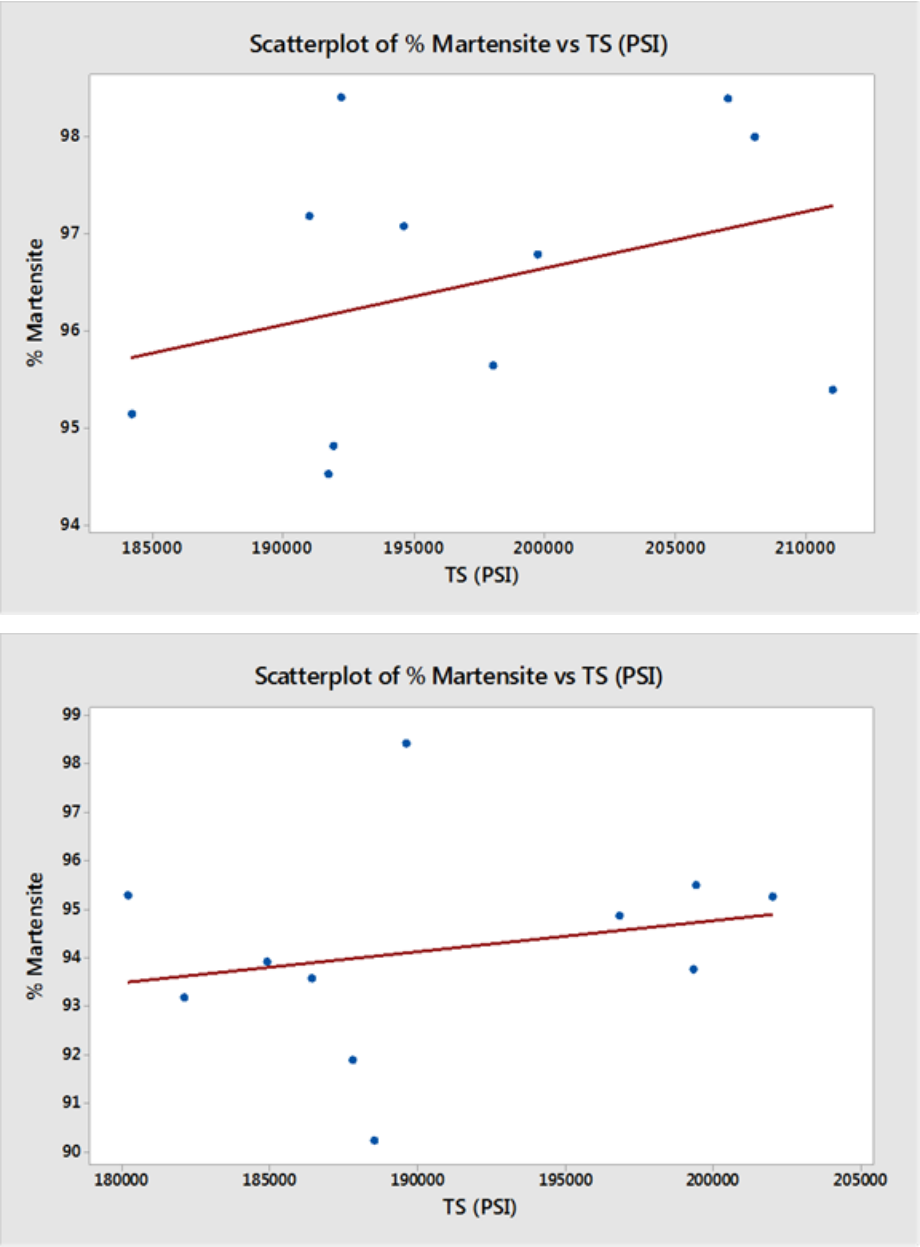

Figure 5-101: 3.375-inch bar - UTS versus % Martensite at the Mid-radius (Top) & Core (Bottom) locations

As for the effect of different heat treatment conditions, the 3.375-inch bar is also influenced by different quench and tempering temperatures. An optimum % of Martensite was achieved at the respective quench temperature of 1550 - 1585°F for the mid-radius position and 1515 - 1585°F for the core location - see Figure 5-102. This ties in with the optimum target properties / recommended operating window established within Table 5-13. The same however, can be said with regards the resultant values achieved at the different tempering temperatures, with the Table 5-

13 stating an optimum condition was achieved at 750 - 830°F for the mid-radius & 750 - 778°F for the core locations. Figure 5-103 highlights that these respective values are consistent with one and other.

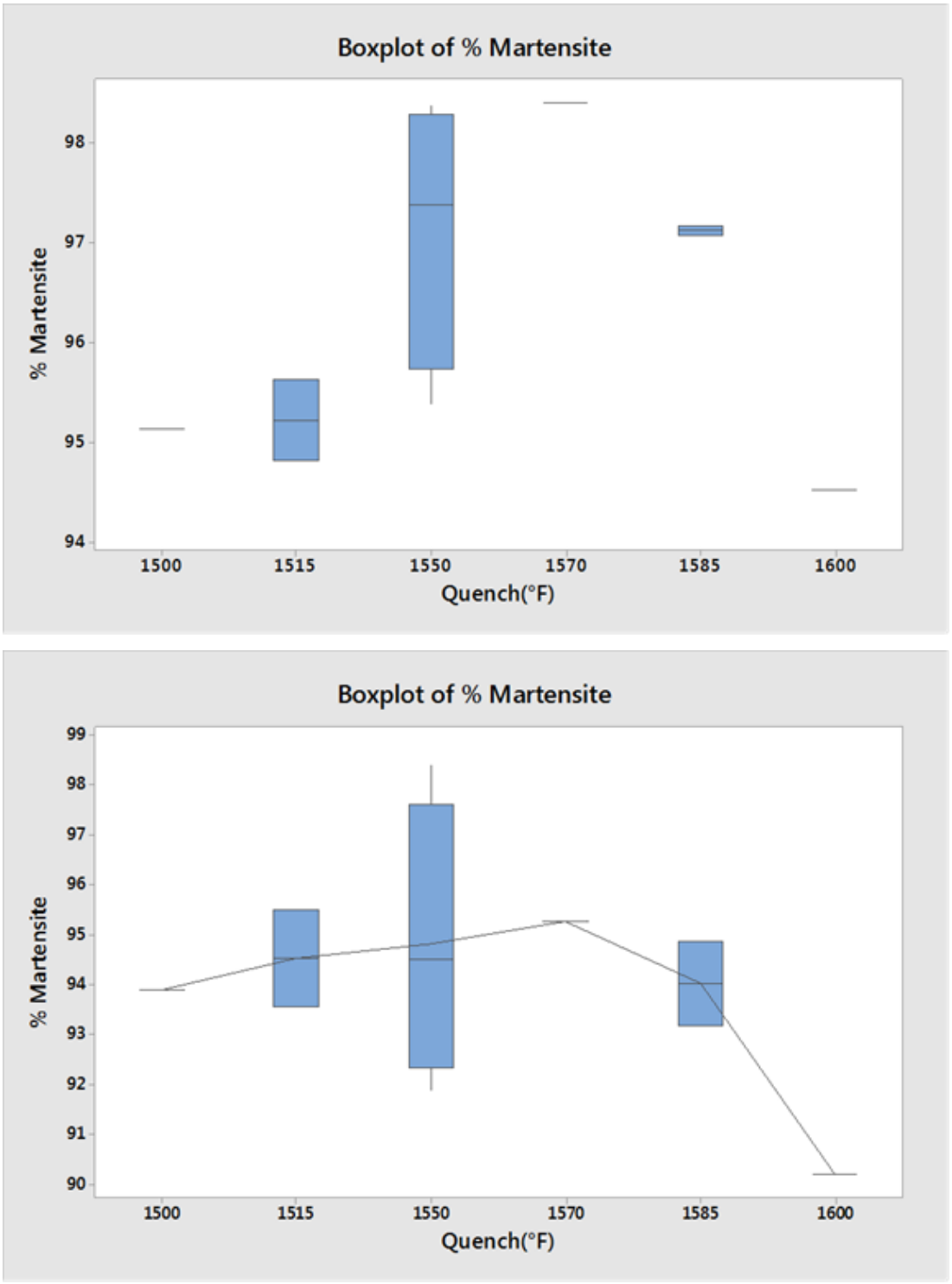

Figure 5-102: Boxplots of %Martensite at the DoE Quench Temperatures (Top - Mid-Radius, Bottom- Core)

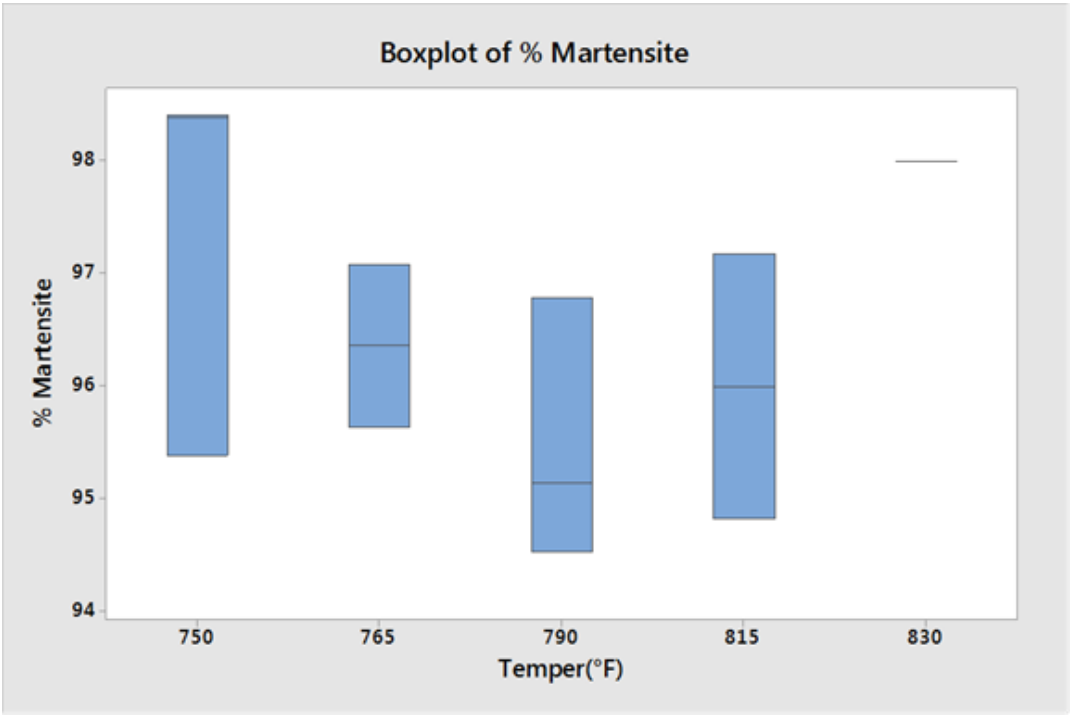

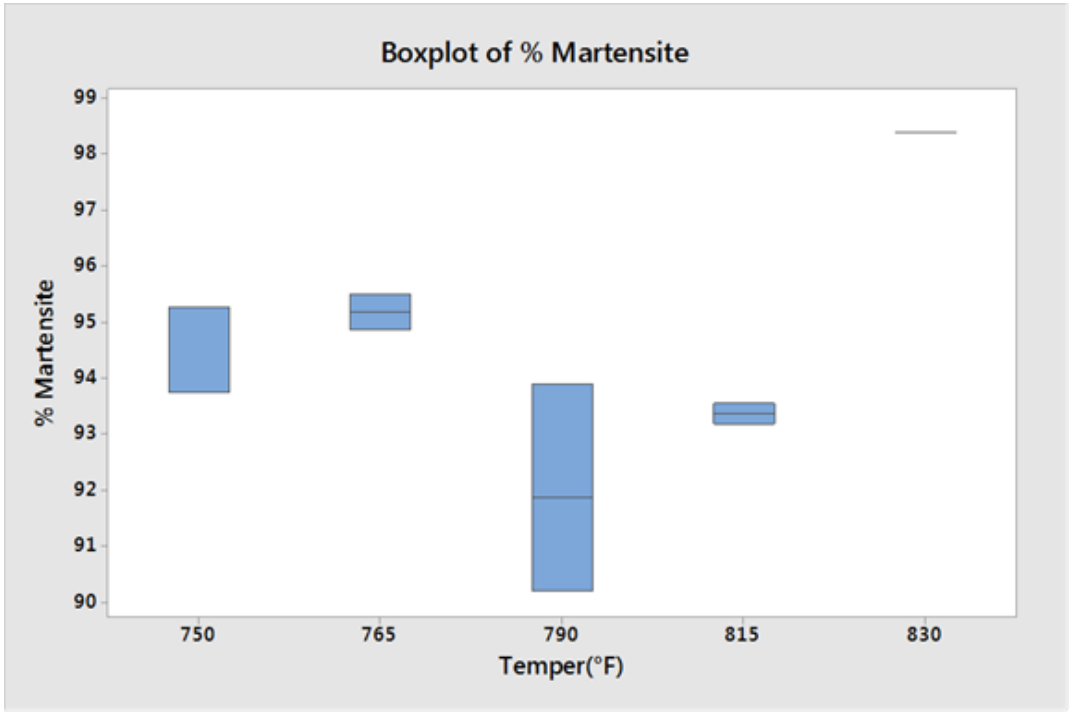

Figure 5-103: Boxplots of %Martensite at the DoE Temper Temperatures - (Top - Mid-Radius) / (Bottom - Core)

The final set of results are for the 4.0-inch bar analysis, which are detailed within Table 5-38 and summarised within Figure 5-105 and Figure 5-106. Like the previous bar sizes, a state of phase equilibrium was achieved in the as-quenched condition for both the mid-radius and core locations. This subtly changed with the quench & temper operation, with an average increase of 6% in relation to the amount of matrix present within the resultant microstructure (50% - As Quenched v 56% Q and T condition).

The microstructure of both the band and the matrix phases were the same as that exhibited by the 2.875 & 3.375-inch material, with in an increase in the amount of Bainite present across the respective matrix locations of the bar (10%, mid-radius & core) - Reference Table 5-38 & Figure 5-104.

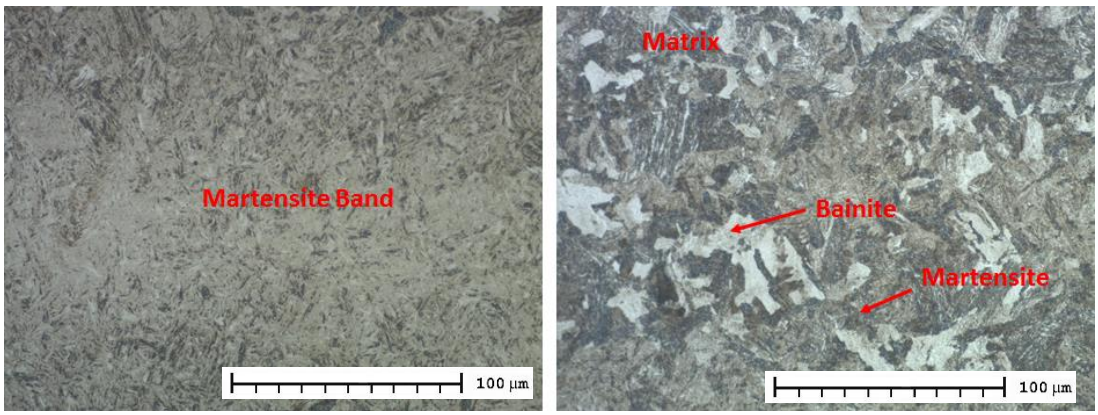

Figure 5-104: Example of the identified microstructures in the Q & T condition (left Martensite Band / right Martensite & Bainite Matrix) Mag X500

Table 5-38: 4.0-inch bar Microstructural Assessment Results

	Air Cool						Air Cool					
Sample No.	Mid radius No. of Martensite bands	Mid radius max band width µm	Mid radius min band width µm	Mid radius total band width µm	Mid radius % Martensite band µm	Mid radius% Matrix	Core No. of Martensite bands	Core max band width µm	Core min band width µm	Core total band width	Core % Martensite band	Core % Matrix
AC	6	157	93	771	45	55	4	180	76	529	31	69
Average	6	157	93	771	45	55	4	180	76	529	31	69

	Quench						Quench					
Sample No.	Mid radius No. of Martensite bands	Mid radius max band width µm	Mid radius min band width µm	Mid radius total band width µm	Mid radius % Martensite band µm	Mid radius% Matrix	Core No. of Martensite bands	Core max band width µm	Core min band width µm	Core total band width	Core % Martensite band	Core % Matrix
1515	5	357	75	945	55	45	5	236	57	767	44	56
1550	8	246	57	874	50	50	5	271	75	774	45	55
1585	5	314	79	896	52	48	3	638	168	1048	61	39
Average	6	306	70	905	52	48	4	382	100	863	50	50

							Quench and Temper							
Sample No	10% value	Bainite Phase %	Mid radius value	Bainite Phase %	Core	Bainite Phase %	Mid radius No. of Martensite bands	Mid radius max band width µm	Mid radius min band width µm	Mid radius total band width µm	Mid radius % Martensite band	Mid radius% Matrix	Mid radius Total White / Grey Phase %	Mid radius Total Martensite %
O1	158946	3.2	389528	7.7	464941	9.2	9	171	62	909	52	48	3.7	96.3
P1	146009	2.9	212882	4.2	567979	11.3	5	206	59	637	37	63	2.7	97.3
Q1	118248	2.3	287109	5.7	429270	8.5	7	212	80	892	52	48	2.8	97.2
R1	269712	5.4	435958	8.7	547947	10.9	7	147	64	757	44	56	4.9	95.1
S1	312586	6.2	343654	6.8	496763	9.9	6	179	59	605	35	65	4.4	95.6
T1	231578	4.6	247464	4.9	343037	6.8	8	125	32	703	41	59	2.9	97.1
U1	119434	2.4	313521	6.2	358349	7.1	6	293	46	889	51	49	3.0	97.0
Average		3.8		6.3		9.1	7	190	57	770	44	56	3	97

							Quench and Temper							
Sample No	10% value	Bainite Phase %	Mid radius value	Bainite Phase %	Core	Bainite Phase %	Core No. of Martensite bands	Core max band width µm	Core min band width µm	Core total band width µm	Core % Martensite band	Core % Matrix	Core Total White / Grey Phase %	Core Total Martensite %
O1	158946	3.2	389528	7.7	464941	9.2	6	201	40	601	35	65	6.0	94.0
P1	146009	2.9	212882	4.2	567979	11.3	3	470	64	774	45	55	6.2	93.8
Q1	118248	2.3	287109	5.7	429270	8.5	6	184	43	579	33	67	5.7	94.3
R1	269712	5.4	435958	8.7	547947	10.9	7	340	32	620	36	64	7.0	93.0
S1	312586	6.2	343654	6.8	496763	9.9	4	235	68	546	32	68	6.8	93.2
T1	231578	4.6	247464	4.9	343037	6.8	5	435	50	1252	72	28	1.9	98.1
U1	119434	2.4	313521	6.2	358349	7.1	4	393	93	910	53	47	3.4	96.6
Average		3.8		6.3		9.1	5	323	56	754	44	56	5	95

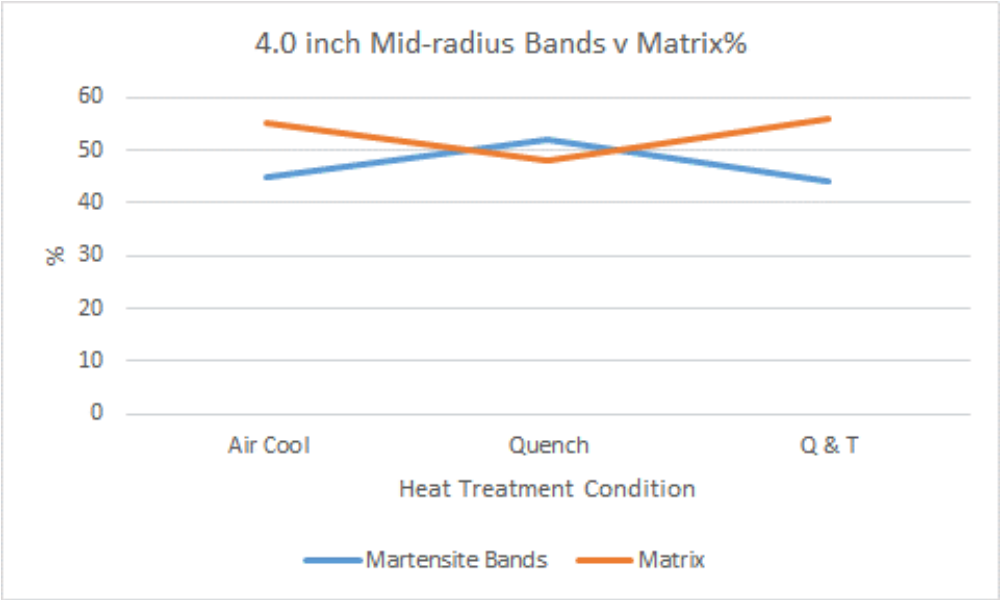

Figure 5-105: 4.0-Inch Mid-radius position - Band versus Matrix distribution for all heat treatment conditions

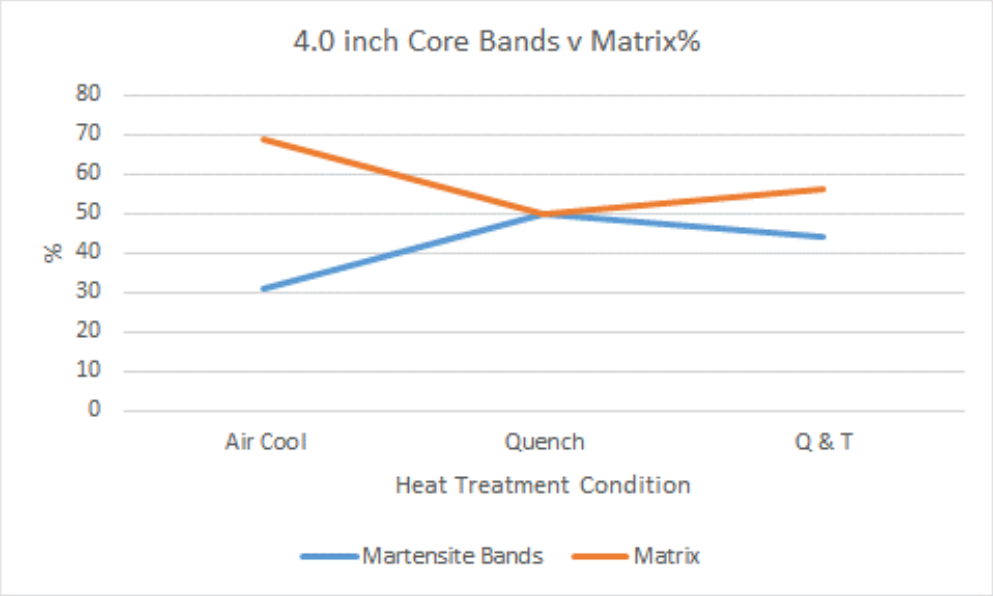

Figure 5-106: 4.0-Inch Core position - Band versus Matrix distribution for all heat treatment conditions

Like the other materials analysed, the amount of Martensite present within the overall microstructure has a direct influence on the resultant UTS properties - Reference Figure 5-107.

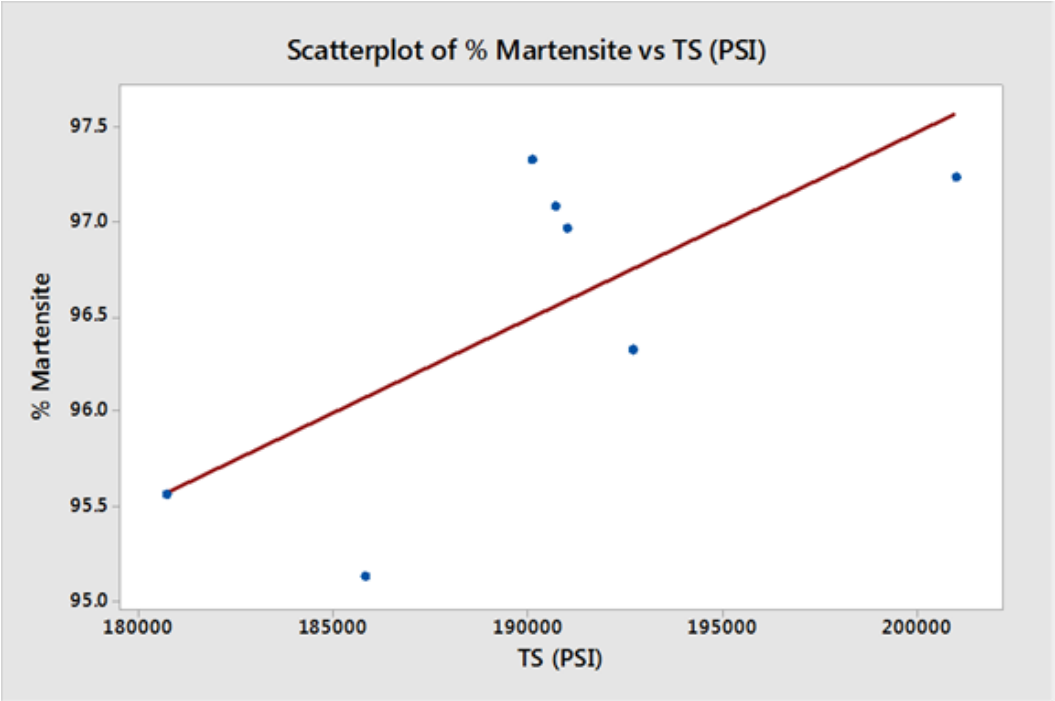

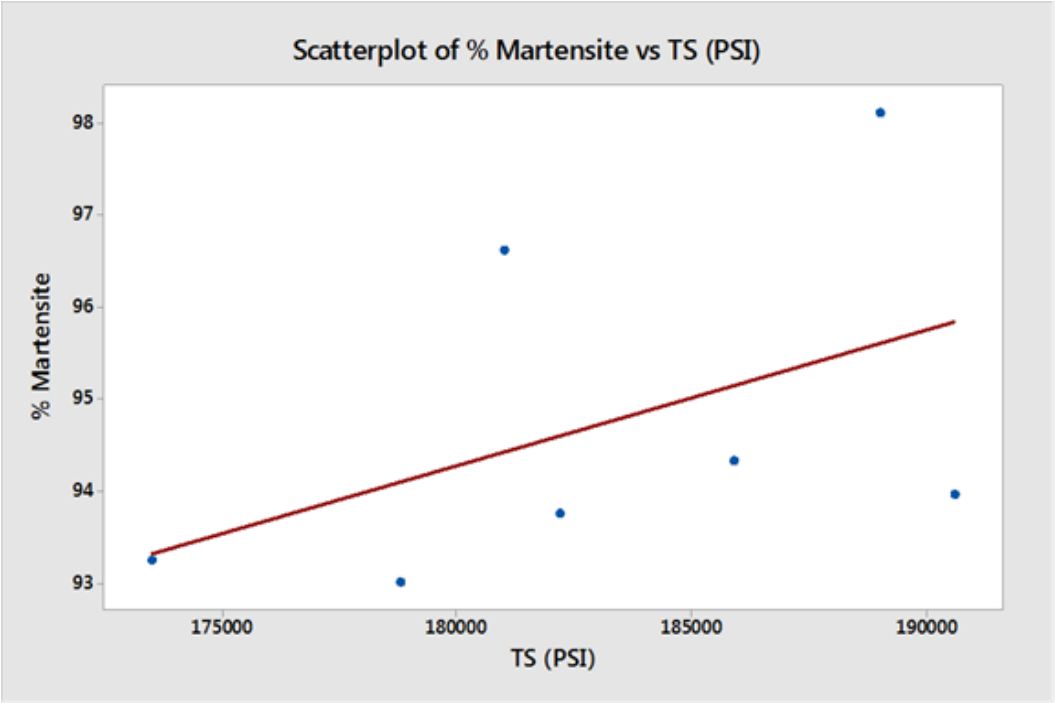

Figure 5-107: 4.0-inch bar - UTS versus % Martensite at the Mid-radius (Top) & Core (Bottom) locations

In addition, both the quench and tempering temperatures had a direct influence on the proportion of Martensite within the microstructure - reference Figure 5-108 and Figure 5-109.

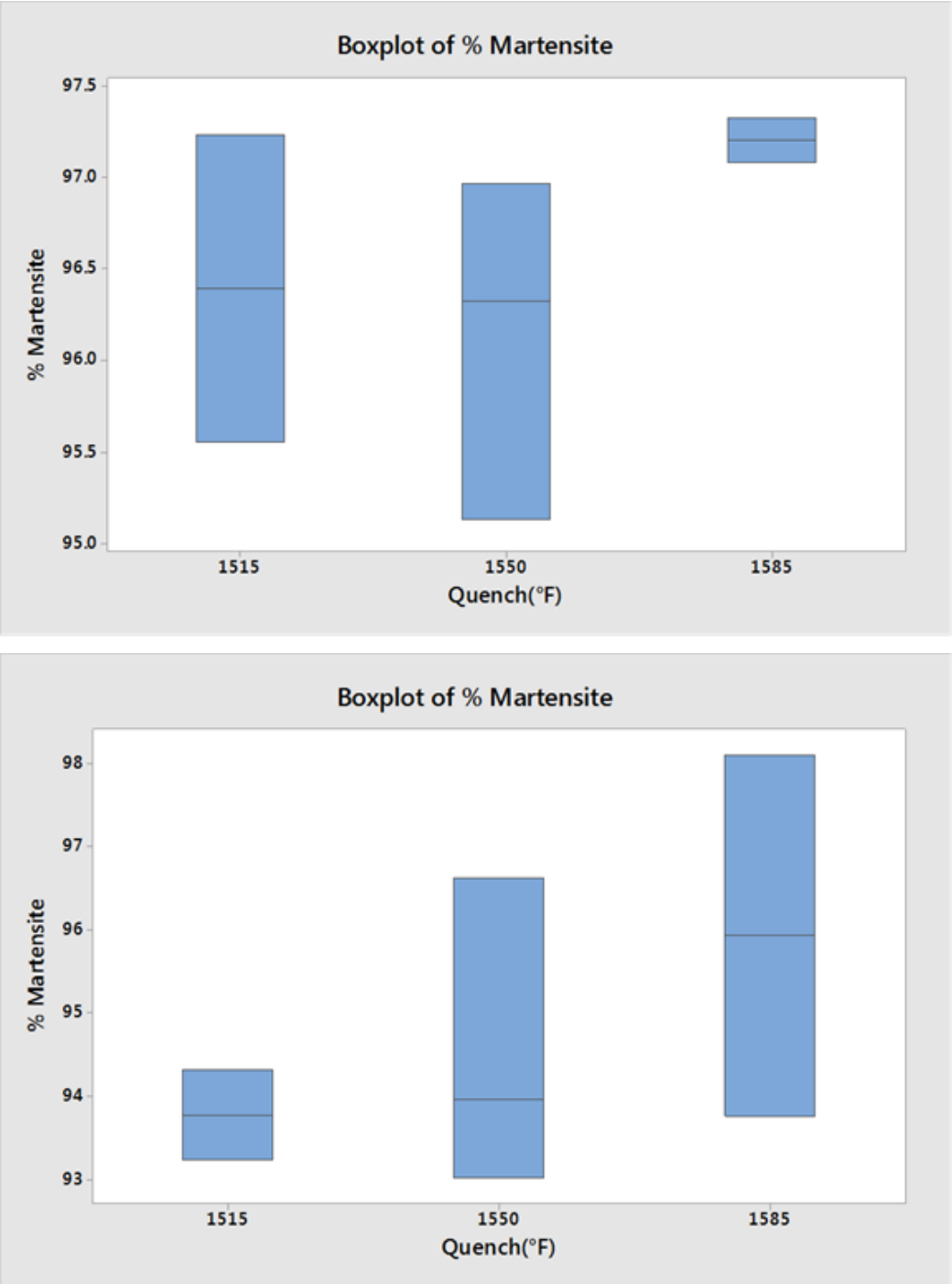

Figure 5-108: Boxplots of %Martensite at the DoE Quench Temperatures - (Top - Mid-radius) / (Bottom - Core)

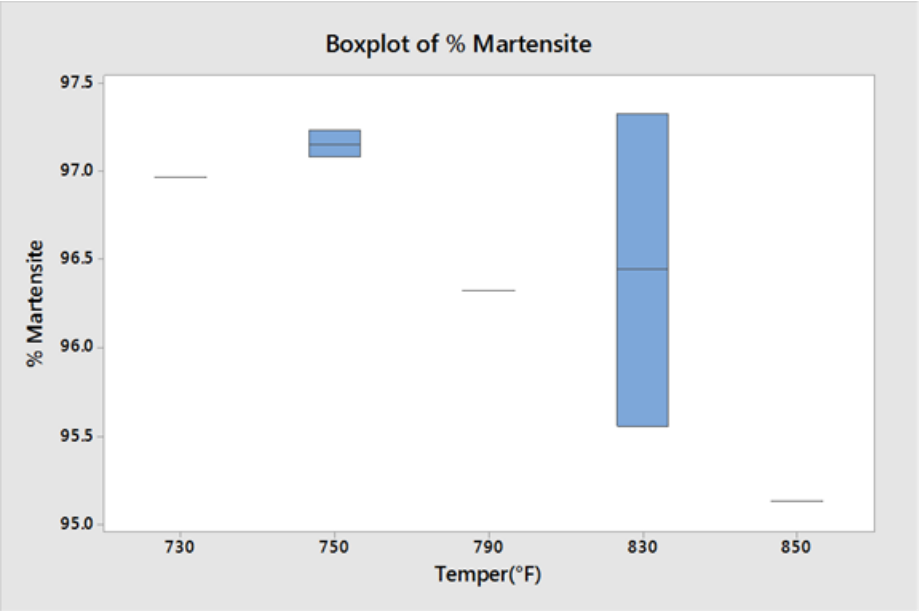

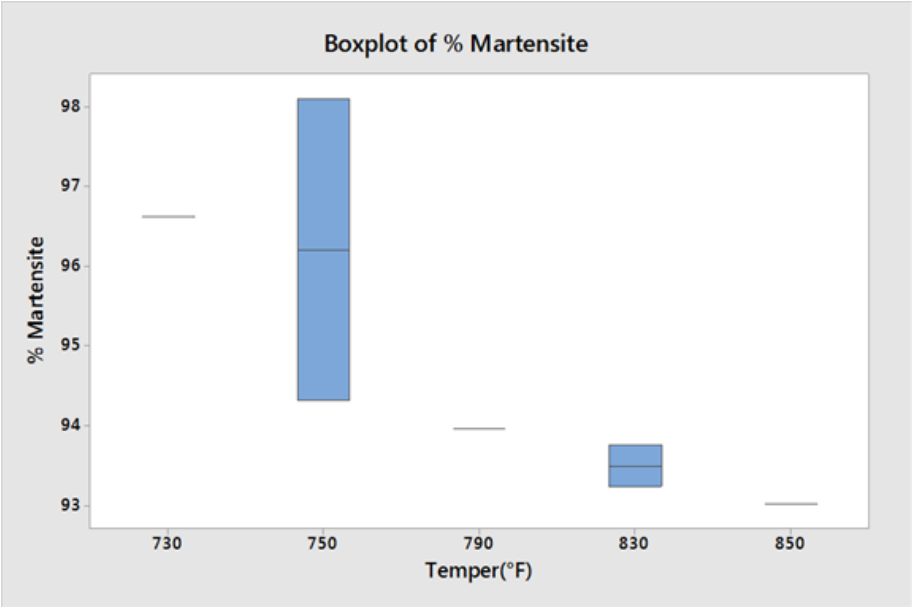

Figure 5-109: Boxplots of %Martensite at the DoE Temper Temperatures - (Top - Mid-radius) / (Bottom - Core)

5.3.9.15 Microstructural Evaluation Summary

The microstructural evaluation has determined that the heat treatment operations have a direct influence on the resultant microstructure in terms of phase distribution (band v matrix). In summary - Reference Figure 5-110:

- The Air Cooling (Normalize) operation produces a phase distribution where the % band is at its lowest within the resultant microstructure.

- This ratio of band to matrix changes to a more homogenous distribution (50: 50) when the material is subjected to the Quenching operation.
- The subsequent Quench & Temper treatment decreases the amount of banding within the microstructure, with an increase in matrix phase produced.

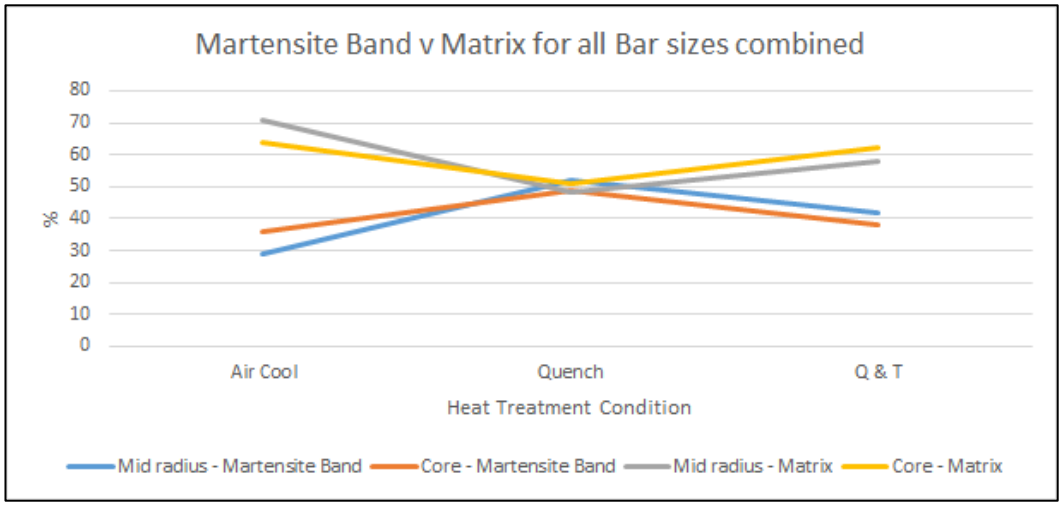

Figure 5-110: Average Phase Distribution (Band versus Matrix) for all Bar Sizes Combined, When Exposed to Different Heat Treatment Conditions

The evaluation has also enabled a detailed understanding of the microstructure in the finished Quench and Tempered condition, which is paramount in the understanding of a coil spring for subsea applications.

- The band phase within all bar sizes has been identified as having a fully Martensitic microstructure, with the matrix exhibiting a mixture of both Martensite and Bainite.
- Martensite is the predominant phase within the matrix, with different levels of Bainite found across the bar cross-section. The percentage of Bainite within the matrix increases from the surface to the core location.
- The amount of Martensite within the microstructure has a direct influence on the resultant UTS properties. An increase in % Martensite corresponds to an increase in the resultant material strength.
- The amount of Martensite within the resultant microstructure is affected by changing the Quench and Tempering temperatures.

6 EXPERIMENTATION AND LITERATURE APPRAISAL

6.1 Introductory Remarks

This chapter presents a detailed examination of the experimental and academic research, to give a fuller understanding of the AISI 416H material in terms of both mechanical and metallurgical properties when subject to different heat treatment conditions. In addition, consideration is given as to why the material is not homogenous and why there are differences in resultant properties across the 3 bar sizes. This is thereafter brought together to enable a better understanding of the material limitations and functionality of the coil spring for subsea applications.

6.2 AISI 4161H Material

Research initially identified that the raw material used for coil spring manufacture is subjected to the continuous casting process, which inherently produces centre line segregation within the billet during the solidification process [6]. The level of segregation is dependent on the carbon content and alloying elements within the bulk material, with hypo-eutectoid steels such as AISI 4161H being more susceptible. This is because the diffusion coefficients of the material elements are "higher in ferrite than in austenite" [6], which results in micro segregation for high carbon steels. Furthermore, the level of segregation is influenced by the hot rolling process, where the material is reduced from the billet form to the required bar diameter. This process breaks up the as-cast structure to a fine-grained material and disperses the segregation throughout [7]. However, this is dependent on the level of hot work in terms of forging reduction ratio. D'Errico et al [17] stated that "the ultimate quality of steel products is determined from the steelmaking technological cycles and casting process technologies employed".

From the outset, this suggests that the raw material used for coil spring manufacture will indeed have some form of variability, even before the bar is further processed (hot coiled & heat treated) to form a coil spring. This phenomenon was initially substantiated with the early work conducted within Chapter 3, which identified the

effect of hot working two 2.875-inch bars at the respective forgings reduction ratios of 5.3:1 and 21.1:1. The levels of micro segregation, identified as microstructural banding was significantly different in terms of microstructure and resultant mechanical properties - see Figure 3-7.

D'Errico et al [17] and Penha et al [18] confirmed that the hot working process used to form the respective material, will align the segregation to form elongated bands, and that during mechanical deformation "dendritic micro-segregation strung out into stringers parallel to the dominant flow direction" [18]. Krauss [29] further verified these findings by concluding that "hot rolling aligns interdendritic variations in chemistry in bands parallel to the rolling direction producing alternating regions of high and low concentrations of various solute elements". In addition, Krauss [29] identified that the level of banding was very much dependent on the hot working processes and the diffusion coefficients of the elements within the material.

D'Errico et al [17] and Penha et al [18] developed this theory further by confirming that the degree of banding is influenced by several key factors, such as alloying elements, cooling rates, austenitization temperatures and prior austenite grain size.

The literature has clearly established that continuous cast material will be prone to centre-line segregation, which when hot rolled can manifest into elongated zones of bands. These bands can exhibit both low and high concentrations of the individual elements stated within the bulk chemistry. This will however be dependent on the element and its respective diffusion coefficient, which can influence the mobility of the elements and reaction with carbon during heat treatment operations.

Because of the chemical composition differences, each band will have its own transformation temperatures, which will result in an independent CCT curve for each respective zone [18].

These findings align with the results found within the DoE evaluation presented within Chapter 5. The AISI 4161H material has been confirmed as having a dual phase / duplex type microstructure, containing elongated bands and a matrix, in the As-Received, Air Cooled (Normalised), As-Quenched and Quenched & Tempered

condition. Also, the bands and matrix contain different chemical compositions with variability evident between the two phases and between the different heat treatment conditions. This therefore warrants an understanding on the effect of Diffusion and Transformation Temperatures during the subsequent heat treatment operations.

6.2.1 Elemental Material Diffusion

The effect of diffusion was studied to determine why the DoE results within Chapter 5, produced different levels of elemental composition (expressed as Ideal Diameter), across the AISI 4161H material.

Arrhenius [62], established that the level of diffusivity of an element would increase with temperature, and that the instantaneous level of diffusion could be calculated from Equation 6-1:

$$D = D_0 e^{\left(\frac{-Q}{RT}\right)}$$

Equation 6-1

where: D is the instantaneous diffusivity, D_0 is the diffusion coefficient, Q is the activation energy, R is the gas constant, and T is the instantaneous temperature.

To collate the level of diffusivity with regards the DoE results, 3 elements were selected for analysis; these were Cr, Mn and Mo. The respective diffusion coefficient and activation energy for the elements were selected from References [31] & [32], along with the gas constant. The methodology employed, was one that determined both the instantaneous and cumulative diffusion during the hold / soak time for the austenitisation temperature. This is paramount, as during standard manufacture the bars used for coil spring manufacture, are held at this temperature prior to quenching. Therefore, time and temperature will have a direct influence on the amount of diffusion experienced by each element. In addition, consideration must be made to the differences experienced at the surface and the core of the material. During the DoE experimental phase, several sample bars were subjected to real time temperature measurement at these respective locations - Figure 5-1.

Therefore, the aim of this study was to establish the amount of cumulative diffusion for the three selected elements, and to determine whether the amount of diffusion would vary between the surface and the core locations.

For research purposes, the mid-sized bar (3.375-inch) was selected for analysis, which produced the time / temperature chart detailed within Figure 6-1.

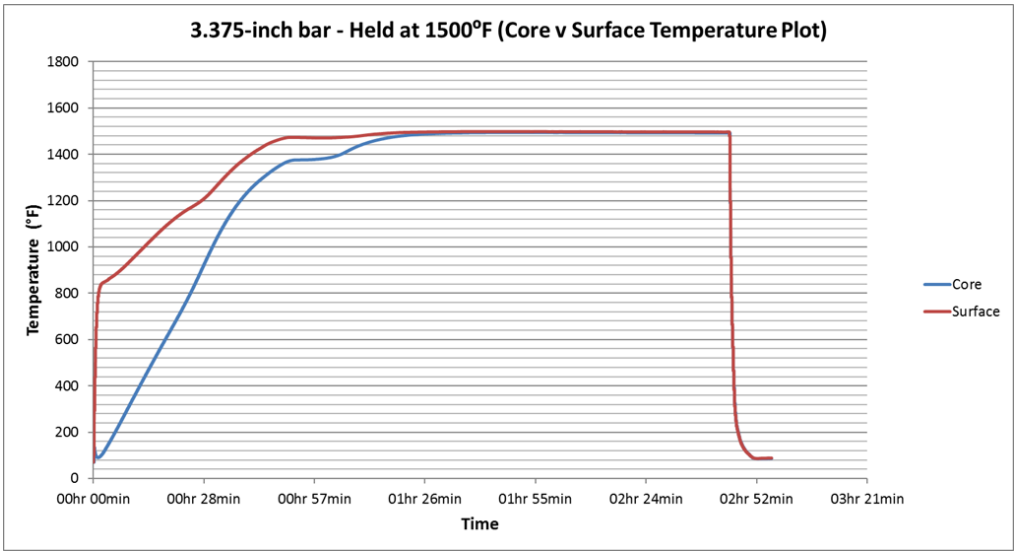

Figure 6-1: Time / Temperature chart for the 3.375-inch bar held at 1500°F

To determine the diffusivity values, an Excel spreadsheet was setup using the diffusion formula, activation energy and gas constant for the respective elements. The calculation took the temperature at a given point to determine the instantaneous diffusion values and then subsequently the level of cumulative diffusion (area under the curve) - Reference Table 6-1.

Table 6-1 Extract from Diffusion Calculation Spreadsheet [31] [32]

Diff Consts	Cr	Mn	Mo		Interface	dx [m]	dc Cr [mol]	dc Mn [mol]	dc Mo [mol]		
D_0 [m^2/s]	0.00108	0.000016	0.0367		Surface	8.00E-05	0.12	0.11	0.09		
Q [kJ/mol]	291.8	261.7	286.8		Core	0.000105	0.5	0.77	0.63		
R [KJ/mol]	0.008314				dc/dx [mol/m]:	Surf	-1.50E+03	-1.38E+03	-1.13E+03		
						Core	-4.76E+03	-7.33E+03	-6.00E+03		
Quenching											
Core											
Inst. Diffusion [m^2]			Inst. Flux [mol/m^2s]			Cummulative Diffusion [m^2]			Cummulative Flux [mol/m^2s]		
Cr	Mn	Mo	Cr	Mn	Mo	Cr	Mn	Mo	Cr	Mn	Mo
1.67E-55	5.48E-52	4.40E-53	7.98E-52	4.02E-48	2.64E-49	1.67E-55	5.48E-52	4.40E-53	7.98E-52	4.02E-48	2.64E-49
1.67E-55	5.48E-52	4.40E-53	2.51E-52	7.54E-49	4.94E-50	3.35E-55	1.10E-51	8.79E-53	1.05E-51	4.77E-48	3.13E-49
1.67E-55	5.48E-52	4.40E-53	2.51E-52	7.54E-49	4.94E-50	5.02E-55	1.64E-51	1.32E-52	1.30E-51	5.53E-48	3.63E-49
2.01E-55	6.44E-52	5.25E-53	3.01E-52	8.86E-49	5.90E-50	7.03E-55	2.29E-51	1.84E-52	1.60E-51	6.41E-48	4.22E-49
2.01E-55	6.44E-52	5.25E-53	3.01E-52	8.86E-49	5.90E-50	9.04E-55	2.93E-51	2.37E-52	1.90E-51	7.30E-48	4.81E-49

The results from the diffusion study have demonstrated that each element has a different level of cumulative diffusivity over the set temperature hold point. This is shown within Figures 6-2 and 6-3, which have established that at the bar core location at a hold temperature of 1500°F, Mo experiences the greatest level of diffusion, which is subsequently followed by Cr and Mn.

- Mo = 3.25E-12 / Cr = 5.48E-14 / Mn = 2.31E-14

With regards the amount of cumulative diffusivity at the core versus the surface; the results have shown there is a fundamental difference between these two locations. This finding is the same for Mo, Cr & Mn, where the levels of diffusion are less at the core location. The resultant diffusion plots demonstrate that the level of diffusion is temperature dependant, since the core takes longer than the surface to reach the respective hold temperature, which results in a lag in time before diffusion takes place. This results in a reduction in diffusion for the same amount of hold time at the respective austenitising temperature - see Figures 6-4 through 6-6.

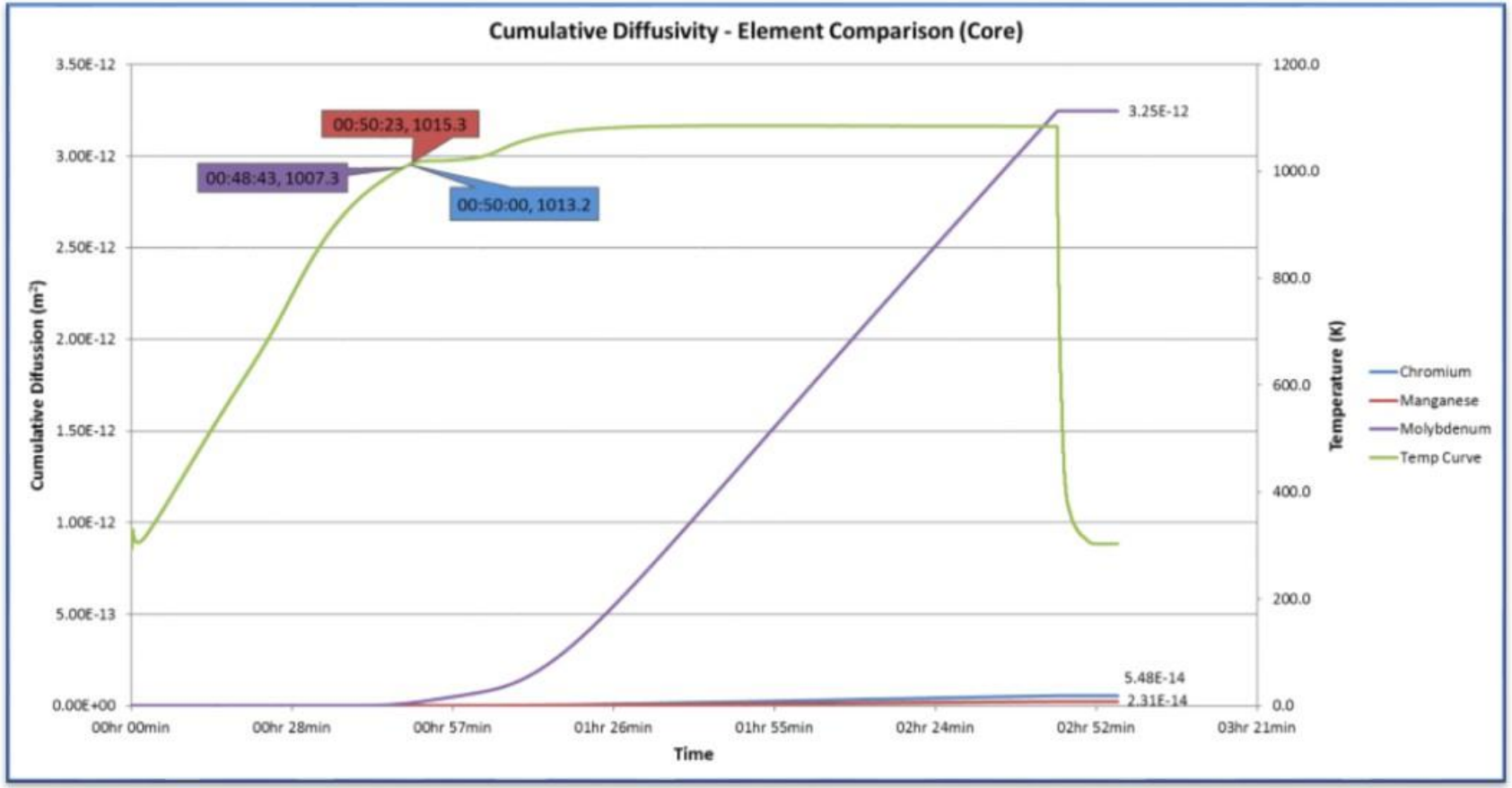

Figure 6-2: Cumulative Diffusion Graph for Mo, Cr & Mn at 1500°F 3.375 -Inch Bar, Core Location

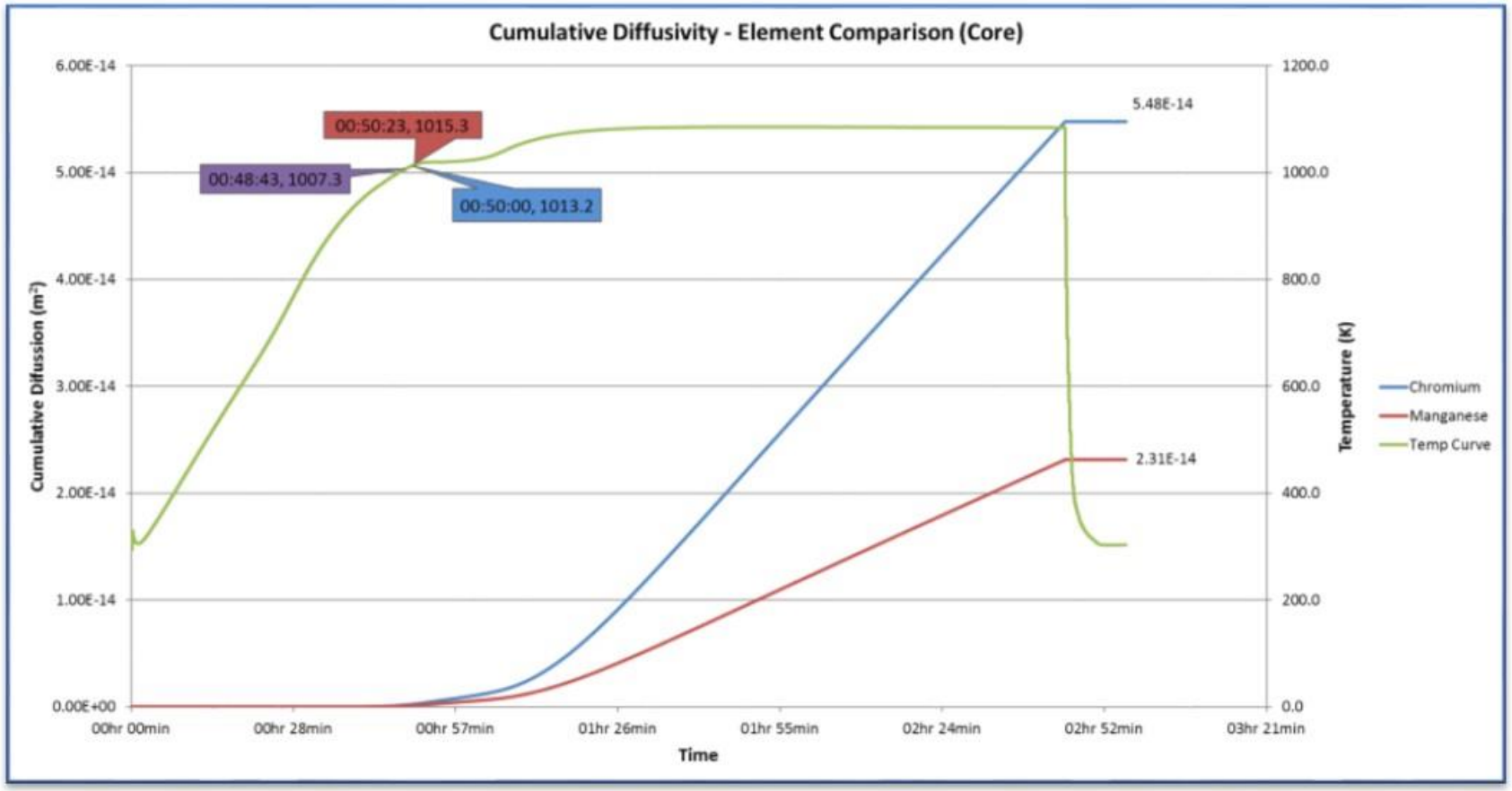

Figure 6-3: Cumulative Diffusion Graph for Cr & Mn at 1500°F 3.375 -Inch Bar, Core Location (Mo Removed for Clarity)

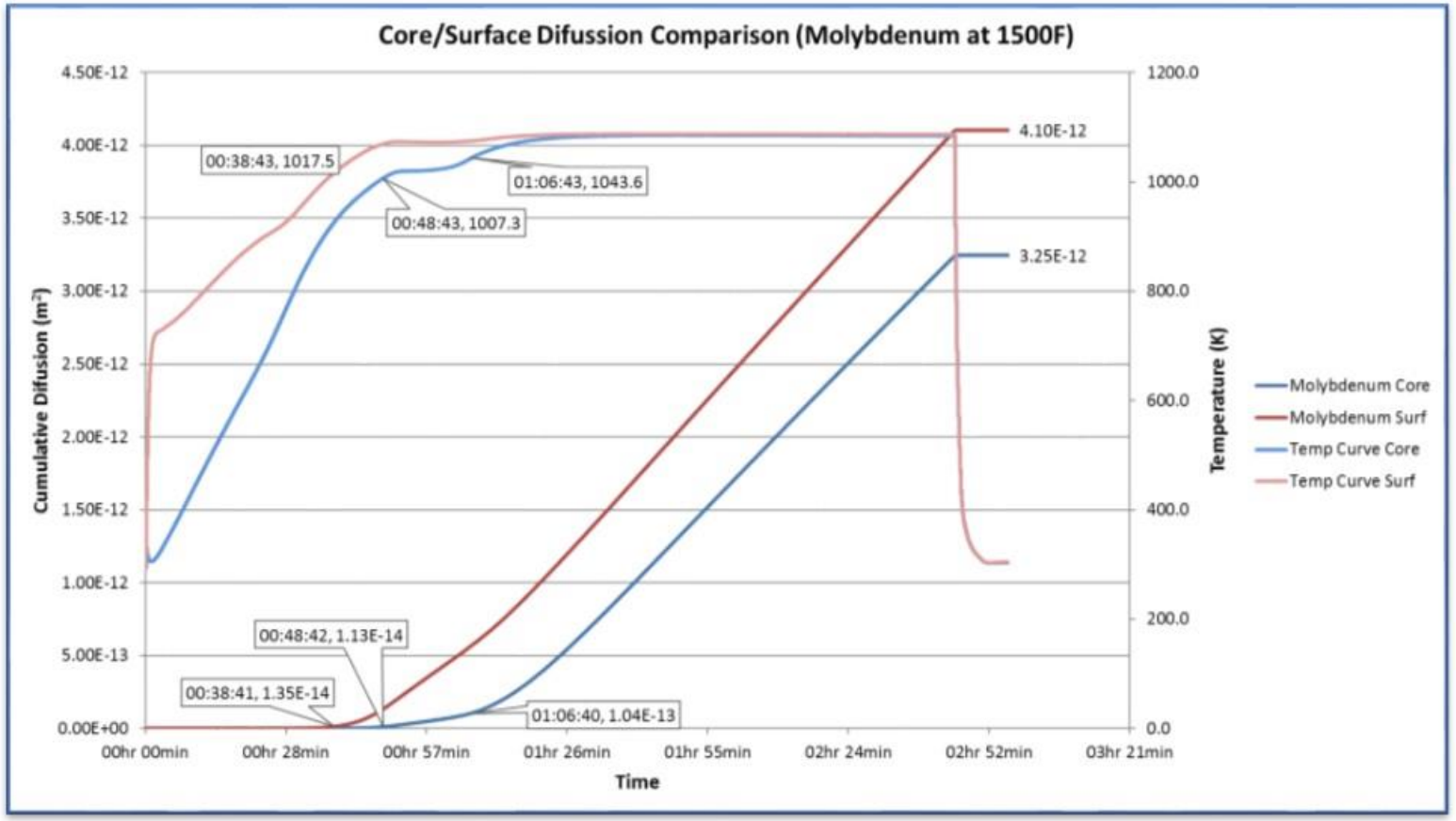

Figure 6-4: Core v Surface Mo Cumulative Diffusion

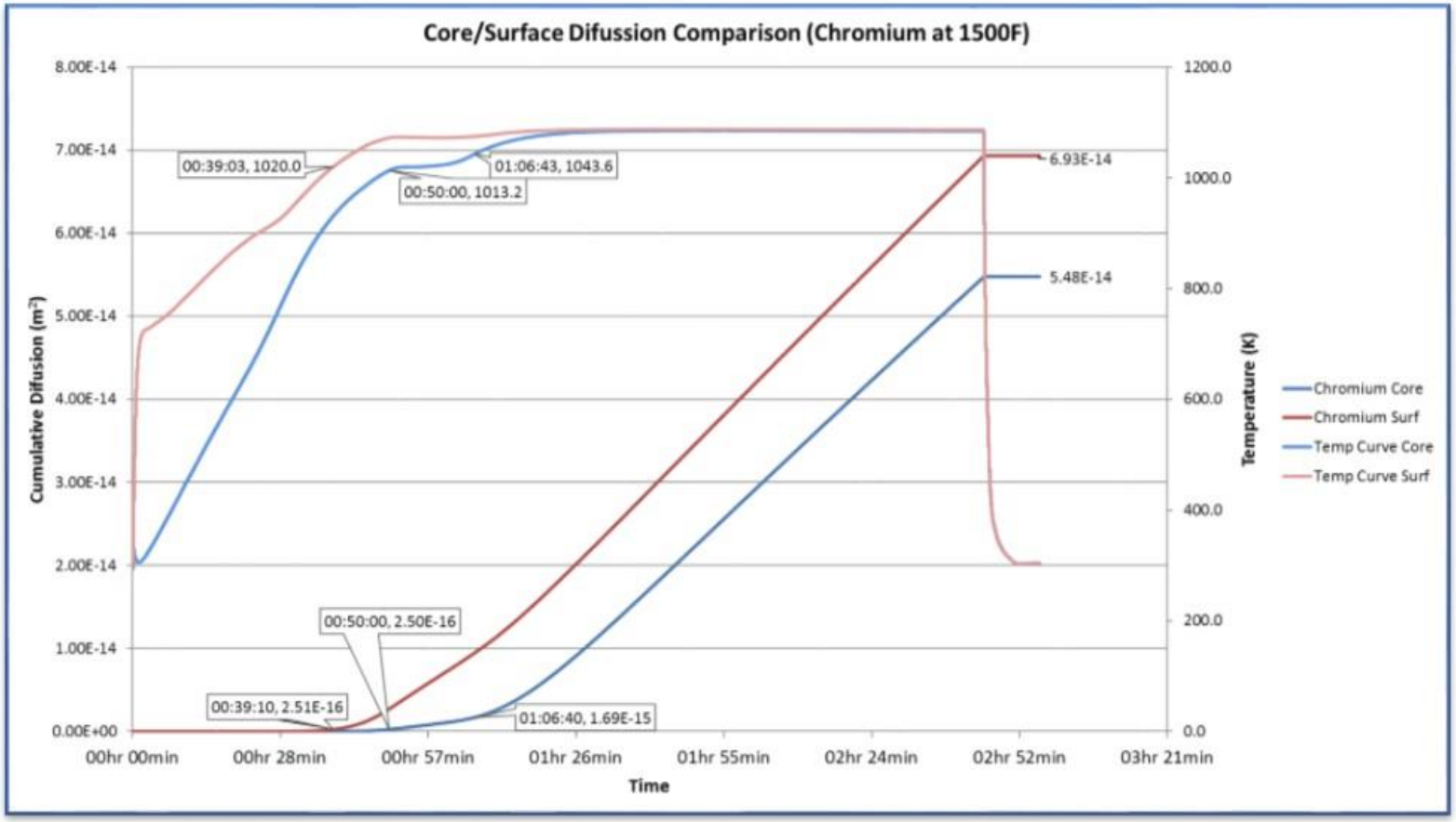

Figure 6-5: Core v Surface Cr Cumulative Diffusion

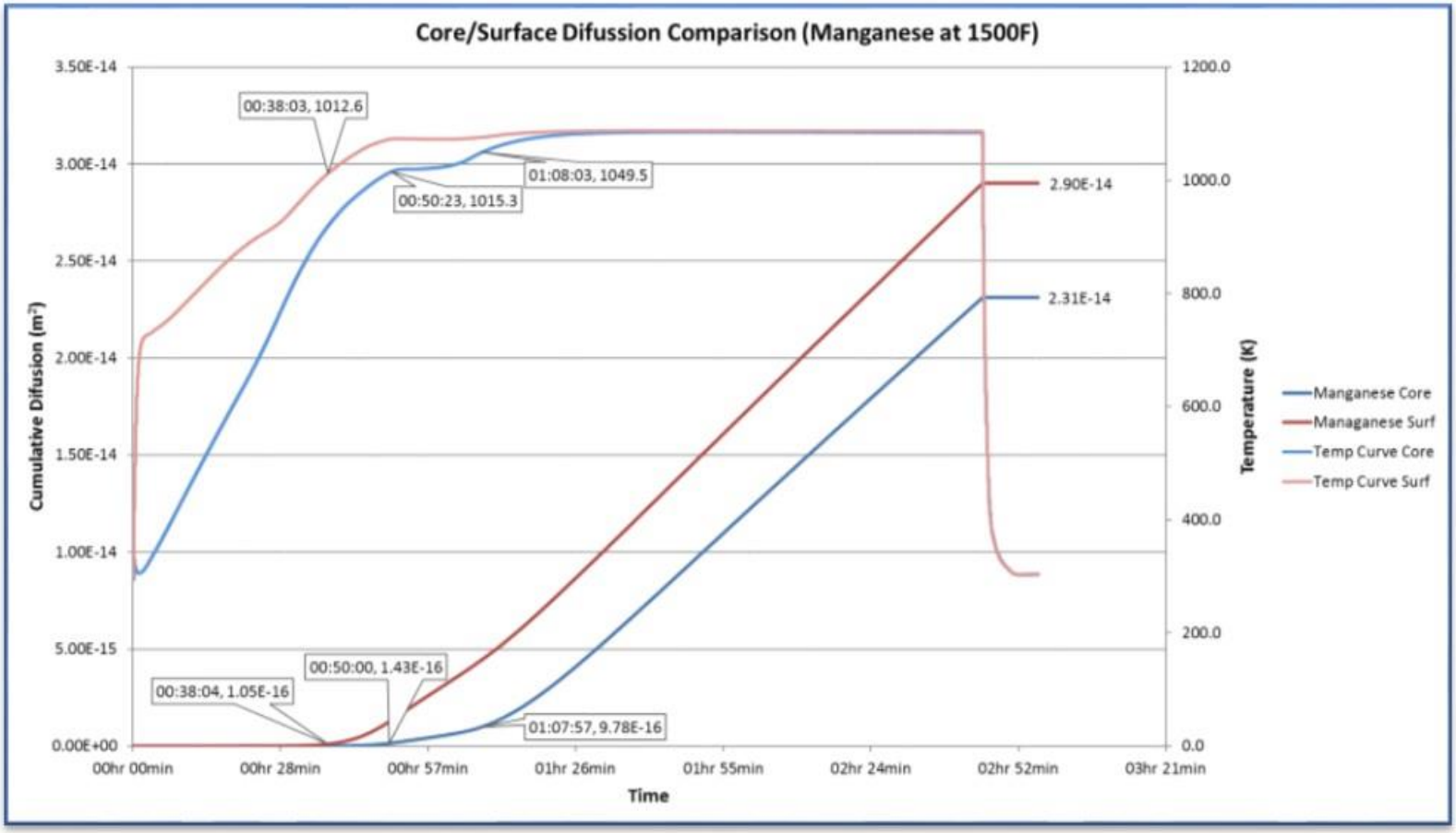

Figure 6-6: Core v Surface Mn Cumulative Diffusion

The study has also confirmed that to obtain the equivalent level of diffusion for each element across the complete DoE bar range, an increase in hold / dwell time at temperature is required. This is demonstrated within Figure 6-7, which demonstrates the time taken to achieve the known level of diffusion e.g. (Cr 1.26E-13) over the three respective bar sizes.

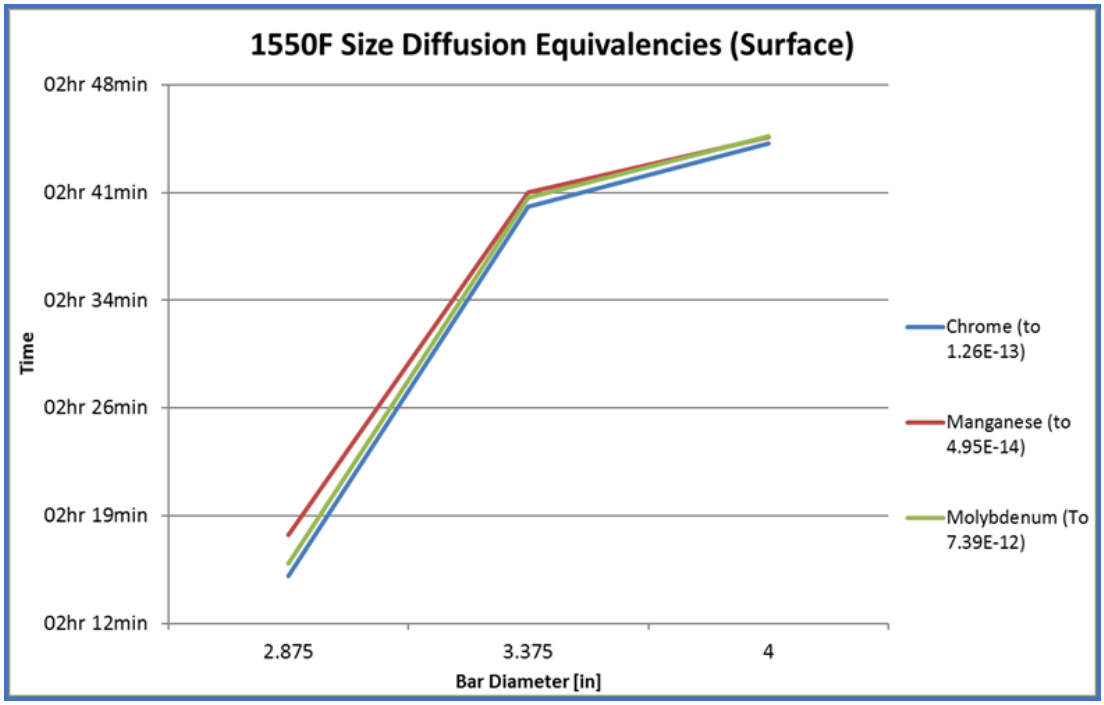

Figure 6-7: Bar size versus time to achieve equivalent levels of elemental diffusion

The results of the diffusion research ties in with both that Krauss [29] and that detailed within the experimental DoE. Krauss [29] established that micro segregation can be reduced / influenced by holding the material for long durations at high temperatures. However, this is dependent on the mobility and composition of the given element [29].

The calculated cumulative diffusion values for Mo, Cr & Mn are different (Figures 6-2 & 6-3), with Mo exhibiting the greatest level of diffusion and mobility within the material. Therefore, when considering the results achieved for the 3.375-inch bar material at 1500°F, and plotting the elemental percentages from the SEM EDAX analysis, the chemical composition changes from the surface to the core – see Figures 6-8 to 6-10.

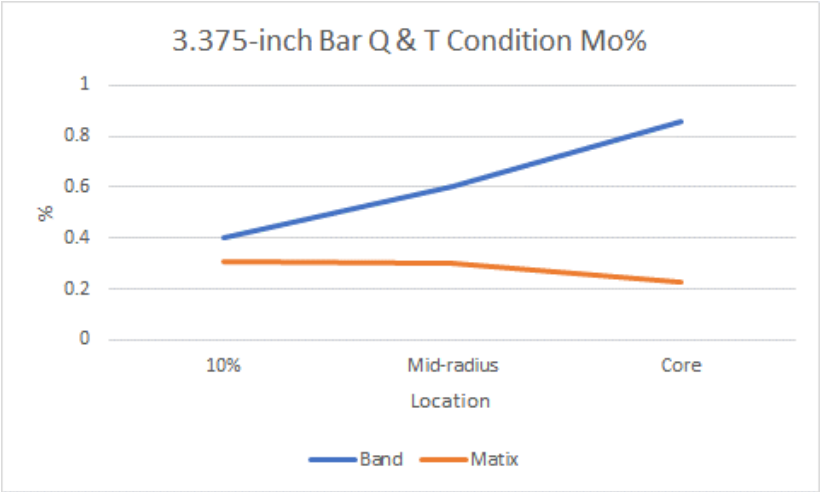

Figure 6-8: Elemental % for Mo across the various bar locations

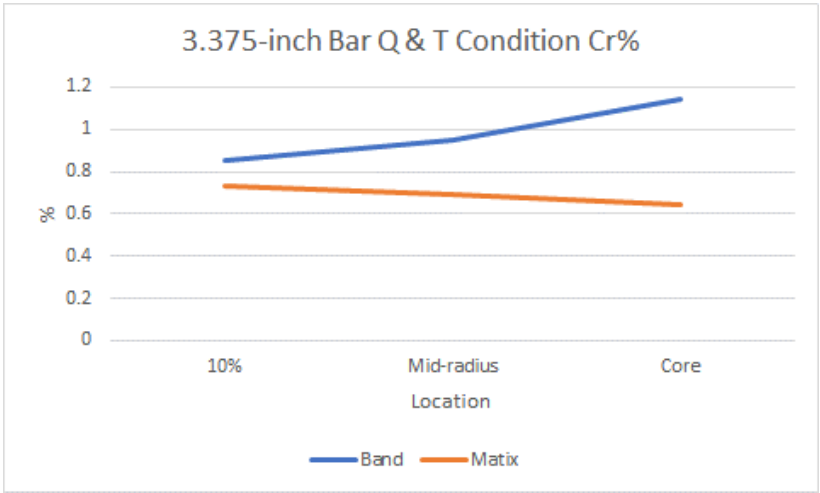

Figure 6-9: Elemental % for Cr across the various bar locations

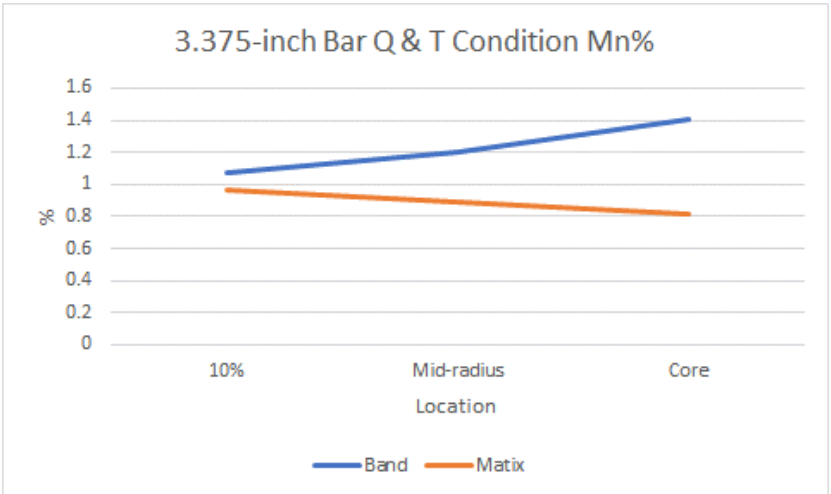

Figure 6-10: Elemental % for Mn across the various bar locations

Figures 6-8 to 6-10, establish that the amount of elemental segregation evident within the band phase, reduces by the greatest extent from the core to the surface with Mo. Both Cr and Mn reduce over the cross-section but the gradient of the line is less. In addition, the elemental% for Mo, Cr and Mn within matrix increases, from the core to the surface. This indicates that more diffusion is taking place between the band and matrix at the surface location; which confirms the analysis presented within Figures 6-4 to 6-6. (Cumulative diffusion is greatest at the surface compared to the core).

It is evident from the research and experimental results that segregation in terms of banding will be present within the raw material, from the continuous casting [6] and hot reduction rolling [7] processes. However, the dispersion of the key alloying elements such as Mo, Cr and Mn, in terms of micro-segregation is dependent on the diffusion coefficients and cumulative mobility of the respective element. This in conjunction with lower diffusion at the core compared to the surface, helps understand the different levels of chemical composition experienced across the bar cross-section, and why different heat treatment conditions (time and temperature) influence the elemental percentages achieved at different locations within the AISI 4161H material.

6.2.2 Chemical Composition and Transformation Temperature

The results have clearly shown that the as-received material in conjunction with the three different heat treatment conditions, contain chemical composition variability between the banded and matrix zones. It has also been established that response to heat treatment is dependent on time at temperature, cooling medium, geometry and cross-sectional thickness of the bar. However, the chemical composition of the material plays a crucial part in the resultant microstructure and mechanical properties, especially in relation to the TTT diagram / curve [8]. Literature has shown that different elements have a direct influence on the critical transformation temperatures such as the A1 & A3. Austenite stabilizing elements such as Mn & Ni decrease the A1, with Ferrite stabilizing elements, such as Cr, Si Mo & W increasing the A1 [9]. However; TTT curves do not consider the effect of different cooling rates, as they are specific to phase transformations at constant temperatures [8]. The CCT curve / diagram however, has shown to be the best representation of a material resultant microstructure, as it considers the effect of different chemical compositions and cooling rates for a given material - see Figure 4-9.

Kirkaldy et al [23] [24] [25] determined that the transformation temperatures and respective phases can be determined through the development of experiment and correlation of empirical formula to create a full CCT / TTT model. Others such as Steven / Haynes [26] and Andrews [27] developed formula for key transformation zones such as Bainite and Martensite start temperatures. Therefore; it is paramount to understand how the chemical composition variability and individual elemental percentage has on the critical phase transformation temperatures and resultant TTT / CCT curves.

Almost all alloying elements will influence the transformation temperatures and transformation times to varying effect. However, the AISI 4161H material has four main elements that were considered (Mn, Si, Mo & Cr) along with a constant carbon content of 0.58%. The equations used to obtain the Austenitisation start & finish temperatures (Ac1 & Ac3), were first derived by Andrews [27].

$$Ac1\ (°C) = 723 - 16.9Ni + 29.1Si + 6.38W - 10.7Mn + 16.9Cr + 290\ As$$

Equation 6-2

$$Ac3\ (°C) = 910 - 203\sqrt{C} + 44.7Si - 15.2Ni + 31.5Mo + 104V + 13.1W - 30Mn + 11Cr + 20Cu - 700P - 400Al - 120As - 400Ti$$

Equation 6-3

In a similar fashion, the Martensitic Start temperature was also derived from equations defined by Andrews [27]. However, due to lack of scientific data, an accurate equation to define the Martensite finish temperature has not yet been derived. Literature [27] has suggested that the temperature can be estimated as a function of the Martensite start temperature, which this analysis methodology has taken. The Martensitic temperatures were therefore defined as:

$$Ms\ (°C) = 539 - 423C - 30.4Mn - 17.7Ni - 12.1Cr - 11.0Si - 7Mo$$

Equation 6-4

$$Mf\ (°F) = Ms\ (°F) - 387$$

Equation 6-5

Finally, the Bainite temperatures were also calculated. Equations derived by Steven and Haynes [26] can accurately predict the Bainite start temperature for low carbon steel, with a similar approach taken to define the Bainite finish temperature as with Martensite.

$$Bs\ (°C) = 830 - 270C - 90Mn - 37Ni - 70Cr - 83Mo$$

Equation 6-6

$$Bf\ (°C) = Bs - 120$$

Equation 6-7

Like the diffusion set of results, Excel spreadsheets were utilized to determine the key transformation temperatures, which were calculated for the band and matrix zones across the 3 bar sizes. An example of the MS Excel model used is demonstrated within Figure 6-11.

Condition	Bar Size	Location	Phase	C	Si	Cr	Mn	Mo	AC1 Temperature C	AC1 Temperature F	AC3 Temperature C	AC3 Temperature F
As received	2.875	Core	Band	0.58	0.46	1.62	1.24	1.12	750.50	1382.89	791.86	1457.35
As received	2.875	Core	Matrix	0.58	0.36	0.92	1.04	0.49	737.90	1360.21	765.85	1410.52

Condition	Bar Size	Location	Phase	C	Si	Cr	Mn	Mo	BS Temperature C	BS Temperature F	Bf Temperature C	Bf Temperature F
As received	2.875	Core	Band	0.58	0.46	1.62	1.24	1.12	355.44	671.79	235.44	455.79
As received	2.875	Core	Matrix	0.58	0.36	0.92	1.04	0.49	474.73	886.51	354.73	670.51

Condition	Bar Size	Location	Phase	C	Si	Cr	Mn	Mo	MS Temperature C	MS Temperature F	Mf Temperature C	Mf Temperature F
As received	2.875	Core	Band	0.58	0.46	1.62	1.24	1.12	222.22	432.00	7.22	45.00
As received	2.875	Core	Matrix	0.58	0.36	0.92	1.04	0.49	242.48	468.47	27.48	81.47

Figure 6-11: Extract from Transformation chart for the As-received 2.875-inch bar

The first set of analyses taken, was that of the as-received material; as this is the datum state prior to any subsequent heat treatment. To understand the effect of the chemical composition the results were presented in graphical format.

The trend established from the results - Figures 6-12 to 6-15, is that chemically rich bands, compared to the matrix, have the greatest impact on the transformation temperatures seen. Regarding the austenisation temperatures, Ac1 & Ac3, the bands with greater chemical content have a higher austenisation temperature compared to the matrix. It can also be noted that moving from the core to the outer radius of the bar also corresponds with a decrease in austenisation temperature of the bands, while the matrix temperature remains approximately constant. This is a result of the reduced chemical composition in the bands at the surface compared to the core.

It is also apparent that the austenite transformation temperatures for the 2.875-inch bar are consistently higher than that of the 3.375 & 4-inch bars. This relates to the Ideal Diameter values presented within Figure 5-69 - 2.875-inch.

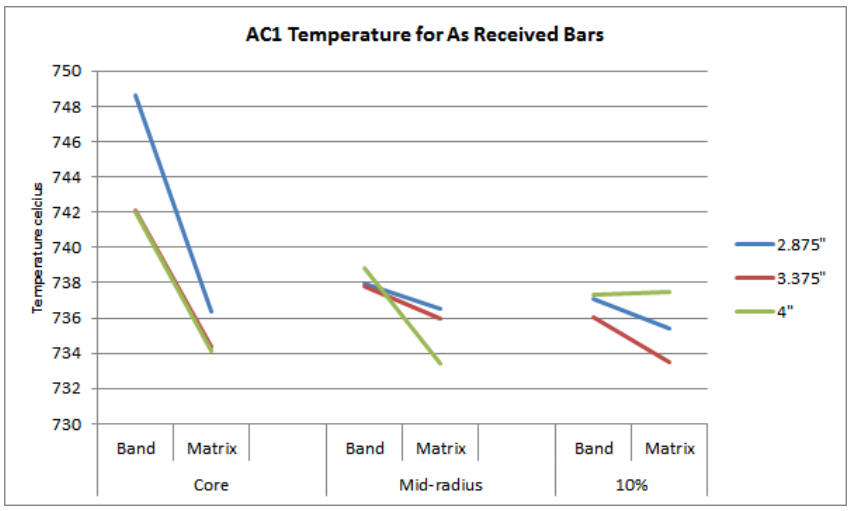

Figure 6-12: Chemical composition effect on the Ac1 transformation temperature

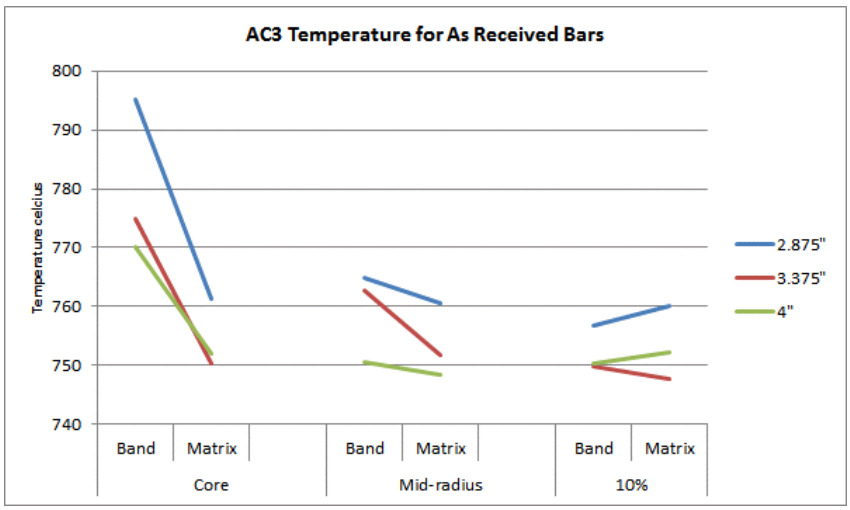

Figure 6-13: Chemical composition effect on the Ac3 transformation temperature

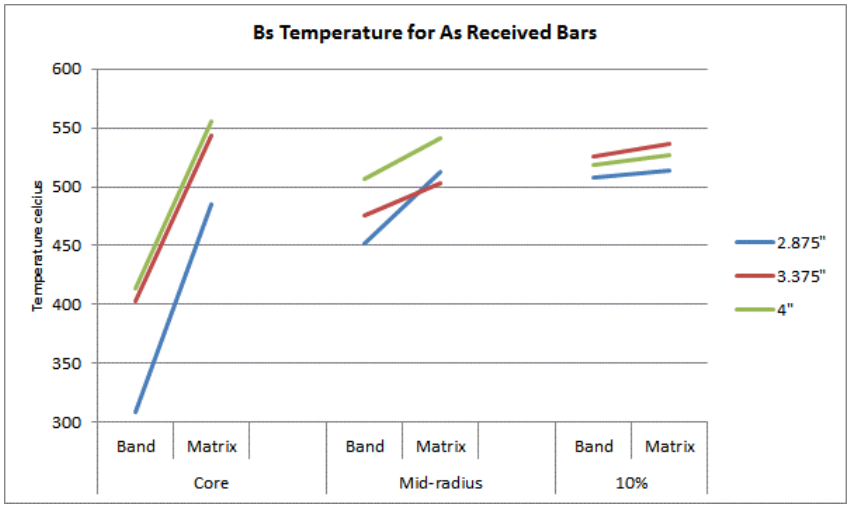

Figure 6-14: Chemical composition effect on the Bs transformation temperature

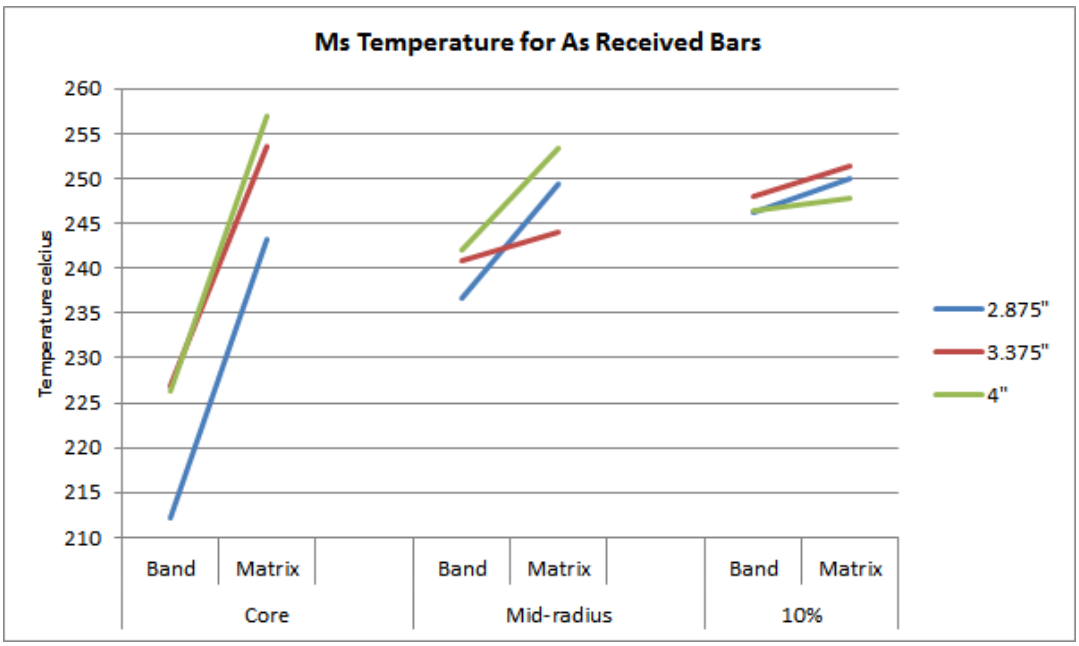

Figure 6-15: Chemical composition effect on the Ms transformation temperature

Both the Ms and Bs transformation temperatures follow similar trends, with the rich chemical compositional bands lowering these respective values. This effect reduces as you move from the core to the surface. The values at the surface are more consistent with a minimum delta in temperature between the two phases; however, the lower chemical composition values result in an increase in the Ms and Bs temperature - see Figures 6-14 and 6-15.

To aid in understanding how elemental chemical composition affects the transformation temperatures; graphs plotting the percentage content of the main alloying elements (Mn, Si, Mo & Cr) were created. The principle of this study, was to take the standard raw material mill analysis and initially establish the respective Ac1, Ac3, Bs & Ms temperatures, using the formula created by Steven / Haynes [26] and Andrews [27]. Once calculated, the effect of individual elements was studied by first changing selected element percentage to zero, while keeping all other elements as a constant - see Table 6-2. The value of the respective element was then changed to see what affect this would have on the key transformation temperatures. Table 6-2 demonstrates an extract from the excel spreadsheet that establishes the temperature change for a given element % increase for the key transformation temperatures. The example shown is for Si.

Table 6-2: Extract from Excel Model - Effect of Si% on the Critical Transformation Temperatures

Si Content %	AC1 - temperature°C	AC1 % change in temperature	AC3 temperature °C	AC3 % change in temperature	Bs - temperature °C	Bs % change in temperature	Bf - temperature °C	Ms - temperature °C	Ms % change in temperature	Mf - temperature °C
0	725.076	0	726.914806	0	522.53	0	402.53	256.65	0	41.65
0.05	726.531	0.20066862	729.149806	0.307463816	522.53	0	402.53	256.1	-0.21429963	41.1
0.1	727.986	0.401337239	731.384806	0.614927632	522.53	0	402.53	255.55	-0.42859926	40.55
0.15	729.441	0.602005859	733.619806	0.922391447	522.53	0	402.53	255	-0.64289889	40
0.2	730.896	0.802674478	735.854806	1.229855263	522.53	0	402.53	254.45	-0.857198519	39.45
0.25	732.351	1.003343098	738.089806	1.537319079	522.53	0	402.53	253.9	-1.071498149	38.9
0.3	733.806	1.204011717	740.324806	1.844782895	522.53	0	402.53	253.35	-1.285797779	38.35
0.35	735.261	1.404680337	742.559806	2.152246711	522.53	0	402.53	252.8	-1.500097409	37.8
0.4	736.716	1.605348957	744.794806	2.459710526	522.53	0	402.53	252.25	-1.714397039	37.25
0.45	738.171	1.806017576	747.029806	2.767174342	522.53	0	402.53	251.7	-1.928696669	36.7
0.5	739.626	2.006686196	749.264806	3.074638158	522.53	0	402.53	251.15	-2.142996298	36.15
0.55	741.081	2.207354815	751.499806	3.382101974	522.53	0	402.53	250.6	-2.357295928	35.6
0.6	742.536	2.408023435	753.734806	3.68956579	522.53	0	402.53	250.05	-2.571595558	35.05
0.65	743.991	2.608692054	755.969806	3.997029605	522.53	0	402.53	249.5	-2.785895188	34.5
0.7	745.446	2.809360674	758.204806	4.304493421	522.53	0	402.53	248.95	-3.000194818	33.95
0.75	746.901	3.010029293	760.439806	4.611957237	522.53	0	402.53	248.4	-3.214494448	33.4
0.8	748.356	3.210697913	762.674806	4.919421053	522.53	0	402.53	247.85	-3.428794078	32.85
0.85	749.811	3.411366533	764.909806	5.226884869	522.53	0	402.53	247.3	-3.643093707	32.3
0.9	751.266	3.612035152	767.144806	5.534348684	522.53	0	402.53	246.75	-3.857393337	31.75
0.95	752.721	3.812703772	769.379806	5.8418125	522.53	0	402.53	246.2	-4.071692967	31.2
1	754.176	4.013372391	771.614806	6.149276316	522.53	0	402.53	245.65	-4.285992597	30.65

The first element scrutinized was the manganese content throughout the bar section. Manganese is an austenite former and its composition in the bar will influence the Ac1 and Ac3 temperatures. Manganese encourages the formation of the austenite at lower temperatures due to it having a similar FCC crystal structure [33]. This improves its solubility in the austenite, and hence a reduction in the Ac1 and Ac3 temperatures occurs with an increase in the respective Mn% - Figure 6-16.

The addition of Mn to the steel also results in a reduction in the Ms and Bs temperatures. Mn does not ably form carbides and, therefore, delays pro-eutectoid ferrite, Pearlitic, and bainitic reactions [33].

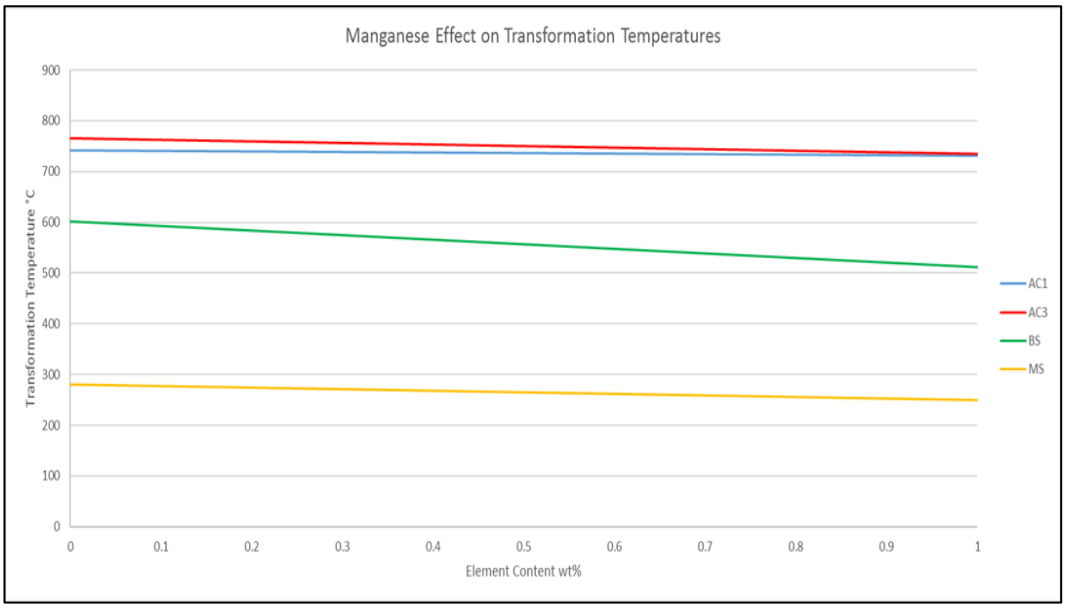

Figure 6-16: Effect on the Transformation Temperatures (% difference) for Different Mn% Contents

The results have shown that in the As-received condition the manganese content across the bar cross-section varies - Figure 6-17. Higher percentages of manganese are located at the core, which steadily decreases to the outer surface, with the band phase always richer in chemistry compared to the matrix. The higher Mn content at the core will therefore result in lower Ms and Bs temperatures compared to the surface. This could be problematic when cooling directly through bainitic region of the CCT curve, as the core will cool slower compared to the surface, which could result in the formation of a ferritic or pearlitic microstructure (carbon & alloy content specific).

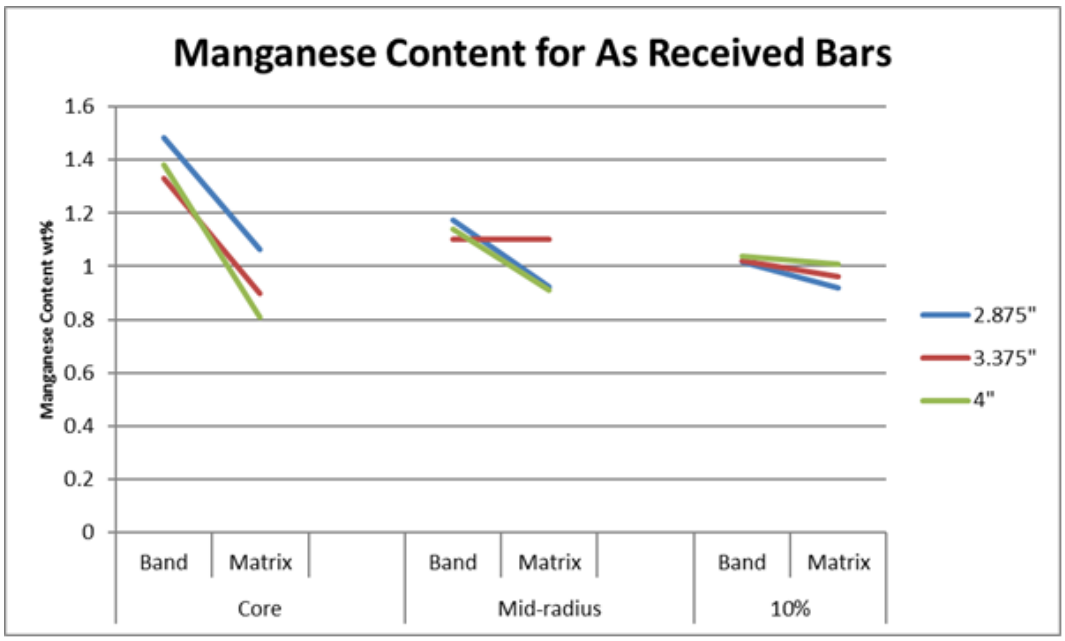

Figure 6-17: Mn Chemical Composition Distribution throughout the As-Received Material

The second element scrutinized was the silicon content throughout the bar section. Silicon is a ferrite stabilizer, due to it being found in solid solution within the ferrite because of its BCC crystal structure. This structure also effects the solubility of carbon in austenite; the lowering of this solubility creates an increase in the amount of carbon in solution increasing the amount of carbides in the steel [33]. The decrease in carbon solubility therefore, results in an increase in the start and finish temperature for austenite transformation, which can be seen in Table 6-2 and Figure 6-18.

Another effect of the low carbon solubility is a decrease in the Ms temperature, which is a result of more carbon being in solution, resulting in the growth of both ferrite or pearlite regions [33].

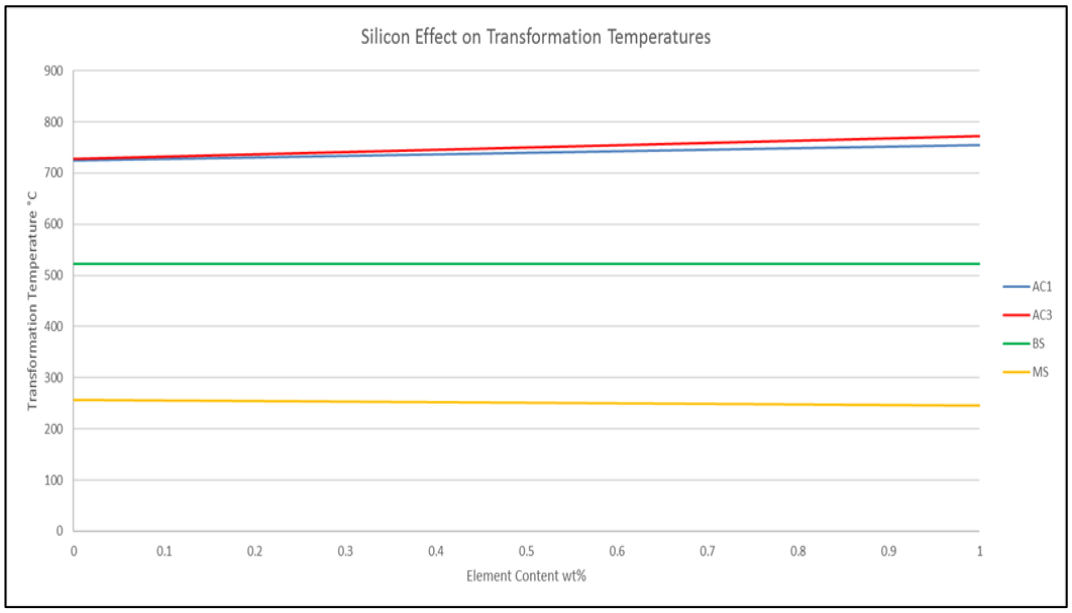

Figure 6-18: Effect on the Transformation Temperatures (% difference) for Different Si% Contents

The silicon content across the bar radius at the various bar sizes has been plotted in Figure 6-19. Like manganese, the bars core contains the highest silicon content, while the band always remained richer in chemistry compared to the matrix.

Higher silicon content at the core will therefore result in lower Martensite start temperatures compared to the surface.

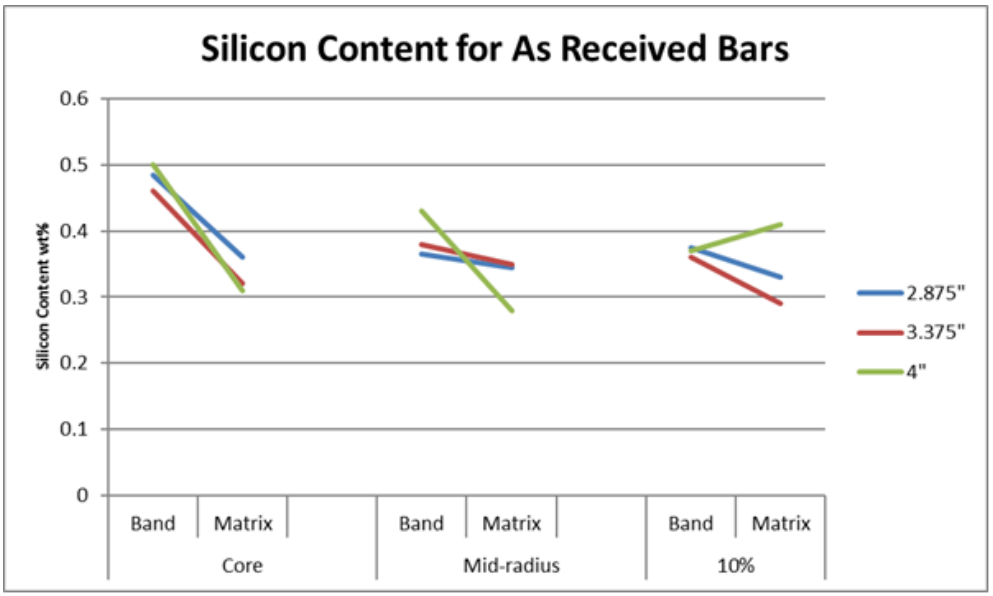

Figure 6-19: Si Chemical Composition Distribution throughout the As-Received Material

The third individual element examined was Mo. Molybdenum, like silicon, is a ferrite stabilizer due to its BCC structure. This structure increases the elements solubility in ferrite phase, which increases the austenization temperature [33]. This is depicted within Figure 6-20.

Unlike silicon, molybdenum is a strong carbide former, which will not only effect the magnitude of the transformation temperatures, but also the microstructure of the material. As molybdenum has a high affinity to form carbides, its ability to remove carbon from the ferrite is greater, resulting in a reduced rate of carbon diffusion, hence a lowering of the transformation temperatures of Martensite, Bainite and Pearlite [33].

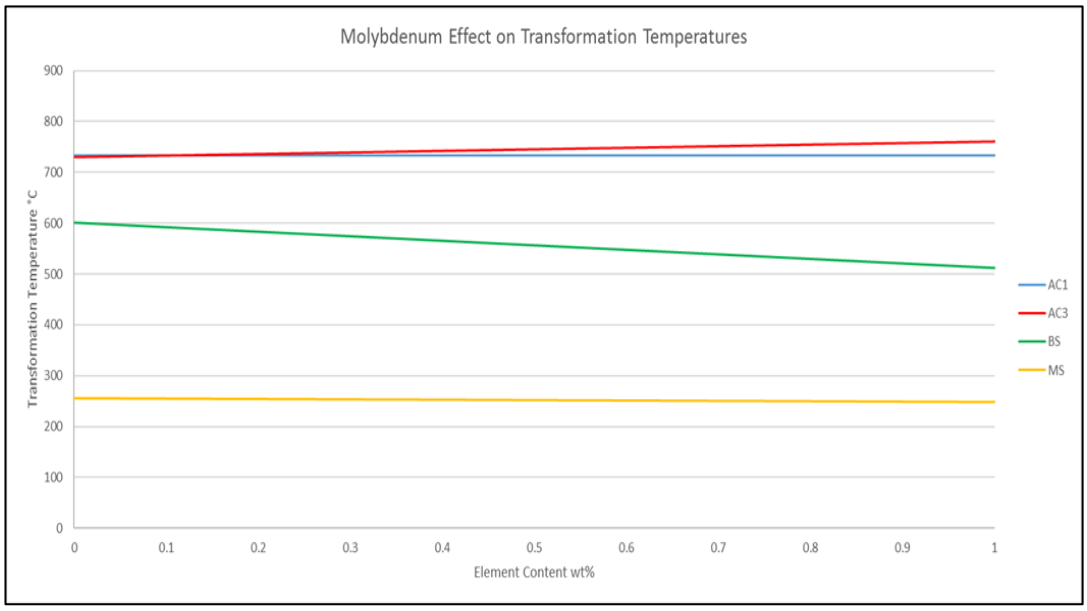

Figure 6-20: Effect on the Transformation Temperatures (% difference) for Different Mo Contents%

Depicted by an isothermal transformation diagram, the effect of adding molybdenum would not only reduce the martensite and bainite transformation temperatures, but also the cooling time to form these structures, which would subsequently move the curve to the right (Figure 6-21). Therefore, the appearance of the respective curve changes from a smooth line to a graph where two distinctive peaks are visible - Figure 6-21.

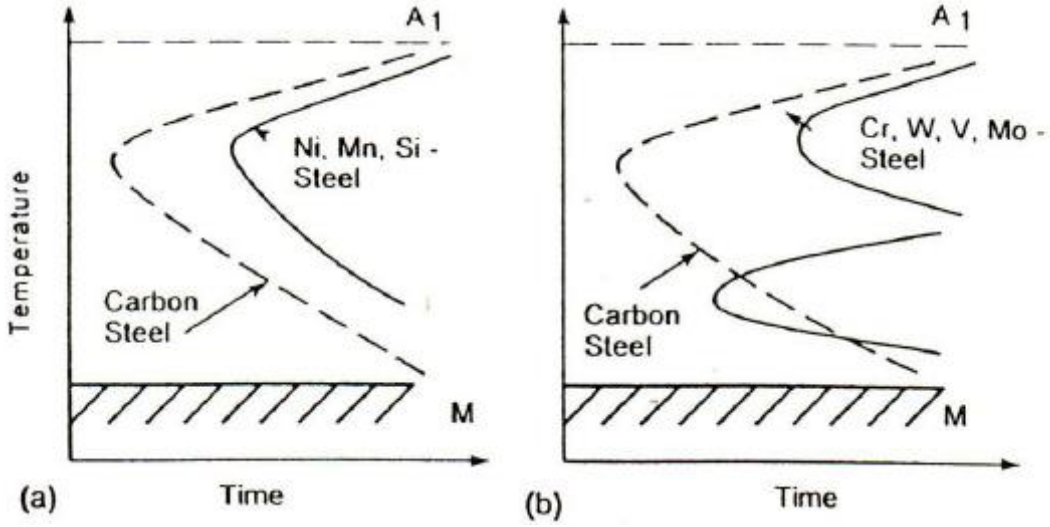

Figure 6-21: Isothermal transformation (a) Carbon steel & steel alloyed with non-carbide forming elements; (b) carbon steel and steel alloyed with carbide forming elements [33]

The molybdenum content exhibited across the respective bar cross-section, has seen the greatest variation of any of the elements investigated - see Figure 6-22. Like the other elements investigated, the core location contains the highest content of Mo, with the band always remaining richer in chemistry compared to the matrix. Molybdenum is also the only element to show a noticeable difference in content between bar sizes, with the 2.875" bar having the highest content throughout - Figure 6-22. This difference is noticeable, especially when analysing the overall Ac3 and Bs transformation temperatures for 2.875-inch material within Figure 6-20.

The average molybdenum content (matrix & band) decreased from 0.915% at the core to 0.24% at the surface, resulting in the decrease of the Ac3 temperature (decreasing from 3.95% to 1.12% across the bar). The bainite temperature is also dramatically altered, from a 13.69% decrease in temperature to a 3.89% decrease at the surface. It therefore can be deduced that molybdenum plays a vital role in the determination of the austenitisation and bainite transformation temperatures.

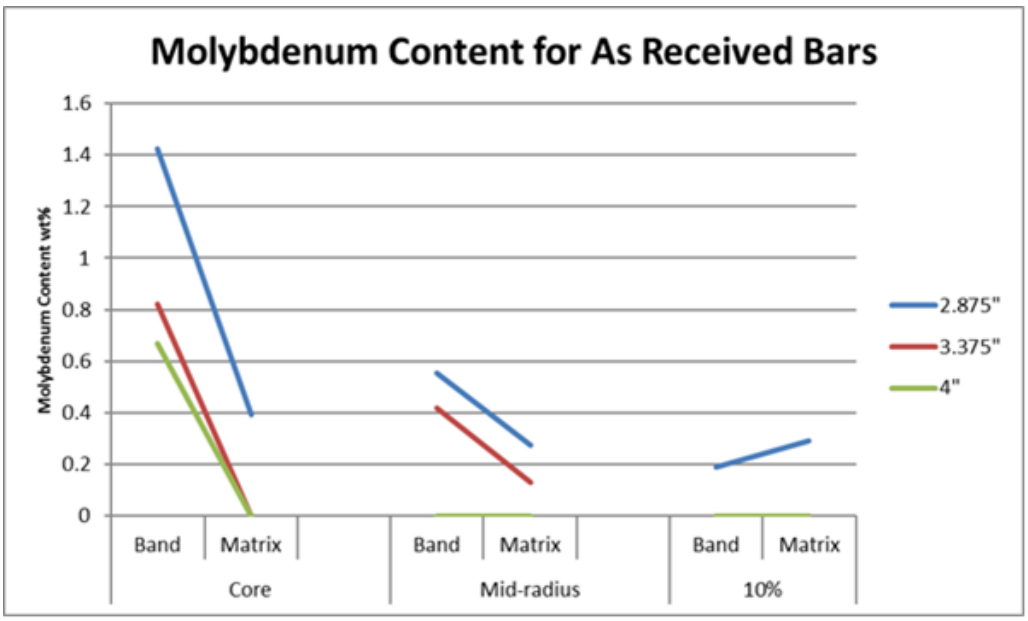

Figure 6-22: Mo Chemical Composition Distribution throughout the As-Received Material

The final element reviewed was the effect of chromium content throughout the bar section. Chromium, as an alloying element in steel, is similar to molybdenum, being a ferrite stabilizer with a BCC structure. Again, this structure increases its solubility in ferrite, which lowers the solubility in austenite, increasing the austenization temperatures as seen in Figure 6-24.

Chromium is also a carbide former, but with a lower affinity to carbon than molybdenum [33]. However, through the same processes as described earlier within this section for molybdenum, martensite and bainite starting temperatures will be lowered. The addition of chromium also forms a twin peak within the isothermal transformation diagram see Figure 6-21.

The chromium content across the bar section, contains the highest content at the core location, while the band always remained richer in chemistry compared to the matrix. For the 2.875-inch bar there is a noticeable increase in chromium content at the core, while the 3.375 and 4.0-inch material exhibited similar % contents - see Figure 6-23. This effect of chromium is noticeable, especially when analysing the overall effect of Ac1, Ms and Bs transformation temperatures in Figure 6-24, where considerable temperature changes are exhibited with increases in respective elemental values.

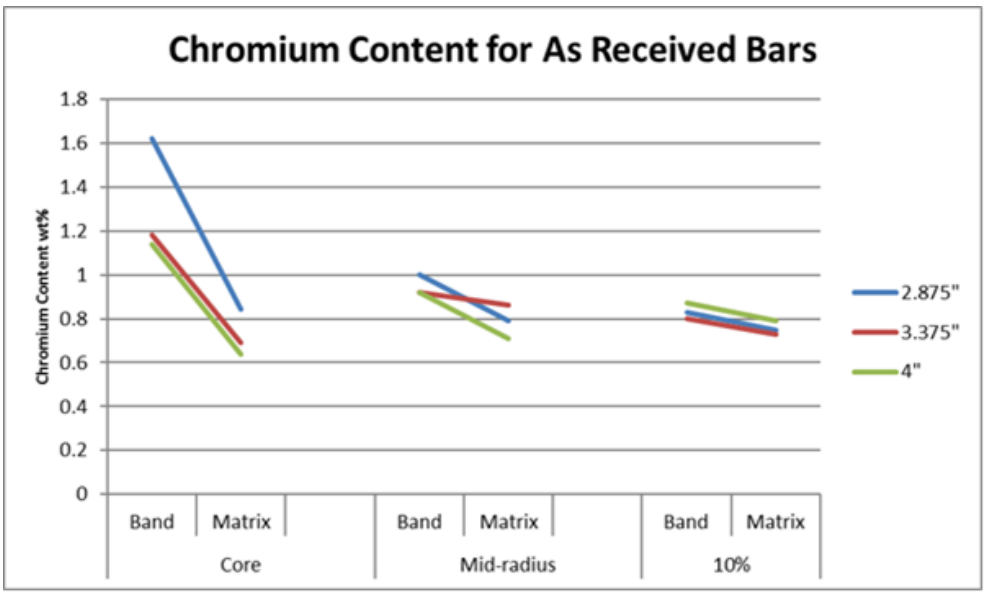

Figure 6-23: Cr Chemical Composition Distribution throughout the As-Received Material

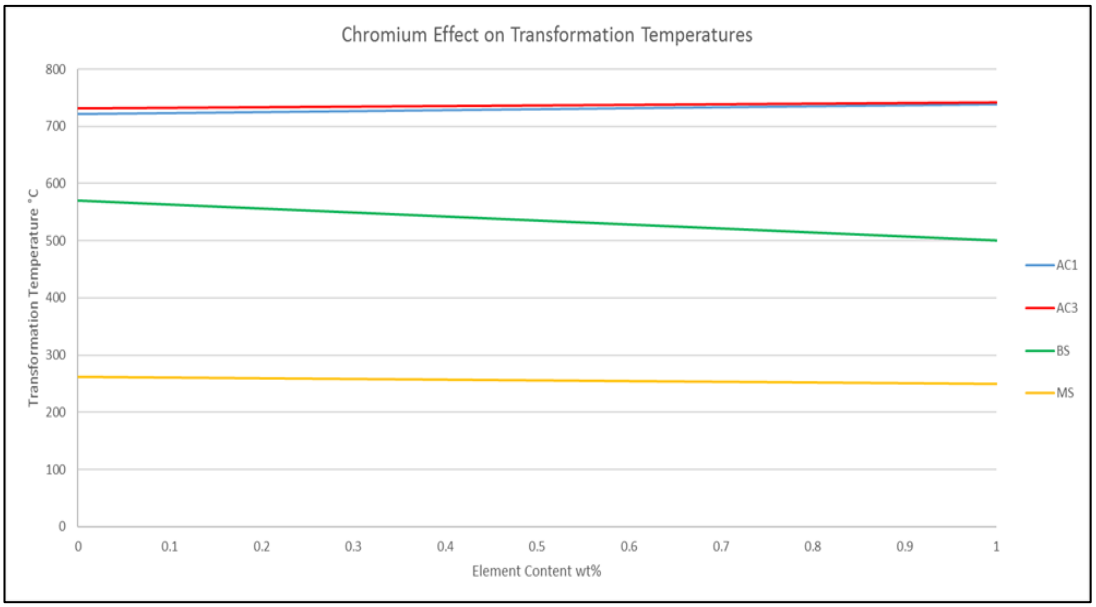

Figure 6-24: Effect on the Transformation Temperatures (% difference) for Different Cr% Contents

From analysing the effects of the various elements on the transformation temperatures; maximum and minimum temperature ranges were plotted, using the worst-case element data from the as received bars - Reference Table 6-3.

Values which do not form part of the calculation for that respective transformation temperature, are noted as N/A within the table.

Table 6-3: Calculated Max / Min Transformation Temperatures for the As-Received Material with different elemental weight %.

		C%	Si%	Cr%	Mn%	Mo%	Temperature °C
Ac1	Highest	0.58	0.51	1.62	0.95	N/A	755.05
	Lowest		0.28	0.64	1.1	N/A	730.19
Ac3	Highest		0.51	1.62	0.95	1.73	822.01
	Lowest		0.28	0.64	1.1	0	741.96
Bs	Highest		N/A	0.64	0.95	0	543.10
	Lowest		N/A	1.62	1.1	1.73	317.41
Ms	Highest		0.28	0.64	0.95	0	253.01
	Lowest		0.51	1.62	1.1	1.73	221.80

From Table 6-3, one of the most important temperatures is the austenisation completion temperature, Ac3. At this temperature, all the ferrite has transformed into austenite and any carbides present have been dissolved into the crystal. During the investigation, the austenization temperatures were 1500°F (815°C), 1515°F (824°C), 1550°F (843°C), 1570°F (854°C), 1585°F (863°C), 1600°F (871°C). Examining the 1500°F and 1515°F hold temperatures, it is apparent that these may not be high enough to convert all the ferrite to austenite, if the worst case chemical composition is to be taken. This could result in small areas of ferritic material owing to the high alloy content. However, the scale of this will be minimal, since the hold period is much greater than the worst case austenisation start temperature, Ac1.

Table 6-3 also highlights the large range in which bainite transformation could start with varying chemical composition. With the maximum start temperature of 543.1°C and a minimum of 317.41°C the difference between these two is approximately 226°C. From approximating that the bainite finish temperature is 120°C below the start temperature it is entirely possible for incomplete transformation to occur, or for the overcooling of the steel leading to the formation of martensite.

To fully understand the effect of the chemical composition variability and to validate the theory developed within this section, the work of Saunders et al was examined [34 - 38]. The research considered the development of a model that could provide both TTT & CCT diagrams for alloy steels. This was accomplished through the creation of empirical formula [34].

This provided an opportunity to determine the effect of the combined chemical compositions of high alloyed zones (bands) and that of the lower alloyed matrix in terms of their respective TTT diagram.

To produce an actual TTT diagram for these respective phases, an excel model was created using the formulas presented within this section for Ac1, Ac3, Bs. Bf, Ms & Mf. These provided the key transformation temperatures for the model however, the formula presented by Saunders et al provided the information required to make the respective shape of the curve [34].

$$\tau_F = \frac{60.\%Mn + 2.\%Ni + 68.\%Cr + 244.\%Mo}{6\times 2^{N/8}\Delta T^3 D_F} I$$

$$\tau_P = \frac{1.8 + 5.4(\%Cr + \%Mo + 4.\%Mo.\%Ni)}{6\times 2^{N/8}\Delta T^q D_P} I$$

$$\tau_B = \frac{(2.3 + 10.\%C + 4.\%Cr + 19.\%Mo).10^{-4}}{6\times 2^{N/8}\Delta T^2 \exp(-27,500/RT)} I$$

Where:

$$I = \int_0^x \frac{dx}{x^{2(1-x)/3}(1-x)^{2x/3}}$$

For x=1, x=0

Df & Dp are transformation constants

N = Grain Size

$$D_F = \exp(-23,500/RT)$$

$$\frac{1}{D_P} = \frac{1}{\exp(-27,500/RT)} + \frac{0.5Mo}{\exp(-37,000/RT)}$$

Equation 6-8

where [34]:

- τ_F = transformation of ferrite
- τ_P = transformation of pearlite
- τ_B = transformation of bainite
- ΔT= undercooling below the transformation temperature of ferrite, pearlite & bainite [34]
- I =volume fraction integral [34]

An extract of the Excel model, which uses the specified formula is detailed within Table 6-4. However, prior to inputting the respective elemental analysis for the band and matrix phases, the model was first validated against the work conducted by Saunders et al for a given chemical composition (0.7% C, 0.35% Mn, 0.16% Si, & 3.24%

Ni, 0.96% Cr & 0.06% Mo). Figure 6-25 demonstrates that the model created is equivalent to that developed within the researched literature [34].

Table 6-4 Extract from Excel Model that Creates the Researched TTT Curve

Banitie Calculations				
			Time (seconds)	
Temperature °C	Undercooling °C	Banite Constant	Initial	Final
600.655	262.645	4.13E-05	2.09E-05	1.21E-04
603.655	259.645	4.53E-05	1.95E-05	1.13E-04
606.655	256.645	4.95E-05	1.82E-05	1.06E-04
609.655	253.645	5.41E-05	1.71E-05	9.92E-05
612.655	250.645	5.90E-05	1.61E-05	9.32E-05
615.655	247.645	6.43E-05	1.51E-05	8.76E-05
618.655	244.645	6.99E-05	1.42E-05	8.26E-05
621.655	241.645	7.59E-05	1.34E-05	7.79E-05
624.655	238.645	8.23E-05	1.27E-05	7.37E-05
627.655	235.645	8.91E-05	1.20E-05	6.98E-05
630.655	232.645	9.63E-05	1.14E-05	6.62E-05
633.655	229.645	1.04E-04	1.09E-05	6.29E-05

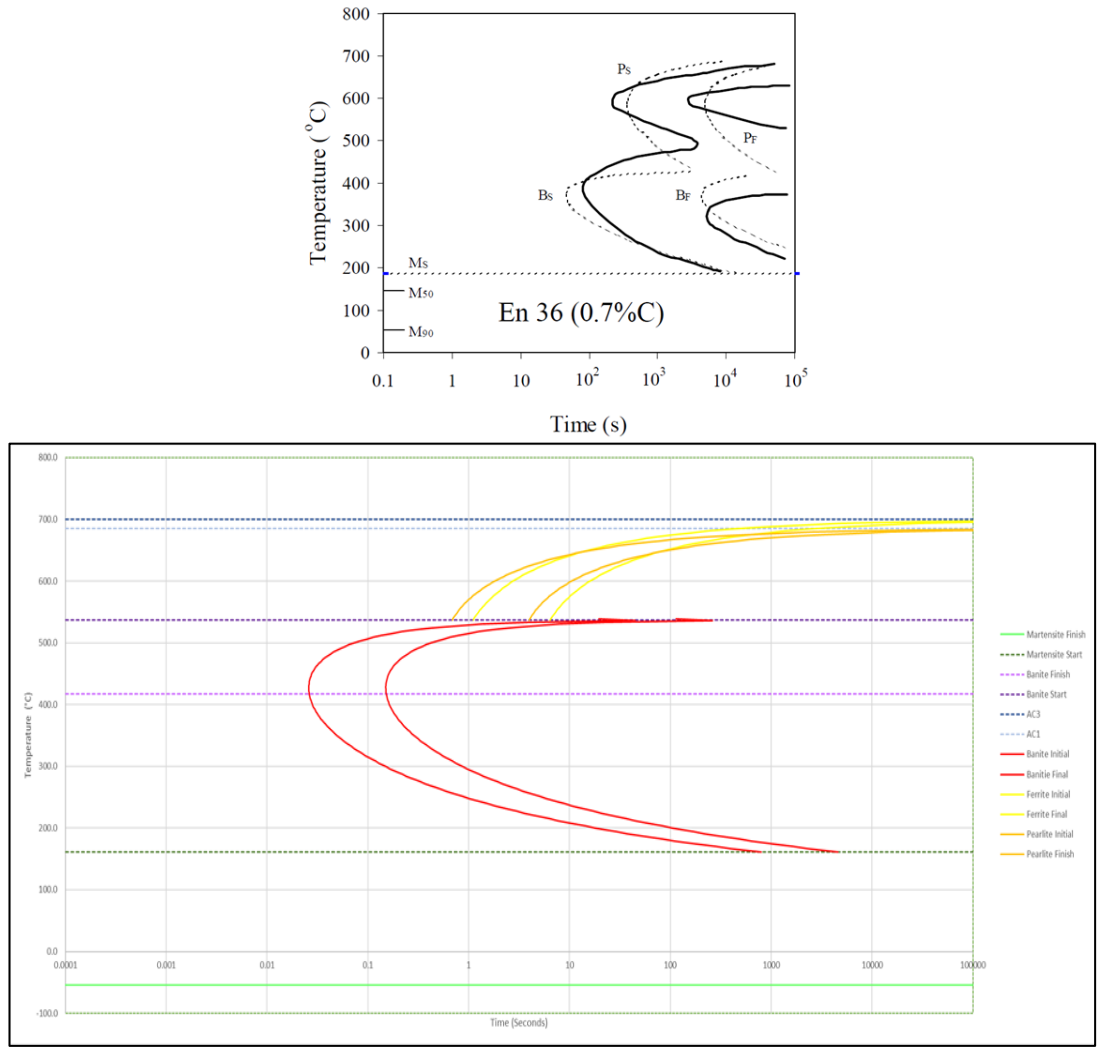

Figure 6-25: TTT Model Validation: Academic Paper (Top) [34] V Excel Model (Bottom)

Although the model was fully validated against the work conducted by Saunders et al [34]; it must be noted that the quench rates specified on the x-axis of figures 6-25, 6-26 and 6-27, are out by 10^3. However, this is based on the calculations specified within the respective authors published literature, which does not contain a correction factor for the TTT curve time axis.

The model was then used to evaluate the TTT curves for the 3.375-inch material for both the band and matrix phases at the core location.

This analysis was conducted to establish the influence of the chemical composition of each respective zone and how it would affect the transformation temperatures and resultant TTT curve.

Figure 6-26 represents the matrix, which exhibits a low alloy composition of C – 0.58% Mn – 0.78% Si – 0.24% Cr – 0.68% Mo – 0 %, with Figure 6-27 displaying the results of an increase in chemistry to C – 0.58%, Mn – 1.31%, Si – 0.46% Cr – 1.07% Mo – 0.76%.

The analysis has established that an increase in the percentage of alloying elements will result in a significant change in the shape and orientation of the respective TTT curve, which subsequently moves to the right. This is in conjunction with changes to the key transformation temperatures, which aligns with the assessed literature [33] (Figure 4-14), and the detailed analysis of the individual elements and their compound effects presented within this chapter - see Figure 6-12 through Figure 6-15.

In summary, an increase in chemical composition has increased the relative Ac1 and Ac3 temperatures, along with a reduction in the Bs and Ms transformation temperature. This information is key for heat treatment operations, especially when heating up to the austenitising temperature and then rapid cooling during the quenching process. Different TTT curves must therefore be considered for each zone / phase across the bar, as their respective position and associated transformation temperature will dictate the resultant microstructure and mechanical properties - see Figure 4-9.

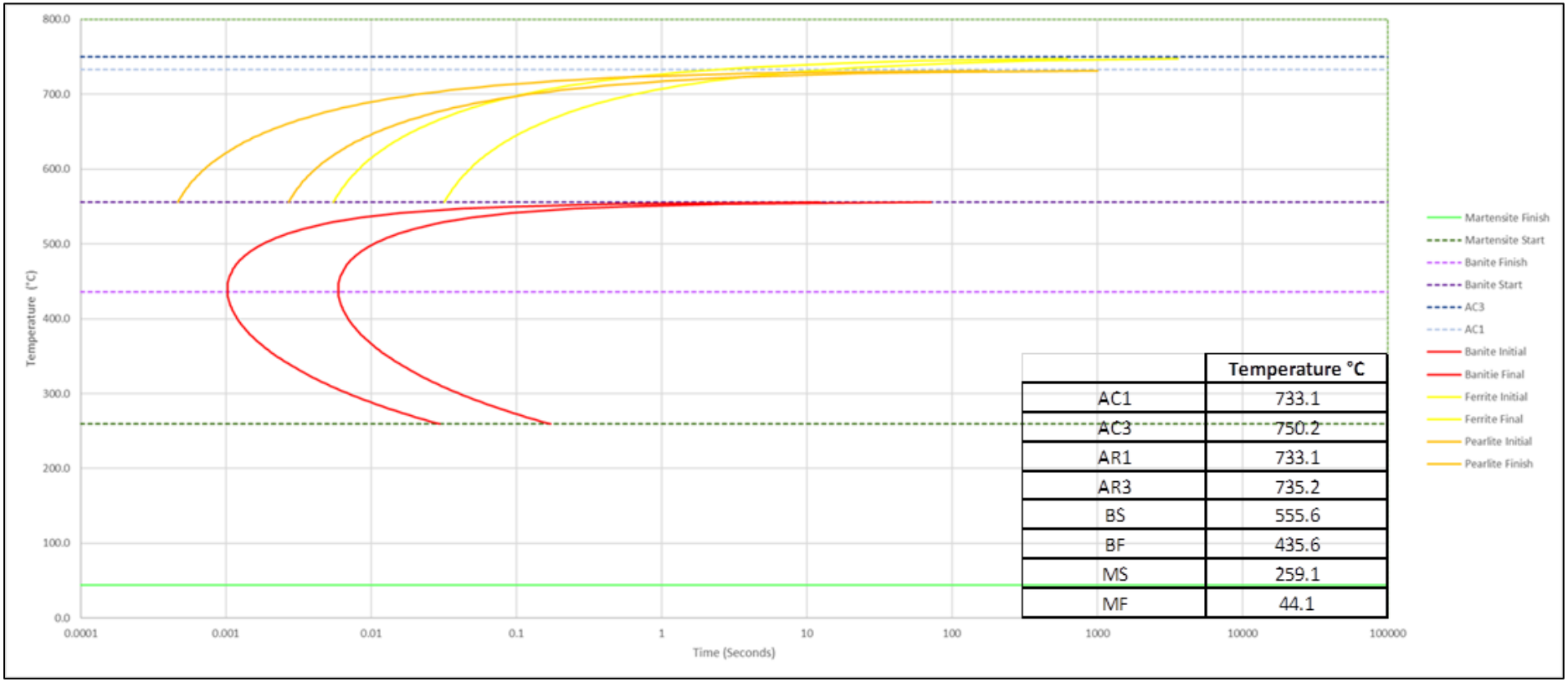

	Temperature °C
AC1	733.1
AC3	750.2
AR1	733.1
AR3	735.2
BS	555.6
BF	435.6
MS	259.1
MF	44.1

Figure 6-26: TTT Curve for 3.375-Inch Bar Core Matrix Location

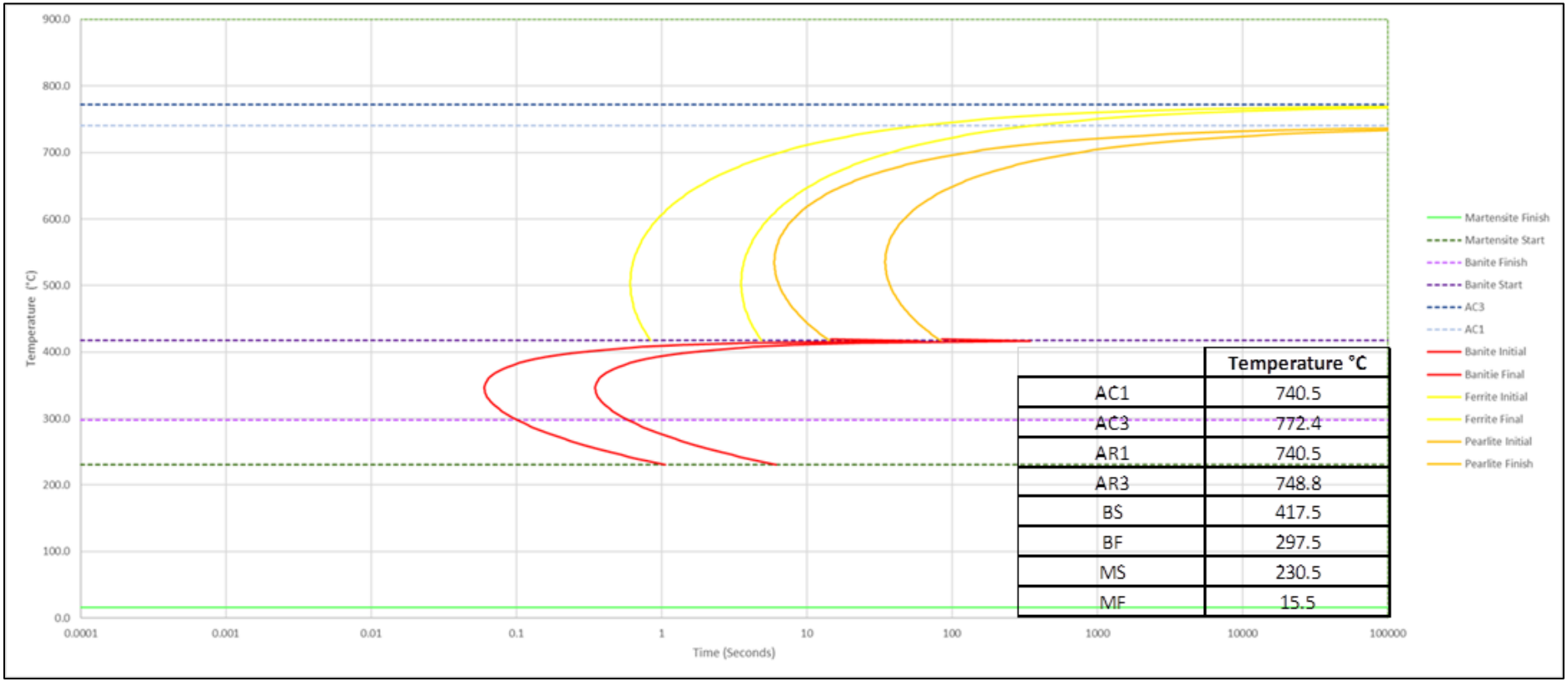

	Temperature °C
AC1	740.5
AC3	772.4
AR1	740.5
AR3	748.8
BS	417.5
BF	297.5
MS	230.5
MF	15.5

Figure 6-27: TTT Curve for 3.375-Inch Bar Core Band Location

6.2.3 Material and Heat Treatment Response

It is clear from the research and experimental study that the AISI 4161H material exists as a duplex form of a matrix / band distribution. These two phases can be considered as separate materials, with different chemical compositions, that react in an unique way when subjected to changes in heat treatment conditions.

The research has shown that the chemical composition effects the respective TTT curve for a given zone within the bar, by changing the isothermal transformation temperatures, and the positioning of the respective curve (Pearlite nose / Bainite chin) - see Figure 6-25. This key attribute in combination of different cooling rates across the bar (core to surface), will determine the resultant microstructure of the material.

But prior to this, one needs to also consider the relative diffusivity of the elements within each zone and their respective position across the bar. The study has established that certain elements are more mobile than others, and the level of diffusion is both temperature and time dependent.

Therefore, the distribution of the %band and %matrix and the respective chemical composition of each phase, will define the resultant properties based on the cross-section of the material and exposure to different heat treatment conditions (time & temperature).

The effect on the chemical composition of the different zones can be clearly seen within the resultant microstructure achieved within chapter 5. The banded zones produced a fully martensitic phase and the matrix exhibiting a combination bainite & martensite in the fully treated quench & tempered condition. This is because the rich chemical zone (bands) move the respective TTT curve to the right allowing the full transformation from austenite to martensite during the subsequent quenching operation (Figure 6-27) [28]. The matrix on the other hand exhibits a low alloy composition (Figure 6-26), which will pull the TTT curve to the left, which results in a CCT curve that crosses the bainite chin prior to passing through the Ms transformation line, producing the mixed phase exhibited by the matrix.

However, different heat treatment conditions (time & temperature), effect the mobility of the elements within the material. Cumulative diffusion rates are higher at the surface compared to the core, therefore the chemical delta composition variability at the surface will be less compared to that at the centre of the material. During the austenitising stage, the surface will enable greater levels of diffusion between the band and the matrix, resulting in lower chemical compositional differences, and similar microstructures. Whereas the core exhibits shorter times where diffusion occurs, which results in the banded zones retaining more of its high elemental chemistry creating a bigger delta between itself and the adjacent matrix (Figure 5-71).

The microstructure in the quenched and tempered condition and the chemical composition delta between the two phases (band & matrix) is the governing factor in the resultant properties of the AISI 4161H material. Not only that, different heat treatment conditions have a major impact on these key attributes, which affect the mechanical properties of the material. The results established that the UTS of the material is directly related to the amount of resultant martensite within the microstructure - see Figure 6-28. However, there are other factors that influence the UTS, such as the austenitising temperature & chemical compositional delta between the band and the matrix.

This is demonstrated by the 2.875-inch Q & T core example (Figure 6-28), where the highest % of martensite was achieved at a quench temperature of 1600°F; however, the greatest UTS was achieved at 1550°F. This is because the ideal diameter delta at the 1550°F was significantly different - see Figure 6-29.

The impact of the delta between ideal diameter of band and matrix on tensile strength is significant, in that a reduction in DI delta increases the tensile strength of the material. This can be explained by considering the 1500°F result, which shows the effect of having the lowest % martensite and highest band/matrix delta. Whereas the 1550°F has the optimum condition of the lowest DI delta and tightest / consistent boxplot in terms of % martensite within the microstructure - see Figure 6-28 and Figure 6-29

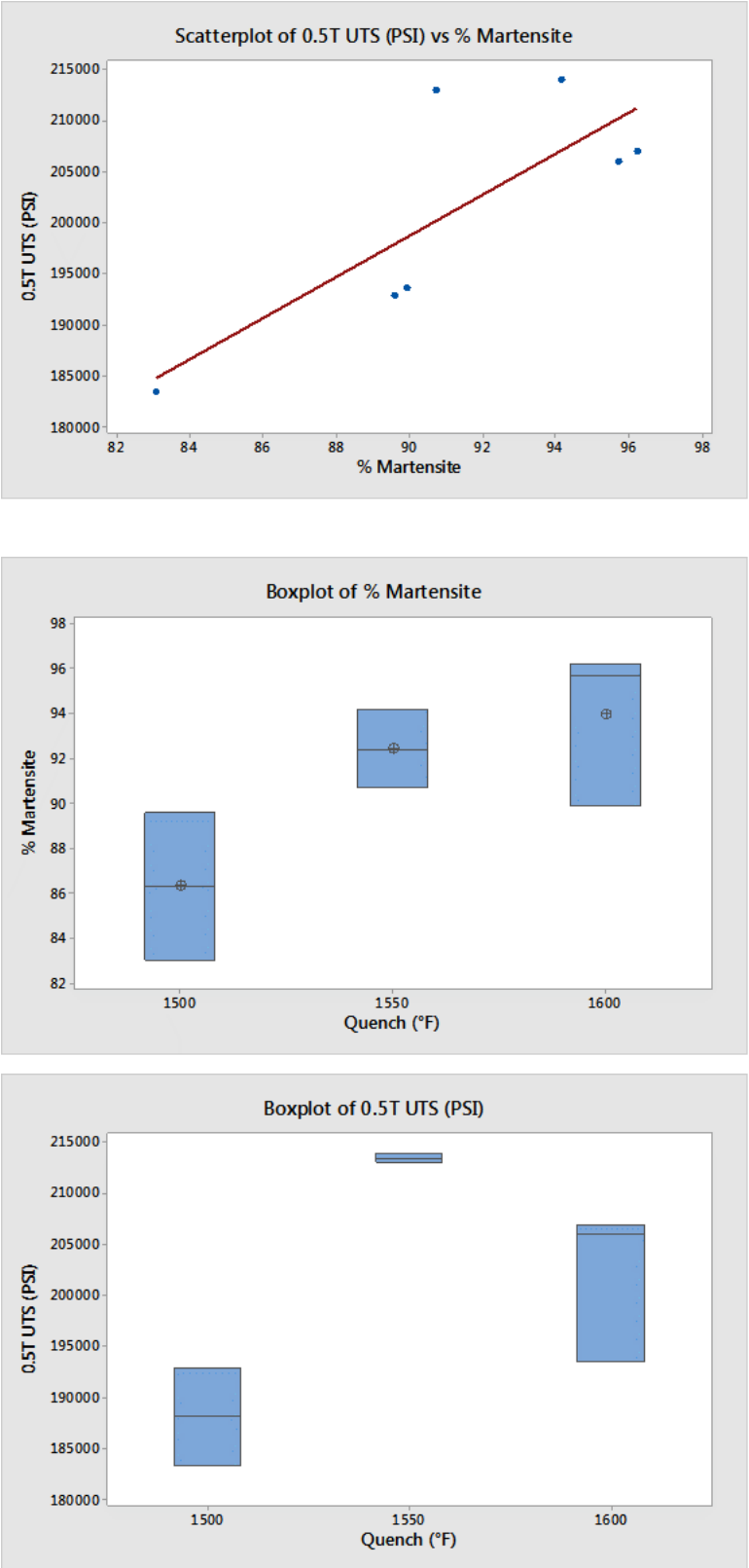

Figure 6-28: 2.875-inch bar - effect of % martensite & Quench temperature on UTS

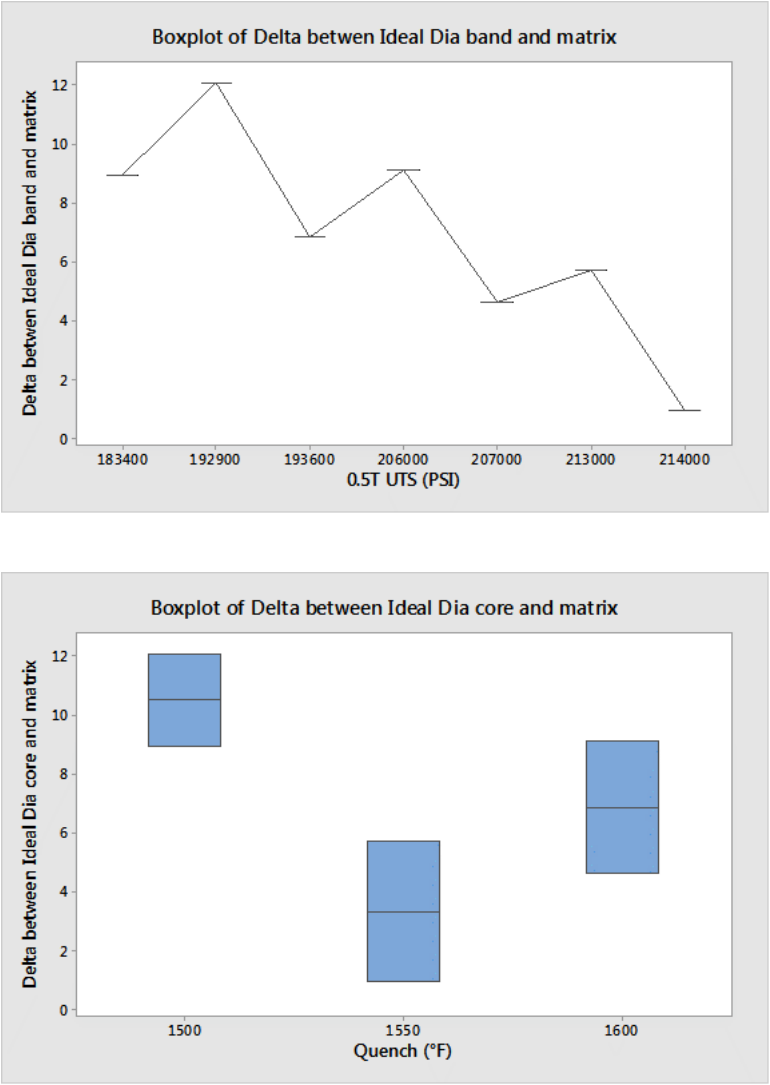

Figure 6-29: 2.875-inch bar - effect of DI delta on UTS (Top) & quench temperature of DI delta (Bottom)

In a comparable way, the tempering temperature has an influence on the % martensite and chemical compositional delta. The box plot of temper temperature against % martensite demonstrates that as the tempering temperature is increased from 790°F to 830°F, the amount of % martensite in the sample decreases - Reference Figure 6-30.

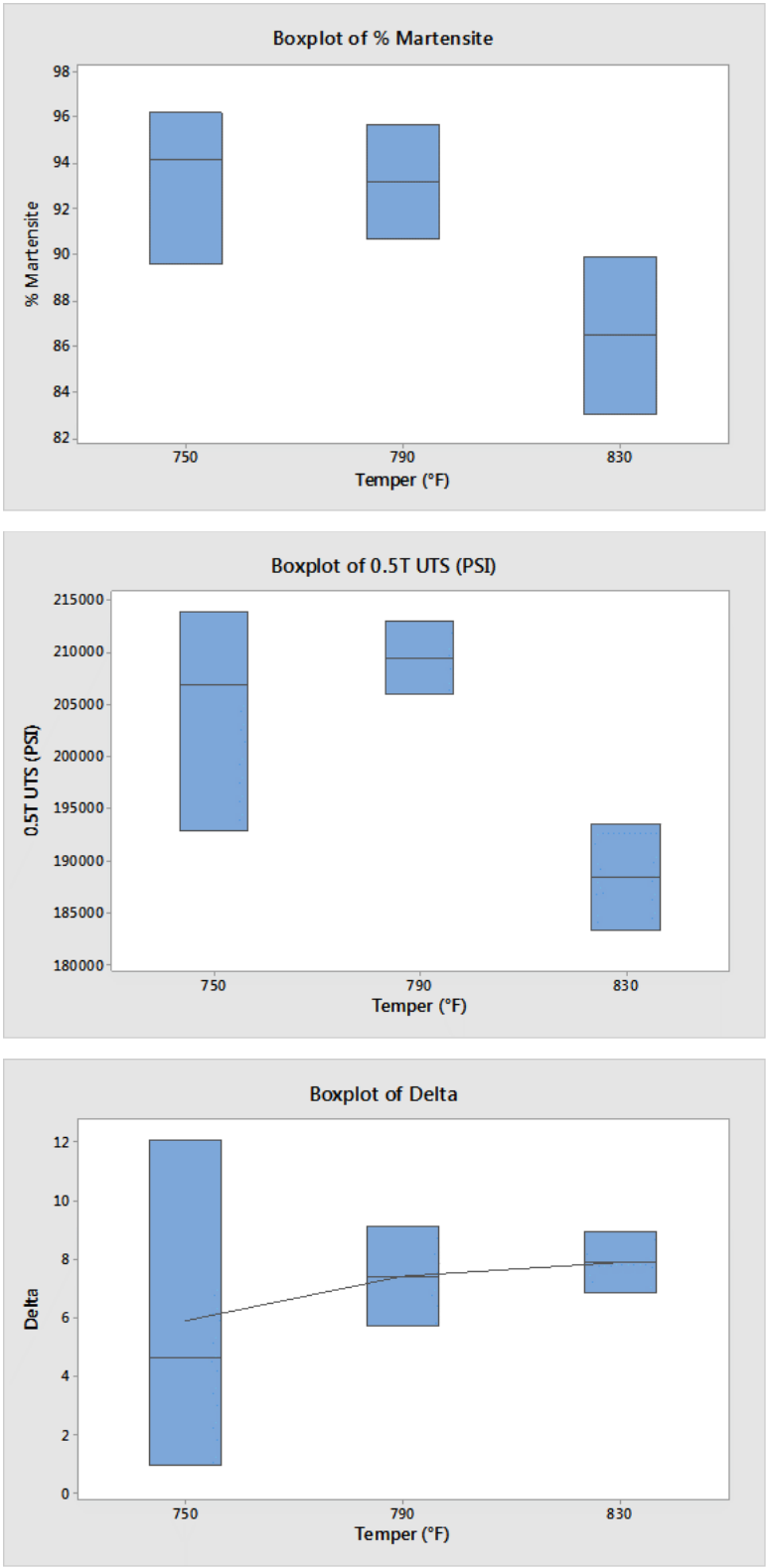

Figure 6-30: 2.875-inch bar - effect of % Martensite & Temper temperature on UTS (Top and Middle) - effect of Tempering temperature on DI delta (Bottom)

This decrease in % Martensite at 830°F leads to a reduction in tensile strength of the material when tempered at this respective temperature - Figure 6-30.
The 750°F and 790°F treatments provide a similar amount of % Martensite however; the variation in tensile strength is greater at 750°F than that of 790°F. The increased variation is due to the increased delta in ideal diameter between band and matrix. Therefore, the optimum conditions for the example selected (2.875-inch diameter - core location) is 1550°F Quench and 790°F Temper, which clarifies and substantiates the graphs and results presented within Chapter 5 - Figures 5-17 to 5-20, Figures 5-27 to 5-28 and Table 5-13.

These findings are significant and help explain the reasons why the AISI 4161H material is not homogenous throughout its sectional thickness and why different heat treatment conditions change the metallurgical properties.
D'Errico & Penha et al [17] [18], confirmed that the degree of banding is influenced by the type and amount of alloying elements; with Krauss [29] highlighting the effect of elemental diffusion, and Kirkaldy et al [23] [24] [25] demonstrating the effect of chemical composition on the key transformation temperatures of the material. However, to date, the literature has not established the extent of material variability and the influences observed on the metallurgical and mechanical properties within bar material used for coil spring manufacture.
The experimental work undertaken herein, has established that a set of optimum conditions can be set in terms of heat treatment temperatures to achieve the engineering desired properties. That is, if the material has the capability in meeting the desired design intent.
The bar material in the fully heat-treated condition, exhibits differences across its thickness, with greater mechanical properties achieved at the ¼T mid-radius compared to the ½T core location. This trend is further verified, when the bar diameter is increased from 2.875-inch to 4.0-inches, where the mechanical properties reduce to values out with the TechnipFMC requirements. However, the trends and results found, can be used to set limitations of the material, which is not currently known by industry, where homogeneity is presumed throughout.

The tensile results align well with the surface hardness values achieved, especially in the quenched and tempered condition, where the smaller bar diameter experienced the greatest surface and through-thickness hardness values compared to the thicker materials [9]. As for the through-thickness results, they highlighted the effect of the different heat treatment operations on the resultant values, with the As-Cooled (normalised) conditions producing lowest values, followed by the Quench and Temper results, and finally the As-Quenched, which achieved the highest values.

The effect of heat treatment was further verified through the detailed assessment of the matrix and band, in terms of the resultant delta of the two phases exhibited during both micro hardness and chemical composition (Ideal Diameter) assessment. This clearly established that the hardness delta between the 2 phases increased from the surface location to the core, irrespective of bar diameter - see Figure 5-57. However, the delta changed when exposed to different heat treatment operations, with the Air Cooled (Normalised) condition yielding values of 26.8 HRC, and the Q and T process achieving typical values of 11.1 HRC (2.875-inch core location).

The work also established that there was one predominant phase that was changing more compared to the other, which was the matrix. During the heat treatment trials, the matrix was the phase that changed in terms of resultant hardness, thus creating the delta between the microstructural bands. This aligns with the microstructural results, where the matrix phase in the Q & T condition changes. The percentage of the Bainite phase within the matrix increases from the surface to the core, thus reducing the amount of martensite. This would therefore create a hardness delta between the rich chemical composition band, which contains elements such as Mo & Cr (Carbide formers) that produce a hard martensite phase and the now depleted adjacent matrix. The effect of the delta would therefore reduce, as movement is made towards the surface where a more uniform chemical compositional balance is present between the matrix and band phases.

The heat treatment processes have shown to have a major influence on the resultant ideal diameter and chemical composition of the analysed material. The experimental approach has demonstrated that the As-received material in the hot rolled condition can change significantly when exposed to different processes such as Air Cool (Normalise), Quench (Austenitise) and Quench & Temper. It has also confirmed that the banded zones are rich in chemistry, which are more prone to change (reduce in alloy content) during subsequent heat treatment operations. However, this is dependent of the diffusion coefficient and the time at temperature of the respective element and location within the bar.

In summary, the experimental and literature research has established that the AISI 4161H material will contain centre line segregation from the raw material Mill and continuous casting process. This will subsequently be dispersed during the hot working process, which will re-align the segregation as elongated bands parallel to the rolling direction. The as-received material will not be homogenous, but in fact a duplex form, containing two phases across the full thickness of the bar.

Both phases shall contain different chemical compositions, which will result in different relative elemental diffusion rates across the material thickness. This will have a direct influence of the critical transformation temperatures and respective TTT / CCT curve during subsequent heat treatment operations, which is responsible for the resultant metallurgical and mechanical properties of the material.

The study has established that the properties vary across the respective bar thickness however; the variability can be altered and influenced by exposing the AISI 4161H material to different heat treatment conditions.

7 COIL SPRING FUNCTIONALITY

7.1 Effects on Material Variability on the Coil Spring Functionality

From the experimental study and the results presented, it is important to understand what effect a heterogeneous material will have on the operation of a functional coil spring. It is also essential to understand the forces that act on the current design in terms of stress distribution in a homogenous state and as hybrid material that consists of metallurgical variability across its respective thickness. To examine the impact on the component, two design approaches are considered:

- Classic Analytical
- Finite Element Analysis

7.1.1 Classical Analysis

Helical compression springs on the macroscopic scale, provide an axial load proportional to the mechanical deflection from the free height. This is until the spring solid height is reached. For close coiled helical springs (pitch angle 'α' is small), the curvature effects have traditionally been neglected during practical spring design [39]. Assuming homogeneous, isotropic material properties; the stress distribution across the bar diameter of a helical compression spring under axial loading reaches a maximum at the bar's inside diameter (ID). The maximum shear stress at this location is approximately given by the formula depicted below [40], where K is the Wahl correction factor, F is the axial load, D is the coil diameter and d is the bar diameter.

$$\boldsymbol{\tau_{max} = K\left(\frac{8FD}{\pi d^3}\right)}$$

Equation 7-1

On closer inspection of the coiled bar, there are several components of stress induced which superimpose to provide the spring's load during axial deflection. These components are detailed within Figure 7-1 and defined by Case et al [41]. Only circular cross sections are considered in this analysis.

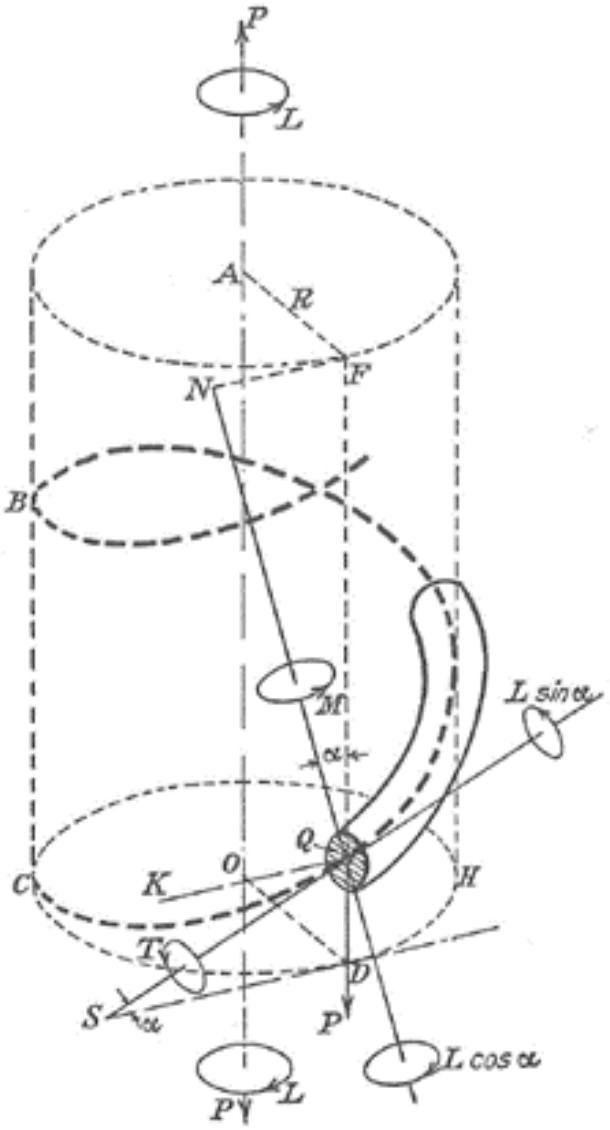

Figure 7-1: Loading Actions at a Section of Helical Spring [41]

Assuming the ends of the spring are free to rotate (for example, in a subsea linear actuator where compression springs are typically mounted on a thrust bearing), the components of stress are reduced to four (4). Using approximate theory [39], the remaining components of stress can be described in terms of the Axial Load 'P', the bar radius 'r', and the pitch angle 'α' - see Figure 7-2.

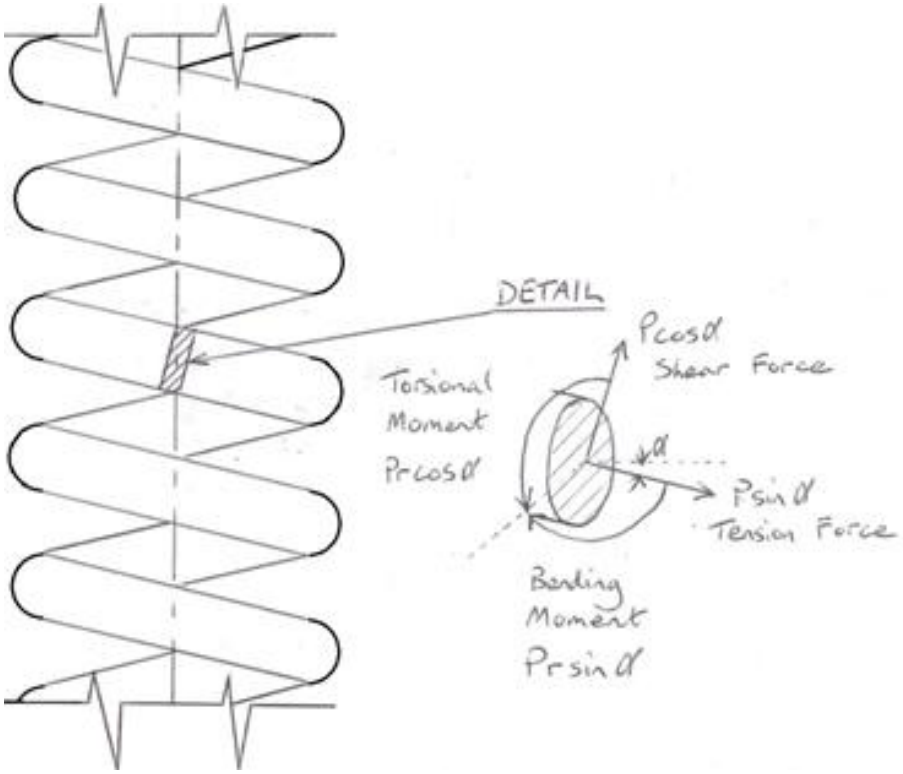

Figure 7-2: Helical Spring subject to Axial Load 'P' with Ends Free to Rotate; Approximate Loading Components

An exact, close form, analytical solution to the stress distribution across a ‘thin slice’ of helical spring was proposed by Ancker and Goodier [42] [43] [44]. This derivation assumes uniform circular cross section, and equal loading conditions on every cross-section along the bar length. The resulting formulae facilitates the calculation of the components of stress at any point across the thickness of a helical spring. The solution is in the form of an iterative series. Ancker and Goodier’s formulas [42] [43] [44] are still considered current, fitting measured data more closely than the original equations proposed by Wahl [45].

W.G. Jiang et al [46] conducted FEA on a variety of helical spring designs. Using a 2D ‘thin slice’ method they determined the stress distribution across the bar thickness and compared the results with those predicted by Ancker and Goodier. W.G. Jiang et al [46] established a correlation between FEA and analytical solutions when the pitch angle ‘α’ and the ratio bar dia. / coil dia. ‘d/D’ were considered. The results of the stress distribution of the homogenous coil slice sections are detailed within Figure 7-3 [46]. This is a visual display of the level of resultant stress distribution in relation

to an axial force bring applied over four (4) separate scenarios - relationship of changing the bar diameter (d) with the mean coil diameter (D) and the respective pitch angle (α).

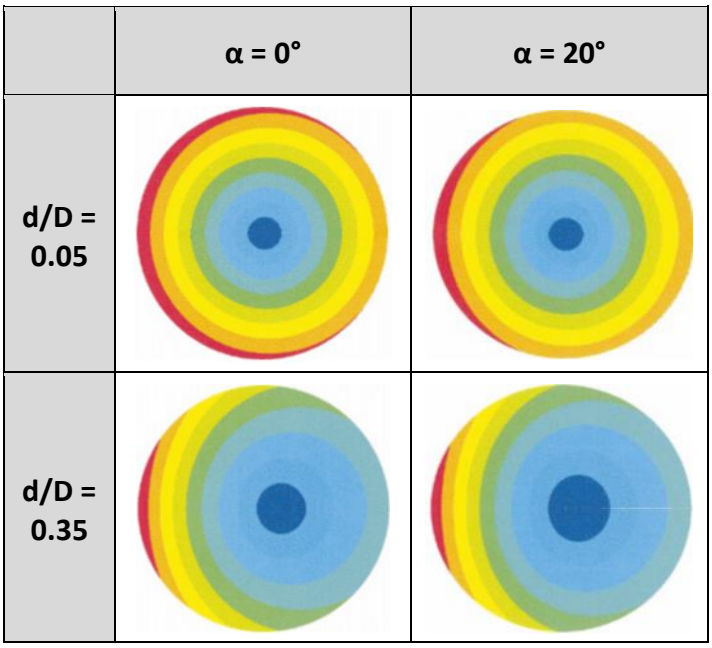

Figure 7-3: Representative Stress Distribution through the Helical Spring Cross Section [46], ID Shown on Left

Whilst no data has been collected to quantify the variation of the elastic or shear moduli with heat treatment conditions and bar diameter; it follows that if the material strength changes as a function of radius, then so will the elastic properties. Assuming that the elastic properties reduce towards the centre of the bar, and that the coiled spring is required to resist the same loading as an equivalent homogeneous material, then the material in the core will respond with a lower stress for the same strain. It follows that the stress distribution through the cross section will tend to increase towards the OD and decrease towards the centre.

To make an approximate analytical model to determine the effect of changing mechanical properties, the following simplifying assumptions are made:

- The torsional moment is the only component of stress considered in the analysis.
- The Shear Modulus (G) of the material varies linearly as a function of radius.

In a helical spring, the torsional moment is given by:

$$T = \frac{FD}{2}$$

Equation 7-2

where F is the spring axial load and D is the coil diameter, as depicted within Figure 7-4

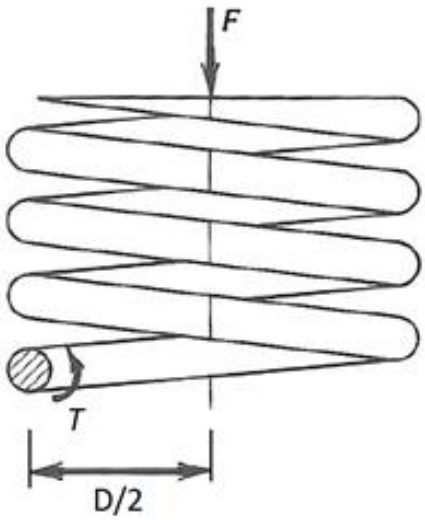

Figure 7-4: Free Body Diagram Showing Torsional Resistance to Axial Load at an Arbitrary Section of the Coil Spring

For the remainder of this analysis, the bar is considered a straight section under a pure shear torque of magnitude FD/2. Through the bar cross section, the modulus of rigidity (Shear Modulus), G, is assumed to vary linearly as a function of radial distance:

$$G = \left(\frac{G_{outer} - G_{Core}}{r}\right).a + G_{Core}$$

Equation 7-3

where G is the shear Modulus; a is the radial distance from bar centre, G-outer and G-core are constants representing the shear modulus at the bar surface and core; r is the radial distance when a=surface.

Using a method similar to that devised by Gere and Timoshenko [47], the Torque induced in the bar is in equilibrium, and may be split into a sum of individual torques (dT) resisted by small circumferential elements - see Figure 7-5.

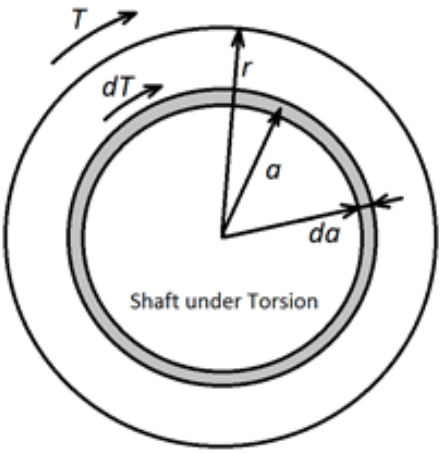

Figure 7-5: Circumferential element resisting torsion [47]

$$dT = Area_{element} \,.\, Lever\ Arm \,.\, Shear\ Stress$$
$$dT = 2.\pi.a.da \ \ . \ \ a \ \ . \ \ \tau$$
$$dT = 2\pi\tau a^2 da$$

Equation 7-4

where dT is the torque resisted by the circumferential element; τ is the shearing stress induced; a is the radial distance to the element from bar centre, da is the element radial 'width'.

The shear stress τ induced due to torsion in the element is given by:

$$\tau = aG\theta$$

Equation 7-5

where θ is the angle of twist per unit meter (Radians / meter), and is constant under static loading. θ can be determined for a given loading condition using Engineer's simple torsion formula:

$$\theta = \frac{T}{GJ} = \frac{FD}{2GJ} = \left(\frac{D}{2GJ}\right)F$$

Equation 7-6

Using the definition of G:

$$\tau = a\left(\left(\frac{G_{outer} - G_{Core}}{r}\right).a + \ G_{Core}\right)\theta$$

$$\tau = \left(\frac{G_{outer} - G_{Core}}{r}\right)\theta a^2 + G_{Core}\theta a$$

Equation 7-7

Therefore, the shear stress induced varied in a quadratic fashion with radial distance, rather than linear, as would be the case for a homogeneous material. Using the relationship dT=2πτa^2 da allows an integral to be determined, thus summing the torques resisted by the circumferential elements.

$$dT = 2\pi\left(\left(\frac{G_{outer} - G_{Core}}{r}\right)\theta a^2 + G_{Core}\theta a\right)a^2 da$$

$$dT = 2\pi\theta\left(\left(\frac{G_{outer} - G_{Core}}{r}\right)a^4 da + G_{Core}a^3 da\right)$$

$$\int 1\, dT = 2\pi\theta\left(\left(\frac{G_{outer} - G_{Core}}{r}\right)\int_0^r a^4\, da + G_{Core}\int_0^r a^3\, da\right)$$

$$T = 2\pi\theta\left(\left(\frac{G_{outer} - G_{Core}}{r}\right)\frac{r^5}{5} + G_{Core}\frac{r^4}{4}\right)$$

$$T = \frac{\pi}{2}r^4\theta\left(\frac{4}{5}(G_{outer} - G_{Core}) + G_{Core}\right)$$

Equation 7-8

where T is the total torque resisted by the shaft.

It is noted that if G-outer = G-core = G then the expression becomes:

$$T_{Homo} = \frac{\pi}{2}r^4\theta G$$

Equation 7-9

Since $\frac{\pi}{2}r^4$represents the polar moment of area, J, the expression once again describes engineer's torsion theory.

To summarize, if the bar must support the same torsional loading, the elastic stress response through the bar diameter with varying mechanical properties takes the form shown in Figure 7-6. This assumes the Shear Modulus varies linearly as a function of radial distance.

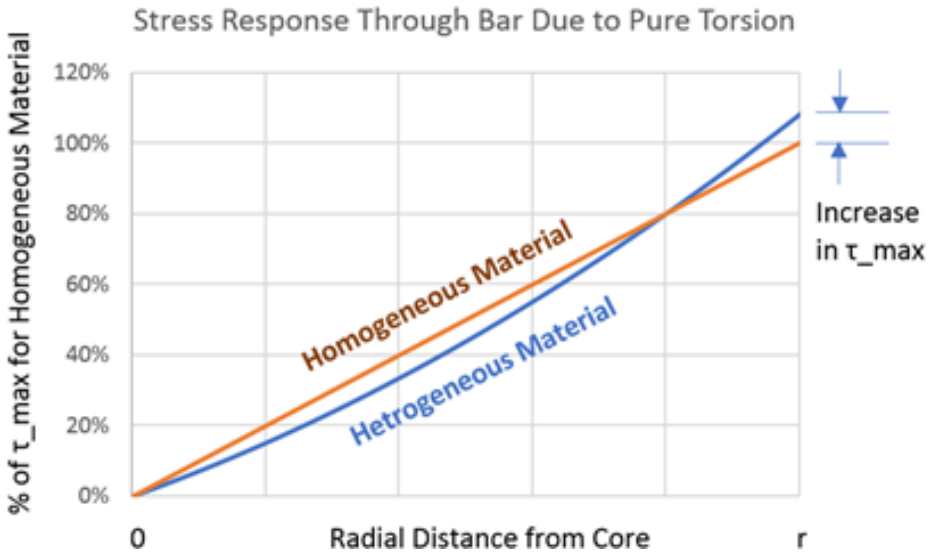

Figure 7-6: Comparison of Stress Distribution between a homogeneous and heterogeneous bar in pure torsion

Where the increase in maximum shear can be plotted against the fraction of Shear Modulus in the Core, to that on the surface - Reference Figure 7-7.

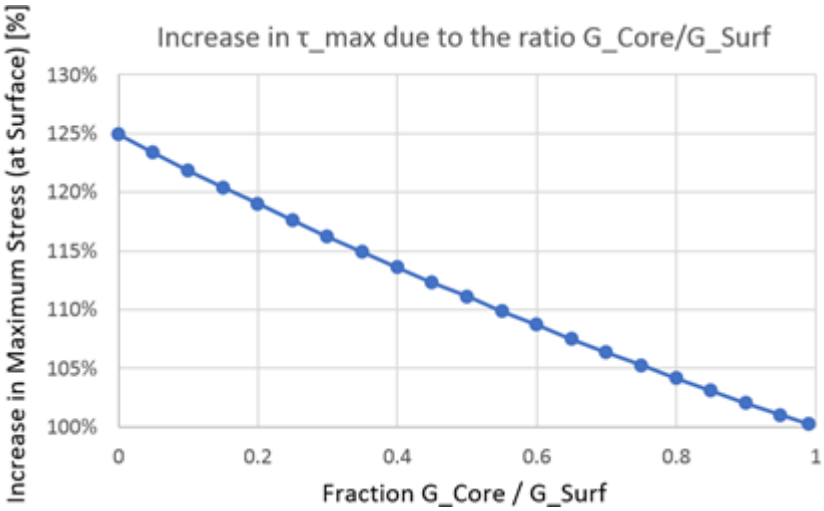

Figure 7-7: Increase in Maximum Stress due to Changing Mechanical Properties through the Bar Diameter

Within this evaluation, no account has been made for plastic deformation at the most highly stress point in the coil spring. Out with the pre-setting operation, helical springs are generally designed to operate within the elastic range.

To simplify the problem the loading conditions other than torsion were neglected. Therefore, to account for the changing yield strength, and hence the plastic strain induced during deflection, a comprehensive FEA study detailing the repercussions of the research published herein, has been performed, see Section 7.1.2.

7.1.2 Finite Element Analysis of Coil Springs

FEA was conducted to determine what affect the different mechanical properties would have on the functionality of an operational coil spring. This approach fits in well with research presented within this thesis, as typically FEA is only conducted on a material that is considered to have homogenous properties throughout its complete cross-sectional thickness.

To investigate the effects of a material, which has through thickness variability in terms of mechanical and metallurgical properties, three FEA models were considered for a coil spring.

- Hybrid bar (Condition 1, 2 and 3) - where three regions across the bar section have different mechanical property conditions - Table 7-2.

The purpose of the hybrid bar was to base a model on the mechanical properties of the ½T core results of the 3 bars combined in the final Quench and Tempered condition. This mindset was to try and create one material type with known mechanical properties at set distances from the surface. By using 3 different sets of conditions, this would simulate the changes exhibited by a hybrid 4-inch bar having concentric properties within one material type - Reference Figure 7-8.

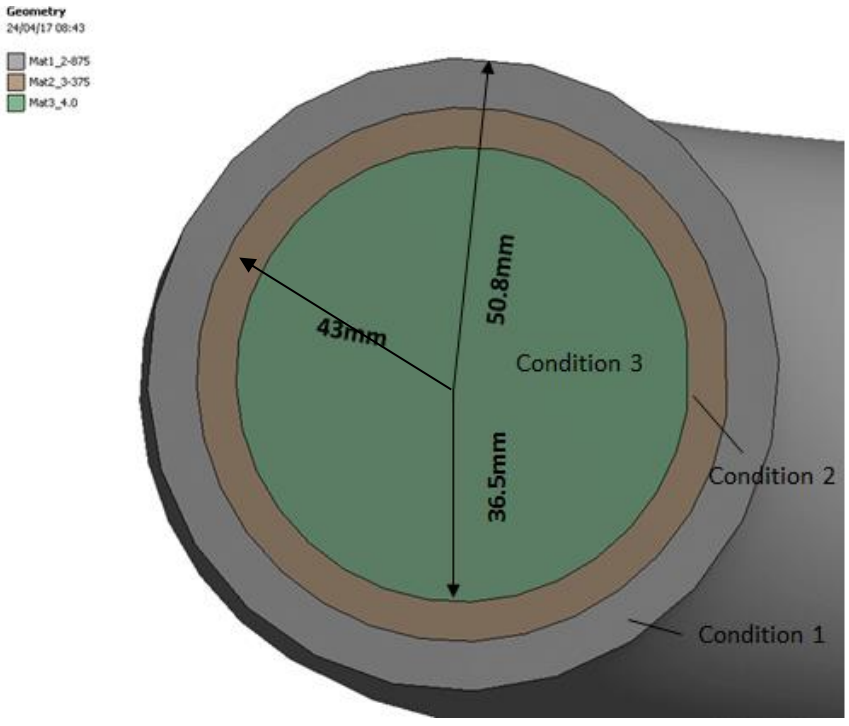

Figure 7-8: Hybrid bar created from three (3) different material types

- 4 -inch Homogenous bar (Condition 3) - material properties are consistent throughout the material thickness - Table 7-2.

The purpose of modelling the homogenous bar, was to create a simulation based on the current set up that industry utilise for FEA analysis. This would act as a datum and be based on uniform mechanical properties throughout the cross-section of the coil spring - Reference Figure 7-9.

- Optimised bar (Condition 3 & 3b) - where the material has two different regions across the bar thickness at ¼ & ½T - Table 7-2.

The purpose of the optimised bar model, was to base a simulation on the actual values achieved for the 4.0-inch material in the fully heat-treated condition - Reference Figure 7-9.

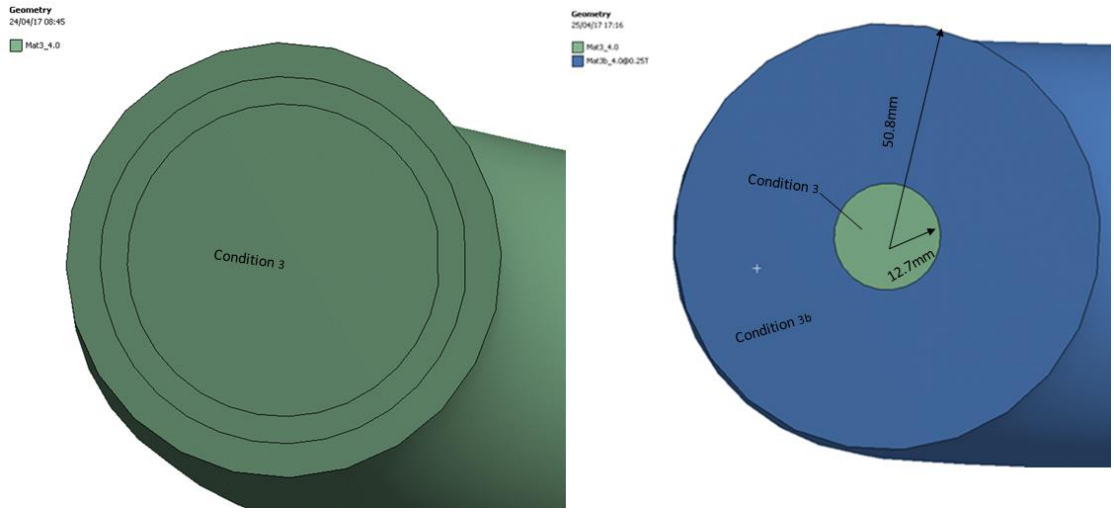

Figure 7-9: Homogenous bar (uniform properties) left & Optimised bar (2 different properties) right

The dimensions of the model were based on the TechnipFMC 4.0-inch coil spring design [30], which are summarized within Table 7-1 & Figure 7-10.

Table 7-1: Dimensions Utilized for the FEA Analysis

Parameter	in	mm
Mean diameter of coil	21.125	536.6
Wire Diameter	4	101.6
Free Length	52.647	1337.2
Pitch	9.346174	237.4

Load step	Description	Applied displacement (compressive)	
		in	mm
1	Compress to preload length	10.15	257.73
2	Compress to minimum working length	19.28	489.79

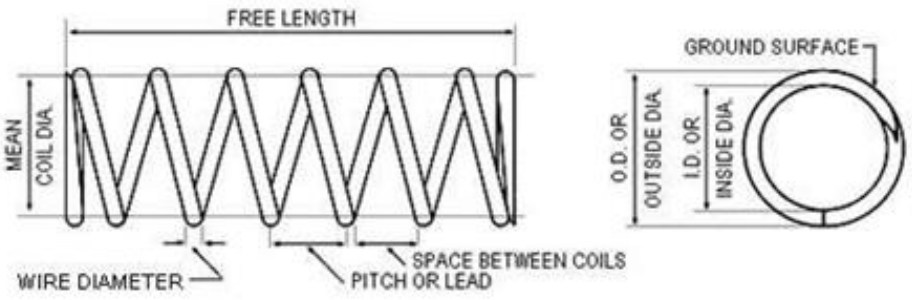

Figure 7-10: Drawing view of key dimensions

The finite element model represents the free length of the spring plus one-half inactive coil. Compression of the spring was modelled by a longitudinal displacement applied evenly across the diameter of this inactive coil, representing the design working stroke of the spring. The other end of the spring was fixed in all degrees of freedom (Figure 7-11). The commercial FEA software ANSYS 17.1 Workbench was used for the analysis.

The model was then meshed using higher-order (20-noded) hexahedral brick elements throughout (ANSYS element Solid186). A mesh density was chosen to give 32 elements around the circumference and an aspect ratio less than three along the length of the spring (Figure 7-11). This mesh density was checked and found to give a converged result.

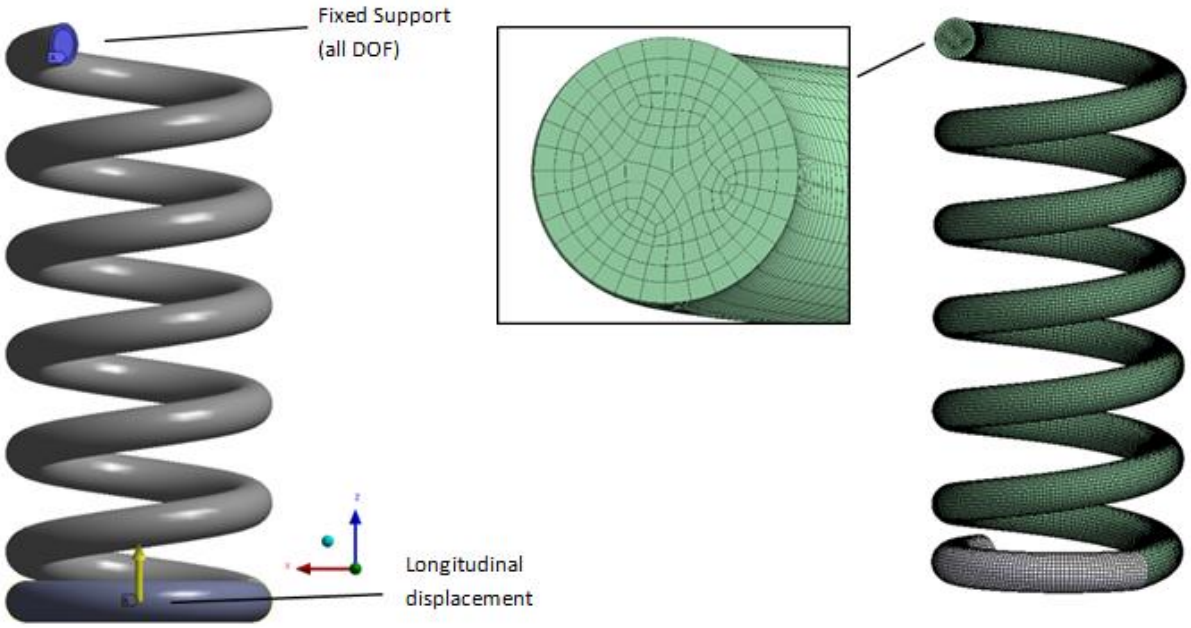

Figure 7-11: (Left) Spring Displacement / Load Conditions (Right) Finite Element Mesh

Prior to conducting the FEA analysis, True stress strain curves were generated using the data detailed within Table 7-2 The values specified within Table 7-2. are the actual mechanical properties exhibited during the tensile test DoE for the 3 bar sizes in the Quench and Tempered condition. Also, the elastic modulus (Young's modulus) generated from the physical testing was included within the data set.

Elastic-plastic stress-strain curves were then generated (Figure 7-12) from the data in Table 7-2. using the method specified in ASME VIII-2 Annex 3.D [53], which fits a power-law curve through the specified yield strength and ultimate strength (UTS).

The elastic modulus was taken as 207 GPa in each case. Perfectly plastic behaviour was assumed from the end of the generated curve up to a true strain of 0.2.

These material curves were then applied to specified regions of the spring model cross-section, which enabled the following three cases to be analysed - see Table 7-2 & Figure 7-12:

- Hybrid bar - Incorporates conditions 1,2 & 3
- Homogenous bar - Incorporates condition 3 only
- Optimised bar - Incorporates condition 3 & 3b

Table 7-2: Mechanical Properties Taken for DoE & Optimised for FEA

Condition	Bar size	Location	Boundary radial distance		Yield Stress	UTS	Yield Stress	UTS	True UTS
	in		in	mm	PSI	PSI	MPa	MPa	MPa
1	2.875	½T - Core	1.4375	36.5	183,900	216,800	1267.9	1494.8	1637
2	3.375	½T - Core	1.6875	42.9	162,600	191,000	1121.1	1316.9	1440
3	4	½T - Core	2	50.8	148,600	187,500	1024.6	1292.8	1464
3b	4	¼ T - Mid-radius	0.5	12.7	160,000	196,700	1103.2	1356.2	1517

The results of the FEA have shown that the three models exhibit different behaviours. It can be concluded that the composition of the coil (degree of variability across its sectional thickness) has a direct effect on the force response, stress distribution and level of plastic strain exhibited.

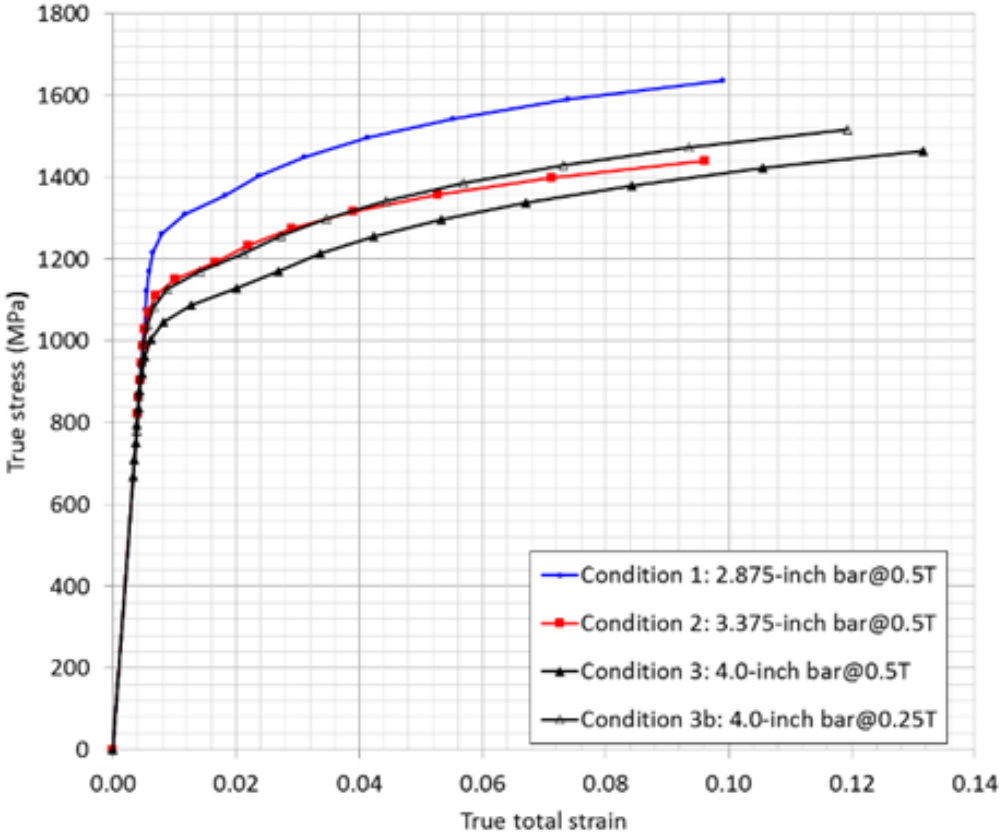

Figure 7-12: True stress strain curves generated for FEA from optimised properties using ASME VIII-2 Annex 3.D [53]

Figure 7-13 shows the difference is reaction force achieved once the individual coils are displaced axially beyond 325mm. The resultant graph clearly shows that the

homogenous condition produces the lowest force, with the hybrid bar delivering a higher KN value over the same level of spring displacement. This suggests that the hybrid material is indeed stiffer compared to the other model / material types.

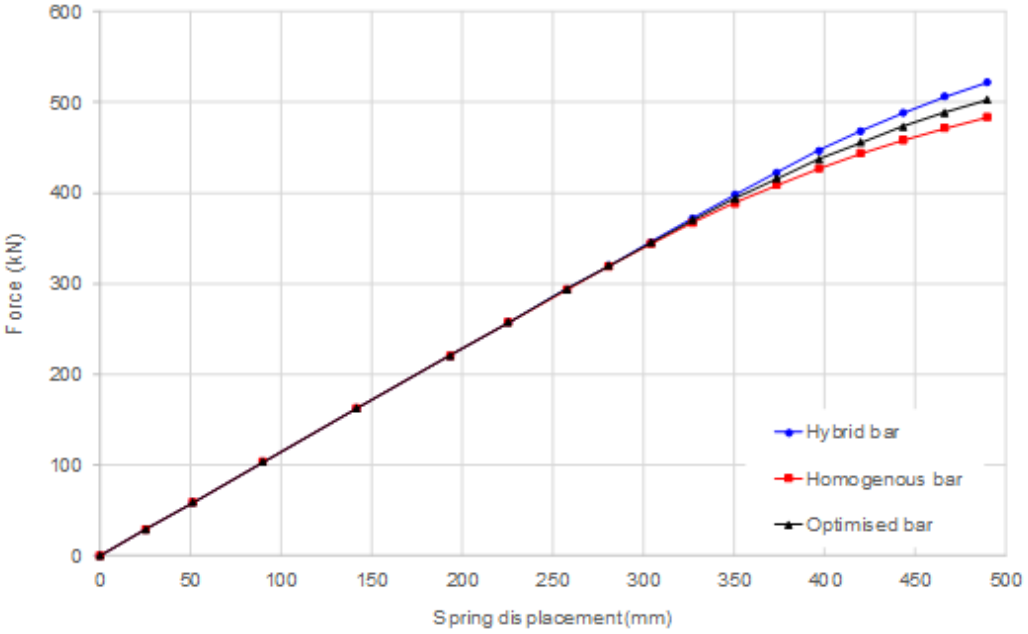

Figure 7-13: Axial Force Exerted by the Compressed Spring - Three Models

To understand the difference in behaviour in more detail, the equivalent stress & plastic strain at full compression were modelled for each mode of coil spring - see Figure 7-14 and Figure 7-15.

The FEA established that the stress distribution is different for all 3 conditions; with the hybrid model exhibiting the highest levels of stress over a greater area of the coil spring - see Figure 7-14 and Figure 7-15.

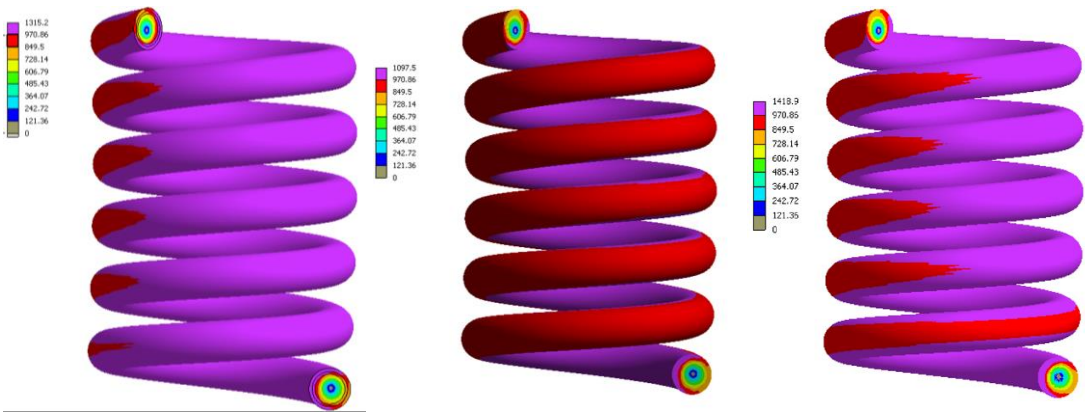

Hybrid Bar Homogenous Bar Optimised Bar

Figure 7-14: Equivalent stress (MPa) at full compression for all conditions

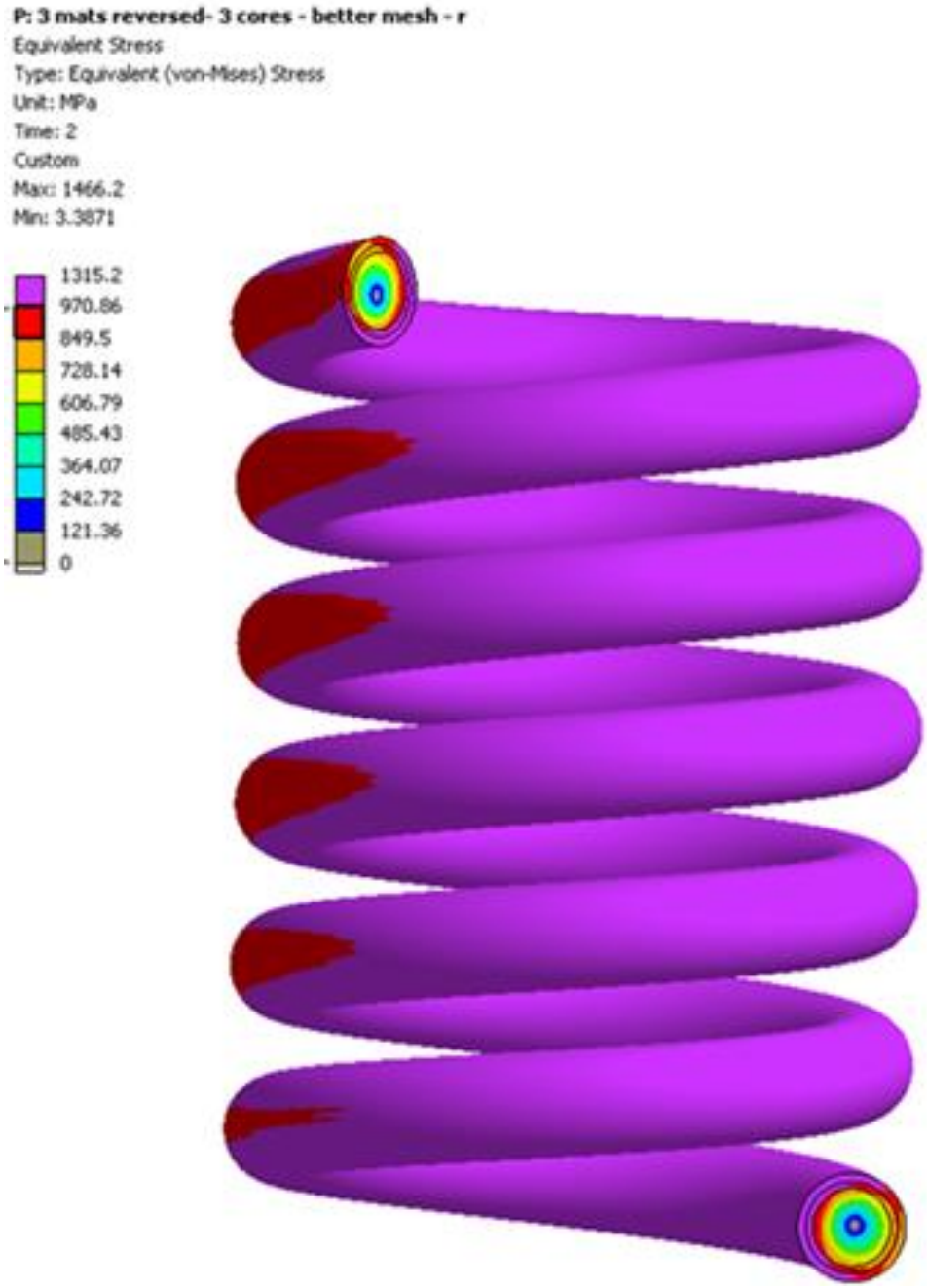

Figure 7-15: Detailed view of the Hybrid bar - Equivalent stress (MPa) at full compression

It can also be concluded that there is a difference in the predicted strain and stress distribution between the three models; notably, there is more plasticity in the homogenous bar at full compression than in the other two models see Figure 7-16 and Figure 7-17.

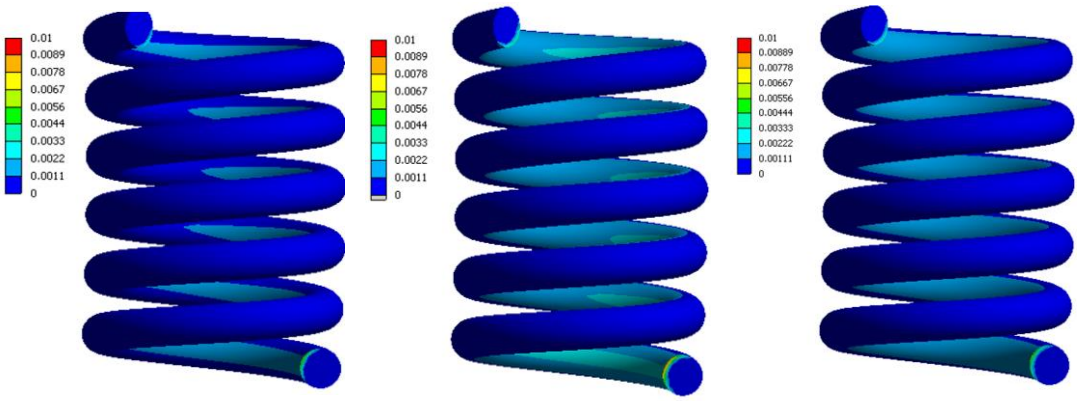

Hybrid Bar Homogenous Bar Optimised Bar

Figure 7-16: Equivalent plastic strain at full compression

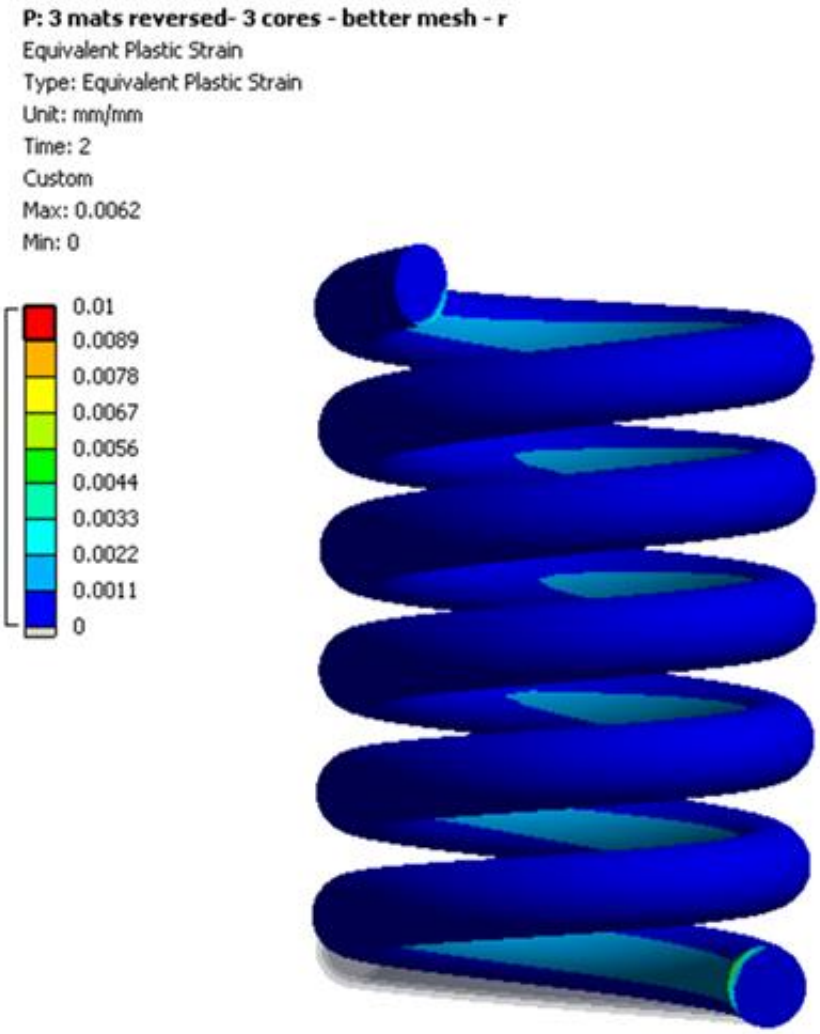

Figure 7-17: Detailed view of the Hybrid bar - Equivalent plastic strain at full compression

Figure 7-18 shows the development of this plastic strain as the spring is compressed; the cases begin to diverge after about 225 mm compression (i.e. as the "working preload level" is approached). The results establish that the homogenous bar exhibits more plasticity.

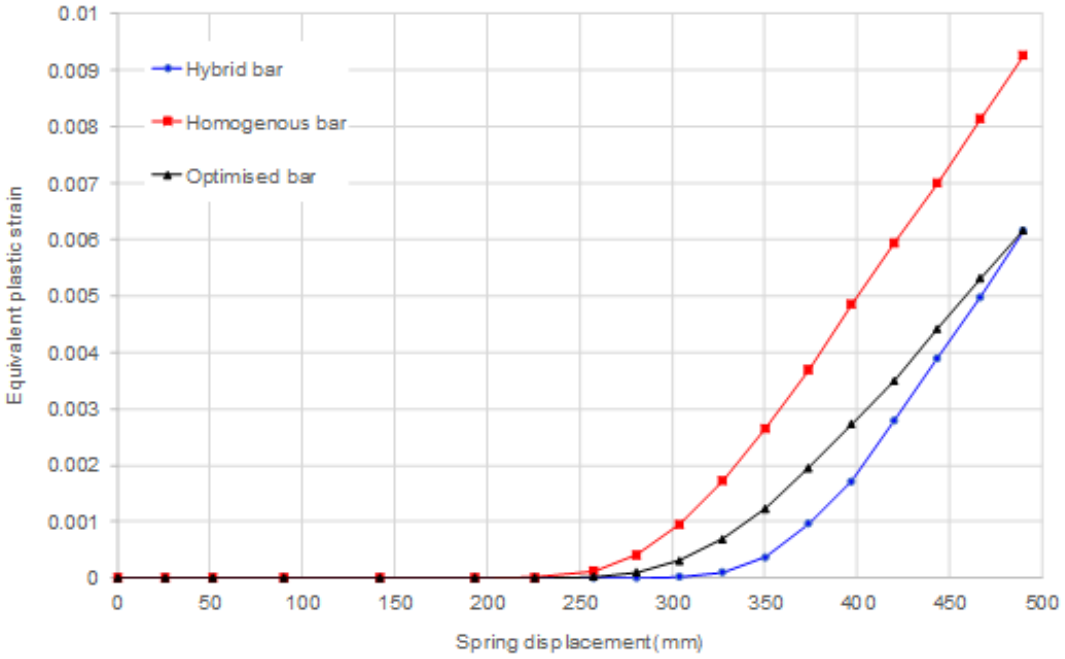

Figure 7-18: Equivalent plastic strain over the full spring displacement

Examination of the material data in Figure 7-18 shows that the material in condition 3, (used for the core of the hybrid and optimised bars but for the entirety of the homogenous bar), has a notably lower yield strength than the other conditions; which explains the greater plastic strain in model 2 - Figure 7-16.

It is suggested that this plasticity (permanent deformation) can be related to the slightly lower reaction force calculated for that model.

The FEA has demonstrated that different heat treatment conditions, and the consequent changes in mechanical properties over different regions of the bar, can result in a measurable effect on the mechanical behaviour of the spring. Specifically, there is a change in the longitudinal / axial force, which the actuator spring can exert during its ability to function.

7.1.3 Analysis Summary

The analysis has shown that the stresses acting on the coil spring will change due to the material variability exhibited throughout the bar thickness. As the material strength changes as a function of radius, this will affect the elastic and plastic properties when the coil is compressed axially.

The work established that the AISI 4161H material will respond differently in relation to the exhibited properties through its respective cross-section. There is a marked difference in a homogenous material to one that is considered a hybrid; with the hybrid displaying greater compressive loads at higher stress levels and reduced plasticity over the operating coil spring displacement range.

8 CONCLUSIONS AND RECOMMENDATIONS

8.1 Introductory remarks

The main objective of this work was to investigate the reasons why the AISI 4161H material used for coil spring applications exhibited variability in terms of both metallurgical and mechanical properties. It was also to establish the effects of various heat treatment operations and conditions, and the characterisation of the resultant properties including the impact on the coil spring design and functionality. These key findings would enable engineers to work within the limitations of the material for subsea applications. The conclusions and recommendations are summarised within this chapter.

8.2 Experimental Investigation - Material

An extensive design of experiments study has established that the material used for coil spring manufacture namely, AISI 4161H, is not homogenous throughout its cross-sectional thickness. Instead the material (ranging between 2.875 - 4.0 inches) comprises of a duplex form, of both a banded zone and matrix.

This material can therefore be considered as heterogeneous, with variability exhibited from the surface to the core of the bar. The variability appears as two separate zones (band & matrix), which contain differences in chemical composition and resultant microstructure, which have a direct influence on the metallurgical and mechanical properties of the material.

However, the variability across the bar section, changes from the surface to the core, with a reduction in material strength, and an increase in the chemical composition and hardness delta between the two phases (band & matrix) exhibited.

The variability within the coil spring can be altered by subjecting the material through different heat treatment operations (Air Cool - Normalise / Quench / Quench and Temper) and by processing the bar at different temperatures and time.

The chemical compositional differences between the two respective zones, result in concentric islands of different material, which respond contrarily due to their

elemental content, which has a direct influence of the key transformation temperatures and respective TTT / CCT curve. This in conjunction with different diffusion rates, produces a material with mixed metallurgical properties.

Therefore, the AISI 4161H material does not follow the traditional homogenous academic literature, where straight lines and linear comparisons exist for changes in both Austenitise (Quench) and Temper conditions. Instead the material will respond under optimum conditions, which considers the duplex material, and associated variability.

This thesis has demonstrated that optimum conditions can be met through the creation of a heat treatment (Quench / Temper) model, which characterises the material properties, and determines the limitations of each bar size. This is required by engineers, for current and future designs, that utilise low alloy steel bar stock.

Appendix E, summarises the key effects of the material variability, which can be used for engineering clarity when designing subsea coil spring components.

8.3 Functionality Investigation - Coil Spring

Based on the experimental evidence, it is apparent that the mechanical properties within the coil spring are not homogenous. To understand this effect, two concept models were analysed, a classic analytical model and a computational model.

Initially a mathematical derivation was performed to vary the elastic properties through the cross section to simulate a heterogenous stress distribution.

The analytical model established that an increase in maximum stress would occur when the shear modulus reduces towards the centre of the bar cross section. It also established a theoretical stress distribution through the cross section of a heterogenous bar, where the shear modulus varies linearly as a function of radius. This distribution can be directly compared with a homogeneous bar by assuming the same overall torsional load is resisted.

However, to create a more representative model that quantifies the effect of changing mechanical and metallurgical properties through the bar cross section, FEA was employed. This model considered all components of stress acting through the

compressed helix. The model was used to determine the induced axial load of the coil, even as plastic deformation is considered through the strata of the coiled bar.

The FEA has demonstrated that different heat treatment conditions, and the consequent changes in mechanical properties over different regions of the bar, can result in a measurable effect on the mechanical behaviour of the spring. Specifically, the axial force, which the actuator spring can exert during its ability to function.

There is a marked difference in a homogenous material to one that is considered a hybrid (three different sets of material properties across its section); with the hybrid displaying greater compressive loads at higher stress levels and reduced plasticity over the operating coil spring displacement range.

8.4 Standards and Industry Recommendation

The work conducted and presented within this thesis has found that the governing standards for coil spring manufacture (ASTM / BS EN) only consider the material in a homogenous form, with uniform properties throughout. This does not take into consideration the material in the raw form and the effect different heat treatment conditions have on its resultant properties. This is applicable for both metallurgical and mechanical (FEA) standards.

In addition, industry standards do not mandate adequate testing requirements that can assess for the effects of material variability. Instead they prescribe minimum metallurgical assessment criteria, which does not consider the material strength and through thickness properties.

It is recommended that:

- A technical paper and or journal is created to make industry aware of the duplex type material, which is produced for coil spring manufacture.
- The respective governance standards include tensile testing with set minimum requirements. A test location of ¼T should be mandated for this purpose.
- Raw material mills consider using Rotary Continual Casting machines, as these will help disperse the centreline segregation produced during bar production.

- Hot working / forging reduction ratio is set at a minimum of 10:1, as this will disperse the segregation and reduce chemical compositional variability throughout the material cross section.
- All FEA models for coil spring application, consider models with materials that have concentric properties, to accurately predict how the part will behave under operational conditions.
- TechnipFMC remove the specification governance that limits a 5 HRC hardness delta between the band & matrix phase at the surface location. This requirement is not sustainable for bars with dimensions > 2.875 inches.

8.5 Further Work

Further research is needed at the raw material source, where the initial centreline segregation manifests. A detailed study on the different types of continuous casting methodology would be beneficial, as this would help determine the best technique and input parameter conditions that would reduce the chemical compositional variability throughout the material.

Another aspect of work would be to create a study on the effect of putting in a reheating step after the continuous casting process. This would assess the effect of heating the billet at various soaking temperatures and times, to encourage the diffusion of the elemental segregation prior to hot rolling.

Finally, it would be worthwhile examining and analysing other material types that have less of a tendency in forming segregation, such as a material with a lower carbon content. This is because the diffusion coefficients of many elements are higher in ferrite than in austenite. Therefore, higher carbon steels such as AISI 4161H are disadvantaged from the outset.

9 REFERENCES

[1] S. MacIntyre, "Design Guideline, Valves - Actuators, Helical Compression Springs", TechnipFMC., Dunfermline, DGL20026224, 2013.

[2] "Design Guidelines", Institute of Spring Technology., Sheffield, 2016.

[3] M. Hayes, "Pre-stressing", Institute of Spring Technology., Sheffield 2016.

[4] C.H. Simmons, D.E. Maguire, N. Phelps, "Manual of Engineering Drawing", 3rd ed, Elsevier Ltd, Oxford, UK, 2009, ch 2, pp. 225-232.

[5] "AISI 51B60H & 4161H High Strength Steels, E3 Generation Coil Springs, Non-H_2S Compatible", TechnipFMC., Houston, M20905, 2015.

[6] S. Louhenkilpi, "Continuous Casting of Steel", in *Treatise on Process Metallurgy*, vol 3, Elsevier, 2014, pp. 373-434.

[7] Mechanical Engineering, "Hot Working of Metals", Dec 2011. Available: sainsmechanical.blogspot.com/2011/12/hot-working-of-metals.html

[8] D. R. Askeland *et al*, The Science and Engineering of Materials, 6th ed, Stamford, Connecticut, 2011.

[9] "Heat Treating", American Society of Metals International Handbook, vol 4, Materials Information Company, USA, 1991.

[10] "Quenching of Steel", American Society of Metals International Handbook, vol 4, Materials Information Company, USA, 1991.

[11] Mark Hayes, "Heat Treatment Problems", Institute of Spring Technology., Sheffield 2016.

[12] B. R. Kumar *et al,* "Premature fatigue failure of a spring due to quench cracks," Materials Characterization Division, National Metallurgical Laboratory, Jamshedpur India, Nov 2009.

[13] D. H. Herring, "A Discussion of Retained Austenite", March 2005. Available: IndustrialHeating.com

[14] G. V. Voort, "Martensite and the Control of Retained Austenite", Vac Aero International Inc.

[15] "Tempering of Steel", American Society of Metals International Handbook, vol 4, Materials Information Company, USA, 1991.

[16] K.B. Lee *et al,* "On Intergranular Tempered Martensite Embrittlement," Department of Metallurgy & Materials Engineering, College of Engineering, Kookmin University Seoul – November 8 1994.

[17] F. D'Errico, "Failures Induced by Abnormal Banding in Steels", Journal of Failure Analysis & Prevention, vol 10, Oct 2010

[18] R. N. Penha, J. Vatavuk, A. A. Couto, S. A. de Lima Pereira, S. A. de Sousa, Lauralice de C.F. Canale - "Effect of chemical banding on the local hardenability in AISI 4340 steel bar", Journal of Engineering Failure Analysis, April 2015

[19] BS EN 13906-1:2002, "Cylindrical helical springs made from wire and bar – Calculation and design", Part 1: Compression springs
[20] P.S. Valsange, "Design of Helical Coil Compression Spring", International Journal of Engineering Research and Applications, vol 2, issue 6, pp.513-523.
[21] Rockford Spring, "Relaxation of Springs". Available www.rockfordspring.com/relaxation-of-springs
[22] Y. Prawoto, M. Ikeda, S.K. Manville, A. Nishikawa, "Design and failure modes of automotive suspension springs", Feb 2008
[23] J.S. Kirkaldy *et al,* "Hardenability Concepts with Applications to steel," eds. J.S. Kirkaldy and D.V. Doane, (Warrendale, PA: AIME, 1978),82.
[24] C. Zener, "Kinetics of decomposition of austenite" *Trans.AIME*, vol 167, pp. 550-595, 1946.
[25] M. Hillert, "Role of interfacial energy during solid-state phase transformations," *JKA*, vol 141, pp 757-789, 1957.
[26] W. Steven and A.G. Haynes, "The Temperature of Formation of Martensite and Bainite in Low Alloy Steels," *J. Iron and Steel Inst.*, vol 183, pp. 349-359, 1956.
[27] Andrews, K.W, "Empirical Formulae for the Calculation of Some Transformation Temperatures", Journal of the Iron and Steel Institute, 203, Part 7, July 1965, pp. 721-727.
[28] N. Saunders, Z. Guo, X.Li, A.P. Miodownik and J.-P. Schille, "The Calculation of TTT and CCT diagrams for General Steels".
[29] G. Krauss - Solidification, Segregation, and Banding in Carbon and Alloy Steels, 2003.
[30] "Design Specification", TechnipFMC., Dunfermline, SPC1008424, 2014
[31] Hiroyuki Nitta, Kensuke Miura, Yoshiaki Iijima - Self-diffusion in iron-based Fe–Mo alloys; 2006.
[32] Smithells Metals Reference Book, 7th ed., Butterworth-Heinemann, Oxford, 1992.
[33] Technische Universität Graz, Mehran Maalekian, "The Effects of Alloying Elements on Steels" (I); October 2007.
[34] N. Saunders, Z. Guo, X. Li, A.P. Miodownik & J.-P. Schille, "The Calculation of TTT and CCT diagrams for General Steel"; October 2007.
[35] J.S. Kirkaldy, B.A. Thomson, and E.A. Baganis, Hardenability Concepts with Applications to Steel, eds. J.S. Kirkaldy and D.V. Doane, (Warrendale, PA: AIME, 1978), 82.
[36] C. Zener, "Kinetics of decomposition of austenite" *Trans.AIME*, vol 167, pp. 550-595, 1946.

[37] M. Hillert, "Role of interfacial energy during solid-state phase transformations," *JKA*, vol 141, pp 757-789, 1957.
[38] J.S. Kirkaldy, "Diffusion-controlled phase transformations in steels. Theory and applications," *Scand. J. Metall.*, vol 20, pp. 50-61, 1991.
[39] A. M. Wahl, *Mechanical Springs*, 2nd ed, McGraw-Hill, 1963.
[40] R. F. "Neathery, "Statics and Applied Strength of Materials", Wiley. 1985, pp 494-499.
[41] J. Case and A. H. Chilver, “Strength of Materials and Structures”. London, Edward Arnold, 1971. pp. 335.
[42] C. J. Ancker and J. N. Goodier, “Pitch and Curvature corrections for helical springs”. ASME Journal of Applied Mechanics, 25, 1958, pp. 466-470.
[43] C. J. Ancker and J. N. Goodier, “Theory of Pitch and Curvature Corrections for the Helical Spring -I (Tension)”. ASME Journal of Applied Mechanics, 25, 1958, pp. 471-483.
[44] C. J. Ancker and J. N. Goodier, “Theory of Pitch and Curvature Corrections for the Helical Spring -II (Torsion)”. ASME Journal of Applied Mechanics, 25, 1958, pp. 484-495.
[45] Wahl "Mechanical Science; Reports by T.S. Bockwoldt and Co-Researchers Describe Recent Advances in Mechanical Science", 2013, Technology & Business Journal, pp. 727.
[46] W.G. Jiang and J.L. Henshall, “A novel Finite element model for helical springs”, Finite Elements in Analysis and Design, 35, 2000. Pp. 363-377.
[47] Gere and Timoshenko [J. M. Gere and S. P. Timoshenko, "Mechanics of Materials", 4th Ed. PWS, 1997, pp 222-225.
[48] SAS Institute Inc, JMP Statistical Discovery TM.
[49] Minitab Inc, Minitab 17TM.
[50] "Irons, Steels, and High-Performance Alloys", ASM Engineers Handbook, 10th ed., vol 1, 1990.
[51] Lean Six Sigma Minitab - The Complete Toolbox Guide for all Lean Six Sigma Practitioners.
[52] ASME VIII, Boiler and Pressure Vessel Code, 2015.
[53] ASME VIII-2, Rules for Construction of Pressure Vessels, Division 2 Alternative Rules, 2015. Annex 3-D.
[54] ASTM A29, Standard Specification for General Requirements for Steel Bars, Carbon and Alloy, Hot-Wrought, 2016.
[55] ASTM A125 Standard Specification for Steel Springs, Helical, Heat-Treated, 2013.
[56] ASTM A255, Standard Test Methods for Determining Hardenability of Steel, 2010.

[57] ASTM 304, Standard Specification for Carbon and Alloy Steel Bars Subject to End-Quench Hardenability Requirements, 2016.
[58] ASTM A689, Standard Specification for Carbon and Alloy Steel Bars for Springs, 1997.
[59] ASTM E112, Standard Test Methods for Determining Average Grain Size, 2013.
[60] ASTM A370, Standard Test Methods and Definitions for Mechanical Testing of Steel Products, 2017.
[61] BS EN 10089, Hot Rolled Steels for Quenched and Tempered Springs - Technical Delivery Conditions. 2002.
[62] Svante Arrhenius, "Worlds in the making microform, the evolution of the universe", Harper, New York; London, 1908.
[63] M. Atkins, "Atlas of continuous cooling transformation diagrams for engineering steels", British Steel Corporation, Sheffield, UK.

10 APPENDICES

List of Appendices

Appendix A: Metallurgical / Mechanical Test Result Data Tables

A1: 2.875-inch bar results

A2: 3.375-inch bar results

A3: 4.000-inch bar results

Appendix B: Additional Micrographs

B1: 2.875-inch bar, as received, as cooled, quenched, quenched and tempered

B2: 3.375-inch bar, as received, as cooled, quenched, quenched and tempered

B3: 4.000-inch bar, as received, as cooled, quenched, quenched and tempered

Appendix C: Residual Plots

A1: 2.875-inch bar results at 0.5T

A2: 3.375-inch bar results at 0.25T and 0.5T

A3: 4.000-inch bar results at 0.25T and 0.5T

Appendix D: Material Certificate of Conformity

D1: Super S® Quench Oil 521

Appendix E: Key Effects of Material Variability

E1: Effect of Increase in Bar Diameter

E2: Effect of Changing Heat Treatment Parameters

Appendix A

Metallurgical / Mechanical Test Result Data Tables

Appendix A1: 2.875-Inch Bar Results

Test Piece	Description					Average Surface Hardness (HRC)									Brinell	Through Thickness Hardness (HRC)					Tensile Test Results						Banding						
						"As received"			"As quenched"			"As tempered"				Location							Y/UTS		Surface Hardness		Delta						
	Material	Heating Temp	Cooling Medium	Quench Temp	Temper Temp	Front End	Middle	Back End	Front End	Middle	Back End	Front End	Middle	Back End		1	2	3	4	5	Yield (psi)	UTS (psi)		Elong (%)	R. of A. (%)	Front End	Back End	10% Dia Ave delta	10 % Dia Dark Ave	10% Dia Light Ave	Mid r Ave delta	Mid r Dark Ave	Mid r Light Ave	Centre Ave delta	Centre Dark Ave	Centre Light Ave
T1	Timken	1700	Air	-	-	38.4	36.0	37.7	32.0	31.9	29.9	-	-	-		30.9	31.4	38.8	31.2	30.9	-	-	-	-	-	-	-	12.8	34.4	47.2	23.4	34.2	57.6	27.2	36.4	63.6
T2	Timken	1800	Air	-	-	38.5	35.7	36.8	30.7	31.0	31.7	-	-	-		28.7	30.2	34.7	29.7	29.4	-	-	-	-	-	-	-	12.0	34.2	46.8	18.4	34.2	55.6	20.4	31.8	58.2
T3	SDI	1700	Air	-	-	34.2	30.9	31.7	30.8	32.4	32.2	-	-	-		27.4	32.7	42.8	33.2	29.3	-	-	-	-	-	-	-	6.6	40.2	46.8	15.8	41.4	57.2	22.4	38.8	61.2
T4	SDI	1800	Air	-	-	38.5	34.3	34.8	33.1	31.3	32.6	-	-	-		28.9	31.1	38.1	32.1	31.3	-	-	-	-	-	-	-	10.6	38.4	49.0	24.2	38.2	62.4	26.8	36.2	62.2
A1	Timken	1800	Oil	1550	790	36.8	34.7	34.0	35.0	32.8	34.0	47.1	46.4	48.3		46.4	45.7	47.0	47.6	47.4	192,000	221,000	0.87	8.2	27.2	47.5	45.0	0.6	49.6	50.2	4.0	46.0	50.0	8.8	43.2	52.0
A2	Timken	1800	Oil	1550	790	38.0	33.2	35.5	39.2	32.2	40.3	49.9	48.4	49.1		47.0	47.0	47.2	46.8	46.1	203,000	228,000	0.89	8.6	28.5	45.9	43.9	4.0	47.0	51.0	6.8	43.6	50.4	5.8	46.2	52.0
A3	Timken	1800	Oil	1550	790	33.9	32.5	31.4	35.2	31.2	35.6	47.7	47.3	49.3		47.3	46.4	47.4	47.1	46.9	178,200	209,000	0.85	10.3	37.0	45.3	45.9	0.8	49.2	50.0	2.9	47.1	50.0	4.9	45.3	50.2
A1a	Timken	1800	Oil	1550	790	29.9	31.0	30.2	-	-	-	47.7	48.3	42.7		46.3	46.3	43.0	44.7	46.2	175,000	207,000	0.85	10.4	29.1	44.5	42.3	1.6	47.8	49.4	1.3	45.8	47.1	7.2	41.6	48.8
A2a	Timken	1800	Oil	1550	790	31.2	30.3	30.9	-	-	-	46.6	47.5	46.4		46.3	46.0	43.7	43.7	44.6	187,500	217,000	0.86	8.7	24.0	45.0	45.1	0.2	50.2	50.4	1.2	50.0	51.2	-0.8	49.4	48.6
A3a	Timken	1800	Oil	1550	790	32.6	32.2	34.0	-	-	-	50.8	44.9	45.2		46.3	46.7	45.6	46.9	47.4	193,500	221,000	0.88	10.0	28.3	45.0	46.3	0.8	47.8	48.6	0.8	47.8	48.6	8.7	40.2	48.9
B1	SDI	1700	Oil	1550	790	31.5	29.4	30.2	-	-	-	47.6	45.6	45.5		47.3	45.3	46.7	45.0	47.3	171,900	207,000	0.83	7.9	17.8	44.2	45.3	0.4	44.4	52.8	8.8	44.0	54.4	11.4	42.8	54.2
B2	SDI	1700	Oil	1550	790	31.3	29.2	30.4	-	-	-	44.8	42.7	43.2		46.5	47.1	46.5	47.6	48.2	170,200	205,000	0.83	7.3	22.6	42.7	43.6	3.0	49.2	52.2	2.7	49.8	52.3	11.4	42.8	54.2
B3	SDI	1700	Oil	1550	790	32.5	30.8	31.3	-	-	-	46.0	43.7	42.3		44.1	44.2	47.2	44.8	48.6	181,300	217,000	0.84	4.8	10.1	43.4	43.6	-0.8	51.0	50.2	-0.9	50.0	49.1	9.4	42.8	52.2
C1	Timken	1550	Oil	1550	790	36.5	33.3	35.3	-	-	-	46.7	48.9	48.9	477	46.9	44.1	46.5	46.5	45.6	185,800	221,000	0.84	9.7	27.2	42.2	45.2	1.8	48.8	50.6	1.2	46.4	49.6	3.6	48.4	52.0
C2	Timken	1550	Oil	1550	790	34.0	33.4	32.7	-	-	-	48.4	49.1	49.9	495	46.8	47.4	47.8	48.1	48.7	180,900	215,000	0.84	10.0	26.9	44.3	43.5	4.0	45.2	49.2	5.6	44.8	50.4	10.2	40.4	50.6
C3	Timken	1550	Oil	1550	790	31.3	33.0	33.8	-	-	-	49.8	49.6	48.8	477	45.3	45.7	45.8	46.0	47.7	179,600	213,000	0.84	11.0	30.9	42.4	44.0	4.0	43.8	47.8	4.0	48.6	50.6	6.4	44.4	50.8
E1	Timken	1600	Oil	1600	830	34.2	33.7	33.2	-	-	-	45.7	46.3	45.5	461	43.1	43.8	40.8	44.2	42.6	158,400	191,800	0.83	13.7	35.9	42.3	40.4	3.2	43.2	46.4	3.6	44.4	48.0	1.2	48.6	49.8
E2	Timken	1600	Oil	1600	830	32.1	31.3	31.8	-	-	-	43.9	45.6	43.2	444	44.5	44.8	41.6	45.3	45.1	168,900	206,000	0.84	13.5	37.1	42.0	42.7	3.4	44.4	47.8	6.6	41.2	47.8	11.8	37.8	49.6
E3	Timken	1600	Oil	1600	830	31.6	33.2	32.0	-	-	-	43.3	42.7	43.0	429	47.6	44.6	43.7	44.7	44.9	162,100	193,600	0.84	11.2	31.5	43.2	43.6	2.6	46.6	49.2	6.2	43.8	50.0	12.0	41.0	53.0
F1	Timken	1600	Oil	1600	750	36.1	33.0	35.1	-	-	-	40.8	41.1	41.1	472	42.8	42.1	40.1	40.9	40.7	170,800	207,000	0.83	11.5	35.1	43.0	41.5	2.6	46.4	49.0	8.8	41.0	49.8	12.6	40.2	52.8
F2	Timken	1600	Oil	1600	750	33.0	32.2	31.7	-	-	-	45.3	45.4	44.3	446	46.1	45.6	44.9	45.1	46.0	175,900	209,000	0.83	10.4	29.6	41.9	42.4	3.2	49.4	52.6	11.0	42.4	53.4	14.2	41.6	55.8
F3	Timken	1600	Oil	1600	750	33.0	34.1	33.4	-	-	-	47.8	45.6	47.8	459	49.0	48.0	46.7	48.2	47.5	170,400	207,000	0.82	12.1	35.7	40.5	42.6	0.4	50.2	50.6	8.8	42.6	51.4	12.8	41.0	53.8
G1	Timken	1500	Oil	1500	830	32.4	32.4	34.7	-	-	-	42.0	42.0	44.0	435	42.8	43.3	40.7	42.3	43.3	146,500	181,400	0.80	12.7	36.4	40.8	41.7	3.4	42.6	46.8	7.8	40.8	48.6	12.4	36.2	48.6
G2	Timken	1500	Oil	1500	830	34.1	33.4	33.9	-	-	-	47.3	46.2	47.5	456	44.6	43.7	42.0	43.5	45.1	162,400	196,800	0.83	10.8	29.2	41.4	41.4	3.4	43.4	46.8	13.2	37.0	50.2	12.8	38.8	56.6
G3	Timken	1500	Oil	1500	830	32.3	33.1	31.9	-	-	-	46.1	45.5	47.0	440	45.6	46.4	42.0	43.9	45.2	153,700	185,700	0.83	11.2	29.2	41.7	41.7	1.8	47.8	49.4	8.6	41.2	49.8	8.8	44.0	48.8
H1	Timken	1500	Oil	1500	750	32.8	32.6	31.7	-	-	-	48.9	46.8	48.7	473	45.4	44.2	42.4	44.1	45.6	155,500	195,200	0.80	11.3	28.1	42.8	42.2	5.2	44.4	49.6	8.6	44.0	51.0	11.8	40.2	51.8
H2	Timken	1500	Oil	1500	750	33.4	32.7	32.2	-	-	-	47.7	46.3	45.9	466	45.8	45.7	43.6	44.6	46.3	152,000	198,600	0.77	9.8	27.3	44.0	43.3	3.4	49.8	53.2	9.8	42.6	52.4	9.6	44.6	54.2
H3	Timken	1500	Oil	1500	750	33.3	31.3	33.9	-	-	-	48.0	48.2	48.7	478	46.5	45.6	43.6	45.0	46.4	150,800	192,900	0.78	11.1	29.6	40.4	40.0	4.4	47.8	52.2	8.4	43.6	52.0	13.8	40.4	54.2
I1	Timken	1550	Oil	1550	750	33.5	34.3	32.5	-	-	-	47.1	48.1	47.6	455	48.0	48.1	47.2	47.8	49.1	188,400	221,000	0.85	10.8	33.8	45.8	46.7	3.4	46.8	50.2	7.2	43.2	50.4	7.6	42.2	49.8
I2	Timken	1550	Oil	1550	750	33.1	33.3	32.5	-	-	-	45.6	45.2	44.6	450	48.6	48.5	48.1	48.0	48.3	185,400	214,000	0.87	10.2	31.5	44.2	43.2	4.8	42.6	47.4	4.0	45.8	49.8	10.8	41.0	51.8
J1	Timken	1600	Oil	1600	790	33.8	33.7	33.6	-	-	-	47.7	47.9	47.9	461	47.5	47.2	47.1	46.7	46.9	183,700	214,000	0.86	10.4	28.6	43.2	43.3	2.8	46.8	49.6	6.0	44.2	50.2	5.8	44.4	50.2
J2	Timken	1600	Oil	1600	790	33.3	33.2	33.3	-	-	-	48.4	49.2	47.7	477	49.2	48.6	48.4	48.9	48.9	175,500	206,000	0.84	9.4	27.1	43.2	43.3	3.8	47.0	50.8	5.6	45.0	50.6	8.8	40.8	49.6

Test Piece	Material	Heating Temp	Cooling Medium	Quench Temp		Av. Surface Hardness (HRC), Middle "As Received"			Av. Surface Hardness (HRC), Middle "As Quenched"			Brinell, Middle "As Quenched"		
A1**	Timken	1800	Oil	1550	-	-	31.9	-	-	60.6	-	-	653	60 HRC
B1**	SDI	1700	Oil	1550	-	-	29.4	-	-	58.0	-	-	627	59 HRC
C1**	Timken	1550	Oil	1550	-	-	32.9	-	-	62.7	-	-	653	60 HRC
E1**	Timken	1600	Oil	1600	-	-	33.2	-	-	55.7	-	-	601	58 HRC
G1**	Timken	1500	Oil	1500	-	-	33.2	-	-	57.6	-	-	578	56 HRC

Test Piece	Through Thickness Hardness (HRC)																															
	Location																															
	1	2	3	4	5																											
A1**	59.8	59.5	59.5	58.9	58.4	-	-	-	-	-	-	-	-	-	5.6	58.6	64.2	11.8	52.6	64.4	17.2	45.6	63.0									
B1**	59.6	59.9	59.1	60.5	59.4	-	-	-	-	-	-	-	-	-	0.6	64.4	65.0	2.6	64.2	66.8	4.8	61.8	66.4									
C1**	59.3	58.3	58.0	58.9	59.2	-	-	-	-	-	-	-	-	-	0.6	60.8	61.4	1.8	59.0	62.8	10.2	48.4	64.6									
E1**	57.4	57.1	55.1	58.1	59.1	-	-	-	-	-	-	-	-	-	0.2	66.4	66.2	1.0	65.8	66.8	2.2	65.6	67.8									
G1**	58.8	58.0	57.0	57.6	59.5	-	-	-	-	-	-	-	-	-	0.2	59.8	59.6	1.6	58.8	56.4	8.8	53.0	61.8									

Appendix A2: 3.375-Inch Bar Results

Test Piece	Description					Average Surface Hardness (HRC)						Ave	Through Thickness Hardness (HRC)						Tensile test results 0.25T					Tensile Test Results 0.5T						Banding							
						"As received"			"As tempered"				Location							Y/UTS					Y/UTS			Surface Hardness		Delta						
	Material	Heating Temp	Cooling Medium	Quench Temp	Temper Temp	Front End	Middle	Back End	Front End	Middle	Back End	Brinell	1	2	3	4	5	6	Yield (psi)	UTS (psi)		Elong (%)	R. of A. (%)	Yield (psi)	UTS (psi)		Elong (%)	R. of A. (%)	Front End	Back End	10% Dia Ave delta	10 % Dia Dark Ave	10% Dia Light Ave	Mid r Ave delta	Mid r Dark Ave	Mid r Light Ave	Centre Ave delta	Centre Dark Ave	Centre Light Ave
I1	Timken			1590	790	31.2	31.4	32.2	46.0	45.0	45.3	388.0	44.0	42.4	42.1	44.6	44.0	43.4	149200	184200	0.81	14.2	41.1	146300	184900	0.79	10.5	27.8	39.5	40.0	5.8	41.8	47.6	8.8	39.8	48.2	11.0	39.0	50.0
I2	Timken			1590	790	31.2	31.1	30.8	48.5	47.2	47.2	429.0	43.1	42.6	41.2	43.5	44.2	42.4	157800	192700	0.82	14.0	43.0	153400	192900	0.80	10.6	28.3	39.5	40.4	6.0	44.0	53.0	7.2	43.6	50.8	13.8	38.2	52.0
I3	Timken			1680	790	30.1	29.4	28.8	43.8	40.7	40.3	366.0	40.2	39.2	39.0	40.1	41.5	40.0	156500	191700	0.82	13.6	41.1	143400	188500	0.76	10.5	29.4	40.9	40.9	4.6	43.4	48.0	8.2	40.4	48.6	11.6	39.2	50.8
I4	Timken			1680	790	32.9	32.5	32.9	44.0	42.6	41.6	392.0	39.6	37.4	38.9	38.9	38.7	38.1	157400	190400	0.83	12.4	41.4	134200	175000	0.76	12.9	37.0	39.0	39.0	6.6	41.4	48.0	10.0	40.2	50.2	16.2	34.6	50.8
K1	Timken			1590	790	32.3	33.1	33.9	45.5	42.5	43.9	419.0	44.1	43.9	44.8	43.3	45.1	44.2	169800	199700	0.85	14.2	39.2	148300	187800	0.79	11.3	31.2	40.3	40.5	6.2	42.6	48.8	9.8	38.8	48.6	15.2	35.0	50.2
K2	Timken			1590	790	32.5	31.9	32.5	45.3	44.7	45.0	434.0	45.3	45.7	46.3	44.2	43.6	45.0	163300	195500	0.84	13.0	41.0	139200	182500	0.76	12.0	34.6	40.1	40.6	2.6	44.8	47.4	4.2	43.6	47.8	10.0	37.8	47.8
K3	Timken			1550	750	30.2	32.3	31.6	48.5	45.5	44.9	455.0	46.1	44.8	43.8	43.5	45.8	44.8	179200	211000	0.85	13.1	42.2	157900	199300	0.79	9.3	24.6	41.3	42.9	3.8	45.4	49.2	3.4	45.2	48.6	8.8	41.6	50.4
K4	Timken			1550	830	26.8	27.1	26.8	46.8	47.5	46.2	444.0	43.6	43.0	43.7	43.4	43.0	43.4	184400	208000	0.90	13.0	42.3	158700	189900	0.84	12.0	33.8	40.5	41.0	5.6	41.6	47.2	11.2	37.2	48.4	11.2	39.0	50.2
K5	Timken			1550	830	31.7	30.6	31.3	46.9	45.8	46.7	444.0	45.0	44.6	42.5	41.9	44.4	43.7	175500	203000	0.86	13.0	42.0	148800	185300	0.80	12.3	37.1	40.4	39.9	3.0	45.2	48.2	5.2	42.8	47.8	12.6	36.4	49.0
K6	Timken			1590	750	31.4	29.9	29.9	46.4	47.2	43.9	458.0	46.1	44.2	43.9	44.7	46.8	45.1	172800	207000	0.83	11.0	39.0	157900	202000	0.78	9.8	23.8	43.6	43.4	0.8	49.0	49.8	9.8	42.2	51.2	8.4	40.0	48.4
L1	Timken			1515	815	32.4	31.5	32.1	43.3	43.7	42.7	461.0	46.0	44.2	46.9	43.6	44.4	45.0	176000	202000	0.87	13.3	38.8	153500	189800	0.81	10.8	28.2	40.9	41.2	2.4	46.2	48.6	7.8	41.6	49.4	9.8	40.4	50.2
L2	Timken			1515	815	27.5	29.3	28.6	44.9	45.0	46.4	439.0	45.5	45.3	44.3	45.6	44.6	45.1	163000	191900	0.85	13.3	43.8	151700	186400	0.81	12.0	36.0	40.1	40.0	2.0	46.8	46.8	6.2	41.0	47.2	10.6	37.8	48.4
L3	Timken			1515	765	30.1	29.0	29.8	44.1	42.7	44.2	423.0	44.1	43.2	43.0	41.9	44.9	43.4	155800	193800	0.80	14.2	41.4	139000	185100	0.75	11.7	31.4	40.8	40.6	6.8	44.6	51.4	14.8	36.4	51.2	8.8	41.2	50.0
L4	Timken			1515	765	29.7	31.3	31.0	45.8	46.7	47.4	450.0	46.0	43.9	44.6	44.5	46.8	45.1	159400	198000	0.81	12.8	41.0	156300	199400	0.78	10.2	25.3	43.7	43.8	5.0	44.4	49.4	7.8	42.8	50.2	12.8	39.0	51.8
M1	Timken			1585	815	31.6	33.1	33.6	43.8	43.6	42.2	397.0	38.1	38.6	38.8	39.5	41.7	39.2	155800	190700	0.82	13.8	43.0	141300	182000	0.78	12.0	37.8	40.3	40.1	3.8	41.0	46.8	10.8	40.2	50.2	14.6	37.0	51.6
M2	Timken			1585	765	31.4	31.2	31.9	45.2	43.5	44.5	444.0	43.3	41.8	41.8	42.2	44.6	42.7	173800	208000	0.84	12.8	41.0	151100	194700	0.78	12.0	35.8	42.6	43.0	5.4	44.0	49.4	5.8	44.8	49.8	15.6	38.2	51.8
M3	Timken			1585	815	32.4	31.6	32.7	48.3	41.3	39.1	388.0	39.5	39.5	42.6	36.6	38.3	39.3	161200	191000	0.84	13.3	44.1	147800	182100	0.81	12.8	34.2	40.5	40.1	1.4	42.0	43.4	4.2	41.0	45.2	9.6	37.6	47.2
M4	Timken			1585	765	31.8	31.3	31.1	47.8	47.5	46.5	444.0	42.1	42.0	40.7	39.3	39.5	40.7	157000	194000	0.81	12.9	42.0	156800	196900	0.80	13.0	34.8	42.1	40.9	9.6	41.0	50.6	10.8	39.8	50.2	12.6	38.0	50.6
N1	Timken			1570	750	33.8	33.2	33.4	44.3	42.7	46.4	397.0	46.1	45.5	43.1	42.5	44.4	44.3	174600	209000	0.84	12.4	39.0	162900	199800	0.82	9.7	23.4	40.8	39.2	5.8	44.6	50.4	5.8	45.8	51.6	15.2	38.4	53.6
N2	Timken			1570	750	35.0	33.3	34.8	44.4	44.5	44.7	415.0	41.5	42.1	39.6	41.6	39.1	40.8	155800	192200	0.81	13.6	42.6	137900	188200	0.76	13.9	37.3	42.8	41.1	9.8	41.0	50.8	8.8	40.8	49.6	13.4	37.8	51.2
1800	Timken	1800	Air cool			30.5	31.6	31.6	31.3	31.1	31.1	299.0	29.0	28.8	30.9	28.9	29.8	29.5												9.4	28.8	38.2	6.0	35.0	41.0	20.0	39.2	59.2
1700	Timken	1700	Air cool			34.0	32.1	31.8	30.8	31.2	30.0	299.0	29.6	29.9	30.1	31.1	29.5	30.0												8.4	31.0	39.4	14.2	33.2	47.4	18.4	37.8	56.2

Test Piece	Material	Heating Temp	Cooling Medium	Quench Temp		Surface Hardness (Brinell), "As Received"			Brinell, Hardness "As Quenched"		
	Timken		Oil	1680	-	293	300	296	601	601	601
	Timken		Oil	1585	-	296	294	293	653	653	653
	Timken		Oil	1550	-	290	288	283	653	627	653
	Timken		Oil	1515	-	298	301	300	627	627	633
	Timken		Oil	1580	-	293	295	293	653	627	653

Appendix A2: 4.0-Inch Bar Results

Test Piece	Description					Average Surface Hardness (HRC)						Ave	Through Thickness Hardness (HRC)						Tensile test results 0.25T					Tensile Test Results 0.5T					Banding							
						"As received"			"As tempered"				Location								Y/UTS					Y/UTS			Surface Hardness		Delta					
	Material	Heating Temp	Cooling Medium	Quench Temp	Temper Temp	Front End	Middle	Back End	Front End	Middle	Back End	Brinell	1	2	3	4	5	5	Yield (psi)	UTS (psi)		Elong (%)	R. of A. (%)	Yield (psi)	UTS (psi)		Elong (%)	R. of A. (%)	Front End	Back End	10% Dia Ave delta	10 % Dia Dark Ave	10% Dia Light Ave	Mid r Ave delta	Mid r Dark Ave	Mid r Light Ave	Centre Ave delta	Centre Dark Ave	Centre Light Ave
Q1	Timken	1550	Oil	1580	790	35.2	34.3	32.6	48.1	45.8	44.7	415.0	37.1	37.7	38.2	38.4	36.1	37.5	157400	152700	0.82	13.6	38.6	154900	150900	0.81	11.5	29.8	36.4	37.8	8.2	40.6	48.8	10.2	38.2	48.4	11.0	39.8	50.8
Q2	Timken	1550	Oil	1560	780	35.5	35.2	33.3	42.4	41.5	41.3	363.0	37.6	37.1	38.7	37.6	37.1	36.0	148400	144400	0.80	13.9	42.2	143800	138700	0.80	13.6	35.2	38.9	38.1	0.0	0.0	0.0	0.0	0.0	0.0	0.0	0.0	0.0
P1	Timken	1585	Oil	1600	790	33.4	34.4	34.6	42.9	40.7	42.2	415.0	39.3	39.0	40.4	40.6	39.6	39.8	159700	150100	0.84	13.1	39.6	156000	152200	0.82	10.9	29.7	39.3	39.1	6.2	38.2	44.4	9.8	37.4	47.2	13.0	35.6	48.6
P2	Timken	1585	Oil	1601	791	34.1	33.5	32.2	41.3	41.2	43.3	388.0	37.9	37.2	39.1	37.8	37.1	37.8	147800	142100	0.81	14.0	44.0	138500	134600	0.79	12.0	35.0	38.7	37.6	0.0	0.0	0.0	0.0	0.0	0.0	0.0	0.0	0.0
Q3	Timken	1515	Oil	1590	790	32.3	32.5	34.1	49.5	48.2	48.2	419.0	44.7	43.0	42.5	43.5	43.9	43.5	161300	201000	0.80	14.0	38.0	143900	185900	0.77	11.0	30.8	38.8	39.0	7.6	42.6	50.2	9.8	41.6	51.4	15.0	37.4	52.4
Q4	Timken	1515	Oil	1590	790	34.3	32.9	33.5	45.8	44.5	47.1	425.0	39.3	37.3	38.7	37.9	40.1	38.7	150200	188900	0.80	13.0	41.0	141000	185700	0.76	10.0	27.0	39.3	39.8	0.0	0.0	0.0	0.0	0.0	0.0	0.0	0.0	0.0
R1	Timken	1550	Oil	1590	750	33.4	34.3	33.9	44.9	44.5	43.7	406.0	42.0	41.3	38.4	39.8	38.2	39.8	156400	185800	0.84	13.0	41.0	147800	178800	0.82	12.0	33.8	39.5	38.8	3.2	41.6	44.8	10.8	38.0	48.8	13.4	36.8	50.2
R2	Timken	1550	Oil	1590	830	34.2	33.2	32.1	42.5	42.2	43.3	415.0	37.8	37.3	38.1	38.5	39.5	38.2	155500	185600	0.84	12.9	35.2	157900	187900	0.84	13.2	41.1	40.8	38.1	0.0	0.0	0.0	0.0	0.0	0.0	0.0	0.0	0.0
S1	Timken	1515	Oil	1590	830	32.5	32.4	32.9	40.4	40.5	40.3	359.0	39.3	40.3	40.2	39.5	40.4	39.9	147000	180700	0.81	16.0	44.0	137800	173500	0.79	13.0	35.0	37.9	37.9	6.2	39.0	45.2	11.4	38.2	49.6	12.0	37.6	49.6
S2	Timken	1515	Oil	1590	750	33.4	32.6	34.3	43.0	42.7	44.0	392.0	39.2	37.5	38.9	38.8	37.2	38.5	153400	185100	0.83	13.0	39.0	140500	175600	0.80	12.0	35.0	35.7	37.2	0.0	0.0	0.0	0.0	0.0	0.0	0.0	0.0	0.0
T1	Timken	1585	Oil	1615	815	35.0	33.5	33.1	45.1	44.4	43.4	392.0	39.0	39.4	38.3	38.5	37.4	38.6	148300	190700	0.78	12.3	40.1	143500	189000	0.76	10.8	30.9	38.6	36.2	5.8	43.4	49.2	10.8	42.2	52.2	14.4	35.8	50.2
T2	Timken	1585	Oil	1555	815	33.9	33.0	33.1	43.9	43.2	43.2	392.0	37.5	37.7	39.8	37.1	38.2	38.0	150600	189100	0.80	13.6	42.5	146100	188900	0.78	11.2	29.8	36.7	35.8	0.0	0.0	0.0	0.0	0.0	0.0	0.0	0.0	0.0
U1	Timken	1550	Oil	1525	765	33.3	32.8	32.6	44.8	45.3	45.6	415.0	39.6	37.9	39.7	39.1	40.3	39.3	162200	191000	0.85	14.0	41.0	149200	182000	0.82	13.0	34.0	40.5	39.3	4.2	39.4	43.6	8.4	41.0	49.4	11.0	38.4	49.4
U2	Timken	1550	Oil	1525	765	34.2	33.0	32.4	58.2	47.0	46.4	425.0	39.8	40.1	39.4	40.8	40.1	40.0	154900	193000	0.80	15.0	41.5	143900	186800	0.77	13.0	31.2	38.5	38.2	0.0	0.0	0.0	0.0	0.0	0.0	0.0	0.0	0.0
AC 1800 (Surf)	Timken	1800	Air Cool	1585	-	32.2	32.0	33.5	33.6	31.4	31.2	298.0	30.3	31.2	30.2	32.2	30.6	30.9	0	0	0	0.0	0.0	0	0	0	0.0	0.0	0.0	0.0	1.2	37.6	36.4	11.0	34.0	45.0	22.0	34.0	57.6
AC 1800 (Core)	Timken	1800	Air Cool	1585	-	32.2	32.0	33.5	33.6	31.4	31.2	298.0	30.3	31.2	30.2	32.2	30.6	30.9	0	0	0	0.0	0.0	0	0	0	0.0	0.0	0.0	0.0	1.2	37.6	36.4	11.0	34.0	45.0	22.0	34.0	57.6
AQ 1515	Timken			1515	765	0.0	0.0	0.0	0.0	0.0	0.0	0.0	0.0	0.0	0.0	0.0	0.0	0.0	0	0	0	0.0	0.0	0	0	0	0.0	0.0	0.0	0.0	0.0	0.0	0.0	0.0	0.0	0.0	0.0	0.0	0.0
AQ 1550	Timken			1550	815	0.0	0.0	0.0	0.0	0.0	0.0	0.0	0.0	0.0	0.0	0.0	0.0	0.0	0	0	0	0.0	0.0	0	0	0	0.0	0.0	0.0	0.0	0.0	0.0	0.0	0.0	0.0	0.0	0.0	0.0	0.0
AQ 1585	Timken			1585	765	0.0	0.0	0.0	0.0	0.0	0.0	0.0	0.0	0.0	0.0	0.0	0.0	0.0	0	0	0	0.0	0.0	0	0	0	0.0	0.0	0.0	0.0	0.0	0.0	0.0	0.0	0.0	0.0	0.0	0.0	0.0

Test Piece	Material	Heating Temp	Cooling Medium	Quench Temp		Surface Hardness (Brinell), "As Received"			Brinell Hardness "As Quenched"		
	Timken		Oil	1580	-	293	300	296	601	601	601
	Timken		Oil	1585		296	294	293	653	650	650
	Timken		Oil	1550	-	290	288	283	653	627	650
	Timken		Oil	1525	-	298	301	300	627	627	633
	Timken		Oil	1590	-	293	293	293	653	627	650

Appendix B

Additional Micrographs

Appendix B1: 2.875-Inch Bar, As Received Condition

2.875-inch bar - Mag X50: As-received 10% location

2.875-inch bar - Mag X50: As-received mid-radius location

2.875-inch bar - Mag X50: As-received core location

Appendix B1: 2.875-Inch Bar, As Cooled Condition

2.875-inch bar - Mag X50: As-cooled 10% location

2.875-inch bar - Mag X50: As-cooled mid-radius location

2.875-inch bar - Mag X50: As-cooled core location

Appendix B1: 2.875-Inch Bar, As Quenched Condition

2.875-inch bar - Mag X50: As-quenched 10% location

2.875-inch bar - Mag X50: As-quenched mid-radius location

2.875-inch bar - Mag X50: As-quenched core location

Appendix B1: 2.875-Inch Bar, Quenched and Tempered

2.875-inch bar - Mag X50: Q & T 10% location

2.875-inch bar - Mag X50: Q & T mid-radius location

2.875-inch bar - Mag X50: Q & T core location

Appendix B2: 3.375-Inch Bar, As Received Condition

3.375-inch bar - Mag X50: As-received 10% location

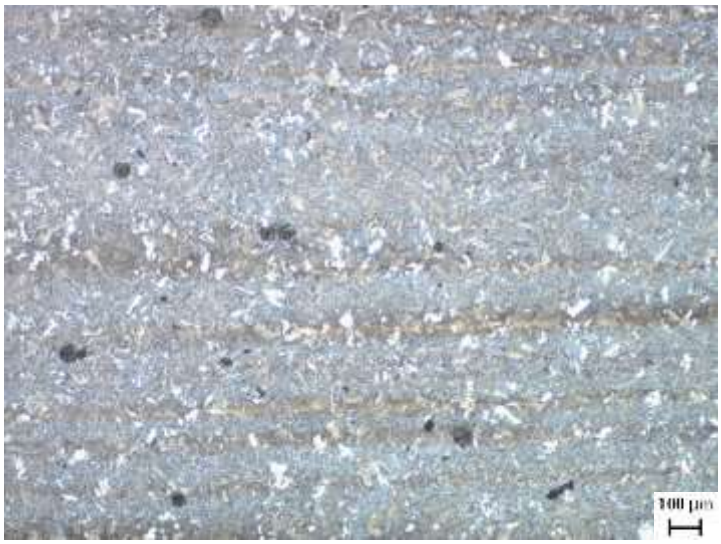

3.375-inch bar - Mag X50: As-received mid-radius location

3.375-inch bar - Mag X50: As-received core location

Appendix B2: 3.375-Inch Bar, As Cooled Condition

3.375-inch bar - Mag X50: As-cooled 10% location

3.375-inch bar - Mag X50: As-cooled mid-radius location

3.375-inch bar - Mag X50: As-cooled core location

Appendix B2: 3.375-Inch Bar, As Quenched Condition

3.375-inch bar - Mag X50: As-quenched 10% location

3.375-inch bar - Mag X50: As-quenched mid-radius location

3.375-inch bar - Mag X50: As-quenched core location

Appendix B2: 3.375-Inch Bar, Quenched and Tempered

3.375-inch bar - Mag X50: Q & T 10% location

3.375-inch bar - Mag X50: Q & T mid-radius location

3.375-inch bar - Mag X50: Q & T core location

Appendix B3: 4.0-Inch Bar, As Received Condition

4.0-inch bar - Mag X50: As-received 10% location

4.0-inch bar - Mag X50: As-received mid-radius location

4.0-inch bar - Mag X50: As-received core location

Appendix B3: 4.0-Inch Bar, As Cooled Condition

4.0-inch bar - Mag X50: As-cooled 10% location

4.0-inch bar - Mag X50: As-cooled mid-radius location

4.0-inch bar - Mag X50: As-cooled core location

Appendix B3: 4.0-Inch Bar, As Quenched Condition

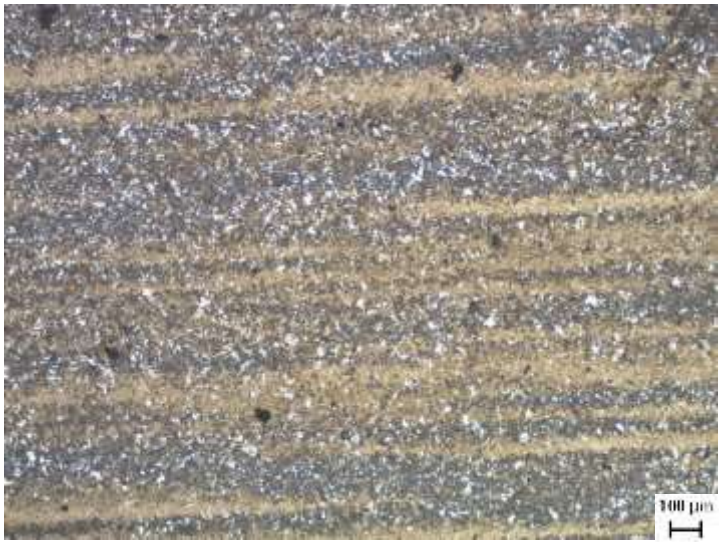

4.0-inch bar - Mag X50: As-quenched 10% location

4.0-inch bar - Mag X50: As-quenched mid-radius location

4.0-inch bar - Mag X50: As-quenched core location

Appendix B3: 4.0-Inch Bar, Quenched and Tempered

4.0-inch bar - Mag X50: Q & T 10% location

4.0-inch bar - Mag X50: Q & T mid-radius location

4.0-inch bar - Mag X50: Q & T core location

Appendix C

Residual Plots

Appendix C: Explanatory Text

The optimized model takes account of all test data to generate a graph that best represents the complete data set. This leads to a residual value around the optimized model, which is expected to be normally distributed. The following residual plots represent how the experimental value is distributed around the optimized model. The Normal Probability Plot represents how many experimental results are within the required residual value. Generally, the probability plot is centered with 50% of the test results having either a positive or negative residual. The Versus Fits plot shows residuals on the y axis and fitted values (estimated responses) on the x axis; it is used to detect non-linearity, unequal error variances, and outliers[1]. The Histogram shows the frequency of each residual value. The Versus Order Chart represents the run order of the test program, which shows that test results were normally distributed around the optimized model.

[1] The Pennsylvania State University. (2017). *A residuals vs. fits plot* [Online]. Available: https://onlinecourses.science.psu.edu/stat501/node/36

Appendix C1: 2.875-Inch Bar Results at 0.5T

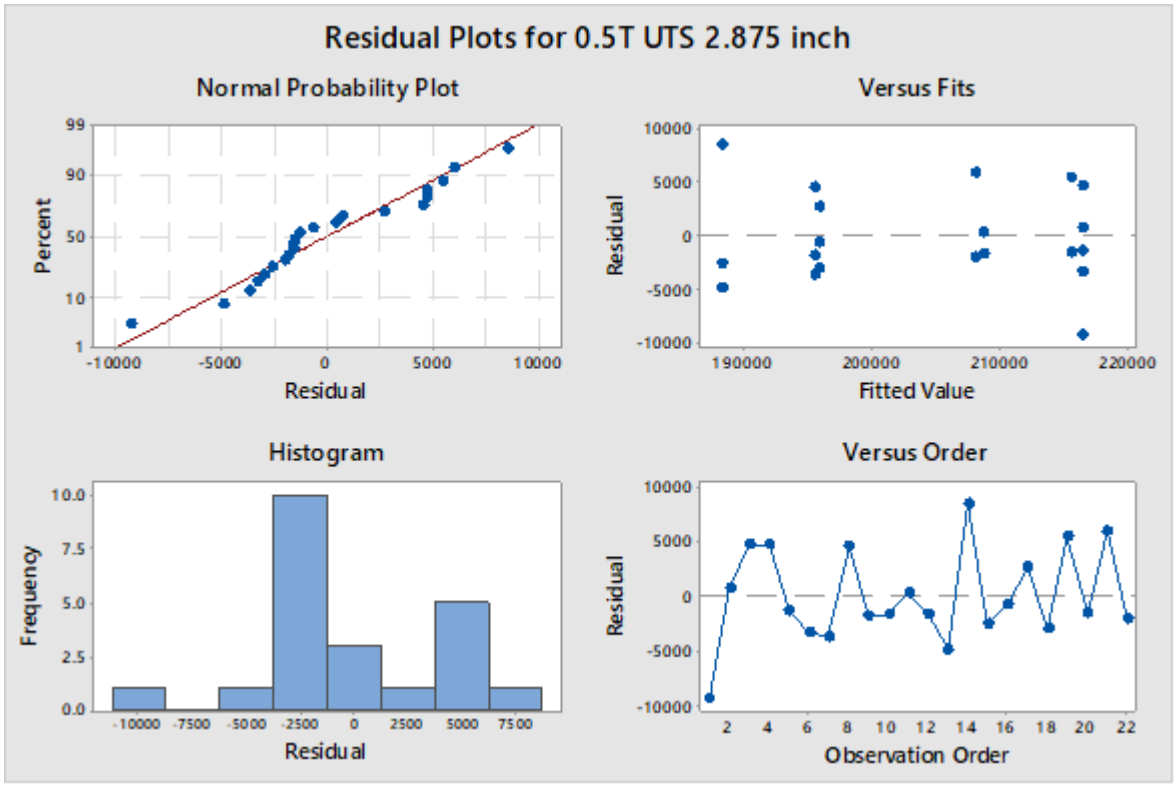

The above graph shows that 98% of test results will be within 10000psi of the value predicted by optimized model.

Appendix C2: 3.375-Inch Bar Results at 0.25T and 0.5T

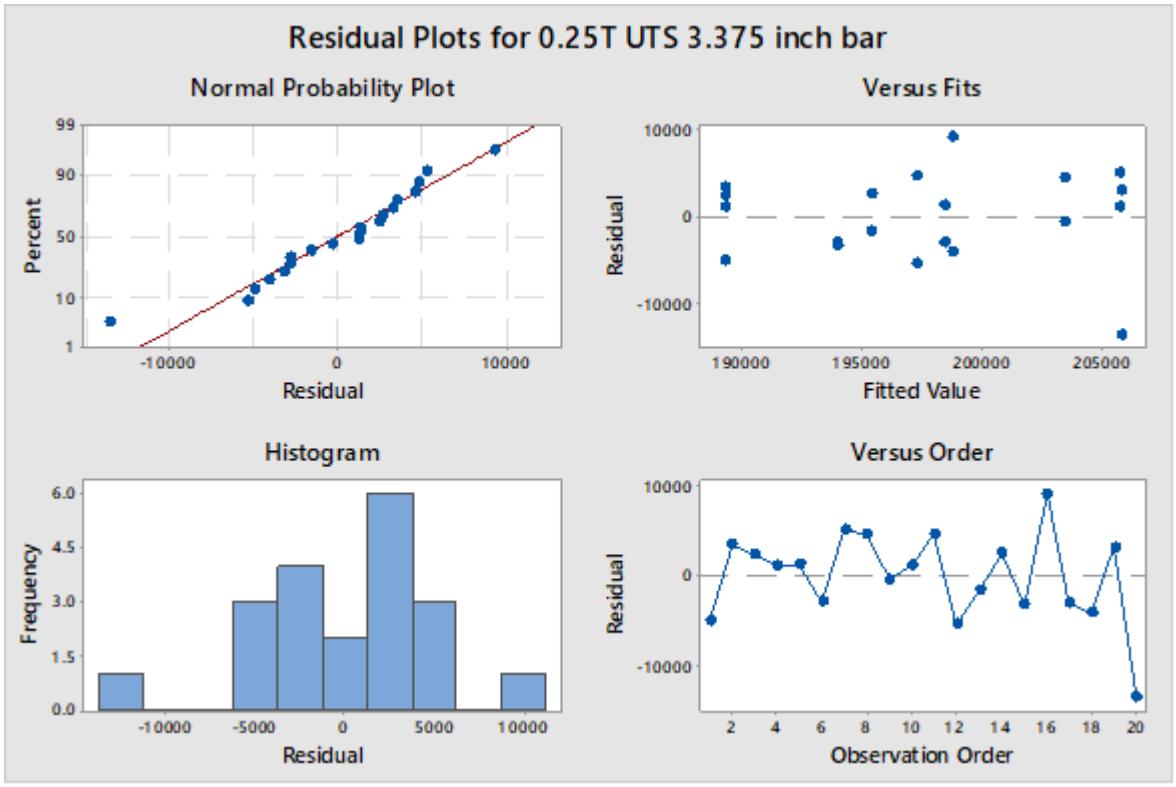

The above graph shows that 98% of test results will be within -12000 / +10000psi and 80% of test results will be within +/-5000psi of the value predicted by optimized model

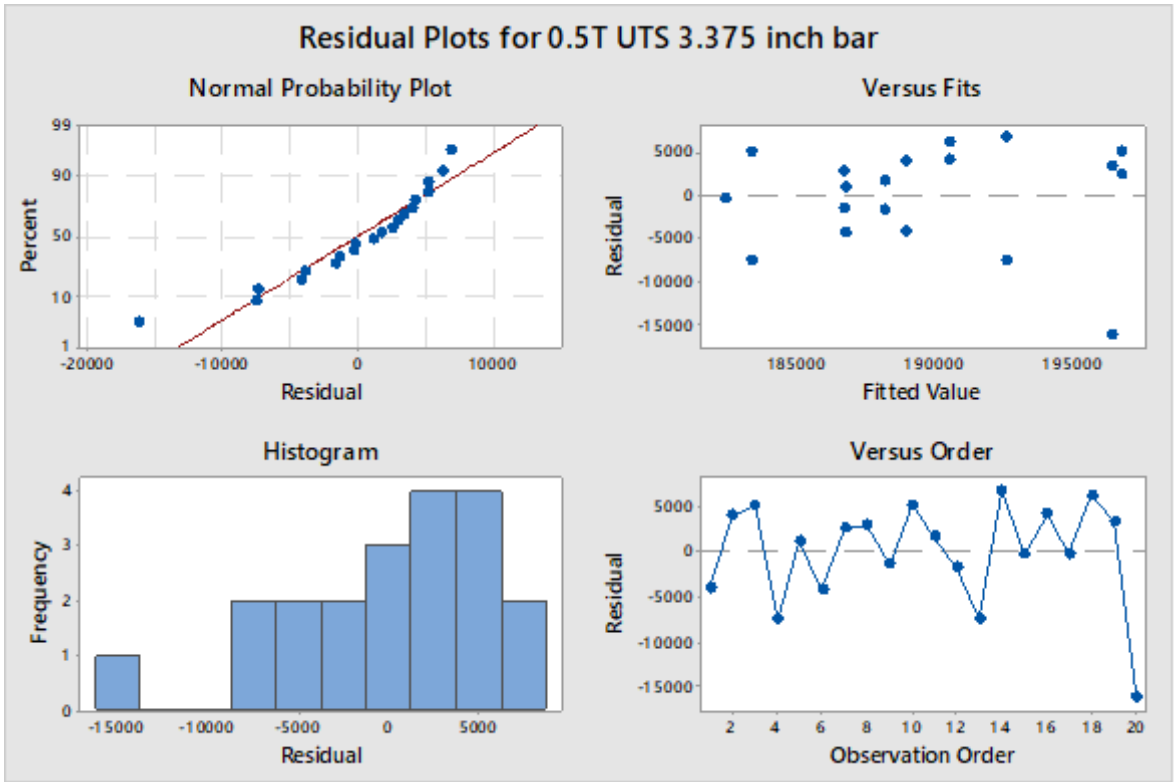

The above graph shows that 98% of test results will be within -15000/-7500psi of the value predicted by optimized model.

Appendix C3: 4.000-Inch Bar Results at 0.25T and 0.5T

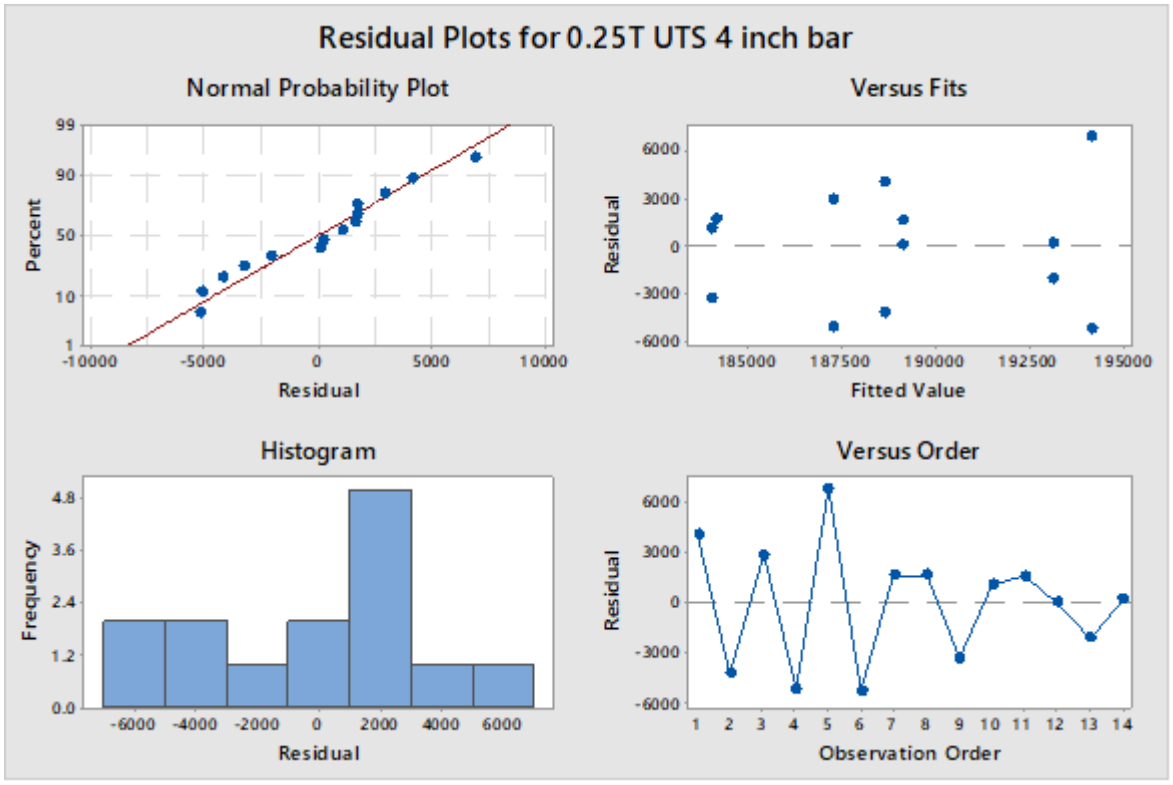

The above graph shows that 98% of test results will be within +/-8000psi of the value predicted by optimized model.

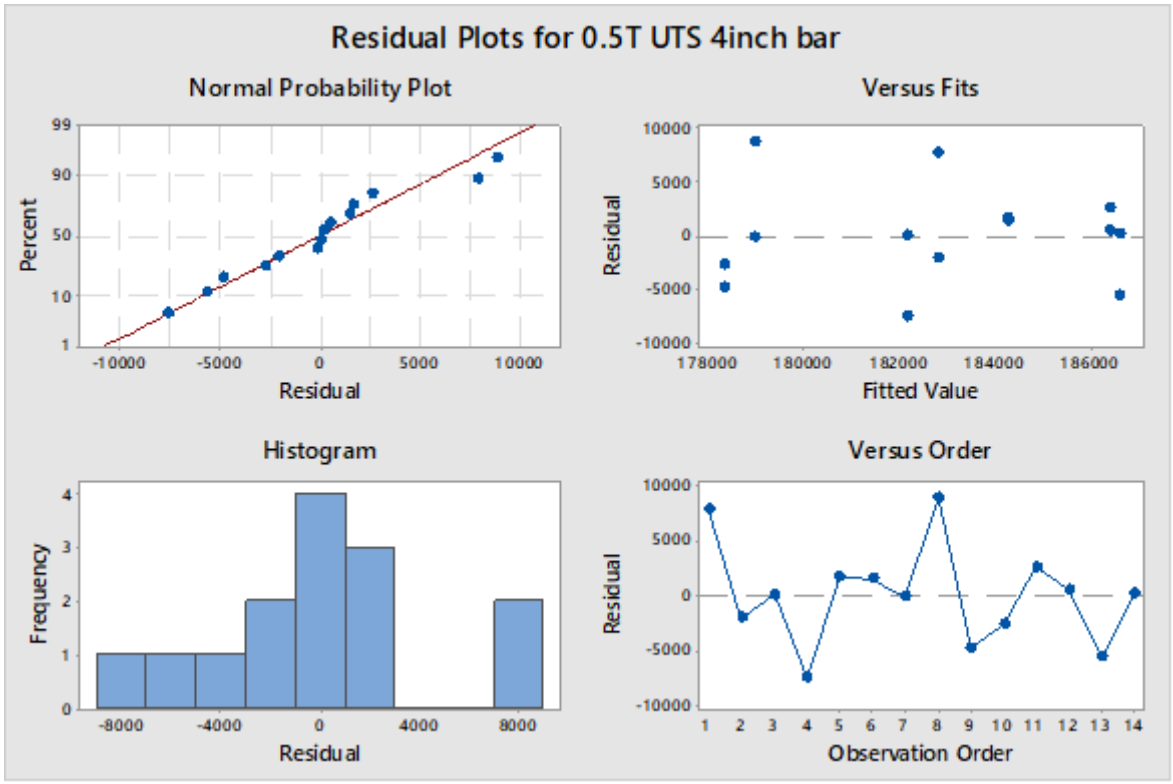

The above graph shows that 98% of test results will be within +/-11000psi of the value predicted by optimized model.

Appendix D

Material Certificate of Conformity (CoC)

Appendix D1: Super S® Quench Oil 521

Super S® Quench Oil 521

TECHNICAL PRODUCT INFORMATION

Super S Quench Oil 521

Super S Quench Oil 521 is a paraffinic based medium speed quench oil used in heat treating of steel

FEATURES/ BENEFITS

Super S Quench Oil 521

- Blended with Hi VI paraffinic base stocks
- Minimum viscosity change during cooling cycle
- Special additive system provides:
- Oxidation resistance
- Excellent wetting ability
- Outstanding cooling capacity

APPLICATIONS

Heat treating of steel

Medium speed quench

SPECIAL HANDLING, NOTICES OR WARNINGS

Handle as you would any petroleum product

TYPICAL CHARACTERISTICS

Super S® Quench Oil 521		
Properties	*Test Method ASTM D-*	*Data*
Gravity, °API	1298	33
Flash Point °C/°F,	92	179/354
Pour Point °C/°F	97	-9/16
Color	1500	3.5
Viscosity cSt @ 40°C SUS @ 100°F	445	 18.5 95
Quench Time	GM Quenchometer	12-16

Typical test data are average values only.
Minor variations which do not affect product performance are to be expected during normal manufacturing.

PRODUCT NUMBERS

SUS 301-55 55 gallon drum

Super S Lubricants *November 12, 2010*

Appendix E

Key Effects of Material Variability

Appendix E1: Effect of Increase in Bar Diameter

1) Reduction in tensile strength.

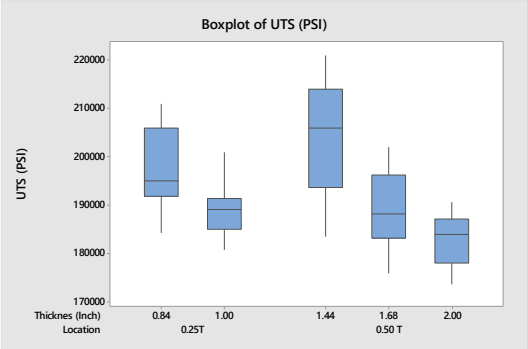

2) Reduction in surface hardness.

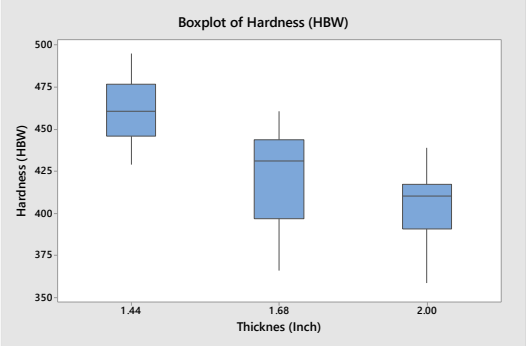

3) Increase in hardness delta between the band and matrix.

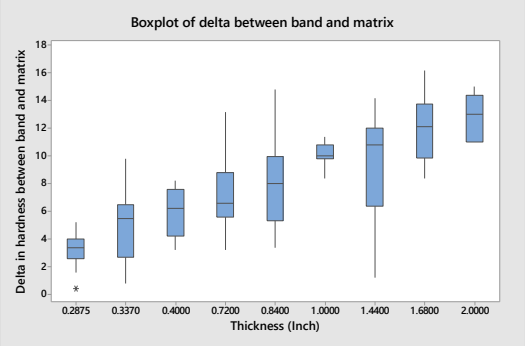

4) Increase in difference between ideal diameter of band and matrix due to increased difference in chemistry between band and matrix.

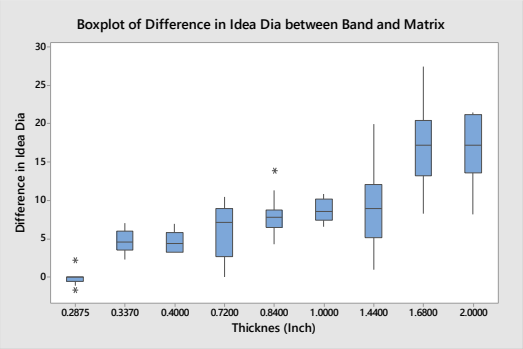

5) Reduction in the proportion of martensite formed within the structure.

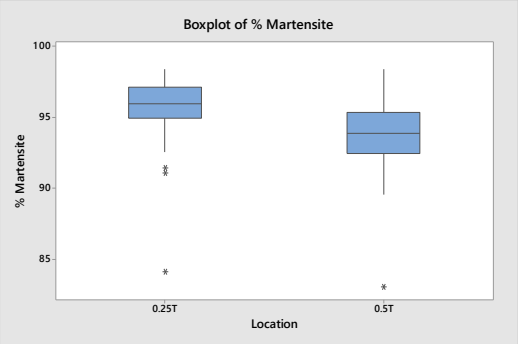

Appendix E2: Effect of Changing Heat Treatment Parameters

The heat treatment parameters, which have a major impact on each tested condition, as indicated by standardised effect plots.

1) Change in tempering temperature has major impact on tensile strength.

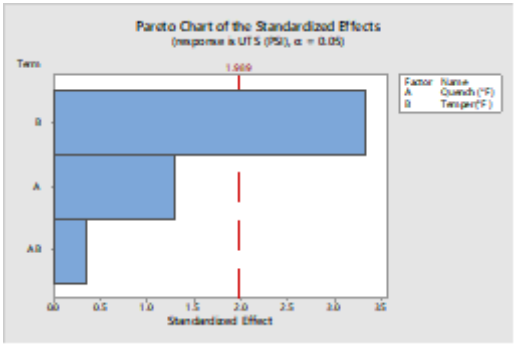

2) Change in tempering temperature has major impact on surface hardness.

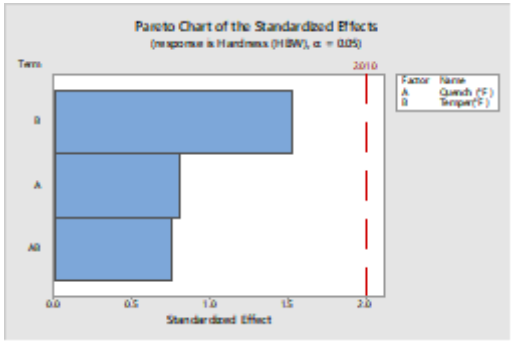

3) Both quenching and tempering temperature have slight impact on delta in hardness between the band and matrix however the impact of tempering temperature is slightly higher than quenching temperature.

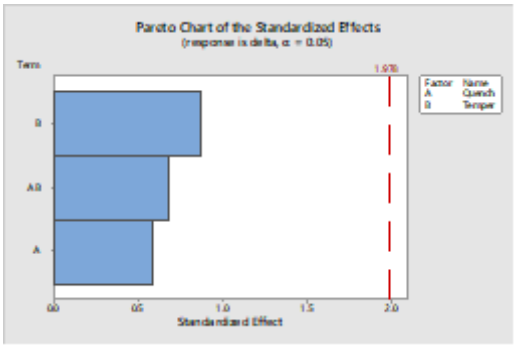

4) Both quenching and tempering temperature have slight impact on delta in ideal diameter and thus chemical composition between the band and matrix however the impact of quenching temperature is slightly higher than tempering temperature.

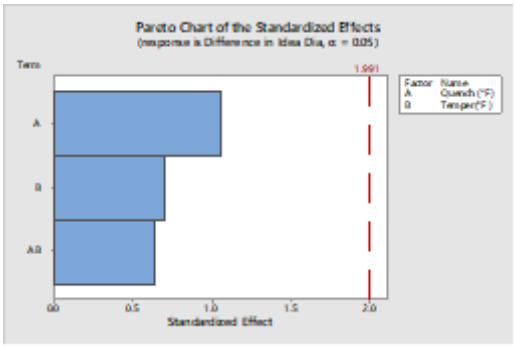

5) Both quenching and tempering temperature have major impact on the proportion of martensite formed within the structure.